Elucidating patterns of Major Histocompatibility complex polymorphism in the Trinidadian guppy (*Poecilia reticulata*) using Next Generation Sequencing

By

Jackie Lighten

Submitted in partial fulfillment of the requirements for the Degree of

Doctor of Philosophy

At

Dalhousie University

Halifax, Nova Scotia

July 2015

Table of Contents

List of Tables

List of Figures

Abstract

This thesis describes patterns of Major Histocompatibility Complex (MHC) evolution in natural populations of the guppy (*Poecilia reticulata*), using Next Generation Sequencing (NGS). I have proposed a redefinition of the molecular and bioinformatic approaches used to gather NGS MHC sequence data, and the theoretical considerations required for accurate interpretation of MHC diversity. The various bioinformatic approaches that are currently implemented in NGS MHC analysis are critically reviewed to provide a clear understanding of how such data should be analyzed. A novel molecular and bioinformatics procedure is introduced to estimate MHC genotypes from NGS data, which performs better than previously used approaches. I also explore the application of NGS to estimate both allelic and loci copy number variation (CNV) among guppy populations. Results suggest that both forms of CNV are widespread among guppies and the complex nature of CNV likely represents an important source of variation both within and among guppy populations. In addition, I provide novel evidence to suggest complex interactions between MHC polymorphism, parasite infection, and male colour, which are implicit in mate choice and believed to be honest signals of immunocompetence. Comparisons among geographic distributions of MHC supertypes and their constitutional alleles provide support for a novel model for how MHC evolution is governed. This identifies a combination of stabilizing selection acting on MHC supertypes (groups of functionally similar/identical MHC alleles) and random genetic drift coupled with Red Queen processes operating on alleles *within* supertypes. Patterns of population differentiation may be misinterpreted to represent high levels of local adaptation at the allelic level if supertypes are ignored. I propose that MHC supertypes are an important unit of selection and patterns of MHC CNV (or haplotype variation) are likely maintained by balancing selection acting on individual loci (or groups of loci), driven by variable parasite communities. This is summarized as the 'stabilized supertypes – balanced loci' model of MHC evolution. Evidence suggests not only that guppies provide a unique system to investigate the interplay between parasite mediated natural selection and sexual selection, but also that the guppy is an ideal model species that can greatly improve our understanding of MHC evolution in natural populations.

List of abbreviations used

A_i	Total number of MHC alleles per individual
A_p	Total number of MHC alleles per population
AVT	Allele validation threshold
BAC	Bacterial artificial chromosome
BLAST	Basic local alignment search tool
b	Bases
Bp	Base pairs
CNV	Copy number variation of genes or alleles
DAPC	Discriminant Analysis of Principle Components
DNA	Deoxyribonucleic acid
dN/dS	Non-synonymous/Synonymous base substitution
dNTP	Deoxynucleoside triphosphates
DOC	Degree of change
HLA	Human Leukocyte Antigen
L_i	Number of loci per individual
MHC I/II/B	Major Histocompatibility Complex class I/class II/beta subunit
MID	Multiplex identifier
mya	Million years ago
MPAF	Maximum per-amplicon frequency
N.	Total frequency (number)
NFDS	Negative frequency dependent selection
NGS	Next Generation Sequencing
PA	Putative allele
PCA	Principle Components Analysis
PCR	Polymerase chain reaction
PBR	Peptide binding region
RAD-seq	Restriction site associated DNA sequencing
RPE	Repeatable putative error
ROC	Rate of change

Sr	The measure of redundancy of PBR amino acid sequences translated from MHC alleles within an MHC supertype
ST	Supertype
ST_i	Total number of MHC supertypes per individual
ST_p	Total number of MHC supertypes per population
TSP	Trans-species polymorphism
x	Sequencing depth

Acknowledgements

I thank my supervisor Dr. Paul Bentzen for his patience, open-mindedness, knowledgeable guidance, and advice throughout this project. I also thank Ian Paterson for the same reasons as well as his invaluable expertise and effort in the lab, which generated the sequence data. Thanks to Dr. Andrew Hendry, along with past and present members of his research group who donated samples alongside parasite and colour data. Many thanks also to Dr. Cock van Oosterhout and Dr. Clive Bennett for their continued enthusiasm and guidance, and to Lyndsey Baillie for providing the microsatellite data.

Thanks to my peers within and outside of the Marine Gene Probe Laboratory, especially to Stanley King, and my long term sounding boards Alexander S.T. Papadopulos, Chris Watson, and Dara Mohammadi for many a fruitful discussion down the pub, excellent constructive criticism on writings, and for putting up with me in general.

I am very appreciative of the financial support provided by research grants to Dr. Paul Bentzen, and the Dr. Patrick Lett Fund, which allowed me to undertake this degree.

Above all I thank my unconditionally loving parents for all of the opportunities, experiences, and support they have given me.

Chapter 1

Introduction

With the rapid developments of Next Generation Sequencing (NGS) and other high-throughput assays over the last ten years, researchers are able to assess diversity at an unprecedented scale across genomes and ecosystems, improving our understanding of the complexities of adaptation among species (e.g. Lamichhaney *et al.* 2015). Notwithstanding cutting-edge NGS genomic approaches, much of what we have learned about adaptation at the DNA level over the past three decades has come from the study of a single set of genes - the Major Histocompatibility Complex (MHC) immune genes. In this thesis I provide significant advances not only in the application of NGS to the study of MHC, but also to the understanding of patterns and processes surrounding MHC evolution in natural populations. I examine MHC diversity across populations of the guppy (*Poecilia reticulata*) and make a case for how this already valuable model species can provide further significant advances in the understanding of MHC evolution in vertebrates. To this end I provide novel insight into the links between MHC diversity and traits that correlate with fitness, and critically, provide evidence in support of a new and potentially paradigm shifting theory surrounding the pattern and processes that characterize MHC diversity.

The Major Histocompatibility Complex (MHC)

The MHC comprises a set of cell surface receptor proteins that are important in the vertebrate immune system. A large gene family encodes these proteins, which have evolved over hundreds of millions of years (Danchin *et al.* 2004), with the specific function of identifying pathogens, and then initiating an immune response to prevent infection (Hedrick 2002). The primary role of MHC molecules is to present antigens (small peptides derived from pathogens) to T-cells. This acts a signaling mechanism for the immune system to make a targeted response in eradicating pathogens (Simpson 1988; Trowsdale 1993). Proteins of the MHC that are involved in these adaptive immunological processes are divided into MHC class I (MHC I) and

MHC class II (MHC II). MHC I is displayed almost ubiquitously among cells and primarily displays antigens derived from intracellular pathogens (e.g. viruses). Conversely, MHC II, although still widespread, is predominantly found on antigen presenting cells (macrophages, B-cells, dendritic cells) and mediates interactions among other immune cells (Lymphocytes; B-cells, T-cells, and dendritic cells) by displaying peptides derived from extra-cellular pathogens (e.g. bacteria, helminthes) (Simpson 1988; Trowsdale 1993).

Broadly speaking, there are four principal reasons for why the MHC has become a model for the study of adaptive evolution at the genetic level. Firstly, the genes that encode MHC proteins are the most polymorphic known in vertebrates (Beck & Trowsdale 2000). This polymorphism is thought to reflect the requirement for species to provide extensive immunological protection against rapidly evolving pathogens (Bernatchez & Landry, 2003; Jeffery & Bangham, 2000; Spurgin & Richardson, 2010), and this is explained by the Red Queen hypothesis (van Valen 1973, see below). It is believed that the selection pressures exerted by pathogens are so strong that high population differentiation at the MHC can arise relatively quickly compared to other neutral or functional loci (Bernatchez & Landry 2003, Spurgin & Richardson 2010). For this reason, studies on the MHC can provide insight in to patterns of local adaptation (Bernatchez and Landry, 2003).

Secondly, the MHC does not only play a central role in immunology, but variation at these genes has also been linked to female mate preference (i.e. pre-copulatory mate choice; e.g. Jordan & Bruford, 1998; Milinski, 2006; Wedekind & Penn, 2000), as well as the viability of embryos (i.e. post-copulatory mechanisms; e.g. Beer *et al.* 1981; Ober *et al.* 1993; Gasparini *et al.* 2015). The MHC therefore allowed behavioural ecologists to study the Good Genes Model (or the Hamilton-Zuk hypothesis, Hamilton & Zuk 1982) at a molecular level for the first time (e.g. von Schantz *et al.* 1996; Bolker *et al.* 2009; Eizaguirre *et al.* 2009). The Good Genes Model suggests that female mate choice is based on particular male traits (e.g. MHC genes) which

provide honest indicators of the ability to optimize reproductive success in offspring.

A third important feature of the MHC is that the functional properties of the amino acids on which diversifying selection acts have been identified through crystallography studies (Brown *et al.* 1993; Stern *et al.* 1994). Given that the majority of protein encoding DNA sequence within genomes is under purifying selection (Asthana *et al*. 2007; Lawrie *et al*. 2013), the identification of the exact amino acids, translated from DNA, that are under diversifying selection is instrumental in evolutionary genetics studies of these genes. Notably, the relative position of the DNA codons that translate these amino acids is highly conserved within the gene sequences across vertebrate taxa (e.g. O'Callaghan *et al.* 1998; Dzuris *et al.* 2000). These codons constitute the region of the MHC complex that interacts with antigens, which is known as the peptide-binding region (PBR). Positive selection at these codons drives adaptation in efficiently displaying unique peptides (Hughes & Nei 1988).

A fourth reason for studying MHC is that the effects of recombination-like processes such as gene conversion and micro-recombination can be studied in detail due to the fact that the MHC is commonly characterized by multiple gene copies. This means that the diversity can be re-arranged between gene paralogues by gene-conversion events and micro-recombination (see below). This can promote rapid expansion of MHC haplotype diversity and immunological repertoires within populations, and various models have been suggested to describe this adaptive expansion and contraction of gene copy number variation (CNV; see below) (cf. the Accordion Model of multigene evolution, Klein *et al.* 1993; and the Birth and Death Model of multigene evolution, Nei *et al.* 1997).

MHC copy number variation (CNV)

Gene copy number variation (CNV) is a form of genomic structural variation where regions of DNA are either lost or duplicated. The study of CNV has gained attention in recent years as genomic analyses increase in sophistication, revealing their importance in disease susceptibility

and fitness (Kondrashov 2012; Katju & Bergthorsson 2013). CNV at the MHC is commonly observed, where ancient gene duplication events have led to an increase in the immune gene repertoire expressed within individuals in order to combat a larger array of pathogens. Copy number variation can be further augmented by unequal crossing over during meiosis, and because gene duplications/deletions are largely heritable (Locke *et al.* 2006), sexually reproducing populations can comprise an array of MHC CNV patterns among individuals (e.g. Chapter 3; Lighten *et al.* 2014a). Consequently, genotypes may consist of different numbers of allele copies among MHC loci (which can also vary in number), meaning that loci can be homozygous (carrying two identical alleles), heterozygous (carrying two distinct alleles), or hemizygous (carry just a single copy of an allele) (e.g. Chapter 3; Lighten *et al*. 2014a). Indeed, because the MHC is a gene dense region containing multiple paralogous gene copies, it is often difficult to fully characterize in non-model species that lack detailed genomic data. As such, gene CNV is often inferred indirectly by counting the number of alleles observed within a genotype. However, such an approach is likely to be inaccurate because it is impossible to discriminate between hemizygous and homozygous genes. Notwithstanding these difficulties, MHC CNV is likely an important source of variation in most vertebrate species given that the number and diversity of alleles within an organism can affect both disease susceptibility and mate choice (e.g. Siddle, 2010, and see below). However, the evolutionary processes operating on MHC CNV remain unclear.

MHC gene conversion

Point mutations in the MHC generate novel sequence variation and an excess of non-synonymous base substitutions in the PBR are a consequence of pathogen driven positive selection (Hughes & Nei 1988). In addition, micro-recombination events can re-distribute existing DNA variation within and among MHC loci, resulting in the formation of new haplotypes (Chen, 2007; Ohta, 1991). Gene-conversion is believed to be an important source for generating variation in MHC functional haplotypes (Högstrand & Böhme 1999; Martinsohn *et al.* 2000; Hosomichi *et al.* 2008). Indeed, a recent study showed that gene conversion events

generated MHC haplotype variation at a rate an order of magnitude greater than point mutations, and these were especially important in augmenting variation in genetically depauperate populations (Spurgin *et al.* 2011). Despite the observation that gene conversion can rapidly generate haplotype variation, over time it is believed to homogenize sequence variation at paralogous loci (Ezawa *et al*. 2010; Takuno *et al*. 2010), and so the extent of gene conversion likely varies between species and along spatial and temporal scales.

Trans-species polymorphism

Trans-species polymorphism (TSP) describes the presence of similar (but not identical) alleles in divergent species (Arden & Klein, 1982; Klein, 1987; Klein *et al*. 1998; Klein *et al.* 2007). This occurs though the retention of ancestral allelic genealogies (and not convergent evolution) from ancestral species to descendent species. In the MHC, balancing selection is believed to drive TSP, and coalescence times of genes displaying TSP are much greater (millions of years) than those of neutrally evolving genes and pre-date speciation events (Takahata 1990; Takahata & Nei 1990). Moreover, a recent comparison between humans and chimpanzees showed that in addition to the MHC, over 100 genomic regions, involved in interactions with pathogens, displayed TSP (Leffler *et al.* 2013). The authors conclude that balancing selection acting on immune genes can persist for millions of years, maintaining critical functionality despite wide-spread genomic divergence between species.

MHC supertypes

The concept of MHC supertypes (or superfamilies) originates from human studies aimed at classifying groups of MHC alleles with similar binding properties for common motifs (supermotifs) derived from pathogens (del Guercio *et al.* 1995). Such classification of supertypes has shown to be valuable in developing vaccines targeting particular group of antigen epitopes (Sidney *et al.* 1996; Sette & Sidney 1998; Sette *et al.* 2002). Revealing the functional characteristics of MHC alleles is crucial in understanding their role in adaptive immunity, but such data have generally been restricted to model organisms, where in-depth

experimental and theoretical research is required (Sette *et al*. 2002). However, bioinformatic approaches have recently been developed which allows statistical characterization of supertypes based on inferred shared functional properties of the amino acids, which constitute MHC genes (Doytchinova *et al*. 2004; Doytchinova & Flower, 2005). In doing so, studies of non-model organisms have been able to adopt MHC supertype analysis in order to infer MHC functionality in studies of adaptation in natural populations (Schwensow *et al.* 2007; Sepil *et al.* 2013a; b). Despite this, the application of such analyses in studies of evolutionary ecology remains sparse, and so the significance of supertypes and their evolution in natural populations remains poorly characterized.

Parasite and mate choice mediated natural selection

Multiple evolutionary hypotheses have been proposed to explain the high polymorphism observed at MHC loci. Parasites are thought to exert balancing selection on MHC polymorphism though negative frequency-dependent selection (NFDS), heterozygote advantage (overdominance), or fluctuating selection over time (reviewed in Edwards & Hedrick, 1998; Spurgin & Richardson, 2010). However, disentangling the relative contributions of each of these processes in natural populations has been difficult, and so convincing empirical evidence in their support is sparse (but see Eizaguirre *et al.* 2012). Moreover, models suggest that heterozygote advantage can explain the high polymorphism observed at MHC loci, but this model requires that the fitness of homozygotes are nearly equal, i.e. symmetric overdominance (De Boer *et al.* 2004). The model by De Boer *et al.* (2004) shows that under asymmetric overdominance, the equilibrium level of polymorphism is considerably lower. Given the large number of MHC alleles, it seems unlikely that all homozygous genotypes have a similar fitness disadvantage (and that all heterozygous genotypes the same fitness advantage). Consequently, overdominance is unlikely to be the only selective force to maintain MHC polymorphism and large allelic diversity at the MHC.

Negative frequency-dependent selection assumes that an ongoing evolutionary arms race between host MHC genes and evolving parasites acts to preserve polymorphism (Spurgin & Richardson, 2010). Rare alleles in a population confer a selective advantage in parasite resistance over more common alleles, and so increase rapidly in a population. Counter-adaptation of parasites will then lead to a reduction in selective advantage of these alleles, and then to an adaptive allele frequency flux as other rare alleles again increase in frequency through novel selective advantages. However, empirical evidence in support of NFDS remains elusive. It has also been proposed that rare-allele advantage may be augmented by mate choice, where females choose to mate with males which carry alleles that increase fitness in offspring (Ejsmond *et al.* 2014; Milinski 2006). Indeed, MHC based mate choice has been observed across taxa (e.g. Winternitz *et al.* 2013), and is believed to be driven by MHC-related odors which convey attractiveness of potential mates (Wedekind & Penn 2000). Females may choose males that have more different MHC alleles to themselves, and so aim to increase the allelic diversity in their offspring (Milinski 2006). Recent evidence also suggests that MHC assortative-mate choice may facilitate local adaptation to endemic pathogens by reducing overall diversity through the increase of crucially functioning alleles (Sin *et al.* 2015).

The Trinidadian Guppy

The guppy is a small freshwater fish native to Northern South America and Central America (Figure 1.1). The contemporary species distribution outside of the neotropics represents human mediated introductions intended to control mosquitos, however its presence on the Caribbean Islands of Trinidad and Tobago is a consequence of natural colonization events from South America during periods of low sea level (Magurran 2005). The ability of guppies to thrive in fresh or brackish water, alongside a high tolerance to relatively harsh conditions, has greatly aided colonization of new habitats (e.g. Lindholm *et al.* 2005). Moreover, their high propensity for rapid evolution and adaptation (aided by relatively short generation times) has not only made guppies a valuable model species in biological studies, but has also gained them global popularity with aquarium hobbyists, where selective breeding has led to a myriad of ‘fancy’

guppy strains and phenotypes (Figure 1.2).

Much of the evolutionary and ecological research on guppies has focused on natural populations in Trinidad. The Northern Range of Trinidad comprises many discrete and diverse riverine ecosystems to test hypotheses of local adaptation. The many isolated populations of guppies in these rivers, coupled with their propensity to evolve independently over relatively small spatial scales in response to local ecological pressures (Reznick *et al.* 1997) has resulted in a "natural laboratory" for studies of vertebrate ecology and evolution (Haskins *et al.* 1961). Guppies show significant variation in genetics, morphology, colouration, feeding behaviour, predator avoidance, courtship, and mating behavior among populations (Meffe 1989; Houde 1997; Magurran 2005; Willing *et al.* 2010; Evans *et al.* 2011; Baillie 2012). The value of guppies as a model species has led to them being extensively studied both in natural populations and under controlled experimental conditions in the lab and field (reviewed in Meffe 1989; Houde 1997; Magurran 2005; Evans *et al.* 2011).

Numerous studies have investigated MHC in guppies and observed reductions in diversity through inbreeding (Sato *et al.* 1996; van Oosterhout *et al.* 2006a), inferred the presence of both random genetic drift and balancing selection in the distribution of MHC allelic diversity (van Oosterhout *et al.* 2006b; Herdegen *et al.* 2014), proposed extensive allelic and loci CNV (Llaurens *et al.* 2012; Chapter 3; Lighten *et al.* 2014a), temporal variation in allele frequencies (Fraser *et al.* 2010), and parasite mediated homogenizing selection (Fraser & Neff, 2010). While each of these findings are interesting in their own right, none have made a case for the guppy to be considered as a model system in MHC studies. This is likely due to similar findings being observed in other species (Bernatchez & Landry 2003; Piertney & Oliver 2006), and so researchers interested in understanding MHC evolutionary ecology (rather than using MHC to understand functional diversity in their focal species) have no impetus to focus solely on guppies. A central aim of this thesis is to demonstrate that guppies offer a unique system for

the study of MHC, and can provide great insight into its evolution and function, which is potentially absent from other study systems.

Overview of the Thesis

This thesis examines MHC evolutionary dynamics in guppy populations using NGS, and examines the relationship between MHC polymorphism and guppy traits that correlate with fitness (colouration, and parasite infections). This study represents the largest study of guppy MHC to date, in terms of the number of studied samples, populations, spatial scale, and data types (MHC and microsatellite genotypes, guppy colouration, and parasite quantification).

Chapter 2 discusses the basic concepts and issues surrounding the implication of NGS in characterizing MHC genotypes. This chapter has been published in *Molecular Ecology (2014) 23(16):3957-72*, and my contributions included conception of the study, development and execution of the analysis, interpretation of the results and writing of the paper. The various bioinformatic approaches that are currently implemented are critically reviewed, and commonly overlooked problems in these procedures are outlined. The aim of this chapter is to provide a clear understanding of how NGS MHC data should be analyzed to provide accurate genotypes in the face of potentially high bias associated with NGS data. In conclusion, I suggest that bioinformatic approaches should adhere to strict genotyping assumptions and follow sequencing depth modeling procedures. This can facilitate accurate separation of real sequenced allelic variants from those that represent sequence artifacts or cross sample contaminants. To date the only procedure that implements such a strategy is that which I describe in the next chapter.

Chapter 3 introduces a novel molecular and bioinformatic procedure to estimate MHC genotypes from NGS data, and is exemplified using individuals from multiple guppy populations. This procedure differs greatly to those previously used and is demonstrated to perform significantly better in reducing both Type I (erroneously including artifacts within a genotype) and Type II (erroneously excluding true alleles from a genotype) genotyping error. This is achieved by strictly adhering to commonly asserted genotyping assumptions (as opposed to previous studies) and modelling the sequencing depth distribution of sequence variants within each sample to accurately separate real alleles and sequence artifacts. Along with the accurate identification of alleles within a genotype, I also explore the application of ultra-deep NGS to estimate both allelic and loci CNV among guppy populations. Results suggest that both forms of CNV are widespread among guppies and the complex nature of CNV likely represents an important source of variation both within and among guppy populations. This chapter was published in *Molecular Ecology Resources (2014) 14(4): 753-767,* and my contributions were the same as in the previous chapter.

Chapter 4 examines the relationship between MHC polymorphism and traits related to fitness in guppies – male coloration and parasite infection. Across populations I reveal significant relationships between MHC population richness, particular MHC supertypes, and changes in particular colouration (which are believed to be an honest signal of male fitness and are implicit in mate choice) and prevalence of *Gyrodactylus* monogean helminthes. Crucially, some of these relationships vary among river drainages, suggesting local adaptation. The most conservative explanation for such patterns is that the metabolic pressure exerted by parasites on the host immune system directly affects colouration believed to signal immunocompetence (Houde & Torio 1992; Houde 1997; Maan *et al.* 2006, c.f. the 'good genes' hypothesis, and the 'indicator' hypothesis, Mays & Hill 2004). In comparisons across populations, MHC supertype richness was positively correlated with *Gyrodactylus* prevalence, and negative correlated with colour area and number of spots. These relationships are likely to be a consequence of

balancing selection acting on MHC supertype diversity driven by local variation in parasite communities. In addition, I demonstrate that MHC allelic diversity is significantly correlated with neutral microsatellite diversity; whereas, MHC supertype diversity and microsatellite diversity are not correlated. This suggests that supertypes are less affected by demographic processes, compared to MHC alleles, and may better represent the unit upon which selection operates (discussed further in Chapter 5). This is the first-time such relationships have been observed among these important fitness and mate choice related traits, and between MHC alleles and supertypes.

Chapter 5 examines in detail the spatial distribution of MHC supertypes across guppy populations. In doing so I describe how population structuring of MHC allelic diversity is affected by neutral demographic processes, whereas supertype population structuring is not. Moreover, the study of MHC supertypes in comparison with their constituent alleles reveals detailed cryptic processes surrounding MHC evolution that cannot be inferred by the study of MHC alleles alone, as is traditional done. I provide the first evidence to suggest that strong stabilizing selection has operated on MHC alleles *within* loci specific supertypes over millions of years in both the guppy and its relative, the swamp guppy (*Poecilia picta*). In concert, I suggest that balancing selection operates directly on loci (supertypes) to produce complex patterns of CNV both within and among populations. This helps to resolve the largely unexplained phenomenon of MHC TSP. The spatial and temporal patterns that stabilizing selection generates in MHC allelic diversity can be erroneously interpreted as widespread divergent selection among populations when supertypes are not considered. This is because as MHC allele frequencies alone may be highly differentiated among populations due to genetic drift, and when supertypes are not considered, this is interpreted as a signature of local adaptation (because each allele is assumed to be functionally important/unique). However, this common interpretation fails to explain the maintenance of TSP. In conjunction with stabilizing selection I suggest that haplotypes of MHC supertype CNV are a central unit upon which balancing selection operates, and high levels of functional similarity among alleles within a supertype

render individual allele frequencies susceptible to random genetic drift. Those alleles within supertypes which differ in fitness effects may rapidly change in frequency due to inter-supertype Red Queen processes. This can help understand TSP and supports previous models showing that TSP cannot be explained by balancing selection on MHC alleles (van Oosterhout, 2009b). The culmination is a description of a new paradigm in the study of MHC evolution, which resolves multiple unexplained and commonly observed paradoxes. I purport that the combined study of MHC alleles, supertypes, and neutral loci is required to accurately interpret temporal and spatial patterns of MHC evolution.

Figure 1.1. The region of Northern Southern America, Trinidad and Tobago within the natural range of the guppy (*Poecilia reticulata*). Genetic evidence suggests that guppies invaded Trinidad and Tobago from ancestral population in the Orinoco River during periods of low sea level (Magurran 2005). (Used with permission from Baillie, 2012).

(a)

(b)

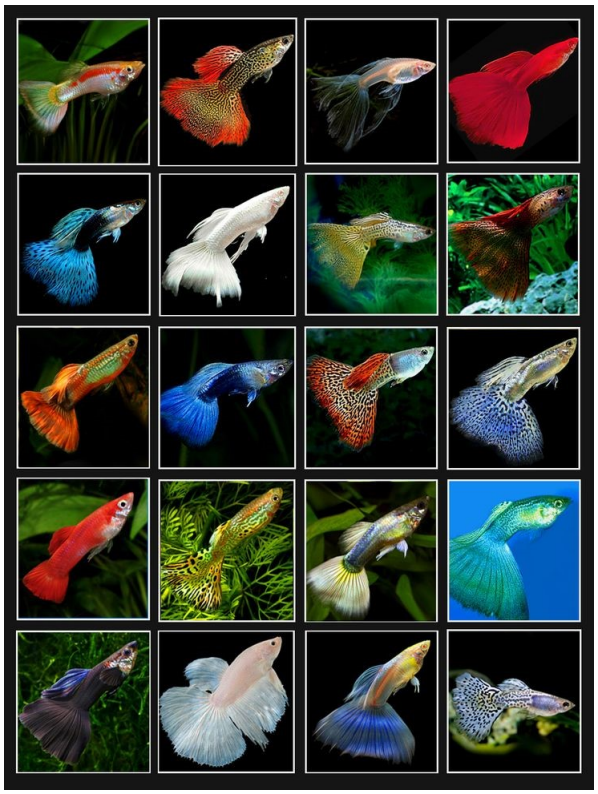

Figure 1.2. (a) Examples of variation in colouration observed among male guppies (*Poecilia reticulata*). Each group of five individuals were taken from separate natural populations in Trinidad. Photo: Andrew Hendry. (b) Selective breeding is able to produce a wide range of male phenotypic variation. These 'fancy guppies' are among the most popular aquarium species. Photo: unknown)

Chapter 2

Critical review of NGS analyses for *de novo* genotyping multigene families

Abstract

Genotyping of highly polymorphic multigene families across many individuals used to be a particularly challenging task because of methodological limitations associated with traditional approaches. Next-generation sequencing (NGS) can overcome most of these limitations, and it is increasingly being applied in population genetic studies of multigene families. Here, I critically review NGS bioinformatic approaches that have been used to genotype the Major Histocompatibility Complex (MHC) immune genes, and I discuss how the significant advances made in this field are applicable to population genetic studies of gene families. Increasingly, approaches are introduced that apply thresholds of sequencing depth and sequence similarity to separate alleles from methodological artefacts. I explain why these approaches are particularly sensitive to methodological biases by violating fundamental genotyping assumptions. An alternative strategy that utilizes ultra-deep sequencing (hundreds to thousands of sequences per amplicon) to reconstruct genotypes and applies statistical methods on the sequencing depth to separate alleles from artefacts appears to be more robust. The 'degree of change' (*DOC*) method avoids using arbitrary cut-off thresholds by looking for statistical boundaries between the sequencing depth for alleles and artefacts, and hence, it is entirely repeatable across studies. Although the advances made in generating NGS data are still far ahead of our ability to perform reliable processing, analysis and interpretation, the community is developing statistically rigorous protocols that will allow us to address novel questions in evolution, ecology and genetics of multigene families. Future developments in third-generation single molecule sequencing may potentially help overcome problems that still persist in *de novo* multigene amplicon genotyping when using current second-generation sequencing approaches.

Introduction

Next-generation sequencing (NGS) techniques allow researchers to provide answers to questions in evolution, ecology and genetics that were previously unobtainable when restricted to traditional molecular approaches (Koboldt *et al.* 2013). Sequence data are relatively cheap and rapidly generated. However, with ever-decreasing costs, genetic data sets become bigger and so do the challenges in analysing them. Ironically, some of the genes that have taught us the most about adaptive processes in the last three decades prove to offer some of the biggest challenges. Consider, for example, the adaptive immunity genes of the Major Histocompatibility Complex (MHC), which are among the best-studied systems in evolutionary genetics. The MHC is a notoriously difficult region to assemble and characterize, even when using non-targeted 'shotgun' sequencing approaches aimed at resolving large unknown genomic regions (Warren *et al.* 2012). Approaches that target individual MHC genes in multiple individuals (i.e. in population genetic studies) have been popular, yet bear a unique set of problems that still hinder accurate MHC characterization (see Babik 2010, and below). Moreover, newly emerging targeted NGS analyses raise novel complications that need to be considered when genotyping highly polymorphic multigene families. In this chapter, I will discuss the current advances made in this field, and although I focus on the MHC, the lessons learned from analysing these genes can be extended and applied to other multigene families, including resistance genes (R-genes) and self-incompatibility genes (SI-genes) in plants; the P450 superfamily and ATP-binding cassette transporter superfamily present in all domains of life; homeobox genes in animals, plants and fungi; the immunoglobin superfamily in vertebrates; effector and virulence genes in pathogens; reptile toxin genes; cadherin cell adhesion genes and many more (e.g. see www.genenames.org/genefamilies; www.genomics.msu.edu/cgi-bin/plant_specific/family_search.cgi).

The vertebrate immune genes of the MHC are perhaps the most studied gene family and remain one of the best systems to investigate the effects of evolutionary forces operating at the nucleotide level (Bernatchez & Landry 2003; Piertney & Oliver 2006; Vandiedonck &

Knight 2009). Major Histocompatibility Complex proteins recognize, bind and present the peptides of pathogens to the T cells of the infected host, which initiates the adaptive immune response. The evolution of pathogens is geared towards escaping immune recognition by the MHC, whereas natural selection in host species favours individuals with an effective immune defense that protects against infections. This results in a series of adaptations and counter-adaptations, which drive the co-evolutionary arms race between host and pathogens. This process has become known as the Red Queen hypothesis (van Valen 1973; Ladle 1992) and is it is believed to be responsible for the high levels of allelic variation that are commonly observed at MHC genes (Piertney & Oliver 2006; Spurgin & Richardson 2010; Eizaguirre *et al.* 2012).

However, the particular MHC genes studied by most researchers (i.e. the MHC class I and class II genes) are just a small part of the suite of genomic regions involved in immunological processes. In humans, for example, the MHC (or the human leucocyte antigen (HLA)) spans 4×10^6 nucleotides and comprises over 128 expressed genes (Mehra & Kaur 2003). In most vertebrates, the MHC in its entirety is a tightly linked, gene-dense region consisting of tens to hundreds of immune- and non-immune-related genes (e.g. The MHC sequencing consortium 1999; Xie *et al.* 2003). Because of this genomic complexity and the fact that natural selection on the MHC interacts with other evolutionary forces (i.e. mutation, recombination, genetic drift and gene flow), many evolutionary processes operate within this relatively small genomic region such as epistasis, pleiotropy, linkage disequilibria, Muller's ratchet, trans-species polymorphism, gene duplication, gene conversion, micro-recombination, transposon accumulation and intron-mediated gene expression regulation (van Oosterhout 2009a; van Oosterhout 2009b; Croisetière *et al.* 2010; Spurgin *et al.* 2011; Llaurens *et al.* 2012).

Besides being part of a complex multigene family, most MHC class I and II genes have undergone multiple independent gene duplication events (Dawkins *et al.* 1999; Kulski *et al.* 2002). These duplications affect host adaptation by augmenting the immune defense repertoires within individuals and populations, or increase the dosage of advantageous alleles across loci. Individuals may contain multiple polymorphic loci at particular MHC genes as a

result of gene duplication, and the total number of loci can vary among individuals, populations, and species, resulting in so-called copy number variation (CNV; i.e. individuals may comprise different numbers of alleles due to different degrees of gene duplication; e.g. Traherne 2008; Eimes *et al.* 2011; Llaurens *et al.* 2012; Cheng *et al.* 2012; Winternitz *et al.* 2013; Chapter 3; Lighten *et al.* 2014a). The high nucleotide similarity between the duplicated gene copies may facilitate recombinational processes such as micro-recombination (exchange of DNA sequence fragments between alleles within or between loci), leading to gene conversion and redistribution of nucleotide variation across MHC gene paralogues (Cullen *et al.* 2002; Eimes *et al.* 2011). Such processes have been implicated in the rapid formation of novel MHC alleles (Spurgin *et al.* 2011; Zhao *et al.* 2013), and recombination may be important in promoting CNV across genomic loci (Völker *et al.* 2010; van Oosterhout 2013). At other non-MHC genomic loci, multiple *de novo* CNVs (believed to be functional) have even been identified in progeny that were not present in either parents (Samarakoon *et al.* 2011), and so CNV may act as an important source of genomic variation in driving rapid adaptation to new or changing environments. Moreover, the adaptive significance of CNV has recently been described in another important immune-related multigene family – the human immunoglobin heavy-chain multigene region (IGH), which encodes the highly variable peptides that constitute antibodies, and is essential in adaptive immunity (Watson *et al.* 2013). The critical task of accurate characterization of MHC (and IGH) diversity within populations is made challenging both by the unknown amount of CNV as well as by the exceptionally high level of polymorphism within individual MHC genes (and the complex gene interactions, which produce extreme diversity in IGH peptides; Watson *et al*. 2013). These issues make it difficult to target individual loci and characterize all variation, and generally with MHC, researchers use degenerate PCR primers to conduct multi-locus genotyping (Babik 2010). Once primers have been designed that maximize the potential to amplify alleles across loci (see e.g. Burri *et al.* 2014), researchers have a choice of multiple strategies to identify unique alleles within multi-template PCR products or amplicons. (Hereafter, I define an amplicon as a set of unique sequences that is derived from the same PCR, and the sequences can include allelic copies as well as copies of paralogous genes). The strategies can be grouped in two categories: (i) those that implement NGS; and (ii) those that apply 'traditional' molecular approaches (e.g. PCR, cloning and Sanger sequencing,

single-strand conformation polymorphism, denaturing gradient gel electrophoresis; see Babik 2010 for an in depth review).

Many protocols have been developed to minimize biases associated with multi-locus genotyping. In particular, they have aimed to identify sequence artefacts generated by sources of methodological error, such as polymerase generated random base-mismatch errors, PCR-associated chimeras and cloning-derived mosaic-sequences (e.g. Lenz & Becker 2008; Cummings *et al.* 2009; Babik 2010). To exclude these errors, genotypes have often been based on the validation of alleles through observing each sequence variant in at least two independent PCR products (Babik 2010). This allele validation threshold (AVT) was set low because of the long and expensive laboratory protocols associated with traditional approaches. The relatively low throughput of traditional methods also means that allele dropout (the failure to include a true allele in a genotype) may reduce genotyping accuracy, especially when PCR bias occurs (Sommer *et al.* 2013). For example, disproportionately fewer clones (each specific to a particular allele) will represent alleles that are less preferentially amplified, and so these alleles have less chance of being sequenced when a low number of clones are screened.

In theory, NGS protocols should not be hindered by allele dropout caused by low throughput because an amplicon can be screened hundreds to thousands of times. This eliminates the shortcoming of being restricted to sequencing just a handful of clonally amplified products per amplicon. Nevertheless, the rationale and thinking that has been developed over decades using traditional approaches continues to resonate in processing NGS data. Contrary to traditional methods, deep re-sequencing allows for the sensitive detection of alleles within an individual even if some are less preferentially amplified (Sommer *et al*. 2013). However, along with this increased resolution comes the potential for NGS to introduce new problems that may reduce genotyping accuracy. Higher error rates and increased sequencing depth also increase the likelihood of observing artefacts (Harismendy *et al.* 2009; see next section). This means that their separation from real MHC alleles has become more challenging in NGS data than in previous methods (discussed below). Although this problem was first emphasized alongside the obvious benefits that NGS offers (Babik *et al.* 2009), it did little to tarnish the perception

generated in initial studies that NGS offers a relatively straightforward bioinformatic approach to genotype MHC loci (Wegner 2009; Babik 2010; Galan *et al.* 2010). However, specific problems were not fully recognized in earlier studies, and therefore, a broadly accepted and rigorously tested theoretical or methodological approach for converting raw NGS data to MHC genotypes is yet to emerge.

The downside of depth

The total re-sequencing depth of an amplicon required to confidently characterize the polymorphism at diploid loci (reviewed in Nielsen *et al.* 2011) is easier to empirically evaluate than the depth required in studies of multigene families. A global minimum re-sequencing depth for accurate genotyping cannot be easily implemented because of unknown CNV. This issue is compounded by (i) PCR amplification bias that may result in unequal amplification of alleles (van Oosterhout *et al*. 2006b; Cummings *et al*. 2010; Sommer *et al*. 2013), (ii) repeatable sequence-specific NGS base-mismatch errors (Harismendy *et al.* 2009; Gilles *et al.* 2011; Chapter 3; Lighten *et al.* 2014a) and (iii) sensitive detection of low copy number DNA sequences in amplicons when using NGS (Li & Stoneking 2012). These factors are problematic because low copy number base-mismatch errors (generated during PCR or sequencing) and cross-sample contamination can be common occurrences, and they can be observed at high sequencing depths when using NGS approaches (Li & Stoneking 2012; Sommer *et al*. 2013; Chapter 3; Lighten *et al*. 2014a). Both PCR bias and the presence of artefacts can vary among amplicons (Sommer *et al*. 2013) and increase the likelihood of including artificial variants in genotypes (Type I genotyping error) or excluding real alleles from genotypes (Type II genotyping error). These problems are common to any NGS approach, and therefore, NGS bioinformatics used to genotype MHC loci and other multigene families should apply much more stringent criteria than traditional approaches in the separation of alleles and artefacts. This requires knowledge of the error distributions specific to NGS technologies, and a shift from the genotyping rationale of traditional sequencing.

The evolution of NGS MHC *de novo* genotyping methods

Since the first application of NGS to genotyping MHC loci (Babik *et al*. 2009), the approach has gained popularity because of improved efficiency in sequence data collection. However, the bioinformatic methods employed to transform raw sequence data into genotypes have been quite variable. Here, I summarize the three main concepts used for NGS *de novo* genotyping of MHC loci, which use (i) allele validation thresholds (AVTs); (ii) variant clustering methods; and (iii) CNV methods (or relative sequencing depth modelling). The latter most recent approach uses expectations derived from NGS assumptions and genetic models of CNV to facilitate genotyping.

Allele validation thresholds (AVTs)

A key assumption in NGS studies of the MHC is that true alleles should be observed at greater depths than artefacts (Babik *et al*. 2009). There are, however, also several largely unspoken assumptions, which are likely to be violated in NGS studies. These include the supposition that all sequencing errors are random (which they are not), that the amplification process does not unduly bias the observed sequence depth of certain alleles (which it can), and the belief that minute amounts of contamination will not be picked up as a signal (which most certainly will be the case when using deep sequencing). Before evaluating the consequences of violating these assumptions, I will discuss the rationale of AVT protocols.

The AVT protocol aims to distinguish artefacts from genuine alleles based on a determined level of variant sequencing replication within and/or among independent PCR amplicons. The AVT method usually comprises two separate components (summarized in Figure 2.1): (i) a minimum required sequencing depth of a variant within and/or among amplicons to initially be considered as a putative allele (AVT_1); and (ii) a minimum within-sample sequencing depth that is required to separate alleles from artefacts in variants that pass the first threshold (AVT_2). Babik *et al*. (2009) set AVT_1 as the observation of a variant in at least

two amplicons at a depth of ≥2× in at least one, or 1× depth in at least three amplicons. Ideally, if an AVT_1 is used, it should be based on an understanding of the error distributions observed among the products of the various stages in a genotyping workflow (e.g. PCR, sequence coverage and specific NGS technologies), and it should not be adopted from traditional sequencing approaches. Galan *et al*. (2010) went further to calculate the probability of sufficiently filtering out artificial sequences under different AVT_1 stringencies. They based their calculation on estimating the probability of observing a single *random* base-mismatch sequencing error derived from a true allele within a sample. They calculated that the probability a sequence occurred with at least one sequencing error in the data set was sufficiently low ($P = 0.11$) so that the overall probability of observing exactly the same error in three or more sequences was negligibly small ($P = 10^{-8}$). Thus, an AVT_1 of 3× was implemented and further justified by the use of similar criteria in cloning and Sanger sequencing studies (e.g. Cummings *et al*. 2010). The two examples were then unified by Zagalska-Neubauer *et al.* (2010) who proposed a genotyping AVT_1 of 3× depth in at least two amplicons for variants to be considered as true alleles. This particular AVT_1 has been commonly applied in NGS MHC studies with the occasional minor modification. However, in some cases, arguments for relaxed AVT_1 criteria were made, evidently to maximize data retention (e.g. Nadachowska-Brzyska *et al.* 2012; Sepil *et al.* 2012), but possibly at the cost of reduced statistical rigour and genotyping accuracy. The problem with setting an AVT_1 based on random sequencing errors is that errors may be nonrandom (Gomez-Alvarez *et al.* 2009; Gilles *et al.* 2011), which means that the probability of detecting the same artefact multiple times will be underestimated. Furthermore, the number of artefacts will increase both with sequence depth and the number of samples, and hence, every study will need to calculate their own AVT_1 value based on the observed error distributions.

Commonly, to estimate AVT_2, the percentage of amplicon sequencing depth attributed to each variant that passed AVT_1 is calculated, and then all unique variants observed among amplicons are ranked in order of their maximum per-amplicon frequency (MPAF; Zagalska-Neubauer *et al*. 2010). By comparing the sequence composition of variants with the lowest MPAF (presumed to be artefacts) to those with higher MPAF (presumed to be real alleles), it is

possible to identify low copy number artefacts that originate from real alleles. When two variants always co-occur among amplicons and differ by just a single base, the variant with the lowest depth is assumed to be a base-mismatch error derived from the more highly sequenced variant. A similar argument can be made for chimeric sequences. Artificial chimeras comprise sequence fragments from real alleles and arise through artificial recombination during co-amplification of multi-template amplicons (Lenz & Becker 2008). To identify potential chimeras, both parental alleles should be present in the same sample and the chimeras are expected to occur at a relatively low frequency. By working up from low MPAF variants towards high MPAF variants, a depth percentage cut-off can be estimated above which only real alleles are likely to occur. The validity of this AVT_2 is then tested in the subset of amplicons and accepted if it filters out the majority of artefacts. This AVT_2 is then applied to the remaining amplicons, assuming that it will just as reliably separate alleles and artefacts as in the subsample of assessed amplicons.

Despite the current popularity of AVTs in NGS studies of the MHC, they are subject to certain problems. Essentially, the use of AVTs may not only violate genotyping assumptions (see below and Figure 2.2 and Table 2.1), but they may also be inadequate in removing artefacts, given that most studies ignore the possibility of cross-amplicon contamination (e.g. Babik *et al.* 2009; Galan *et al.* 2010; Zagalska-Neubauer *et al.* 2010; Kloch *et al.* 2010; Sepil *et al.* 2012; Nadachowska-Brzyska *et al.* 2012; Radwan *et al.* 2012; Sommer *et al.* 2013; Pavey *et al.* 2013; Lamaze *et al.* 2014). Specifically, studies that have used AVTs have reported artificial chimeras that had mimicked putative alleles in disparate amplicons (e.g. Zagalska-Neubauer *et al*. 2010; Radwan *et al*. 2012), which in most cases were apparently identified by visual comparison of aligned sequences within a sample. However, from the commonly observed high rate of occurrences of these supposed 'chimeric alleles' among amplicons, it is more likely that they in fact represent contamination from disparate PCR products (Chapter 3; Lighten *et al*. 2014a). The identification of chimeras is a notoriously difficult task, which is reflected in the fact that multiple programs have been designed to assess the likelihoods of chimeric sequences (e.g. Padidam *et al.* 1999; Posada & Crandall 2001; Edgar *et al.* 2011; Martin & Wang 2011).

Identifying artificial chimeras is particularly difficult in MHC studies because MHC alleles frequently undergo natural recombination (Carrington 1999). Moreover, the likelihood of chimeras perfectly mimicking real alleles in disparate amplicons at such high frequencies seems unrealistic.

Previous studies employing AVTs have not considered the possibility of contaminant variants at relatively low depths, which are identical to real alleles in other samples (i.e. not PCR-derived artefacts). Such low-depth sequences that were not observed with putative parental alleles might be erroneously included as genuine alleles in a genotype. Adding further to potential genotyping error, AVTs have sometimes been modified on an apparently arbitrary basis with no justification. For example, Stiebens *et al.* (2013) redefined AVT_2 and accepted sequences only as genuine alleles when they achieved ≥10% of the depth of the most sequenced allele within the sample. However, they did so without describing an empirical evaluation, and by doing so, they risked losing non-preferentially amplified alleles or including repeatable artifacts. Given the significant variation in amplification rate among alleles, and the more recent realization that cross-sample contamination may be common, in retrospect, this modification of AVT_2 without thorough justification seems ill-advised irrespective of their observed high genotype repeatability (as both alleles and artifacts can be repeatable).

Notwithstanding these problems, if AVTs are empirically assessed on a case-by-case basis, then they may allow replicated genotype estimates if cross-sample contamination is low and all remaining errors can be accurately identified. Accordingly, some studies have suggested interesting patterns of MHC diversity in a variety of taxa (e.g. high number of genes per individual, Zagalska-Neubauer *et al*. 2010; hybridization increasing diversity, Nadachowska-Brzyska *et al*. 2012) and have demonstrated genotyping repeatability between samples when using AVTs. As such, they have formed the basis for further development of genotyping methods and represented an important step in the progression of NGS MHC genotyping (e.g. Stiebens *et al*. 2013). However, deep sequencing exacerbates the problems that AVTs face with contamination (Figure 2.2). With decreasing NGS costs and the advent of ultra-deep sequencing, further developments in AVTs methods are required if they are to remain a reliable

genotyping approach as currently they hold no significant advantage over other available methods (See below and Table 2.2).

Variant clustering

More recently, variant clustering approaches to MHC genotyping have been designed that aim to separate artefacts from alleles based on the sequence similarity among variants within each amplicon (Sommer *et al*. 2013; Pavey *et al*. 2013; Lamaze *et al*. 2014; summarized in Figure 2.1 and Table 2.2). Evaluating sequence variants on a per-amplicon basis is an improvement over applying a rigid AVT across all amplicons because AVTs are usually based on sequence observations on a sub-sample of amplicons taken from the entire data set. Therefore, the aim of clustering approaches has been to increase genotyping accuracy by accounting for variation in error frequencies and PCR bias among amplicons and sequencing runs. However, the attempt to eradicate artefacts by collapsing all closely related (highly similar) sequences to a single representative during clustering is controversial and may oversimplify patterns of diversity. Knowledge of the actual allelic diversity is important because this can inform us about the amount of balancing selection that is acting on the MHC (see e.g. van Oosterhout *et al*. 2006b).

Pavey *et al*. (2013) and Lamaze *et al*. (2014) used a complex iterative procedure in three successive steps, which can help overcome over-reducing diversity estimates using sequence clustering: (i) the first step generates clusters of putative allele sequences within each individual. These clusters each describe a unique variant and the depth at which it has been sequenced. Thresholds are set to discard clusters that fail to meet criteria of sequence similarity and total sequencing depth within each amplicon. These criteria are based on the common premise that artefacts should be observed at lower depths and are similar in sequence to highly sequenced alleles. The sequences are then aligned with Sanger sequences for quality control (e.g. for indel detection); (ii) The second step builds clusters of putative global alleles from all individuals, and a threshold, based on the targeted length of amplicons, is used to distinguish alleles that differ by a single nucleotide; (iii) In the third step, the global consensus alleles for all populations constitute a BLAST database against which the original sequences within each

individual are compared. If a true allele is erroneously discarded from an amplicon during the second step because it is very closely related to a more highly sequenced true allele, this third step should reassign the allele back to that amplicon when its sequences are compared with the BLAST database, assuming that it was correctly identified in other amplicons. Although this step aims to reduce Type II genotyping error, careful consideration must be taken as it also increases the potential to inflate Type I genotyping error if contamination is present. Then, for each global consensus allele, BLAST e-value scores are plotted as a function of the number of reads. A minimal threshold of number of sequences to accurately genotype each individual is established based on a natural break in this relationship (as in Babik *et al*. 2009).

Sommer *et al*. (2013) followed with a similar approach that used an iterative clustering approach of variants within each amplicon individually. They separated alleles and artefacts based on (i) the relative frequencies of variants; (ii) variant replication among amplicons; and (iii) nucleotide similarity among variants. Sequence variants within an amplicon are first clustered based on sequence similarity and ranked by their percentage of amplicon sequencing depth, removing singleton variants represented by just one sequence (i.e. 1× depth – assumed to represent artefacts). Starting from the second highest ranked cluster (a cluster is from here on defined as a unique variant with a particular sequencing depth) and moving down the list, they are compared in sequence composition to more frequent ones. Chimeras are computationally identified based on the probability that they comprise sequence fragments from two different more frequent variants. The remaining variants are classified as either '1–2 base pair (bp) difference' or '>2-bp difference' from its most similar higher frequency variant. The next stage aims to identify putative artefacts by comparing variant composition among replicated amplicons and/or disparate amplicons. When a variant labelled as 1- to 2-bp difference or a chimera is not present in both replicates amplicons of the same sample, it is classified as a putative artefact. However, variants classified as >2-bp differences are identified as putative artefacts only if they are not replicated in any sample amplicon across the entire data set. This stage is reliant on the assumption that even if allele dropout occurs between sample replicates, then that allele will still be identified in disparate samples. However, this

may fail to identify real rare alleles (present in just one individual), especially if they are less efficiently amplified. An additional assumption is that base-mismatch errors are not repeatable among amplicons and thus they are identified primarily by their absence in the replicate amplicon. The final stage then defines putative alleles based on intra-amplicon comparisons of relative depths among putative artefacts and the remaining sequences, where alleles must be seen in both replicate amplicons at greater depth than all putative artefacts (see Sommer *et al*. 2013 for full details).

Interestingly, this approach also introduced measures to estimate the degree to which the amplification of each allele was affected by PCR bias and showed that allele dropout may occur if PCR bias is not accounted for. However, this approach to detect PCR bias (and estimate genotypes) currently requires replicate sequencing of every sample and so reduces the total number of unique samples that can be employed in a single sequencing run. Notwithstanding a reduction in the total number of unique samples that can be included in a sequencing run, currently, the repeated sequencing of a sample is the best way to validate genotypes, but is not enough to call alleles given that artefacts are repeatable among amplicons. Also, their results suggest a benefit of increasing amplicon sequencing depth to hundreds or thousands of sequences, which may increase genotyping accuracy by reducing the impact of PCR bias.

Clustering sequence variants within samples has been shown to be an effective means to filter out erroneous variants and is a popular approach to process NGS data (e.g. in RAD-seq analysis, Catchen *et al.* 2013). However, because of the uncertainties surrounding the observations of alleles and artefacts among MHC amplicons (i.e. CNV, PCR bias, error variance), there are no *a priori* (and objective) parameter settings that can be used to designate clusters and separate alleles from artefacts. Previous methods that intended to do so (e.g. Galan *et al*. 2010; Pavey *et al*. 2013) should be applied with caution because even small changes in the arbitrary parameter settings can significantly alter the resulting allele frequencies (Oomen *et al.* 2013). This is particularly the case in the presence of PCR bias and contamination. The arbitrary distance thresholds used in clustering approaches are similar to the AVT method and lack the

statistical rigour to theoretically validate separation of alleles and artefacts. Such statistical approaches are important and carried out in NGS analyses in other areas of research (e.g. RAD-seq; Catchen *et al*. 2013; Gagnaire *et al.* 2013).

Genotype modelling based on theoretical expectations

Recently, Lighten *et al*. (2014a) (See Chapter 3) aimed to separate alleles from artefacts based on per-amplicon comparisons of relative sequencing depths in a data set derived from ultra-deep sequencing, using two independent yet complementary workflows (see below, Figure 2.1 and Table 2.2). This approach takes advantage of the semi-quantitative nature of NGS and assumes that the number of times a target region has been sequenced is approximately proportional to its copy number in the genome (and so alleles should be sequenced at significantly greater depths than low copy number artefacts within each amplicon). The assumption is that PCR bias is nonexistent or negligible so that relative sequencing depths of multi-allele MHC amplicons can be fitted to expectations derived from theoretical models of CNV (i.e. the allele counts expected in multi-locus genotypes). While the CNV modelling approach of Lighten *et al*. (2014a) (Chapter 3) may be valuable in study systems that have well-optimized primers and few duplicated loci, the impact of higher numbers of loci (e.g. >10) and PCR-biased allele amplification across these loci may be too great to accurately decipher complex patterns of allele and loci CNV. Moreover, the CNV modelling approach was not tested in a system with more than five MHC IIb loci, and the effects of PCR bias were not assessed. Furthermore, the predicted and repeatable CNV patterns reported in the guppy remain to be independently validated by alterative molecular methods (e.g. direct sequencing of entire MHC region), and it would be valuable to apply the CNV modelling approach to an alternative well-characterized genetic system and to fully test the effects of PCR bias on the accuracy of this approach.

In taxa that are believed to harbour tens of MHC loci (e.g. passerine birds, Sepil *et al.* 2012), the most realistic and accurate genotype modelling approach may need to be adapted so to focus on identifying solely the total number of alleles (A_i) if accurate and repeatable CNV patterns cannot be verified. Lighten *et al*. (2014a) (Chapter 3) additionally implemented such an

approach, which appears to provide robust complementary estimates of A_i to those estimated from CNV modelling. Variant depths were also evaluated (independent of CNV model expectations) with respect to identified statistical breakpoints between alleles and artefacts. The rationale is that alleles should occur with higher depth than artefacts so that within each sample, there should be a noticeable drop in the number of reads between the least-amplified allele and the most common artefact. This drop is identified by a statistically significant degree of change (*DOC*) in the sequencing depth attained for alleles and artefacts (see Chapter 3; Lighten *et al*. 2014a). This approach avoids the use of any *a priori* AVTs or parameter settings to separate alleles from artefacts. This has the important advantage that genotyping becomes directly comparable among studies, even if sequencing error distributions differ. Moreover, the requirement of a statistical breakpoint between alleles and artefacts introduced an amplicon quality control measure for reliable genotyping (Figure 2.2). Those amplicon data that could be justified as being of poor quality were identified and removed from downstream analysis to avoid biases in estimates of genetic diversity. Even though this method reliably separates alleles from artefacts, a potential disadvantage of this approach is that severe PCR amplification bias could distort estimates of CNV patterns and hinder the separation of alleles and artefacts (but shouldn't affect *DOC* genotyping, see Chapter 3; Lighten *et al.* 2014a). Indeed, although the multi-locus genotypes were highly repeatable within the same sequencing run (100%), the repeatability (the degree of concordance between the alleles observed in both replicates) was less impressive among fully independent sequencing run data sets (83.7%; but see Chapter 5 where repeatability improves to 99.83%). Yet, this reduction is believed to be a consequence of random effects rather than PCR bias, as the additional alleles found in the second sequencing run were initially observed in the first data set, just at a sequencing depth which erroneously classified them as errors. The method of Lighten *et al*. (2014a) (Chapter 3) also identified and resolved problems associated with cross-amplicon contamination, which is an undesirable yet inevitable feature of PCR-based ultra-deep sequencing methods.

A similar approach has been implemented using deep sequencing ratios to estimate CNV by Hayes *et al.* (2013) who compared CNV estimates with sequencing depths of loci, using both a PCR- and a non-PCR-based (sequence capture-array) approach. By including the method applied in Sommer *et al*. (2013) to identify any PCR bias, the Lighten *et al*. (2014a) approach would be further strengthened. Including population genetics theory and analysing the Mendelian segregation of alleles in multi-locus genotypes could make a possible further advance. This relies, however, on Hardy–Weinberg equilibria, an assumption that is likely to be violated in genes such as the MHC, which are under selection. Also, the use of pedigree or relatedness data could be a fruitful avenue to improve the scoring of multi-locus genotypes by NGS (e.g. Huchard *et al.* 2012).

A point worth emphasizing is the added benefit of estimating genotypes using two independent yet complementary approaches. Using the CNV modelling approach, Lighten *et al*. (2014a) (Chapter 3) allowed for the possibility of up to five MHC IIb loci (10 alleles) based on empirical evidence to suggest that guppies had up to three loci (six alleles). Testing the fit of the data to a higher number of loci than expected does not affect the outcome of the best-fitting model, and although the number of models does not constitute a genotyping threshold, underestimating the number of loci will affect genotyping. In most cases, researchers should have a general idea of the number of alleles present in their study species, as prior optimization of PCR primers (whether it be though cloning and Sanger sequencing or NGS) is always recommended. However, even if these data are lacking, the *DOC* criterion implemented in Chapter 3 (Lighten *et al*. 2014a) is independent of CNV mathematical assumptions, and if the number of modelled loci is underestimated in the CNV workflow, then the inflection point that illustrates the significant increase in the *DOC* would fall above the number of alleles that can be expected based on the modelled number of loci. This allows the user to adjust the number of CNV models implemented in their analysis.

Finally, a common source of error that is largely overlooked in multiplexed amplicon studies, but especially important to recognize in multigene family studies, is that of artificial amplicon barcode (used to identify specific samples) switching during laboratory procedures. This can lead to the formation of novel dual-barcode combinations, which were not employed in the study design, and potentially could lead to a source of 'contamination' among amplicons, where variants from one amplicon become associated with those from a disparate amplicon. However, such variants should be relatively rare across entire data set, as the source of the error is believed to occur when independent PCR samples are pooled together (even without further PCR cycles) for NGS library construction when PCR products have not been thoroughly cleaned to remove primers and primer dimers (Carlsen *et al.* 2012). These artefacts are easily distinguished from real alleles when using the *DOC* criterion (given good quality data; Chapter 3; Lighten *et al*. 2014a) especially in those generated by the Illumina TruSeq protocol, as all samples undergo just one independent PCR each. However, caution should be taken when using protocols that perform additional PCR cycles on pooled multi-template amplicon libraries (each of which has already undergone an initial PCR) as this could inflate the relative frequency of all types of artefacts, potentially impeding genotyping.

The importance of upholding genotyping assumptions

Next-generation sequencing methods to genotype multigene families by PCR make the following two assumptions: (i) different alleles should amplify approximately equally well; and (ii) alleles should be amplified at much greater sequencing depths than low copy number artefacts (e.g. Babik *et al*. 2009; Galan *et al*. 2010; Zagalska-Neubauer *et al*. 2010). Assumption 1 can be validated by the design and testing of degenerate and/or locus-specific primers that amplify all allelic variants equally efficiently (a nontrivial task; Burri *et al*. 2014). Also increasing total amplicon depths can help minimize the effect of PCR bias (Sommer *et al*. 2013), but in some cases, allele dropout may be hard to eradicate. If the primers simply do not anneal efficiently to the priming sites, no sequence depth will help to uncover these alleles. Indeed, it is very likely that MHC studies underestimate the true allelic richness because primers are

designed based on the already known sequence information. Given that the MHC is highly polymorphic, it is likely that some allelic variations will not be amplified and remain unknown. Similarly, the use of additional sequence data can decipher unknown allelic CNV in conserved exons (i.e. the same allele may be duplicated among different loci, and these multiple copies will remain cryptic if the exon sequences are identical at each loci). Llaurens *et al*. (2012) illustrated this point in the MHC by redesigning PCR primers in the conserved neighbouring exon (exon 3), which were used to sequence through the adjacent intron 2. Remarkably, this uncovered 40.9% more MHC alleles that would have been missed if they had amplified the polymorphic exon 2 of the MHC class IIB alone, meaning that some MHC class IIB alleles were observed in multiple copies and were only distinguishable by their associated unique intron variation. Given that MHC class II studies tend to focus just on exon 2, it is not unlikely that most MHC studies have significantly underestimated the 'true' allelic variation.

Despite the possibility that some PCR bias may be unavoidable, assumption 2 should always be enforced; that is, there should always be a noticeable (and statistically significant) difference between relative depths of real alleles and artefacts. This allows for the confident separation of alleles from artefacts, and it is fully achievable using NGS (Chapter 3; Lighten *et al*. 2014a). Obviously, if significant PCR bias does exist, some alleles may not be observed along with highly sequenced alleles. For this reason, primer design and the evaluation of the amplification efficiency of primers by testing different primer combinations on a subset of individuals is of paramount importance.

Moving forward: Elucidating gene family CNV and the use of single molecule sequencing

The number of duplicated loci in multigene families is usually inferred indirectly through estimates of the total number of distinct alleles (A_i) in a genotype. (Note, however, that this usually refers to the number of putative allelic sequences rather than the actual number of 'true' allele copies). A_i can vary greatly among species (e.g. Winternitz *et al*. 2013), and even within species (Piertney & Oliver 2006; Chapter 3; Lighten *et al*. 2014a). Traditionally, variation in A_i has been attributed to CNV in the number of MHC loci between individuals (i.e. the number of gene paralogous), or alternatively, due to the same allele being present at multiple loci (which might be the consequence of gene conversion). However, identifying the actual cause of CNV is difficult. For example, if sequencing depth of an amplicon indicates that an allele is present in two copies, it could suggest there are two alleles at a homozygous locus, but equally, there could be two copies at two heterozygous (or hemizygous) loci. Pedigree studies could shed further light on the genetic architecture by assessing the inheritance of alleles. To my knowledge, few attempts have been made to quantify the frequency of either duplicated alleles or loci at a population level, probably because estimating loci and allelic CNV using traditional PCR-based methods is difficult. An alternative to pedigree-based approaches to verify the structural arrangements of multigene families and the cause of CNV is to analyse bacterial artificial chromosome (BAC) libraries. This approach can produce large DNA constructs from cloned gene fragments spanning entire genomic regions. Although the laborious nature of this technique means that it is not feasibly applied across many individuals, it can be used to initially characterize CNV (assuming this variation resides on the same chromosomal region) and then to develop CNV-specific PCR primers for population studies. Such an approach has been applied to characterizing CNV at the human immunoglobin heavy-chain multigene region (IGH; Watson *et al*. 2013) and MHC in the disease-threatened Tasmanian Devil (Siddle *et al.* 2010; Cheng *et al.* 2012).

Deep sequencing through NGS also offers a potential solution to estimate CNV (Campbell *et al.* 2008; Chiang *et al.* 2009; Xie & Tammi 2009; Yoon *et al.* 2009; Oomen *et al.* 2013; Hayes *et al.* 2013) which may be more feasible on the population level. By comparing the

relative proportions of allelic sequences, it is possible to estimate the CNV at particular loci. CNV estimates are commonly inferred from data collected by sequence capture or exome sequencing approaches. Micro-arrays or targeted gene probes can be implemented to isolate specific genomic regions of interest, which can then be sequenced. For applications in multigene families, this approach is beneficial as it avoids potential PCR bias in designed primers (utilizing ligation-mediated PCR) and can produce long-range haplotype data (Cao *et al.* 2013). The main drawbacks are that sequence capture approaches require significant *a priori* genomic data for probe design and are relatively expensive compared with strictly PCR-based approaches. Nonetheless, the information gained from extended haplotypes of multigene families can be invaluable in elucidating the pattern and processes implicit in their important biological functions (Pröll *et al.* 2011).

Inferring CNV through relative ratios of sequence product observed among variants lacks the definitive validation of directly sequencing the primary genomic architecture of the region suspected to contain copy number variants. Indeed, the ability to actually sequence and genotype entire multigene family complexes efficiently on the population level rather than count allele products at particular loci (by PCR or sequence capture) would be a major step-change in the population genetic analysis of these genes. For example, significant fitness effects of MHC genes are not just due to the additive effects of alleles, but also the combination of alleles both within and between loci (i.e. overdominance and epistasis) plays a major role in the evolutionary genetics of these genes (Gregersen *et al.* 2006; Oliver *et al.* 2009; Lippert *et al.* 2013). The development of methods that allow for multi-locus genotyping will significantly advance our understanding of the evolution of multigene family function, and in the case of the MHC, it will open up new avenues in the study of local adaptation and susceptibility to disease in natural populations (Siddle *et al*. 2010; Cheng *et al*. 2012).

Prospective 'third-generation sequencing' technologies offer promise in overcoming the hurdles in CNV characterization still present even with NGS (or 'second-generation sequencing', Table 2.3), those mainly being the fact that in most cases, CNV is inferred from relative abundance of sequence products and not direct characterization of the entire genomic region.

In particular, single molecule sequencing that relies on nanopore technology holds great potential. Theoretically, this approach is not limited by sequencing read length, complex library preparations and relative sequencing depths as with current NGS platforms, but instead can, in theory, continuously sequence entire DNA fragments. These long reads may provide direct characterization of entire genomic regions, which may be especially valuable in deciphering CNV. Moreover, nanopore technology circumvents the requirement for PCR amplification, which can further reduce the issues in describing highly polymorphic multigene families. Because, for example, MHC and IGH regions have high gene densities (Vandiedonck & Knight 2009; Watson *et al.* 2013), it may be possible to characterize entire gene family regions as one sequenced fragment, providing the opportunity for a much fuller understanding of the complex interactions and evolution among all loci. At the moment, this approach would require the sequence of entire genomes or individual chromosomes to locate the gene family regions if no prior genomic targeting was undertaken. Alternatively, sequence capture approaches could be used to initially target the region of interest (albeit in numerous fragments) prior to single molecule sequencing. For example, sequence capture probes have recently been used to isolate most of the MHC region in humans (HLA; e.g. Cao *et al.* 2013), and by avoiding the need for short-read deep re-sequencing, as with current NGS technologies, single molecular sequencing could dramatically reduce the cost and effort required to genotype entire HLA regions in many individuals. This approach would allow comparatively simpler bioinformatic approaches than to those currently being used in *de novo* multi-locus genotyping, and while it could be used for more efficiently design of PCR primers (being more cost-effective and time effective than BAC libraries), more importantly it would allow the sequencing of entire multigene family regions across a multiplex of samples in a single sequencing run. However, future developments will need to be made to reduce the moderate to high sequencing error rates of single molecule sequencing technologies (Thompson & Milos 2011) and to more efficiently target whole regions containing localized gene duplications.

Conclusion

A gold standard multigene family genotyping protocol based on NGS is yet to be validated and accepted, but the development of bioinformatic approaches to separate methodological artefacts and real alleles within amplicons continue to develop. Although approaches that have used global, and sometimes arbitrary, *a priori* designated AVTs and sequence distance thresholds have been popular, they leave genotype estimates particularly sensitive to biases. Multiple current approaches rely on rationales adopted from traditional studies, despite stark contrasts in characteristics between traditional MHC data and those acquired using NGS. However, by incorporating theoretical expectations about sequencing depth, the genotyping of multigene families can be significantly improved, and complex artefacts can be easily identified and avoided. The future of genotyping of multigene families lies in the increase of amplicon sequencing depth alongside with model-based approaches. This is an extension of the rationale adopted in diploid SNP calling algorithms (reviewed in Nielsen *et al*. 2011). Modelling approaches along with third-generation sequencing technologies may improve our ability to characterize both variation in the number of duplicated loci and the degree to which alleles are duplicated across loci. In doing so, many more widely used population genetics approaches that rely on understanding affiliations among alleles and loci will become available to study multigene families.

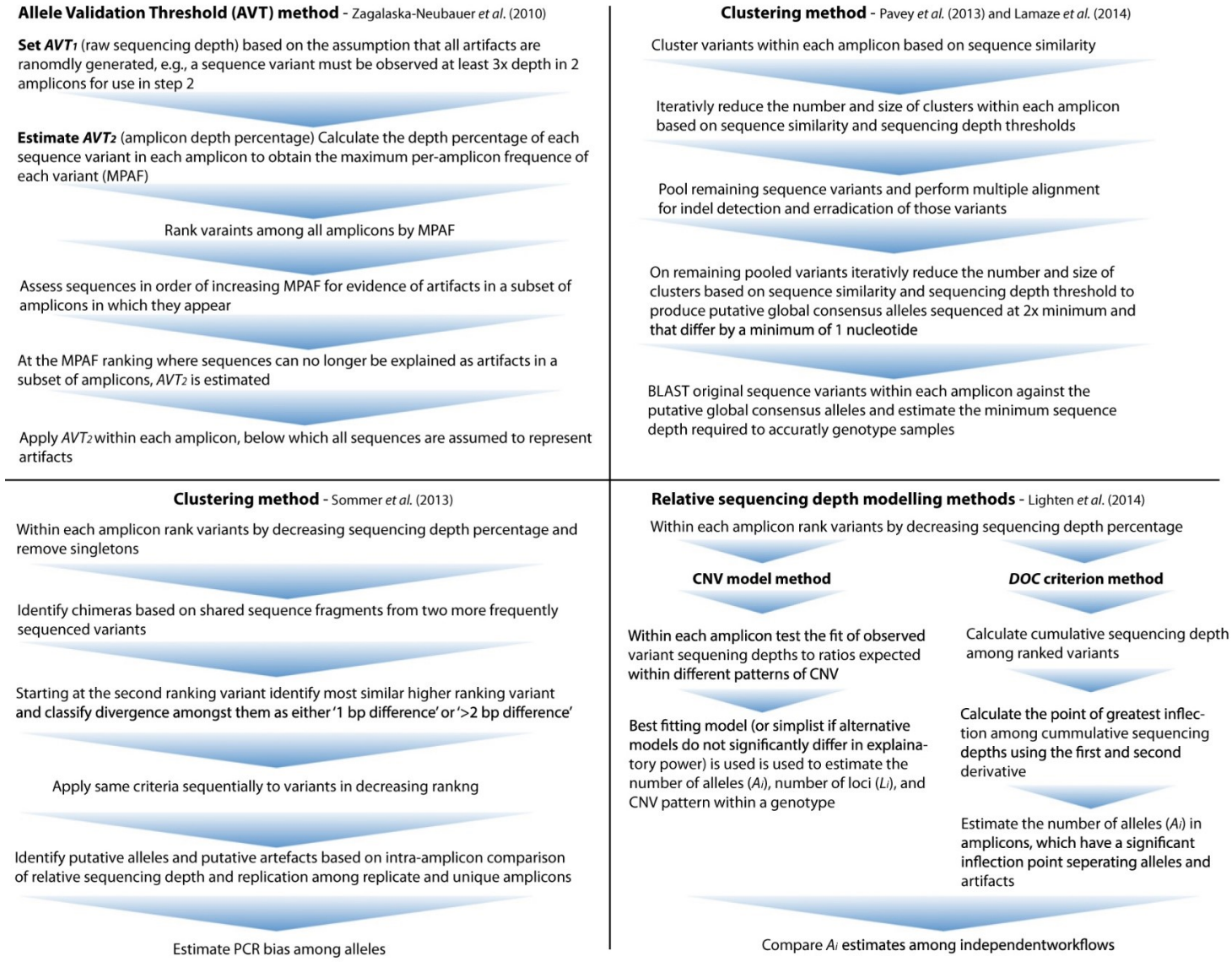

Figure 2.1. The basic stages of analysis used in the current main approaches for *de novo* genotyping of multigene family amplicons.

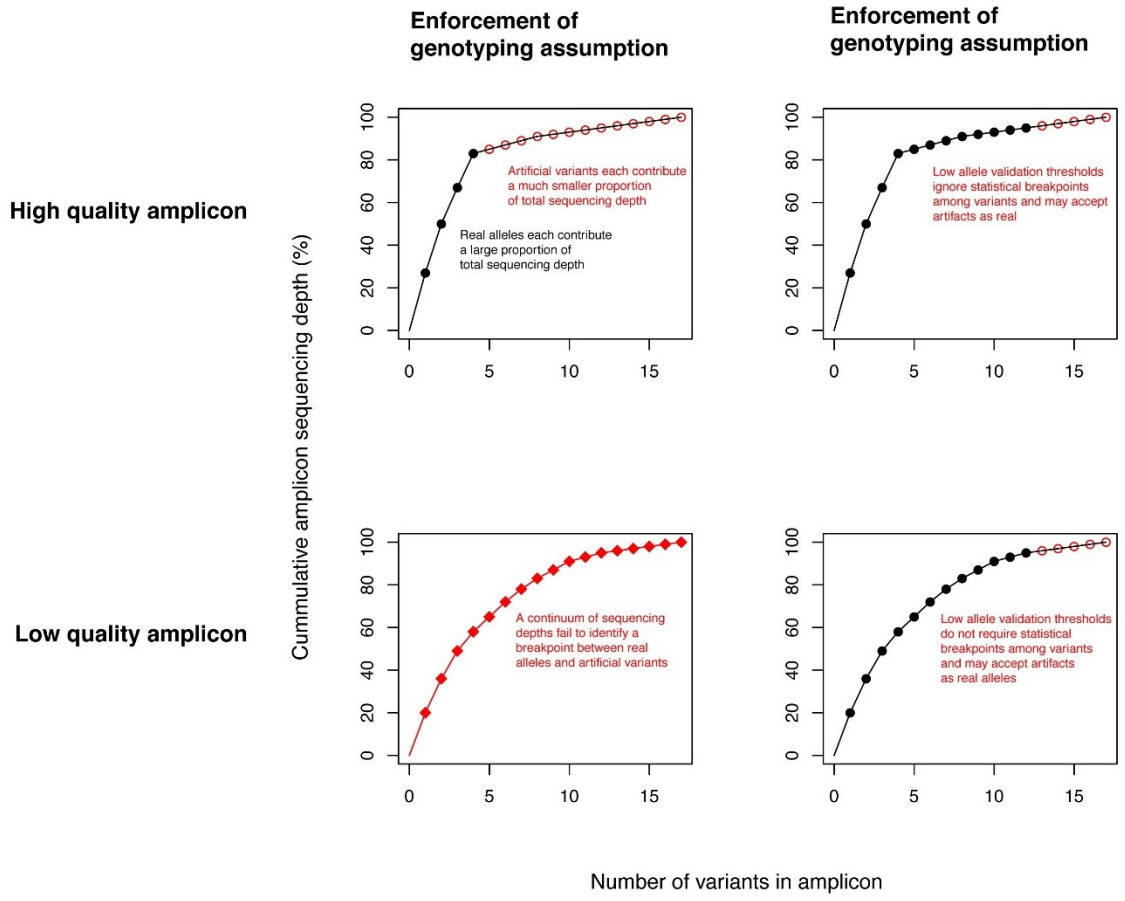

Figure 2.2. Theoretical evaluation of separation of real alleles and artefacts in amplicons through enforcing genotyping criteria. When variants are ranked by descending sequencing depth, high-quality amplicons are characterized by an inflection point in the cumulative depth across variants. This inflection point illustrates a significant increase in the degree of change (*DOC* criterion, Chapter3; Lighten *et al*. 2014a) between the sequencing depths attained for the variants on either side. Based on the assumption that real alleles should contribute a relatively higher amplicon depth percentage than artefacts, variants after the inflection point (which each contribute relatively little to the total amplicon depth) are classified as artefacts if genotyping assumptions are strictly enforced (after visual validation; see Chapter 3; Lighten *et al*. 2014a). If the assumption that alleles should always be observed at higher depths than alleles is ignored, and a strict allele validation threshold (AVT) is enforced, then artefacts can erroneously be included in genotypes, despite the potential for high-quality genotyping. Conversely, poor-quality amplicons, which contain either high levels of contamination and/or poor-quality product, do not demonstrate a significant inflection point. When the cumulative depth among variants is curved, it is difficult to theoretically validate the separation of alleles and artefacts if commonly observed contamination is present, and by enforcing genotyping assumptions, these amplicons should be removed from further analysis. Again, if genotyping assumptions are ignored and AVTs are used, poor-quality amplicons are not identified and can bias downstream analyses with the inclusion of poor-quality data.

Assumption	Expectation	Justifies	Applied in practice by AVTs	Genotyping assumption upheld?
Equal amplification of alleles	Approximately equal ratios of sequencing depth per allele copy in an amplicon.	Prediction of minimum total amplicon sequencing depth for accurate genotyping widely adopted from Galan *et al*. 2010.	Different alleles are accepted at any depth from just a few sequences (or low amplicon depth percentage) to thousands (or high amplicon depth percentage) within the same amplicon. The same allele may be accepted at a depth of just a few sequences (or low amplicon depth percentage) to thousands (or high amplicon depth percentage) within different amplicons.	No. Drastically un-uniform depth representations of the same or different alleles within and among amplicons observed using AVT directly violate assumption of equal amplification of alleles.
Alleles are sequenced at much greater depths than artefacts	A statistical breakpoint between highly sequenced alleles and low copy number artefacts.	NA	Within an amplicon alleles and artefacts may be differentiated by a 1× or 0.01% sequencing depth margin.	No. AVTs stipulate a threshold that apparently separates alleles and artefacts; therefore, there is essentially no buffer zone to confirm that alleles are sequenced at much greater depths than artefacts. This provides scope for considerably inaccurate classification of variants.
NGS base-mismatch errors are randomly distributed along a sequence	There is negligible probability that multiple sequences contain the same sequencing error.	Consideration of putative alleles with very low sequencing depths within an amplicon, that is, more than a random error is expected to achieve.	AVT_1 of 3× in two amplicons	No. Although random error may occur in NGS, there is also a high rate of repeatable base position-specific sequencing error. Therefore, repeatable errors can achieve high sequencing depths.

Table 2.1. Common assumptions in protocols for genotyping multigene families using NGS, and how those that use AVTs treat those assumptions.

Method	Greatest relative advantage	Greatest relative disadvantage	Complexity	Available pipeline?	Use of a priori thresholds?	Requires a priori estimate of A_i?	Strictly adheres to genotyping assumptions?	Number of independent workflows to estimate genotype
Allele validation threshold (AVT)	None	Can greatly increase genotyping error.	Low	No	Yes	Yes	No	1
Clustering – Pavey *et al*. 2013 and Lamaze *et al*. 2014	Can reduce the exclusion of real alleles from genotypes using a BLAST database of putative global consensus alleles.	The same BLAST approach may increase the inclusion of contaminant variants in genotypes.	High	Yes	Yes	No	No	1
Clustering – Sommer *et al*. 2013;	Can estimate PCR bias.	Requires duplicate sequencing of every sample	High	Yes	Yes	No	No	1
Relative depth modelling – Lighten *et al*. 2014	Can estimate CNV. Identifies poor-quality amplicons and contaminants.	CNV estimate accuracy may be effected by PCR bias. Manual assessment is required to confirm 'poor-quality' amplicons in fact do not contain many alleles at low depths.	Medium	Yes	No	No	Yes	2

Table 2.2. Comparisons among aspects of the main approaches used for *de novo* genotyping of multigene family loci using NGS.

Current problem	Impact	Approach to remedy	Data/analytical improvement
PCR primer amplification bias	Unequal amplification of alleles may render real alleles and artefacts difficult to differentiate based on sequencing depth.	Rigorous PCR primer design and optimization using cDNA. Third-generation sequencing can provide better baseline data to design primers (i.e. entire genomic regions), but also provide approaches to avoid PCR-based sequencing altogether.	Will enable full haplotype characterization of multigene families across loci, including CNV characterization.
Sample/PCR cross-contamination	Increase the likelihood of including artificial variants in genotypes (type I genotyping error) or excluding real alleles from genotypes (type II genotyping error).	Individually preserve samples (i.e. no batch preservation in same vial). Pre- and post-PCR laboratory conditions (as used in ancient DNA studies).	Will reduce the need for complex quality filtering of data for accurate genotype estimation. Will decrease genotyping error rates.
Difficult to estimate CNV of alleles and genes	Underestimation of allele frequencies. Restricts study of an important evolutionary aspect of genomic variation.	PCR-based deep re-sequencing of loci and identification of repeatable differential ratios of allele sequencing depth can infer CNV. Cost-effective and multiplexed third-generation sequencing may allow resolution of multigene family genomic architecture and CNV.	Accurate estimates of allele frequencies and population genetics. Reduced complexity of bioinformatics and identification of affiliations between alleles and loci.
Bias of focus on a small number of individual genes/gene families	Lack of understanding of processes governing evolution of entire gene families.	Sequence entire gene family regions. Third-generation sequencing can overcome lack of *a priori* knowledge required to target understudied gene families.	Will allow comparative studies among gene families and ultimately deepen our understanding of the evolution of important genomic regions.

Table 2.3. Central problems associated with PCR-based analysis of multigene families that need to be improve.

Chapter 3

Ultra-deep Illumina sequencing accurately identifies MHC class IIb alleles and provides evidence for copy number variation in the guppy (*Poecilia reticulata*)

Abstract

Here I address the bioinformatic issue of accurately separating amplified genes of the Major Histocompatibility Complex (MHC) from artefacts generated during Next Generation sequencing workflows. I fit observed ultra-deep sequencing depths (hundreds to thousands of sequences per amplicon) of allelic variants to expectations from genetic models of copy number variation (CNV). I provide a simple, accurate and repeatable method for genotyping multigene families, evaluating the method via analyses of 209 b of MHC class IIb exon 2 in guppies (*Poecilia reticulata*). Genotype repeatability for re-sequenced individuals (*N* = 49) was high (100%) within the same sequencing run. However, repeatability dropped to 83.7% between independent runs, either because of lower mean amplicon sequencing depth in the initial run or random PCR effects. This highlights the importance of fully independent replicates. Significant improvements in genotyping accuracy were made by greatly reducing Type I genotyping error (i.e. accepting an artefact as a true allele), which may occur when using low-depth allele validation thresholds (AVT) used by previous methods. Only a small amount (4.9%) of Type II error (i.e. rejecting a genuine allele as an artefact) was detected through fully independent sequencing runs. I observed 1–6 alleles per individual, and evidence of sharing of alleles across loci. Variation in the total number of MHC class IIb loci among individuals, both among and within populations was also observed, and some genotypes appeared to be partially hemizygous; total allelic dosage added up to an odd number of allelic copies. Collectively, observations provide evidence of MHC CNV and its complex basis in natural populations.

Introduction

The genes of the Major Histocompatibility Complex (MHC) have important links to factors influencing individual fitness (Piertney & Oliver 2006). Not only is this region high in gene density, but it also harbours exceptional levels of non-neutral genetic variation that are directly linked to disease resistance, mate choice and sexual attractiveness (Edwards & Hedrick 1998; Trowsdale 2011). Population genetic theory shows that due to its high levels of polymorphism and epistatic gene–gene interactions, the MHC is prone to accumulate recessive deleterious mutations and transposable elements (van Oosterhout 2009a; b), which could explain why this region is associated with many heritable disorders (e.g. Shiina *et al.* 2006). Not surprisingly, MHC genes have been important targets in the study of the genetic basis of immunology, courtship and mating behaviour, and ecology (Bernatchez & Landry 2003; Piertney & Oliver 2006) and have also provided important insights into the interactions among evolutionary forces (van Oosterhout 2009b). Yet, despite several decades of wide scientific interest, progress in evolutionary and population genetic research on the MHC has been hindered by the difficulty of accurately genotyping this highly polymorphic multigene family.

Traditionally, studies examining intraspecific MHC variation identified alleles based on cloned PCR products and Sanger sequencing (see Bernatchez & Landry 2003). This approach is time-consuming and relatively expensive compared to more recent Next Generation sequencing (NGS) approaches (Babik 2010), and these factors impose important constraints on the number of replicates (clones) sequenced per individual and the total number of individuals genotyped. Consequently, traditional methods may underestimate the level of MHC polymorphism at the individual, population or species level.

The advent of NGS can significantly improve the quality of MHC data and analyses. Recently, 454 sequencing has been used to study MHC genes (e.g. Babik *et al*. 2009; Zagalska-Neubauer *et al*. 2010); however, the separation of artefacts (generated during PCR and NGS) from true alleles remains challenging. Previous studies have aimed to separate the two using AVTs (e.g. Galan *et al*. 2010; Zagalska-Neubauer *et al*. 2010). A global depth threshold is

estimated by classifying the read depth of a subset of variants; with read depths below this threshold assumed to represent artefacts (see Zagalska-Neubauer *et al*. 2010).

Unfortunately, there often is a 'grey area' in which the depth distinction between putative alleles (PA; unconfirmed by RNA expression analysis) and artefacts is blurred (e.g. Zagalska-Neubauer *et al*. 2010). The use of strict acceptance thresholds (e.g. 3× depth in two or more individuals, Zagalska-Neubauer *et al*. 2010) can become problematic, especially when many samples are being analysed and among which the error rates and sequence depths can vary. The use of set thresholds may also be problematic because of reoccurring sequence-specific errors associated with NGS (Gomez-Alvarez *et al*. 2009; Gilles *et al*. 2011), as well as low copy number contaminants associated with large multiplexed data sets (Li & Stoneking 2012). Base-mismatch errors and chimeric sequences generated during PCR and sequencing, and low-level contaminants, may reach sequencing depths above the set threshold, especially in deep-sequencing studies. These problems have been acknowledged (excluding contaminants), and it has been recommended that genotyping protocols be adjusted on a case-by-case basis (Oomen *et al*. 2013). A recent example suggests that both the inclusion of low copy number artefacts and exclusion of less preferentially amplified alleles may be minimized when estimating MHC genotypes using higher sequencing depths (Sommer *et al*. 2013).

Here, I build on previous approaches with the application of Illumina sequencing in MHC population analysis and demonstrate a highly repeatable and accurate methodology for *de novo* genotyping co-amplified multi-template amplicons. In doing so, I show that ultra-deep NGS (hundreds to thousands of sequence reads per amplicon) can be employed in studies of multigene families to distinguish alleles from artefacts. By avoiding the use of arbitrary and variable global validation thresholds, it can be consistently applied across ultra-deep NGS data sets.

My method estimates the total number of alleles observed among loci within individuals

(A_i) in populations exhibiting copy number variation (CNV). I compare observed sequence depths of MHC IIb amplicon variants in guppies (*Poecilia reticulata*) to those expected under a range of alternative genetic models that assume different numbers of loci. In addition to model-based estimates of A_i, I also provide estimates of the total number of loci within individuals (L_i) and evidence in support of MHC IIb CNV that includes the occurrence of hemizygous gene copies, that is, MHC gene copies that are present on only one homologous chromosome. My results suggest that in combination with ultra-deep NGS and a robust analytical pipeline, multi-locus MHC genotypes can be accurately reconstructed, which in turn will significantly advance our understanding of the evolutionary, population genetics and fitness consequences of MHC variation.

Methods

Samples

Guppies were collected from seven populations across Trinidad and Tobago. Two populations were sampled from the Guanapo River (Guanapo-1: *n* = 32, Guanapo-2: *n* = 28, Caroni drainage), one from the Quare River (Quare-1: *n* = 31, Oropouche drainage) and two from the Marianne River drainage (Marianne-3: *n* = 28, Marianne-10: *n* = 29, Northern slope). Smaller sample sets were collected from a stream at Cumana Beach, Guayamara Bay (Cumana: *n* = 6, Eastern coast), and from an unnamed river along Winward Rd. in Tobago (Tobago: *n* = 5). A total of 159 individuals were analysed in this study.

Molecular methods

DNA was extracted from 3 to 5 dried scales or pectoral fins using a glassmilk-binding protocol (Elphinstone *et al.* 2003). A 209-base pair (bp) fragment of MHC IIb, encompassing all but three codons predicted to comprise the peptide-binding region (PBR; Brown *et al.* 1993; Bondinas *et al.* 2007), was amplified using the degenerate primer pair DABdegFb – GTGTCTTTARCTCSHCTGARC – (Llaurens *et al*. 2012), and DABdegRei – CTCACCTGATTTAKYYAG.

In guppies, intron 2 of MHC IIb is less polymorphic than exon 2 (Llaurens *et al*. 2012), so the reverse primer was situated spanning the boundary between exon 2 and intron 2, to reduce the likelihood of amplification bias or null alleles. Although the possibility of null alleles or PCR bias cannot be eliminated, PCR trials suggested that this reverse primer produced more robust amplifications than previously used reverse primers (M. McMullan & C. van Oosterhout, unpublished data). Each primer was uniquely modified on the 5' end with a 10-bp multiplex identifier (MID; Roche Diagnostics Technical Bulletin TCB No.005-2009), and samples were amplified using a unique combination of forward and reverse MID-labeled primers, which allowed recovery of the amplicons per individual after de-multiplexing. Because MHC IIb appears to be a multi-locus gene family in guppies (Sato *et al*. 1996; van Oosterhout *et al*. 2006a; b), I expected some amplicons to contain more than two alleles. Polymerase chain reactions (PCRs) contained 0.2 mm dNTPs (New England Biolabs), 0.5 μm forward primer, 0.5 μm reverse primer, 1× Phusion HF buffer, 6% DMSO, ~1–3 ng genomic DNA and 0.4 U Phusion DNA Polymerase (Finnzymes). PCRs were performed in Mastercycler Epgradient S (96 well), or ep384 thermocyclers (Eppendorf), using the following parameters: 98 °C for 3 min; 30 cycles of 98 °C 15 s, 57 °C 40 s, 72 °C 60 s; 10 min at 72 °C, then held at 10 °C. During optimization and testing of molecular methods, I found that no artificial chimeric sequences were generated in amplicons when 30 PCR cycles were employed (data not shown). PCR amplicons were pooled and prepared for 150-bp paired-end Illumina MiSeq (Illumina, Inc., San Diego, CA, USA) sequencing using the vendor's TruSeq library protocol. Additional independent PCRs (1–5) were sequenced for each of 49 individual samples in an independent MiSeq run to validate the genotyping method. Some of these samples were chosen at random, but others were chosen to verify genotypes estimated to contain the minimum, median, and maximum number of MHC PAs. In addition, MHC IIb genotypes were characterized in PCRs using three individual DNAs (three replicate PCRs per individual) via cloning and Sanger sequencing. Each of the amplicons was cloned, and 32 clones per individual PCR (288 in total) were sequenced on ABI 3730 XL sequencers (Genewiz, USA). Sanger/cloning protocols are generally limited in the number of clones that can be feasibly sequenced and so CNV could not be estimated in the respective replicated samples. A total of 154 independent replicate PCR products were sequenced.

Data analysis

Data analysis entailed three major steps: (1) sequence preprocessing, (2) error correction and (3) genotype estimation. The third step included two complementary approaches, the CNV model method and the degree of change (*DOC*) method; the former method provided estimates of A_i, L_i and CNV pattern, whereas the latter independently estimated A_i and provided a quality filter that allowed me to assess which amplicons were of high enough quality to yield reliable genotypes. These steps are summarized in Figure 3.1 and described in detail below.

Sequence preprocessing

Paired-end sequencing products were assembled based on a 26-bp region of overlap, using *FLASH* (Magoc & Salzberg 2011). Per-base quality scores of all sequences were assessed using *PRINSEQ* (Schmieder & Edwards 2011), and I retained those with at least a mean of Q30 (99.99% base call accuracy) that were of the expected product length. Sequences were de-multiplexed and variant depths were quantified among amplicons, along with removal of barcodes and priming sequences in *jMHC* (Stuglik *et al.* 2011).

Error correction

I performed a multiple alignment of sequence variants (assembled contigs) observed within each amplicon and built a neighbour-joining tree in *CODONCODE* aligner 3.5.7 (CodonCode, Dedham, MA, USA) to identify repeatable base-mismatch errors, common in NGS (Gomez-Alvarez *et al*. 2009; Gilles *et al*. 2011). Low copy number base-mismatch errors may dilute the realized sequencing depth of the true allele from which they originate, and were identified based on minor sequence variation (1–3 bp) from a high copy number variant (parental variant; presumed to be a true allele). Repeatable putative errors (RPEs) were identified if they (1) reoccurred at the same base positions or in homopolymer runs, (2) co-occurred with a parental PA variant and (3) never occurred as a high copy number variant. RPEs, which are believed to largely originate during sequencing, in my data acquired depths generally <2% depth of the parental PA. The raw depth value for each RPE was added to that of the parent PA for further analysis.

Genotype estimation

I made the following three assumptions for estimating MHC genotypes: (1) the relative number of reads of an allele is proportional to its presence relative to the number of copies of other alleles in that individual, but otherwise constant across individuals; (2) the number of reads per allele is proportional to the number of copies of that sequence in the genome present at the same locus and other (duplicated) loci; (3) genuine alleles amplify at considerably higher sequencing depths than artefacts.

To estimate genotypes by the CNV model method, I first calculated the depths of up to 10 most sequenced variants in each individual, correcting the depth of each variant for RPEs as described. A previous Sanger-based sequencing study suggested the presence of up to three MHC class IIb loci in guppies (van Oosterhout *et al.* 2006b); therefore, by considering the 10 most abundant variants, I conservatively allowed for the possibility of up to five loci. I then calculated the expected sequence depth (E_{ij}) for each allele j of individual i and did this for each theoretical genetic model, considering different numbers of loci and allelic copies using:

$$E_{ij} = \left(\frac{D_i}{E(A_i)}\right) \times E(N_{ij}),$$

where D_i is the total observed sequence depth of the 10 most sequenced variants in individual i, $E(A_i)$ is the expected number of allelic copies for individual i, and $E(N_{ij})$ is the expected number of copies of allele j in the multi-locus genotype of individual i (sum total of all $E(N_{ij}) = E(A_i)$). For example, if the total sequencing depth of the top 10 variants (D_i) was 1000×, I calculated E_{ij} values in a model that assumed two unique alleles, with the first allele (i_1) in homozygous state at one locus and the second allele (i_2) in hemizygous state at the second locus as:

$$E_{i1} = \left(\frac{1000}{3}\right) \times 2, E_{i2} = \left(\frac{1000}{3}\right) \times 1,$$

and the remaining eight variants each were given $E_{ij} = 0$. By calculating E_{ij} for each of the top 10 variants, I produced expected depth ratios of allele combinations in each model of CNV and removed the effect of many low copy number variants assumed to be artefacts (Assumption 3). I then estimated the goodness of fit of each model across all alleles *j* for each individual *i*, calculating the sum of squares, $\sum (O_{ij}-E_{ij})^2$, where O_{ij} is observed sequencing depth and E_{ij} the expected depth of allele *j* in individual *i*. An *F*-ratio test (d.f. = 1) was used to assess whether the top two best-fitting genetic models (with the lowest sums of squares) were significantly different from each other. When the top two models were significantly different, I used the best-fitting model, and when there was no significant difference between models, I used the simplest (lowest) estimate of the L_i and CNV to explain the data. This provided an estimate of A_i, L_i and CNV of each individual.

I used an additional approach, the *DOC* method, to independently estimate A_i and to assess the suitability of amplicons for genotype calling. In this method, A_i of each individual *i* was estimated by differentiating PAs and artefacts based on the observed sequencing depths (O_i) of the 10 most common variants *n* (O_{in}). I calculated the cumulative sequencing depth of individual *i* (C_i) among the top *n* variants as:

$$C_{in} = \sum_n O_{in.}$$

I then calculated the rate of change (first derivative) in cumulative sequencing depth (ROC_{in}) between each variant *n* of individual *i*, which is equivalent to the raw sequence depths of variants (e.g. $ROC_{i1} = C_{i2}-C_{i1}$). Using the *ROC* values of variants (*ROC*1 to *ROC*9), I calculated the degree of change (*DOC*, second derivative) around each variant, which were then transformed into percentages of the total change among all variants as:

$$DOC_{i1} = \frac{\left(\frac{ROC_{i1}}{ROC_{i2}}\right)}{\sum DOC_{i1-i9}} \times 100.$$

The variant with the highest *DOC* value was deemed the last PA in the top *n* variants, after which the *ROC* reduced considerably due to the much lower sequencing depth of artefacts (Assumption 3; see Results). This approach using the *DOC* criterion is similar in some respects to that employed by Babik *et al*. (2009), but differs in multiple criteria. The most important of these is that our method relies on the conformance of variant depths to theoretical expectations derived from my genotyping assumptions (e.g. the expectation of Assumption 3 is that there should be an obvious reduction in sequencing depths between putative alleles and artefacts, or an inflection point in a linear plot of cumulative sequencing depths at the point of greatest *DOC*; see Results), and I discarded amplicons that violated this core assumption after critical assessment (see below). Critically, this approach is independent of the assumptions made in the CNV model that negligible/non-existent PCR bias exists, and that relative sequencing depths represent allelic copy number, and only follows the assumption that alleles should be sequenced at significantly greater depths that artefacts. By actively enforcing the requirement that observed amplicon depths conform to the expectations of this genotyping assumptions, I was able to theoretically assess the validity of the empirical performance of my genotyping protocol. This allowed identification of samples of poor data quality that may bias measures of MHC diversity. However, samples, which have an exceptionally high number of PAs and/or have a number of poorly amplified PAs, may display a similar pattern of cumulative variant depth to those that are of poor quality. I checked such samples for low copy number PAs that were not observed as high copy number PAs in other amplicons. Such examples would indicate an allele that is consistently poorly amplified by the PCR primers, whereas contaminants would be identical to high copy number PAs in other amplicons. Similarly, it was important to assess discarded variants in all amplicons for the likelihood that they may represent poorly amplified PAs and not contaminants. Calculations for A_i estimates using the CNV model fitting and the *DOC* criterion were performed in a custom Excel macro (Appendix 5).

In order to confirm that the *DOC* A_i estimates explained the majority of the variance in total amplicon sequencing depth (i.e. PAs accounted for the majority of the depth; Assumption 3), I performed a principle components analysis (PCA) using *FactoMineR* (François Husson 2008) in *R* (R Development Core Team 2011) on the mean depth values for each of the top 10 most sequenced variants among individuals that displayed each A_i. I performed another PCA to assess whether the maximum estimate of A_i across all samples explained most of the per-amplicon depth variance and whether I had underestimated maximum A_i. Although our CNV models assumed zero error, and I removed RPEs, I expected to observe low copy number contaminants. However, these should account for an insignificant amount of variation (depth) among variants within amplicons.

To compare my approach to previously employed methods, I also genotyped samples using two separate AVTs. In each amplicon, all variants above (1) 3×, and (2) 10×, that could not be explained as a base-mismatch error or a chimeric sequence of more abundant variants were deemed PAs and included in the genotype.

Validating MHC IIb genotypes

To validate my genotyping protocol, I estimated genotyping repeatability using samples replicated in the same sequencing run and in different sequencing runs. Repeatability was assessed on the repeated observation of each allele within each set of replicate amplicons and calculated using the total number of alleles that were replicated among all re-sequenced samples.

All PAs were aligned using *CODONCODE* aligner 3.5.7 (CodonCode), and the reading frame designated in guppies (van Oosterhout *et al*. 2006a;b) was used to check for stop codons. PAs were compared to the NCBI nucleotide database (www.ncbi.nlm.nih.gov) using *BLAST* (Altschul *et al.* 1990). The program *OMEGAMAP* (Wilson & McVean 2006) was used to identify codons that displayed a strong signal of positive selection, and these were compared to

previous estimates of codons that constitute the PBR in the MHC IIb peptide (Brown *et al*. 1993; Bondinas *et al*. 2007; Llaurens *et al.* 2012; McMullan 2010). The program estimates rates of natural selection (*dN/dS*) in the presence of recombination using a population genetic approach within a Bayesian framework, so may provide a more suitable measure of selection at codons than traditional raw *dN/dS* ratios when examining MHC that is expected to undergo frequent recombination (Carrington 1999). Prior distributions recommended by the program's authors (see *OMEGAMAP* manual) were implemented for all modeled parameters. Two *OMEGAMAP* instances were run for 600 000 interactions with a burn-in of 10 000 and combined upon confirmation of convergence of Markov chains. I inferred codons within the PBR that displayed >0.95 posterior probability of positive selection.

Results

Identifying MHC IIb alleles

A total of 381 677 contigs passed pre-processing and all base calls in retained sequences were highly accurate (>Q30, 99.99% accuracy). Ultra-deep sequencing was achieved across samples (mean: 2484× ± 1456), and 87 MHC IIb PAs were identified among 149 individuals with total depth of at least 84× (range: 84–6611×). These 87 PAs translated into 82 unique polypeptides. Across PAs, 63.2% of nucleotides were variable, as were 72.5% of amino acids in translated polypeptides. Putative alleles differed by 1–76 nucleotides and 0–36 amino acids. Ten samples (6%) that came from five populations were excluded from further analyses because PAs could not be confidently separated from artefacts, due to violation of genotyping Assumption 3, either because of inadequate sequencing depth or suspected PCR-carry-over contamination combined with poor DNA quality (Figure 3.2). These samples generally contained tens of low copy number contaminant variants identical to high copy number PAs in other amplicons.

Of the 87 PAs observed, 82 PAs were novel (GenBank: KF321642–KF321728) and only five (*Pore-DAB*103*, *Pore-DAB*120*, *Pore-DAB*130*, *Pore-DAB*133* and *Pore-DAB**138) had been characterized previously (Llaurens *et al*. 2012). Fourteen PAs were shared across at least

two populations, 73 were unique to single populations (private alleles), and the total number of alleles within each population (*Ap*) varied between 1 and 27 (1: Cumana; 4: Marianne-3; 7: Tobago; 14: Guanapo-1; 23: Marianne-10; 27: Guanapo-2, 27; Quare-1). Ultra-deep sequencing provided confident identification of 36 rare PAs (subset of 82 novel PAs) that were each observed in a single individual. Putative alleles shared 81–100% sequence identity with previously identified MHC IIb alleles in guppies or closely related species (www.ncbi.nlm.nih.gov).

Validating alleles

Three samples were re-sequenced using cloning plus Sanger sequencing, and 49 samples were re-sequenced with an independent MiSeq run. The alleles inferred from the cloning/Sanger sequencing method were identical to those determined by Illumina sequencing. In the second MiSeq run, a total of 719 507 contigs passed preprocessing and all base calls in retained sequences were highly accurate (>Q30, 99.99% accuracy). A mean per-amplicon sequencing depth of 6852× ± 5433 was achieved (range: 327–24, 501×), almost three times higher than the coverage obtained by the first run. Genotype repeatability among amplicons that were of sufficient quality (i.e. could be genotyped using the *DOC* method) in the second run was 100% (Figure S3.1a, Appendix 1), and 83.6% between runs (Figure S3.1b, Appendix 1). For eight (16.4%) of the 49 re-sequenced samples, genotyping confirmed additional PAs in the second sequencing run; all of these additional PAs were observed in the first run, but at insufficient depth to be confidently deemed a PA, despite similarly high total amplicon depths in respective replicated samples (hence, they were considered to be artificial variants).

Use of a low per-amplicon depth threshold (e.g. 3× coverage, Zagalska-Neubauer *et al*. 2010) would have retained these PAs, but would also have artificially inflated the A_i estimates by 133–1600% (mean: 416 ± 359%) if applied to these replicates in the first data set, erroneously adding 3–29 (mean: 9.62 ± 6.95) low-level contaminants per individual (Figure S3.2a–h, Appendix 1). Furthermore, it would have produced highly disparate A_i estimates in the remaining replicated samples, both within and between sequencing runs, resulting in 8.5%

repeatability between replicates within a sequencing run and 0% between runs (Table S3.2, Appendix 5). Using 3× AVT would have resulted in a range of A_i from 2 to 64 across all individuals in the first run, respectively (Figure S3.3, Appendix 1), and a mean A_i of 16.2 (±15.5). Similarly, using a more conservative criterion (e.g. 10× coverage) would have resulted in a range of A_i = 1–32 and a mean A_i of 5.7 (±7.4), erroneously inflating the A_i estimate by 16.6–800% (mean of 124 ± 163%). Given that artefacts can occur at much higher depths than 3×, or even 10× (Figure S3.4, Appendix 1), arbitrary elevation of the depth threshold would not result in the accurate determination of multi-locus genotypes. In particular, these low AVTs would have performed particularly poorly in distinguishing between 'real' alleles (i.e. those that are part of the true genotype of an individual) and those present in the amplicon as a result of contamination.

In total, 36 rare alleles would have been omitted using previous protocols, but were confirmed by the independent sequencing run. All these alleles were accepted as genuine by the new protocol in both runs, which demonstrates that the protocol reduces the need for replicated sequencing. Nevertheless, the new protocol does introduce a small Type II genotyping error (rejecting the existence of 14 PA copies of 302 in total among all samples; Type II error = 4.9%), but it also avoided a very considerable Type I genotyping error compared to previous methods that used the 3× depth threshold criterion and which would have accepted 602 artificial variants (Type I error = 78.6%). Furthermore, the Type II error associated with the new protocol was completely removed in the second run, which shows that the protocol is particularly powerful when using ultra-deep coverage. Equally important is that the new protocol can reconstruct the most likely multi-locus genotypes, including putative homozygotes and hemizygotes, which allows for a more complete population genetic analysis (Table S3.1, Appendix 5).

Genotype estimates

One to six PAs were observed in each individual (mean: 3.15 ± 1.21), consistent with previous estimates of up to three MHC IIb loci in guppies (van Oosterhout *et al.* 2006b). Among all 149 individuals, 5% had one PA, 23% two PAs, 34% three PAs, 19% four PAs, 14% five PAs and 5% six PAs (Figure 3.3a), a distribution consistent with expectations under the optimality hypothesis that a median A_i is maintained in high frequencies within populations through increased fitness benefits (Nowak *et al.* 1992; Woelfing *et al.* 2009). However, the frequency distribution of A_i also varied among populations (Figure 3.3b–h), suggesting spatial variability in processes governing MHC diversity (Eizaguirre *et al.* 2011). Moreover, I observed no meaningful relationship between total amplicon sequencing depth and A_i (Figure S3.5, Appendix 1; linear regression: $P = 0.109$, $r2 = 0.01$), showing that the total number of alleles identified within an amplicon is not significantly affected by increasing sequencing depth.

Individual PAs generated 5.22–97.45% (mean: 29.9 ± 17.7%) of total amplicon sequencing depth (Figure 3.4). Overall, A_i was confidently estimated in 94% of samples using CNV model fitting, *DOC* estimates and PCA validation. The latter approach showed that PAs accounted for 100% of the variance among amplicons (Figure. S3.6, Appendix 1). Only 6% of samples could not be genotyped due to a lack of separation between potential PAs and artefacts.

RPEs frequently deviated from a parental PA by 1–2 bp, and individual RPEs were observed in 1–76 amplicons. Artefacts identical in sequence to PAs in other samples, but at low sequencing depths of 0.02–2.11% (mean: 0.7 ± 0.5%) of total per-amplicon sequencing depth, were observed in all amplicons (Figure 3.4a). The low sequencing depths exhibited by these sequences identical to high copy number PAs in other amplicons caused them to be considered artefacts by my validation methods. They were likely contaminants, which are common in large multiplexed amplicon studies (Gomez-Alvarez *et al*. 2009; Gilles *et al*. 2011). Including contaminants would have reduced the repeatability of the A_i estimate between runs (Table

S3.2, Appendix 5).

The relative proportion of sequence reads attributed to PAs and artefacts varied among amplicons containing varying numbers of PAs, but showed consistent patterns. When sequence variants were sorted in descending order of frequency that they were observed within individual amplicons, the mean *ROC* of cumulative depth was greater among PAs than among variants judged to be artefacts (Mann–Whitney *U*-test: Z = 9.62, *P* = <0.001), affirming that I correctly classified amplicon variants based on relative sequence depth (Figure 3.5a). There was also a considerable increase in the mean *DOC* of cumulative depth at the point of transition between sequence variants classified as PAs and those classified as artefacts (Figure 3.5).

On average, 83.9–94% of amplicon sequencing depth was attributed to PAs, and the remainder to artefacts (Figure 3.5a). Estimates of A_i obtained using the *DOC* criterion showed values of *DOC* ≥ 48.1% marking the boundary between PAs and artefacts (Figure 3.5b). Mean *DOC* values varied depending on total A_i (mean: 61.67%, range: 48.1–86.6%). In addition, *DOC* A_i estimates were corroborated using PCA, which defined PAs and artefacts based on relative sequencing depth among amplicons (Figure S3.7a–f, Appendix 1).

In each of the 41 replicated samples that had confirmed A_i between sequencing runs, I estimated that guppies have between 1 and 4 loci (Table S3.3, Appendix 5). CNV and L_i estimates were confirmed in 100% of these replicate PCRs (Table S3.3, Appendix 5). The presence of odd A_i estimates, with each PA sequenced at approximately equal ratios, infers hemizygous genotypes in progeny of parents containing different L_i.

Sequence polymorphism

Positive selection was identified in 15 codons using *OMEGAMAP* (Figure S3.8, Appendix 1). Of these, 14 codons matched those previously inferred to constitute the PBR in other vertebrates based on X-ray crystallography, either alone (Brown *et al*. 1993) or in comparison with sequence data (Bondinas *et al*. 2007), and nine codons matched those previously inferred in

guppies using *OMEGAMAP* (McMullan 2010, Figure S3.8, Appendix 1), confirming that the correct DNA fragment had been amplified. I observed a high posterior probability of selection for each of two additional codons predicted to reside in the guppy PBR (P = 0.89 and 0.9), which, although below the threshold of P = 0.95, are most likely also under positive selection. The remaining codon found to be evolving under positive selection deviated from previous inferences of PBR designations by one codon.

Discussion

I present a method that can be used to distinguish MHC multi-locus genotypes from artefacts generated during PCR and NGS. My approach differs from previously described methods (e.g. Galan *et al*. 2010; Zagalska-Neubauer *et al*. 2010) in that it does not use AVTs to confirm alleles from artefacts and provides an approach to deal with common cross-sample contamination. In addition, it is relatively simple in comparison with more recent methods that use complex clustering approaches (Pavey *et al*. 2013; Sommer *et al*. 2013). Instead, my approach relies on two independent metrics. The first involves calculating the observed sequencing depths of variants and testing their fit to expected genetic models. The second involves statistically identifying the boundary between true alleles and artefacts using relative sequencing depths. Overall, the application of my genotyping method and the specific assumptions it entails result in a highly repeatable measure of alleles and genotypes per individual. I was able to accurately separate PAs from artefacts in 94% of sufficient quality amplicons and to replicate genotypes with 100% accuracy within a sequencing run, and 83.7% between fully independent runs. To my knowledge, this is the first example of this level of genotyping repeatability among fully independent data sets in a NGS MHC sequencing study.

The combined depth of erroneous and artefactual sequences (namely low copy number contaminants) was similar across all amplicons (range: 0–22%, mean: 4.2 ± 4%), irrespective of total number of unique artefacts, and their individual contribution to total amplicon depth.

Similarly, I observed consistently high proportions of amplicon sequencing depth attributed to PAs (range: 61.8–98.6, mean: 89.18 ± 7.1%) in amplicons of varying A_i (alleles per individual), which is in agreement with the assumption that PAs should account for considerably more sequence depth than artefacts within amplicons.

By assessing sequencing depths of PAs and artefacts on a per-amplicon basis, I minimized both the inclusion of artificial sequences and the exclusion of true alleles. While this approach greatly reduces the inclusion of artificial sequences, it can also exclude PAs with low depths. The rate of this Type II error can be estimated by fully independent re-sequencing of samples, and the Type II error itself is largely avoided by ultra-deep sequencing. Type II error rate between replicates sequenced both in the 1st and in the 2nd run with a mean sequencing depth of 2424× and 6852×, respectively, equaled 4.9%, and then 0% (i.e. 100% repeatability) between re-sequenced samples within the 2nd run.

Individuals that were not accurately genotyped either had very low sequencing depth, or sequence depths could not be used to separate PAs from artefacts due to suspected cross-contamination, which is common in large multiplexed amplicon studies (Li & Stoneking 2012). These problematic samples can be easily identified using the proposed methodology, and they are best removed from further analysis, given that they dramatically reduce genotyping repeatability (but see below). To my knowledge such amplicon quality assessments have not been previously implemented in NGS MHC studies, yet, such quality standards may be important in light of the potential for common DNA/PCR-carry-over contaminants in large multiplexed NGS data sets (Li & Stoneking 2012).

Performance of genotyping method

A significant reduction in the mean *ROC* at the boundary between PAs and artefacts, identified by critical values of *DOC*, and separation of PAs and artefacts using PCA confirms that my genotyping method produced estimates of A_i that conform to theoretical expectations.

Specifically, both findings corroborate the assumption that errors should be observed less frequently than PAs.

Replicates of re-sequenced samples displayed identical genotypes within a sequencing run. However, some re-sequenced individuals were observed to have up to three additional alleles in fully independent replicates that were discarded from original genotypes due to inadequate sequencing depth of particular variants, despite similarly high total amplicon sequencing depths between samples replicated among data sets. This highlights the advantage in estimating genotyping repeatability in fully independent replicates where random effects of sample preparation and data collection may result in allele dropout. However, this also highlights a shortcoming of classifying true PAs and contaminants based on relative sequencing depths, where some real PAs may be erroneously discarded as contaminants, and so it is important to critically evaluate sequences that are discarded within amplicons to reduce this. Importantly, re-sequenced samples displayed repeatable estimates of L_i and CNV despite variation in total amplicon sequencing depth (see below).

An important step in my genotyping protocol is assessing the conformance of variant sequencing depths, within each amplicon, to theoretical expectations derived from genotyping Assumption 3. This acts as a quality control step to filter out samples that display deviations from expectations (i.e. a continuum of variant depths opposed to a breakpoint between highly sequenced alleles and minimally sequenced artefacts) and therefore cannot be reliably genotyped. Previous work that estimated between 1 and 6 alleles per individual in guppies (van Oosterhout *et al.* 2006b; Llaurens *et al*. 2012) was supported by my findings in all amplicons that conformed to theoretical expectations by displaying a noticeable inflection point in cumulative sequencing depth (highest *DOC*) between PAs and artefacts. Not only was the removal of amplicons that displayed a continuum of variant depths warranted based on the violation of genotyping Assumption 3, but the estimated PA count within these samples would have been an order of magnitude greater than those estimated in good-quality amplicons,

previous studies, and test data sets (data not shown). Thus, I believe this is an important step in improving the quality of data sets and accuracy in MHC population genetics analyses. Although the methods allowed me to genotype guppies that acquired depths of tens or hundreds of sequences, ultra-deep depths of thousands of sequences may be required to accurately define a breakpoint between alleles and artefacts in species that are expected to contain tens of MHC alleles. However, this approach does not take into consideration that some alleles may always amplify poorly and attain sequence depths similar to those expected by low copy number contaminants. Therefore, variants should be carefully assessed in samples that lack a clear inflection point in cumulative depth between PAs and artefacts, where contaminants may be distinguished from poorly amplified PAs. Of all samples in my study, 94% met the criterion for reliable genotyping, and with further careful attention to laboratory protocols minimizing the risk of contamination, this number would likely improve.

It is worth noting that the lack of artificial sequences that represented chimeras in this study may have been aided by the relatively reduced number of PCR cycles (30 cycles), compared to other studies that reported higher numbers of artefact when using more PCR cycles (e.g. Sommer *et al*. 2013). A reduction in PCR cycles has been shown to effectively reduce PCR artefacts when genotyping MHC loci and should be employed to avoid the occurrence of problematic chimeric artefacts (Lenz & Becker 2008).

Comparison to previous NGS MHC genotyping methods

My approach differs from previous methods of MHC genotyping using NGS (Galan *et al*. 2010; Zagalska-Neubauer *et al*. 2010) in several key ways. Although I accept a similar genotyping assumption (Assumption 3), I strictly enforce criteria that follow from this assumption, unlike previous methods (e.g. Zagalska-Neubauer *et al*. 2010), making it relatively easy to separate PA from artefacts based on theoretical expectations. I also actively corrected the depth of PAs that are affected by RPEs. This further reduces the number of artificial sequences within individuals and increases accuracy in PA depth ratio estimates. Although assessments of RPE are necessary

to gauge data quality, they may not be crucial in data sets that contain very little cross-contamination among samples and only aim to estimate A_i. However, I recommend their identification to increase retention of useful data and improve genotyping accuracy. Previous studies have eliminated suspected artefacts within amplicons by identifying variants that likely originate as a 1 base-mismatch error from a more common parental variant (e.g. Zagalska-Neubauer *et al*. 2010). However, I identified artificial variants that displayed up to two repeatable base-mismatch errors. Therefore, detailed assessment of closely related variants within amplicons is essential to facilitate accurate genotyping.

The method used here accounts for variation in amplicon sequencing depths. By avoiding global AVTs, I was able to mitigate the effects of the problematic 'grey area' and reduce the effect of variable error rates among individuals. This was especially important in the case of artefacts identical to PAs in different amplicons, where low-allele acceptance thresholds would otherwise have caused severe artificial inflation of A_i across many genotypes. These low-depth artefacts resulted in nonreplicable A_i estimates and violated all assumptions of the genotyping protocol and thus warranted exclusion. In addition, I identified a small number of samples that displayed a continuum of sequencing depths across many variants. The blurring between true PAs and artefacts may be a sign of increased contamination or poor DNA quality in these samples, but in other cases could represent poorer amplification of real alleles.

It is worth noting that previous studies, which have employed AVTs, have in some cases empirically defined the acceptance depth threshold (albeit based on just a subset of samples), and also acknowledged that thresholds may not account for the removal of all artefacts. Thus, while AVTs may have allowed for repeatable genotyping in studies that achieved less sequencing depth per amplicon, I confirm previous evidence that they are not well suited when ultra-deep sequencing is employed (Oomen *et al*. 2013). Similarly, my approach may cause some low copy number PAs to be erroneously discarded from amplicons, and critical

assessment of sequence variants is always required among amplicons, especially in those that display a continuum of sequencing depths among variants.

Recently, it was suggested that low total amplicon sequencing depths used in the majority of 454 sequencing-based studies may be problematic as variable amplification efficacy among PAs may cause some to be mistakenly discarded from amplicons ('allele dropout') if they do not reach a set threshold (Sommer *et al*. 2013). Here, I show ultra-deep sequencing aided accurate genotyping by increasing the power of quantitative appraisals of PAs and artefacts within amplicons, which are less reliable in low-depth sequencing. This was verified by 100% genotype repeatability within a sequencing run and only a small amount of allele dropout between fully independent data sets. However, random PCR effects most likely caused this dropout rather than systematic bias; thus, ultra-deep sequencing is an effective strategy to minimize the effect of allele dropout caused by PCR bias. Admittedly, ultra-deep sequencing and my protocol cannot fully overcome allele dropout caused by problematic PCR bias, but if sample contamination can be reduced to negligible levels, then my approach may permit a quantitative appraisal of the influence of amplification bias and allow simpler identification of poorly amplified PAs. Also, my approach allowed the identification of rare PAs, which I confirmed independently. The application of previous MHC NGS genotyping protocols, which exclude PAs seen in just one amplicon, would have resulted in a 41% reduction in the total number of observed PAs.

Exploring MHC CNV

Although my main focus was to provide repeatable, accurate estimates of A_i, I also observed repeatable evidence of MHC IIb CNV within and among populations. Estimates of CNV were less robust in studies that employed Sanger sequencing because that method offers no practical means to quantify relative abundance of amplicon products. As such, the estimation of allele frequencies in multigene families where the locus affiliation of alleles is unknown, and CNV may exist, has been challenging. Consequently, estimating the number of loci has been equally

difficult. Despite this, traditional MHC genotyping methods have led to speculation that CNV exists within and among populations of guppies based on the observation of odd numbers of alleles (Llaurens *et al*. 2012), and my results support this. Interest in quantifying MHC CNV in natural populations is growing, in part because of increasing evidence of its importance in influencing patterns of susceptibility to disease (Siddle *et al*. 2010; Cheng *et al*. 2012). Recently, studies have also suggested the presence of multiple copies of the same PA within genotypes using relative 454 sequencing depth ratios (Oomen *et al*. 2013; Sommer *et al*. 2013), however with very limited analysis. My detailed approach using ultra-deep sequencing supported a range of repeatable CNV models across 149 guppies (Table S3.1 and Table S3.3, Appendix 5). The fit of the two most probable CNV models to the observed data was significantly different in just eleven samples (and so model 1 was used), whereas the simplest model was used in the remainder of samples when the top two models potentially explained the data equally well (Table S3.1, Appendix 5). Conjecturally, guppies may have between 1 and 5 loci (including hemizygous loci), although I cannot rule out the possibility that individuals estimated to contain 1 diploid locus may actually have 1 hemizygous locus or as many as 5 loci fixed for the same allele loci. Similarly, individuals estimated to have 2.5 loci may actually have 5 loci. Unlike the case with Assumption 3, it is difficult to empirically evaluate Assumptions 1 and 2 of my genotyping criteria; validation of these criteria will require further testing in guppies.

Because of the complexity of possible combinations of PA and number of loci copies in genotypes, coupled with the semi-quantitative nature of NGS, only an estimate can be given of the true CNV pattern exhibited. Moreover, PCR amplification bias, which is known operate during co-amplification of MHC loci (van Oosterhout *et al*. 2006b; Sommer *et al*. 2013), may affect sequencing depth ratios of alleles in some amplicons and so may distort quantitative appraisals of relative depth ratios. Notwithstanding this possibility, complex yet repeatable inferences of CNV suggest that alleles may be duplicated within individuals, in line with other recent evidence describing MHC IIb diversity in guppies (Llaurens *et al*. 2012). Development of further methods that can accurately detect PCR bias and correct sequencing depth ratios

accordingly will strengthen PCR-based methods to quantify CNV using sequencing depth. Measures of A_i and L_i should be less affected by minor variations in PA depth ratios and hence should be the most robust. Nonetheless, fitting ultra-deep NGS data to theoretical models of CNV suggests that variation in the total number of MHC IIb loci and number of PA copies exists within and among populations. It would be interesting to apply my approach to a study system where the genomic architecture and expression levels of the MHC are thoroughly characterized (e.g. humans) to further validate and improve the ability to quantify CNV using PCR and ultra-deep sequencing approaches.

Conclusion

The methods presented here improve on previous NGS protocols to genotype MHC loci by avoiding problematic and sometimes-arbitrary AVTs, and by enforcing genotyping assumptions to produce accurate and repeatable genotypes. My results demonstrate that substantial improvements can be made to traditional MHC genotyping methods through the application of NGS. In doing so, I was also able to provide repeatable comparative evidence to support CNV in the number of MHC IIb loci and allele copies between individuals. Studies involving controlled breeding experiments in individuals with known CNV will help further elucidate the pattern of MHC CNV. I recommend the development of MHC genotyping protocols that strictly enforce genotyping assumptions using ultra-deep NGS (which can be achieved using any of the current popular NGS technologies) while compensating for PCR bias, and believe that methods aimed at exploring CNV of MHC in natural populations may shed light on this previously understudied aspect of MHC evolution.

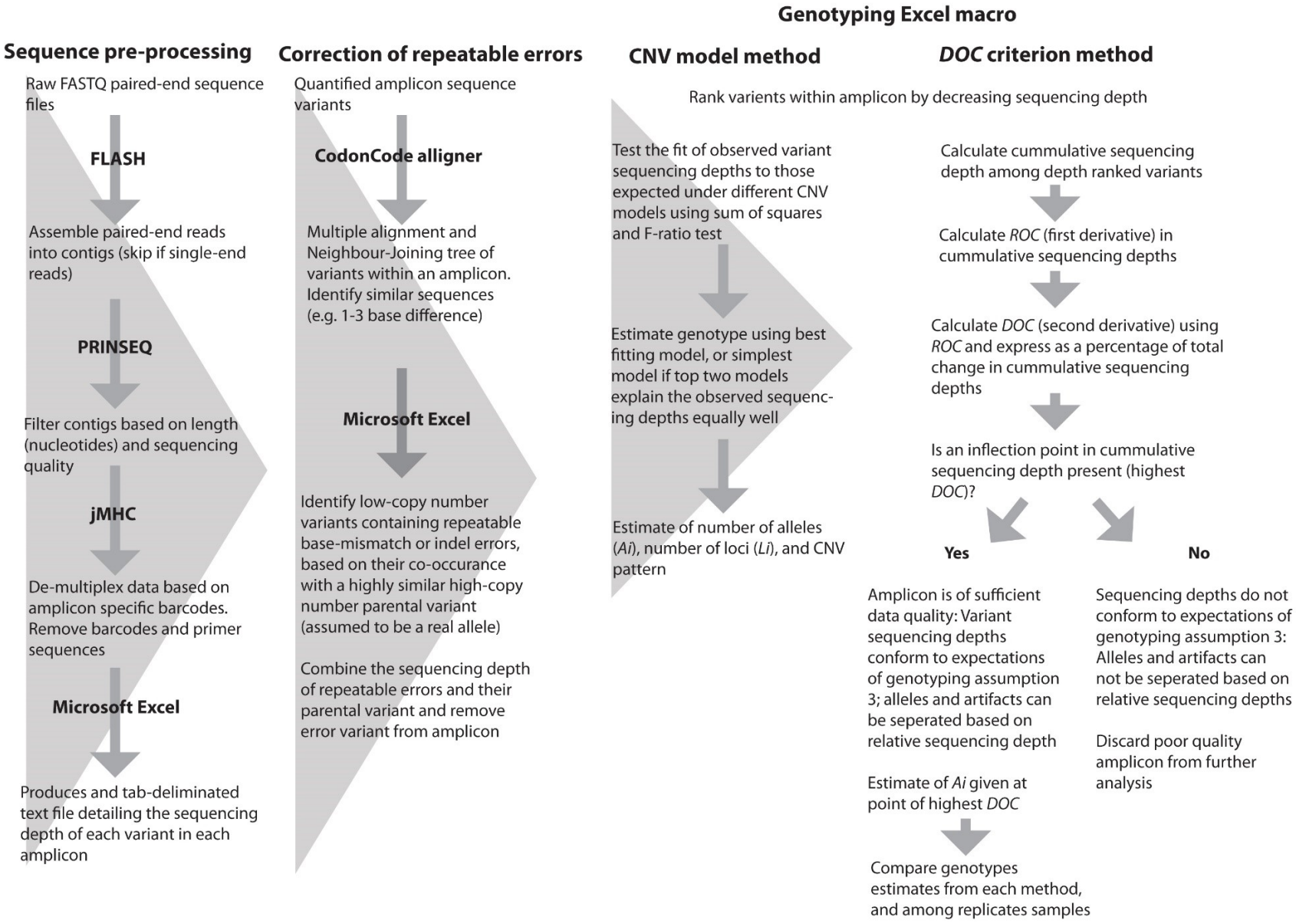

Figure 3.1. Flowchart of analysis steps in the genotyping of multitemplate MHC amplicons.

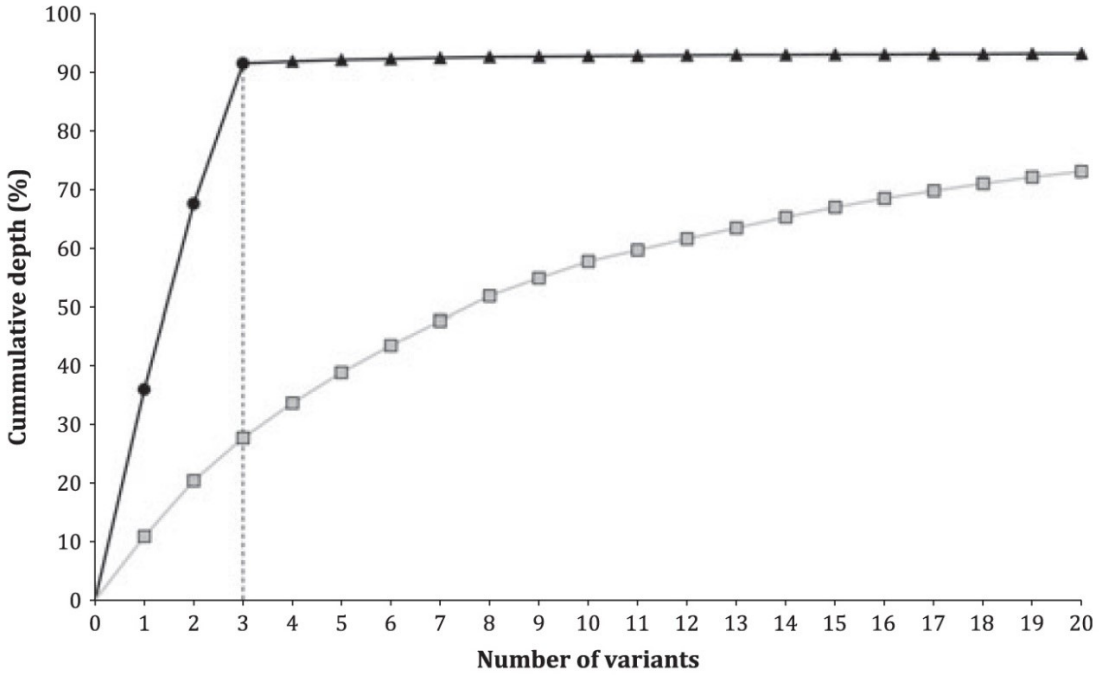

Figure 3.2. A comparison between good- and bad-quality amplicon data. Shown are examples of a good (black)- and poor (grey)-quality amplicon, each sequenced at high depth (2925× and 2498×, respectively). In the good amplicon, ultra-deep sequencing reveals a decrease in rate of change (*ROC*) of the cumulative sequencing depth of the top 20 variants after *n* variants, marked by the hashed vertical line. This inflection point coincides with the final estimate of A_i for this sample (A_i = 3) and clearly marks the boundary between PAs (circles) and artefacts (triangles). The low copy number/depth of individual artefacts contribute relatively little to the total amplicon sequencing depth compared to individually highly sequenced PAs. In contrast, in the poor-quality amplicon, which likely results from some combination of contamination and poor template DNA quality, it is impossible to accurately identify a breakpoint between PAs and artefacts, and variants are indistinguishable (squares). Because this distribution violates genotyping assumptions, such samples are removed from further analysis if assessment of variants suggests the presence of low copy number contaminants derived from high copy number PAs present in disparate amplicons.

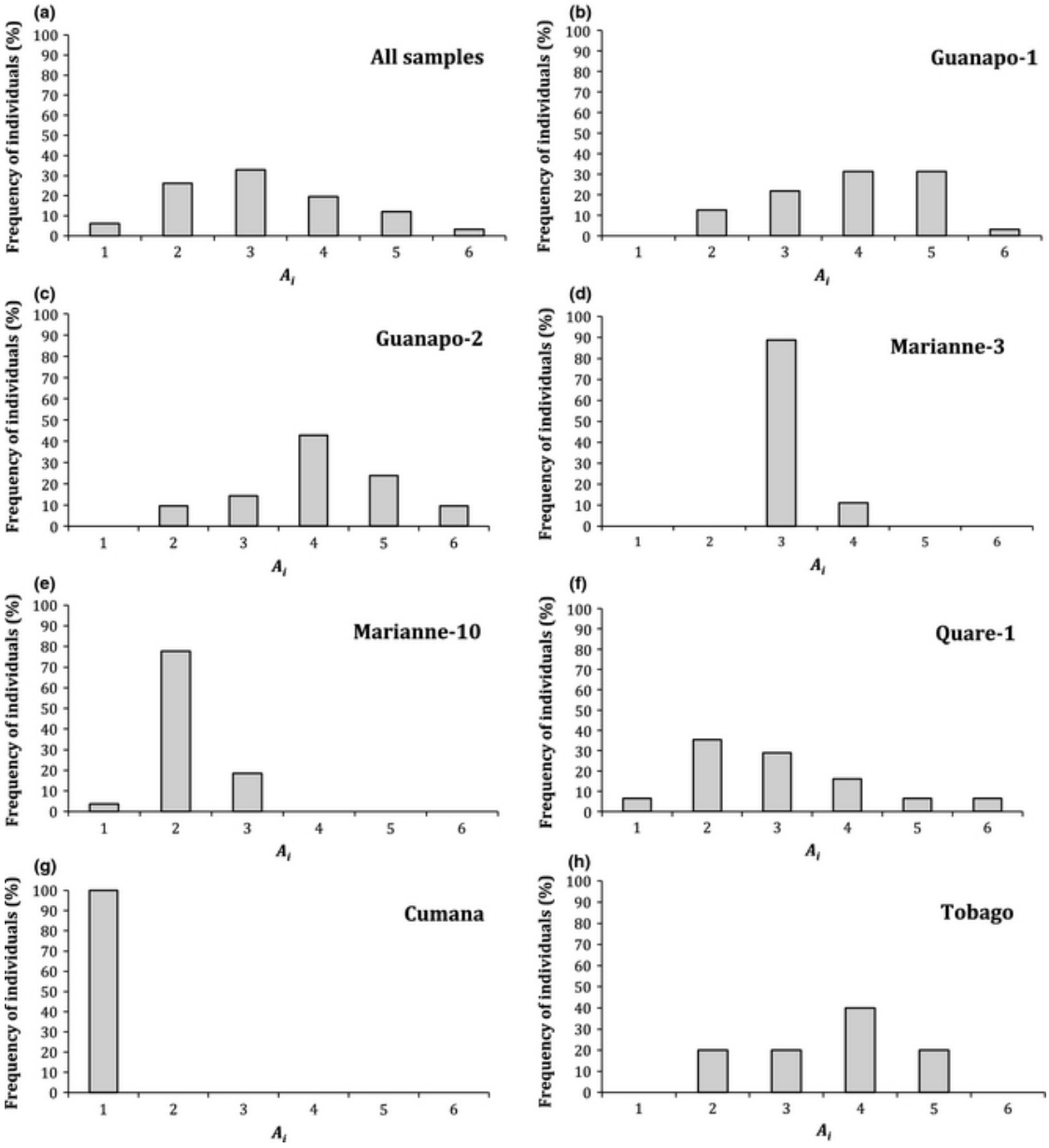

Figure 3.3. Frequency distributions of A_i estimates among individual guppies. (a) The frequency distribution of A_i across all guppies conforms to expectations under the optimality hypothesis that most individuals express an intermediate A_i, (b-h) but varies among populations. In populations where A_i estimates across individuals were particularly skewed (e.g. M3, Cumana), genotypes were confirmed in multiple independent replicates.

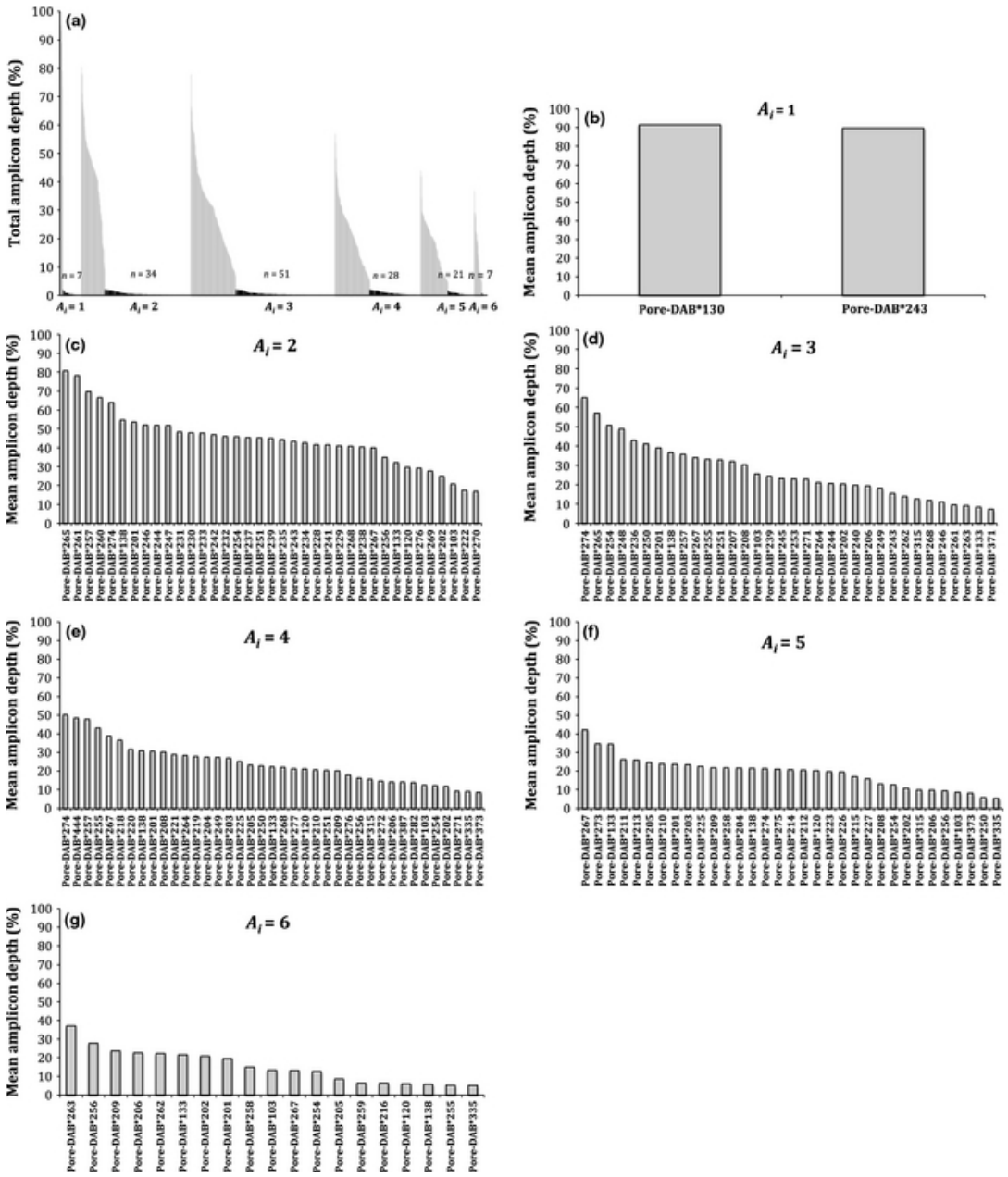

Figure 3.4. Depth distribution of PAs and artefacts among amplicons in all guppy samples with A_i values ranging from A_i = 1 to A_i = 6. (a) Across all amplicons, PAs were observed at between 97.4% and 5.2% of total amplicon depth. Light grey bars show the depth of every instance of PAs in each A_i category. As estimated A_i increases, the maximum depth that a PA contributes to total amplicon depth reduces. However, the distinction between PAs and contaminants (dark grey bars) is maintained even when A_i increases. We see a clear step decrease in total amplicon depth percentage between light grey and dark grey bars, shown here for sequence depths across all individuals in each A_i category, but also evident individually in each amplicon (not shown). (b–g) For clarity, the mean sequencing depth is shown for each PA that was observed among all individuals of in each A_i category (A_i = 1- A_i = 6). The number of unique PAs observed within each A_i category varied as did the mean sequencing depth for each PA.

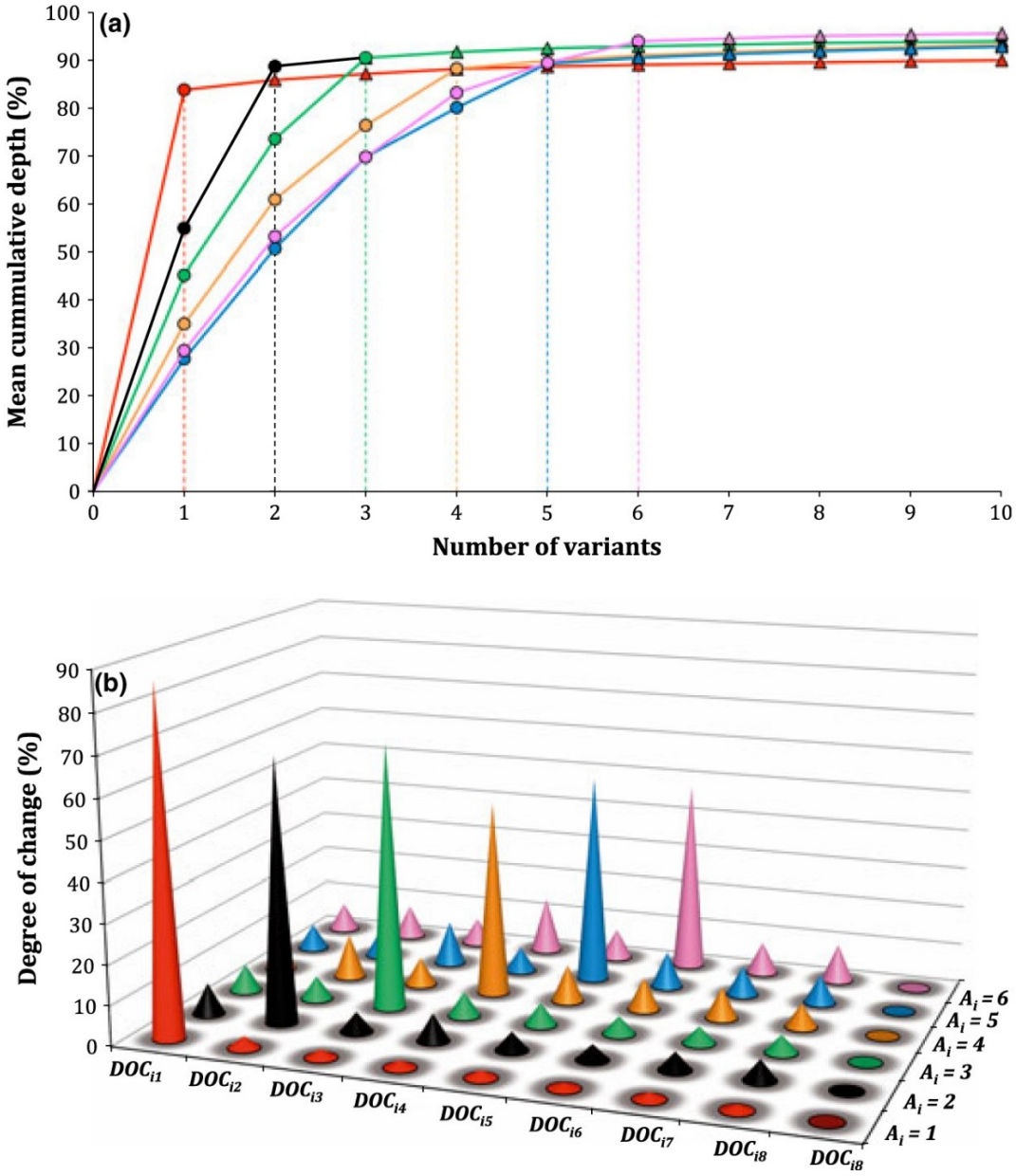

Figure 3.5. Confirmation of the total number of observed unique PAs within genotypes. (a) Across samples grouped by A_i, the mean percentage of cumulative sequencing depth decreases in *ROC* after *n* variants – marked by the hashed vertical line. Across all samples, the mean *ROC* was significantly different between PAs and artefacts (Mann–Whitney *U*-test: Z = 9.62, *P* = <0.001). In the case of each A_i grouping, the point of decrease coincides with the final estimates of A_i for those samples. This point marks the boundary between PAs (circle) and artefacts (triangle), where the low copy number/depth of individual artefacts contribute relatively little to the total amplicon sequencing depth compared to highly sequenced PAs. (b) The greatest *DOC* between variants characterizes this boundary between PAs and artefacts.

Chapter 4

The role of MHC and parasites in the secondary sexual colouration of guppies (*Poecilia reticulata*)

Abstract

The guppy (*Poecilia reticulata*) is a model species in the study of natural and sexual selection. The paradigm focuses on the opposing selection pressures of predators and female mate choice on male colour. Yet this simplistic view ignores other selection pressures individuals may experience, most notably, parasitism. Here I highlight links between colouration, parasitic infections by *Gyrodactylus*, and genes of the Major Histocompatibility Complex (MHC) among 21 guppy populations in Trinidad. I show that across drainages the relative body area of different colours decreases with increasing *Gyrodactylus* prevalence, and that MHC variation is positively correlated with parasite prevalence. These associations suggest differential selection pressure exerted by parasites may directly affect colours believed to be on honest signal of male fitness, and relationships between MHC polymorphism and colour may be an indirect consequence of its role in parasite infections. This supports the Hamilton-Zuk hypothesis which states that genetic variability can be maintained by mate choice driven by preference for sexual ornamentation that indicates parasite resistance. Indeed, some interactions between MHC, parasite prevalence, and male colour seem to be governed by variation between host populations in distinct river drainages. This suggests local adaptation of guppies within drainages, and further supports the hypothesis that populations in each drainage represent distinct evolutionary lineages. Other aspects of ecology (including parasitism) alongside predation pressure and female mate choice may affect adaptation of guppy populations. This is the first time such relationships have been observed in concert among MHC, pathogen infection, and colour.

Introduction

Understanding how organisms adapt to their local environment can help elucidate drivers of species diversification. In this regard, spatially varying phenotypes and genotypes may represent local adaptation of populations, and even evidence of ecological speciation (Wang *et al.* 2013; Shafer & Wolf 2013; Papadopulos *et al.* 2014). Conversely, similarity in ecological conditions between localities can hinder population divergence, for example when balancing selection and stabilizing selection slow down the rate of genetic divergence expected under neutral evolution (e.g. allele frequency changes due to random genetic drift). Indeed, as recent studies have shown, the rate of divergence varies across the genome (e.g. Yang 2010) and allelic lineages in some genes (e.g. Major Histocompatibility Complex; MHC) coalesce much further back in time than the split of the most recent common ancestor (Figueroa *et al.* 1988). Even in allopatry, parallel evolutionary mechanisms (i.e. stabilizing- and balancing selection) may lead to convergence or maintenance of particular phenotypic and genomic variants despite long-term geographic isolation and local adaptation of other traits.

The MHC genes are used to infer patterns of vertebrate adaptation to dynamic pathogen communities (Bernatchez & Landry 2003; Piertney & Oliver 2006), and the links between MHC polymorphism and susceptibility to disease are well established (Trowsdale 2011; Trowsdale & Knight 2013). However, little is known about effects of this polymorphism on phenotypic measures implicit in sexual selection, i.e. those that are believed to represent honest signals of health. Correlations between MHC-polymorphism and parasite loads are used as proxies for the effects of MHC on host fitness, however, other vertebrate traits, such as the quality of secondary sexual colour displays, are believed to confer more direct signals of individual fitness. Colouration may be a reliable indicator of an individual's immunocompetence because colour can be a costly trait and indicative of an honest signal (Saks *et al.* 2003; Kolluru *et al.* 2006; Aguilera & Amat 2007; del Cerro *et al.* 2010; Mougeot *et al.* 2010). For example, carotenoids are used as pigments in colour displays, but also have critical anti-oxidant roles in immunological processes (Grether *et al.* 1999; Stahl & Sies 2003; Chew & Park 2004). The ability

to allocate carotenoids away from these immune processes to displays of colouration is therefore thought to be indicative of an honest signal for high fitness and increased immune defenses against pathogens. Similarly, melanin-based pigments in ornamentation also correlate with parasite resistance and so may be reliable indicators of individual health (Gasparini *et al.* 2009; Jacquin *et al.* 2011). Such processes are outlined in the Hamilton-Zuk hypothesis, which posits that specific genetic polymorphism can be maintained in a population when females choose mates based on sexual ornamentation that indicates resistance to parasites (Hamilton & Zuk 1982; Balenger & Zuk 2014). It follows that studying secondary sexual traits should allow for examination of both pathogen-mediated natural selection (as traits denoting fitness will be affected by the degree of infection), and mate choice mediated sexual selection (as females preferentially chose mates that appeared fitter), e.g. in guppies (*Poecilia reticulata*) (Houde & Torio 1992; Grether *et al.* 1999; Kolluru *et al.* 2006). Resolving the interaction between MHC polymorphism and the display of phenotypic traits that are associated with fitness may elucidate complex interactions among different forms of natural selection.

The guppy is an excellent species to assess the links between MHC genes, pathogen infection, and secondary sexual colouration. Particular MHC polymorphism in guppies may be associated with defense against common *Gyrodactylus spp*. (viviparous monogenean parasites) (Fraser & Neff 2010), and importantly, MHC can play a significant role in mate choice, where evidence suggests that females chose male genotypes in order to optimize the immune repertoire in their offspring (Milinski 2006). Expression of colours that are believed to be an honest signal of immunocompetence (e.g. orange, Saks *et al.* 2003; Aguilera & Amat 2007; del Cerro *et al.* 2010) may be affected at the individual level in guppies by both the degree of parasite infection (e.g. intensity of orange; Houde & Torio 1992), and also past selection though mate choice based on female preference for different male colours (Houde 1997).

The same colours that are preferred by females are also believed to be associated with increased susceptibility to predation (Endler 1980; Houde 1997; Godin 2003) and so are particularly suited to addressing questions focused on the interplay of various drivers of natural

selection. Male guppies in experimental high predation (HP) environments can evolve colour patterns that apparently reduce conspicuousness to predators (e.g. reduction in colour spot size), where as those in artificial low predation (LP) environments can display more carotenoid and black colouration, driven by female mate choice (Endler 1980). The paradigm is that predation pressure is a strong driver of parallel evolution of life history, colour, and mate choice among genetically independent populations, despite long-term isolation (Houde 1997).

Notwithstanding this paradigm, guppy life history (Fitzpatrick *et al.* 2014), and colour (Millar & Hendry 2012) can display non-parallelism among populations of similar predation levels, and importantly there has shown to be negligible variation in the relative fitness of brightly coloured males between HP and LP populations (Weese *et al.* 2010). Male colouration in populations commonly do not conform to expectations derived from the 'predation paradigm', where some LP populations display temporally stable colouration consistent with HP environments (Gotanda *et al.* 2013). Moreover, guppy fitness related colours can vary significantly among drainages, yet it is not clear what causal agent drives these differences (Rodd & Reznick 1991). Interestingly, guppy populations within each of the three main drainages of northern Trinidad represent distinct drainage specific lineages, which increases evolutionary independence and facilitates testing of evolutionary hypothesis. Strictly speaking the North Slope comprises many independent smaller watershed (as opposed to the Caroni, and Oropouche drainages), but genetic data suggest that they represent a single lineage (Willing *et al.* 2010; Baillie 2012).

Here I quantify variation in phenotypic traits and genetic polymorphisms correlated to fitness in guppies and investigate the following questions: (1) Is colour variation in male guppies explained solely by predation pressure; (2) do patterns of parasitism and MHC correlate with adaptive traits (e.g. colour) in guppies, and, (3) is guppy MHC diversity influenced by demographic processes? Defining the interactions between MHC, parasitism, and colour will allow for a clearer understanding of how sexual selection and parasite mediated selection define the adaptive diversity of guppies in relation to the effects of variable predation pressures.

Methods

Sampling and parasite assessment

Male guppies were sampled from 21 populations across 10 rivers in northern Trinidad (Figure S4.1, Appendix 2) in 2009 (total n = 723) and 2010 (total n = 707). Fish were isolated to prevent parasite movement among individuals, and euthanized in 0.02 % Tricaine Methanesulfonate (Finquel MS-222; Argent Laboratories, Redmond, WA, USA) buffered to a neutral pH with NaHCO3. *Gyrodactylus* on each individual were counted using a stereomicroscope, however the three species infecting guppies (*G. turnbulli*, *G*. *poecilia*, *G. bullatarudis)* are indistinguishable while on the skin (Harris 1986; Cable & van Oosterhout 2007), and so as in previous studies (Cable & van Oosterhout 2007; Fraser & Neff 2010), were not distinguished. Because I focused on population level, and not individual level correlates among fitness related traits, infection was quantified only as *Gyrodactylus* prevalence (percentage of infected fish in a population; Bush *et al.* 1997).

Microsatellite and MHC data were only available for male individuals collected in 2010, but colour and *Gyrodactylus* infection data were only available for individuals sampled in 2009. However, I believe that comparisons among these data types across successive years is still valid because: (1) MHC and microsatellite polymorphism were stable in numerous temporal replicates across multiple populations used in this study (unpublished data, and Baillie 2012), and so allele frequencies are not believed to be significantly different between 2009 and 2010. (2) *Gyrodactylus* prevalence and coloration was stable between 2009 and 2010 in the study populations (Gotanda *et al.* 2013; Gotanda & Hendry 2014).

Molecular methods

A 209 bp amplicon of the MHC IIb locus was PCR amplified, Illumina sequenced, and subsequently genotyped in 707 guppies, as previously outlined (Chapter 2; Chapter 3; Lighten *et al.* 2014a; b). All samples were additionally genotyped at 10 polymorphic microsatellite loci using *P. reticulata* specific primers (Watanabe *et al.* 2003; Paterson *et al.* 2005; Shen *et al.*

2006; Baillie 2012, Table S4.1, Appendix 2). DNA was amplified via PCR in 5µl volumes comprising 10-50ng DNA, 0.5µl 10x ThermoPol PCR buffer (20 mM Tris-HCl, 10 mM KCl, 10 mM $(NH_4)_2SO_4$, 0.1 % Triton X-100), 200µM dNTP, 200µM fluorescently labelled forward primer, 200µM reverse primer, and 0.5U *Taq* DNA polymerase (New England BioLabs). PCR amplification consisted of the following: 4 min at 95°C, 30 cycles of 30s at 95°C, 30s at locus specific annealing temperature (Table S4.1, Appendix 2), 30s at 72°C, and 3 min at 72°C. PCRs were carried out in Eppendorf Mastercycler ep thermal cyclers. Microsatellite PCR products were visualized by electrophoresis on 8% denaturing polyacrylamide gels run on a LI-COR IR^2 DNA analyzer at 50°C. All gels included positive control samples, redundant samples, and a molecular weight size standard ladder. All analyses were conducted in the R statistical package (R Development Core Team 2011) unless otherwise stated.

I classified MHC IIb alleles into functional supertypes (MHC-ST) by amino acid polymorphism at the guppy specific peptide-binding region (PBR) (Chapter 3, Lighten *et al.* 2014a). The PBR is under strong directional selection and is the adaptive interface between pathogen recognition and the host immune response. Therefore, PBR diversity should reflect functional differences among alleles. The PBR of each allele was numerically characterized based on the physicochemical properties of each amino acid (Sandberg *et al.* 1998; Doytchinova *et al.* 2004; Doytchinova & Flower 2005), and were clustered using Discriminant Analysis of Principle Components (DAPC) with the *adagenet* package (Jombart 2008). Supertype classification avoided introducing missing data points into correlation analyses where the presence of particular alleles varied greatly among populations, but the presence of MHC-STs were more consistent (see Results).

Population genetic diversity

Locus affiliations of MHC alleles are unknown in guppies (Llaurens *et al.* 2012; Chapter 3; Lighten *et al.* 2014a) so traditional measures of allelic richness cannot be applied. I estimated population level MHC allelic richness (MHC-A_r) using a bootstrapping approach to account for

different population sample sizes. I randomly sub-sampled 10 alleles (as each guppy may have up to five loci; see Chapter 3; Lighten *et al.* 2014a, and Results) from among all individuals within a population and counted the number of unique alleles. I repeated sub-sampling with replacement 1000 times and calculated the mean number of unique alleles sampled. This provided unbiased relative estimates of MHC-A_r in each population. Using the same approach I also calculated MHC-ST richness (MHC-ST_r) within each population.

Microsatellite genotypes were checked using *Micro-Checker v.2.2.3* (van Oosterhout *et al.* 2004). For each population, *GENEPOP v.4.0.10* (Raymond & Rousset 1995; Rousset 2008) was used to estimate frequency of null alleles at each locus. All 10 loci were checked for selection using *LOSITAN* (Beaumont & Nichols 1996; Antao *et al.* 2008), which suggested that one of the ten loci (Pret-46) did not conform to expectations under neutrality. Moreover, inclusion of this locus resulted in inferences of population structure that were bio-geographically implausible and contradictory to those previously reported in guppies (e.g. Willing *et al.* 2010, Baillie 2012) and so was removed. Population level microsatellite richness (Micro-A_r) was calculated in the same manner as with MHC polymorphism.

Male guppy colouration

Full details regarding collection of colour data are given in (Gotanda *et al.* 2013). Briefly, guppy traits were quantified from photographs of 723 male fish sampled in 2009 only. Colour metrics of male fish were quantified from photographs based on classification of individual colour spots on the body and caudal fin into one of eight categories (modified from Endler 1991; Kemp *et al.* 2008; Millar & Hendry 2012) in *Image J* (Schneider *et al.* 2012): Black, fuzzy black, orange (including red), yellow, blue (including purple), green, violet, blue, and silver. For each fish, the total area of each colour was divided by the total fish area (body area + caudal fin area) to yield relative area of a given colour. The population level mean for each colour trait (area, and number of spots) was calculated and used in further analyses.

Effect of predation level, and drainage on guppy trait variation

To test whether predation level had a significant effect, I used a Wilcoxon rank-sum test for each trait of interest (MHC-A_r, MHC-ST_r, Micro-A_r, MHC-ST frequencies; colour area and number of colour spots, and *Gyrodactylus* prevalence), with populations separated by either high or low predation. The same analysis was repeated, but instead populations were classified by drainage. Despite its location in the Oropouche drainage, guppy populations from the Turure river were classified with populations from the Caroni drainage, as they represent a relatively recent introduction (1957, Haskins) from the Caroni drainage (Shaw *et al.* 1992; Suk & Neff 2009; Willing *et al.* 2010). Because only two true Oropouche-type guppy populations remained, both from the Quare River, inter-drainage comparisons of trait variation were only conducted between the North Slope and the Caroni drainage.

Correlations between genetic diversity, colouration, and Gyrodactylus prevalence

All uninfected populations were excluded from analyses of the relationships between parasites, colour, and MHC. I also excluded one population (El Cedro-1) with low infection prevalence from further analysis, as parasite prevalence was an order of magnitude lower than that of other infected populations. This reduced prevalence may have been a sampling artifact, or due to natural demographic stochasticity. All further analyses were conducted using the R package *ade4 v1.5-1* (Dray & Dufour 2007) unless otherwise stated. I assessed the variation among the population mean for each colour trait using a principal components analysis (PCA), which indicated co-variation among the total colour area and the number of spots of five colours (violet, green, silver, yellow, and blue). I retained only measures of area for further analysis of these colours. The correlation between two data matrices, which collectively contained three types of data, was assessed by co-inertia analysis (COIN, Doledec & Chessel 1994) to test if functional genetic diversity was correlated with traits associated with indicating fitness. Data matrix (1) contained MHC-ST frequencies for each population, and data matrix (2) contained colour trait means and *Gyrodactylus* prevalence for each population. COIN is very robust

against autocorrelation (Lamaze *et al.* 2014), compared to other similar approaches (e.g. Mantel test), and derives from studies comparing phenotypic and environmental variables (Doledec & Chessel 1994). A PCA was conducted on each data matrix (i.e. 1 and 2), and COIN (COIN[1]) assessed the global variation among PCA axes between the PCA outputs for data matrix 1 and 2, using 1000 bootstrap replicates. Where a strong correlation was indicated between individual traits of interest from data matrix 1 and 2 (e.g. between the frequency of a particular supertype and a particular colour), a separate one-tailed Pearson's correlation coefficient (PCC) was calculated. The procedure was repeated using the data matrix (1) MHC-A_r, and MHC-ST_r, and (2) male colouration and *Gyrodactylus* prevalence (COIN[2]). Where significant correlations between metrics of genetic diversity and colouration existed in infected populations, they were also examined in non-infected populations. Finally, I fitted separate linear models with MHC-A_r, and MHC-ST_r, as dependent variables and Micro-A_r as an independent variable, across all populations (including non-infected). Using Micro-A_r as a null model of neutral evolution, this tested whether demographic processes affected MHC diversity, assumed to be under strong selection (Bernatchez & Landry 2003).

Results

Identifying MHC polymorphism

A total of 1 634 085 contigs passed pre-processing (mean >Q.30; 99.99% accuracy). Of 707 samples for which genotyping was attempted, 72 (10%) were excluded from further analyses because PAs could not be confidently separated from artifacts, leaving 635 genotyped amplicons that had individual depths of 281x – 13,120x (mean 2391x ± 1380). Among these, 159 MHC IIb PAs were identified, which translated into 120 unique polypeptides.

Across all 158 PAs observed, 77 PAs were novel (GenBank: KR870052-KR870125) and 81 PAs had been characterized previously (Llaurens *et al.* 2012; Chapter 3; Lighten *et al.* 2014a). Among PAs, 76 were shared across at least two populations, 82 were unique to single

populations (private alleles), and the total number of alleles within each population (A_p) varied between 4 and 35 (Table S4.1, Appendix 5). I observed 87 rare PAs, each within a single individual. One to nine PAs were observed per individual guppy (mean 2.385 ± 1.216, Figure S4.2, Appendix 2). The range of A_i measures also varied among populations (mean=3.28, range= 1-9; Table 4.1). Genotype repeatability between sequencing runs was 95.4%.

By clustering PAs based on functional similarity of amino acids constituting the PBR, I identified 12 MHC-STs (ST-1 to ST-12; Figure S4.3-4.4, Appendix 2, Table S4.2, Appendix 5), and the number of alleles constituting each supertype varied (mean=13.16 ± 5, range=5-22, Figure S4.4, Appendix 2, Table S4.2, Appendix 5). The number of MHC supertypes observed within individuals (MHC-ST_i) ranged from one to six (Mean 2.81, Table S4.1, Appendix 5). In most individuals (99.38%) each supertype was represented by a maximum of two unique MHC alleles (Table S4.3, Appendix 5). Four samples from the same population (Aripo-2) each had three alleles that belonged to ST-9. The number of supertypes also varied between populations (*STp*; mean= 7.19 ± 1.96, range=4-10, Table S4.1, Appendix 5).

Linear models showed a significant positive relationship between MHC-A_r and Micro-A_r across all populations (P=0.001, R^2=0.41). The relationship between MHC-ST_r and Micro-A_r among all populations was not significant (P= 0.289, R^2=0.01) (Figure S4.5, Appendix 2). This suggests that variation in MHC-A_r is strongly influenced by demographic processes (such as genetic drift) whereas variation in MHC-ST_r is not. As such the remaining analysis used supertypes as the metric of MHC diversity.

Effect of predation level, and drainage on trait variation

Across all populations (both infected and uninfected) Micro-A_r was significantly higher in HP than the LP sites (Wilcoxon rank sum test: P=0.010, Table 4.2). Remarkably, HP and LP populations did not differ significantly in MHC-ST_r but drainages did (P=<0.001, Table 4.2), with guppy populations in the North Slope displaying lower MHC-ST_r than the Caroni (Figure 4.1). Populations in the North Slope displayed significantly more orange (P=0.001) and yellow body area (P=0.018), and more fuzzy black spots (P=0.001), which, importantly varied very little between HP and LP sites (Table 4.1, Figure 4.2-4.4).

Gyrodactylus were observed in 14 of 21 populations (Table 4.1, Table S4.4, Appendix 5) and one population (El Cedro-1) had a parasite incidence that was an order of magnitude lower than the 13 remaining infected populations. Of the remaining individuals from which MHC IIb genotypes were obtained, 167 (29.3%) were infected with *Gyrodactylus*. Wilcoxon rank sum test showed that variance in *Gyrodactylus* prevalence among populations was significantly correlated with predation level (P= <0.001, Table 4.2).

Correlations between genetic diversity, colouration, and Gyrodactylus prevalence

The COIN analysis between MHC-ST frequencies, male colour and *Gyrodactylus* prevalence (COIN[1]) revealed no significant correlation between the data matrices (global co-inertia coefficient = 0.49, P=0.167), which suggests that the strength of the relationship between individual MHC-STs, colour traits, and parasites varied among populations (Figure S4.6, Appendix 2). Interactions among individual MHC-ST frequencies, colour traits, and infections were observed when co-variation among each factor was examined independently. *Gyrodactylus* prevalence was negatively correlated with orange area (P=0.021, R^2=0.32, Figure 4.5a), fuzzy black area (P=0.012, R^2=0.38, Figure 4.5b), and yellow area (P=0.021, R^2=0.32,

Figure 4.5c), as well as the frequency of ST2 (P=0.017, R^2=0.34, Figure 4.6a), and ST11 (P=0.012, R^2=0.38, Figure 4.6b). The frequency of MHC-ST2 was positively correlated with orange area (P=0.007, R^2=0.43, Figure 4.7a), and yellow area (P=0.023, R^2=0.31, Figure 4.7b). Similarly, MHC-ST11 frequency was positively correlated with fuzzy black area (P=0.035, R^2=0.27, Figure 4.7c). In some rivers there was a similar interaction between MHC supertypes, colour and *Gyrodactylus* prevalence despite predation level, (e.g. M3 (LP) and M4 (LP); Y1 (LP) and Y2 (HP); AP1 (LP) and AP2 (HP) (Figure S4.6, Appendix 2).

Secondly, the COIN analysis between (1) MHC-A_r, MHC-ST_r, and (2) colouration and *Gyrodactylus* prevalence ($COIN^2$) revealed a significant correlation between the two data sets (Global co-inertia RV coefficient = 0.37, simulated P=0.043), and important fitness correlated traits (Figure S4.7, Appendix 2). *Gyrodactylus* prevalence was positively correlated with MHC-ST_r (P=0.001, R^2=0.59, Figure 4.8a) across infected populations. Remarkably, MHC-ST_r was negatively correlated with orange body area (P=<0.001, R^2=0.64, Figure 4.8b), and yellow body area (P=0.006, R^2=0.45, Figure 4.8c). Notably, the relationships between MHC-ST_r *Gyrodactylus,* and colour, seem to be governed by variation in these traits between drainages (Figure 4.8, Table 4.2).

Discussion

Male guppy colouration can evolve in response to female mate choice, presumably because it is a honest indicator of individual fitness (Houde 1997). However, this effect can be counteracted by the benefits of inconspicuous colouration when faced with increased predation (Endler 1991; Houde 1997). Freed from predation pressure, guppies in low predation (LP) sites should consistently display more carotenoid-based colouration, but this is not always the case (Gotanda *et al.* 2013; Gotanda & Hendry 2014). Here I have shown that fitness related colouration of guppies at the population level varies more between drainages than it does according to the classic dichotomous model of predation levels across Trinidad, and further,

that this variation is correlated with MHC polymorphism and parasite prevalence. Specifically, particular MHC polymorphisms are associated both with decreased *Gyrodactylus* prevalence and increases in population mean orange, yellow, and fuzzy black. Moreover, MHC supertype richness (MHC-ST_r) is also related to *Gyrodactylus* prevalence and colour patterns. Notably, correlations between MHC and colouration were absent in non-infected populations. Interactions between MHC polymorphism, *Gyrodactylus* prevalence, and male colouration among populations are consistent with parallel evolution related to variable selection imposed by pathogens across drainages. Although generally not considered in studies of guppy evolution, MHC and parasite diversity are likely important components that contribute to the wide spread adaptation observed in this species.

Is predation driving parallel evolution in guppy colour?

Surprisingly, I found no significant differences in the population mean area and number of spots of any colour trait between predation levels. This is contrary to expectations suggested by previous studies that compared the effects of predation on individual level variation in experimental mesocosms (Endler 1991), and among individuals of populations within the same river (Weese *et al.* 2010; Millar & Hendry 2012; Gotanda & Hendry 2014). In particular, variation in mean orange, and yellow body area (which are believed to indicate health, and susceptibility to predation) was minor and non-significant between HP and LP sites, but substantial (and significant) between drainages. Increased orange area in North Slope populations compared to those in the Caroni has been observed previously, and speculated to be a consequence of reduced predation pressure in this region compared to other drainages (Rodd & Reznick 1991), but this has not been substantiated. I show that this drainage-level trait co-varies with MHC and parasites within drainages. Moreover, the patterns of variation between HP and LP sites in fuzzy black area (which only significantly varied between regions) are reversed between the Caroni drainage and North Slope. The effect of predator driven selection on colouration appears to be inconsistent among populations (and particularly between the Caroni drainage and North Slope), and this fits with observations of non-parallel

evolution among guppy populations (Fitzpatrick *et al.* 2014; Gotanda & Hendry 2014). This suggests that other biological/ecological factors have an impact on species-wide variation of important colours relating to natural selection in guppies.

Similarly, MHC-ST_r did not vary significantly between predation levels, but did between drainages. MHC-ST_r was not correlated with microsatellite allelic richness (Micro-A_r), yet MHC allelic richness (MHC-A_r) was. The fact that MHC-ST_r is independent of Micro-A_r suggests that variation in MHC supertype diversity is less susceptible to demographic processes than MHC alleles. The significant variation in Micro-A_r (subject to drift and gene flow) between HP and LP site is likely a consequence of the larger population sizes in downstream HP environments, and the higher rate of gene flow from upland populations (Crispo *et al.* 2006; Barson *et al.* 2009; Suk & Neff 2009; Willing *et al.* 2010). The difference in MHC-ST_r between drainages is likely explained by variation in pathogen-mediated selection. The reduction in *Gyrodactylus* prevalence in populations with lower MHC-ST_r may represent directional selection towards more focused adaptive immunity against a smaller parasite community; however further work is needed to test this hypothesis. Therefore, supertypes may be more important measures of population and individual level MHC functional diversity than alleles. Signals of natural selection purely at the MHC allelic level could potentially be confounded by demographic process across guppy populations of different sizes (high or low predation).

Similar to Micro-A_r, *Gyrodactylus* prevalence was also significantly greater in HP than LP sites. The higher prevalence of infection in HP sites is most likely a consequence of larger host populations in the larger downstream river habitats, which receive more infected immigrants to sustain pathogen numbers. Moreover, the anti-predation strategy of tight shoaling among guppies in HP environments may facilitate easier transmission of parasites between individuals (Johnson *et al*. 2011). Similarity in patterns of *Gyrodactylus* prevalence are consistent across

drainages and this suggests that they may exert a similar degree of selection pressure on guppies.

Parallel patterns of phenotypic and genetic variation relating to parasite driven natural selection and mate-choice driven sexual selection

Frequencies of MHC-ST-2 and ST-11 were strongly negatively correlated with *Gyrodactylus* prevalence. A previous study (Fraser & Neff 2010) also observed a negative association between *Gyrodactylus* infection prevalence in Trinidadian guppies and the frequency of a particular MHC IIb supertype (supertype 'a'). Based on nucleotide sequences, alleles of the '*Gyrodactylus* resistance' supertype-a (Fraser & Neff 2010) form a clade with alleles in ST-11, which I identified as being associated with reductions in *Gyrodactylus* prevalence (Figure S4.4, Appendix 2). In populations where MHC-A_r and MHC-ST_r were greatly reduced (e.g. Marianne-3, and Marianne-4), all individuals had the same three alleles (Table S4.3, Appendix 5), which each represented a unique MHC-ST. Notably, two of these alleles represented ST-2, and ST-11, and this supports the hypothesis that a reduction in MHC population level diversity may be a consequence of directional selection for polymorphism involved in parasite resistance (Monzón-Argüello *et al.* 2013). Evidently, *Gyrodactylus* has a similar effect on MHC polymorphism in all infected populations, and this corroborates the observation that this parasite species complex may impose homogeneous selection pressures across large spatial scales (Fraser & Neff 2010). However, the fact that guppies express multiple other MHC supertypes among populations suggests that a fitness trade-off exists between ST-2, ST-11, and other supertypes, which presumably function to combat other parasite species. This means that the frequency of supertypes among populations is likely governed by the requirement for immunological defense against variable parasite communities, where individuals are required to express an effecting array of supertypes in relation to the number of potential parasite species that can infect them. It is therefore somewhat surprising that given the multiple species of *Gyrodactylus*, and their probable high-levels of cryptic diversity among isolated drainages (Xavier *et al.* 2015), that when considered as a single complex (species or strain were not

differentiated in this study) significant relationships among their prevalence, colour, and MHC polymorphism are detected. This suggests that individual MHC supertypes evolve efficient functionality against broad but similar parasitic phenotypes.

Across all populations ST-2, and ST-11 frequencies were positively correlated with a significant increase in the colour area of fuzzy black, orange, and yellow. This is consistent with a previous finding that *Gyrodactylus* infections were negatively correlated with carotenoid intensity in laboratory populations of guppies (Kolluru *et al.* 2006). Although intensity of carotenoid pigmentation may be an honest plastic signal of male health based on nutrition (Grether *et al.* 1999), the area, and number of colour spots has a genetic basis (e.g. Tripathi *et al.* 2009). Because particular colour genes may confer some selective advantage through mate choice among populations, they may possibly become linked to other important traits that increase fitness though natural selection (Gordon *et al.* 2012). Indeed a recent study demonstrated that one particular MHC-ST in baboons (*Papio ursinus*) was related to reduced individual condition, and the size and shape of sexual swelling during female estrous, which serve as secondary sexual signals (Huchard *et al.* 2010).

Upon visual examination of correlations among MHC diversity, colour, and *Gyrodactylus* prevalence there appears to be a strong effect of drainage in governing multiple correlations. However, drainage was not included as a factor in correlative models, as combined with the small number of populations examined this led to over parametrization and weakening of correlations between specific traits. However, Wilcoxon tests independently demonstrated which of these traits varied significantly among drainages, and when compared to correlative analyses, the effect of drainage on trait covariation can be assessed.

This study establishes a relationship among MHC-supertypes, and MHC supertype richness, with parasite infections and secondary sexual colouration. This finding is consistent with predictions stemming from the Hamilton-Zuk, or good genes, hypothesis, which posits that

genetic diversity is affected by mate choice for sexual ornamentation that signifies parasite resistance. The fact that female guppies apparently choose mates based on visual colour cues, and not chemosensory MHC related olfactory cues (Houde 1997; Archard *et al.* 2008), leads to speculation that MHC polymorphism, which confers increases in relative fitness, is associated with colour traits. The hypothesis that MHC and body colours are associated suggests that sexual selection plays a large role in shaping population frequencies of MHC alleles, given the established importance of male guppy colouration in influencing female mate choice (e.g. Wedekind & Penn 2000; Milinski 2006). It is likely that natural selection pressures exerted by parasites and predators both influence processes of sexual selection and this can vary among drainages. Particular MHC polymorphisms, which confer resistance to parasites, increase in a population because of fitness benefits. Individuals less energetically burdened by parasites are able to spend more time devoted to courtship over foraging (Kolluru *et al.* 2006), and so sexual selection could operate to increase those colours associated with female preference for indicators of male fitness. These findings are contrary to those of a study that explicitly tested the Hamilton-Zuk hypothesis at the individual level in natural guppy populations, and found no association between *Gyrodactylus* infections and male color (Martin & Johnsen 2007). It may be that within population variation in male color and parasite infections is so large that meaningful relationships between colour and infections are difficult to detect. Moreover, my results suggest that correlations in support of the Hamilton-Zuk hypothesis can be governed by variation among drainages, and so likely result from historical effects driving local adaptation. While disentangling the relative contributions of each type of selection will be difficult, sexual selection is a dominant force in shaping MHC diversity across diverse taxa (Winternitz *et al.* 2013). In guppies, the observed patterns of MHC polymorphism and male colouration likely result from some complex interaction among spatially varying processes of sexual selection and natural selection driven by predators and parasites.

Conclusion

I show significant interactions between MHC polymorphism, parasite infection, and colour traits related to survival and mate choice. To my knowledge this is the first-time such relationships have been observed among these three major features related to fitness. While the difficulties associated with correlative analyses mean that cause and effect of these relationships cannot be definitively identified without further experimental work, they do show that variation in colouration and genetic polymorphism are likely governed by a complex interaction of different drivers of natural selection. The most conservative explanation for such patterns is that immunological pressures exerted by parasites vary over space (among populations or drainages), and this directly affects the strength of selection on colour signals. Thus the correlation between MHC polymorphism and colour may be an indirect consequence of how well particular polymorphism combats parasite infections, and thus MHC polymorphism that confers high immunocompetence will lead to increases in colours that indicate increased health. Aspects of ecology alongside predation pressure likely drive local and parallel adaptations of guppy populations across large geographic scales, of which parasites likely play a major role.

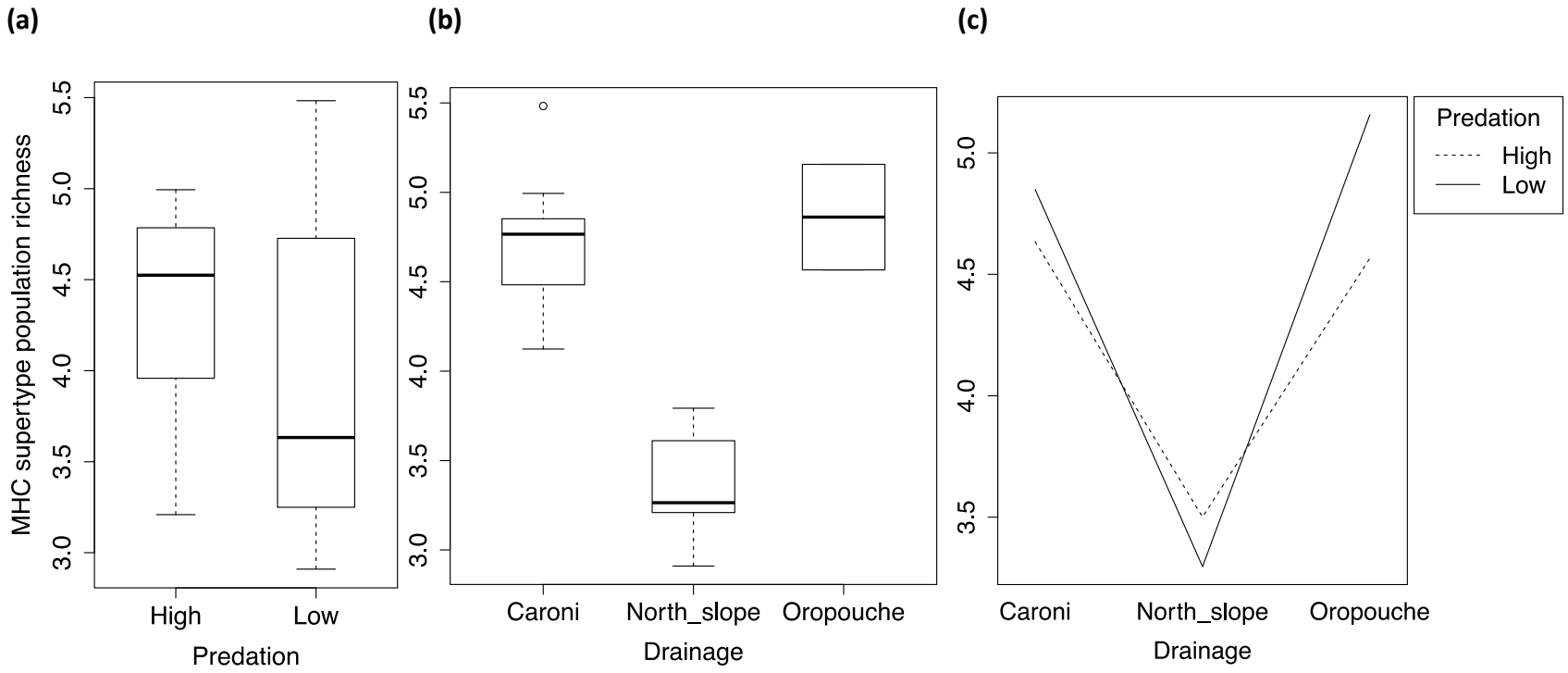

Figure 4.1. Variation in MHC supertype richness (MHC-ST_r) between (a) high and low predation sites, and (b) drainages. Variation in the Oropouche drainage (b) was not included in significance tests among drainages (Table 4.2) as it was calculated from just two populations and so should be interpreted with caution. A two way interaction plot (c) shows how mean MHC-ST_r varies among populations of different predation strengths among drainages, with similar caution needed regarded interpretation of Oropouche variability.

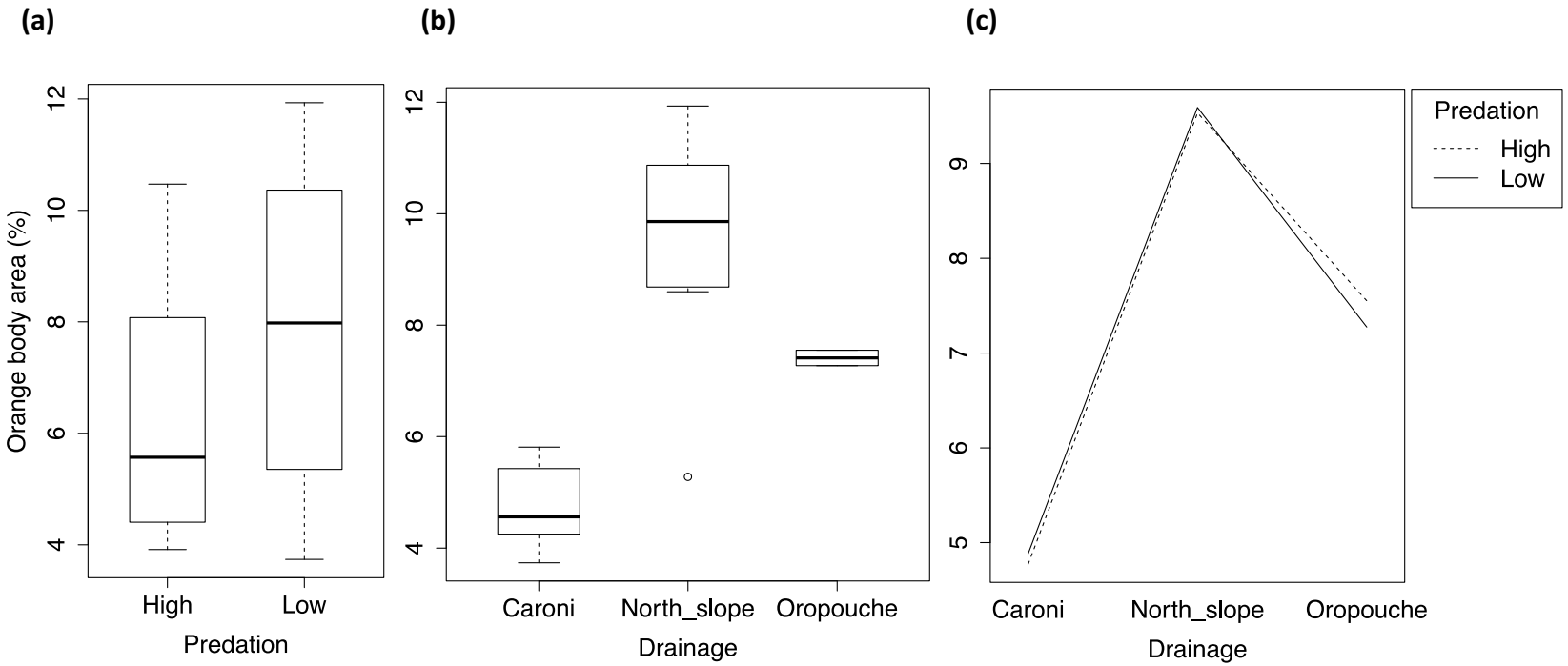

Figure 4.2. Variation in orange body area (%) between (a) high and low predation sites, and (b) drainages. Variation in the Oropouche drainage (b) was not included in significance tests among drainages (Table 4.2) as it was calculated from just two populations and so should be interpreted with caution. A two way interaction plot (c) shows how mean orange area varies among populations of different predation strengths among drainages, with similar caution needed regarded interpretation of Oropouche variability.

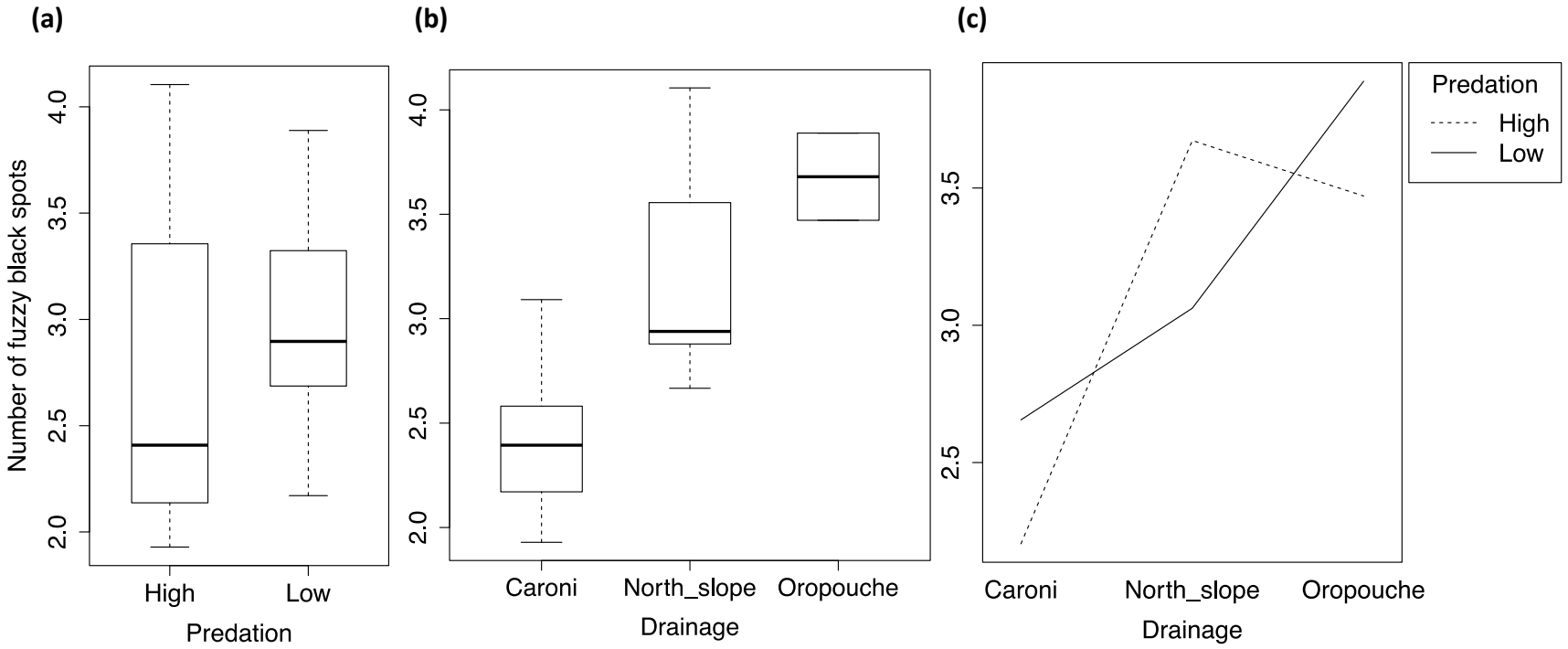

Figure 4.3. Variation in the number of fuzzy black spots between (a) high and low predation sites, and (b) drainages. Variation in the Oropouche drainage (b) was not included in significance tests among drainages (Table 4.2) as it was calculated from just two populations and so should be interpreted with caution. A two way interaction plot (c) shows how mean number of fuzzy black spots varies among populations of different predation strengths among drainages, with similar caution needed regarded interpretation of Oropouche variability.

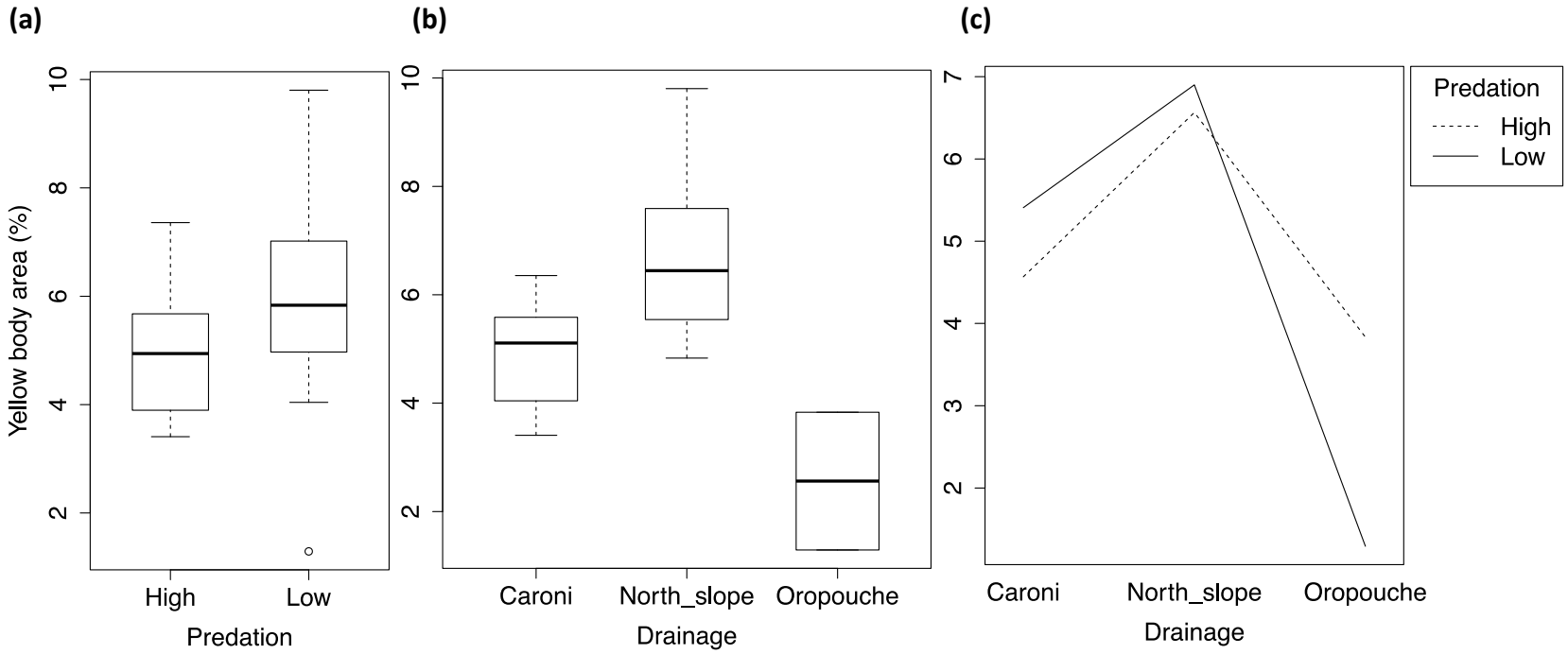

Figure 4.4. Variation in yellow body area between (a) high and low predation sites, and (b) drainages. Variation in the Oropouche drainage (b) was not included in significance tests among drainages (Table 4.2) as it was calculated from just two populations and so should be interpreted with caution. A two way interaction plot (c) shows how mean yellow area varies among populations of different predation strengths among drainages, with similar caution needed regarded interpretation of Oropouche variability.

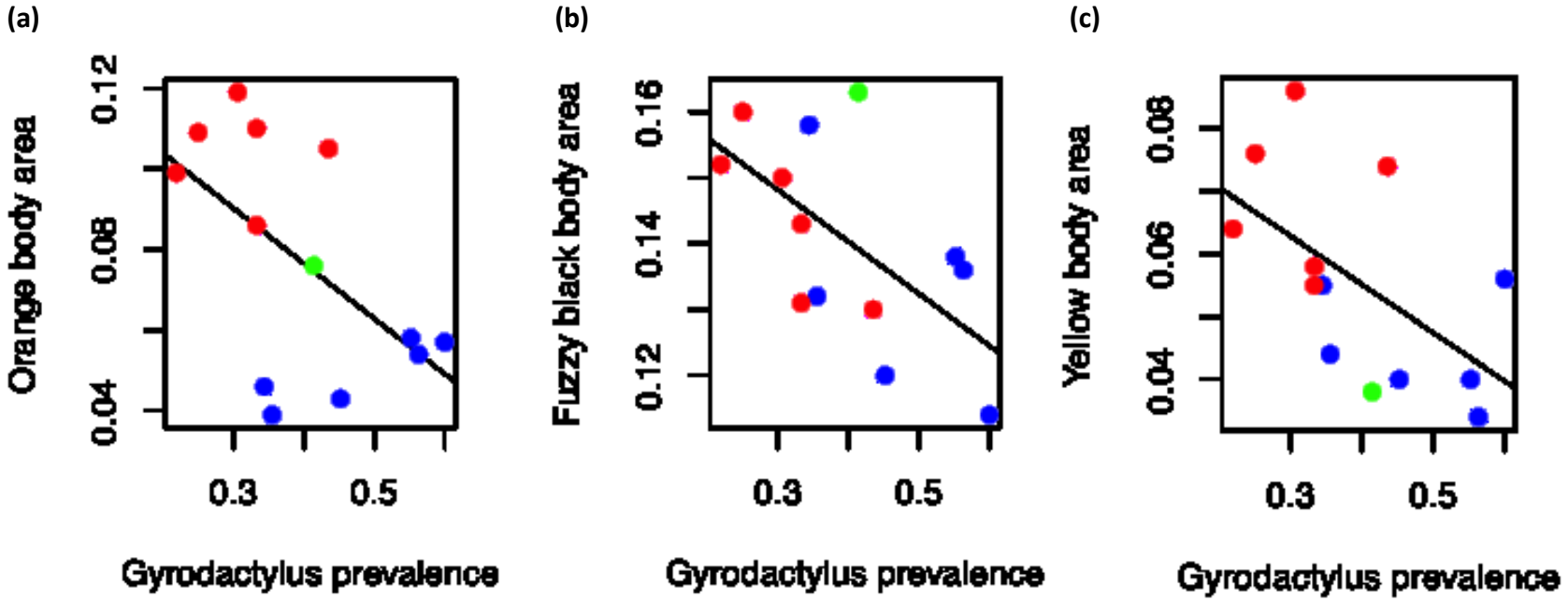

Figure 4.5. Pearson's correlation coefficients demonstrated significant negative association between *Gyrodactylus* prevalence and (a) orange area (P=0.021, R^2=0.32), (b) fuzzy black area (P=0.012, R^2=0.38), and (c) yellow body area (P=0.021, R^2=0.32), In some cases it is evident that the variation in relationships among traits (e.g. a) varies spatially among drainages: Caroni populations (blue), North Slope populations (Red), Oropouche population (Green).

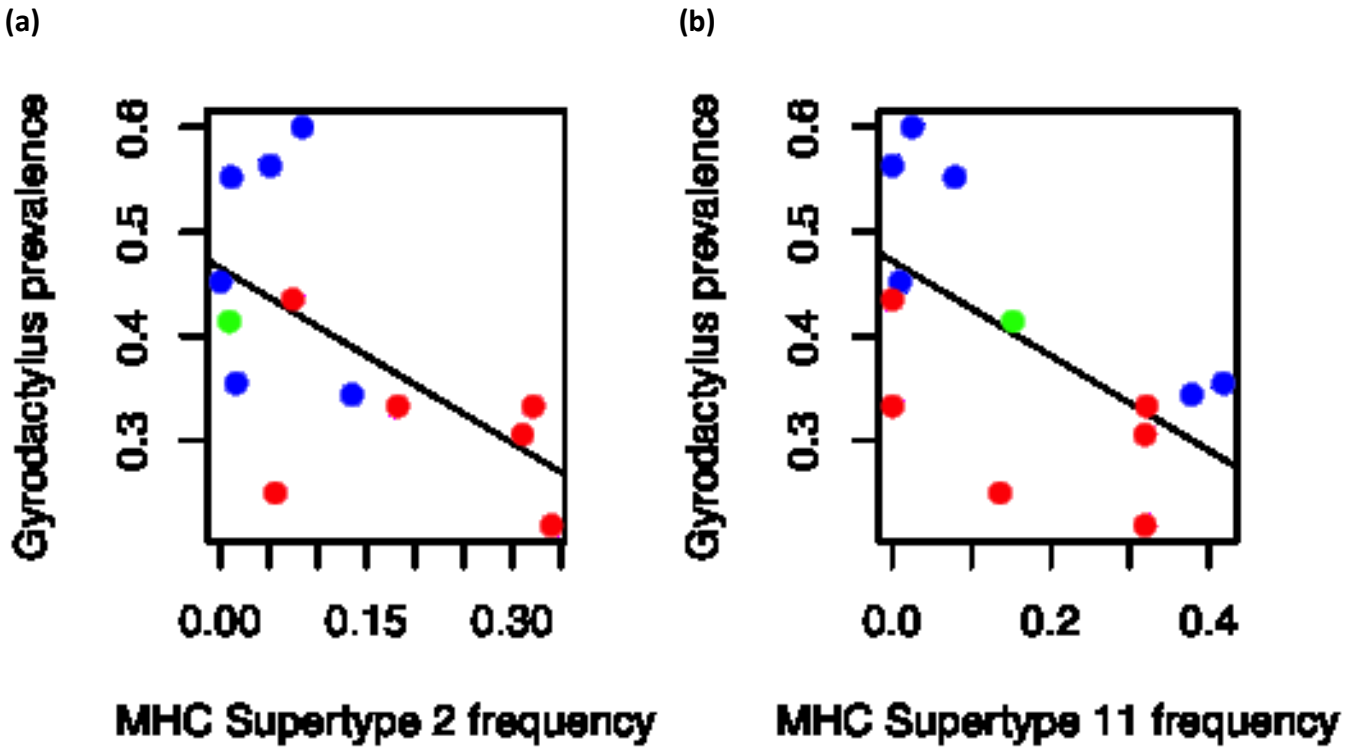

Figure 4.6. Pearson's correlation coefficients demonstrated significant negative association between *Gyrodactylus* prevalence and (a) MHC-ST2 frequency (P=0.017, R^2=0.34), and (b) MHC-ST11 frequency (P=0.012, R^2=0.38). Caroni populations (blue), North Slope populations (Red), Oropouche population (Green).

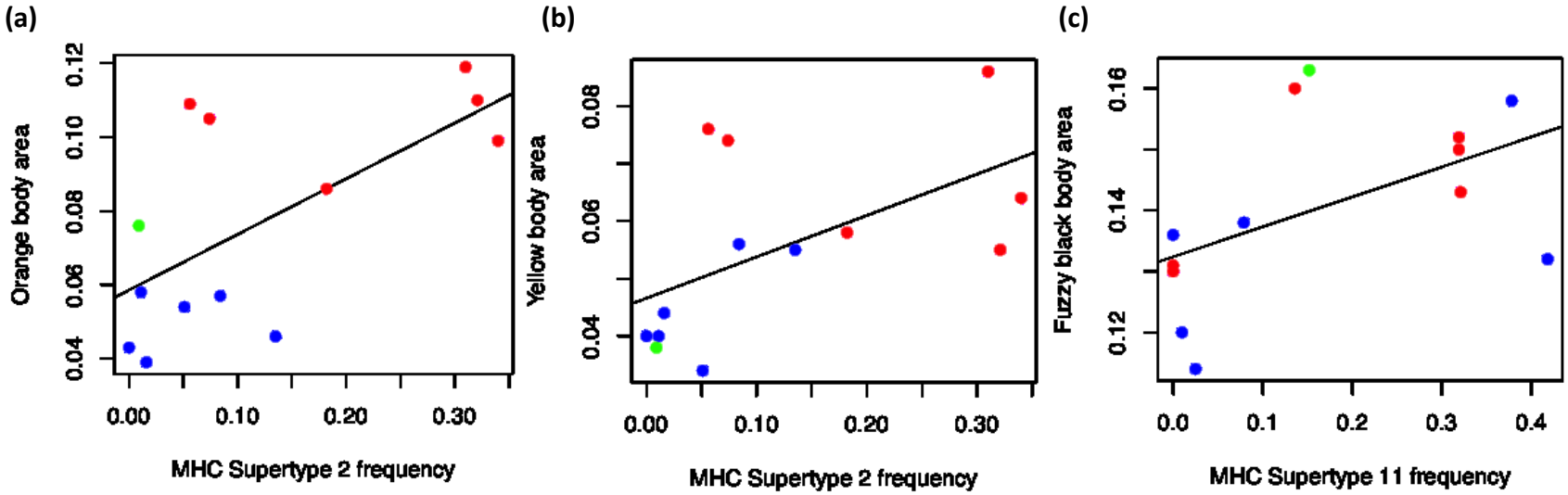

Figure 4.7. Pearson's correlation coefficients demonstrated significant positive association between MHC-ST2 frequency and (a) orange area (P=0.007, R^2=0.43), and (b) yellow area (P=0.023, R^2=0.31). Similarly, MHC-ST11 frequency was positively associated with (c) fuzzy black area (P=0.035, R^2=0.27).), In some cases it is evident that the variation in relationships among traits (e.g. a) varies spatially among drainages: Caroni populations (blue), North Slope populations (Red), Oropouche population (Green).

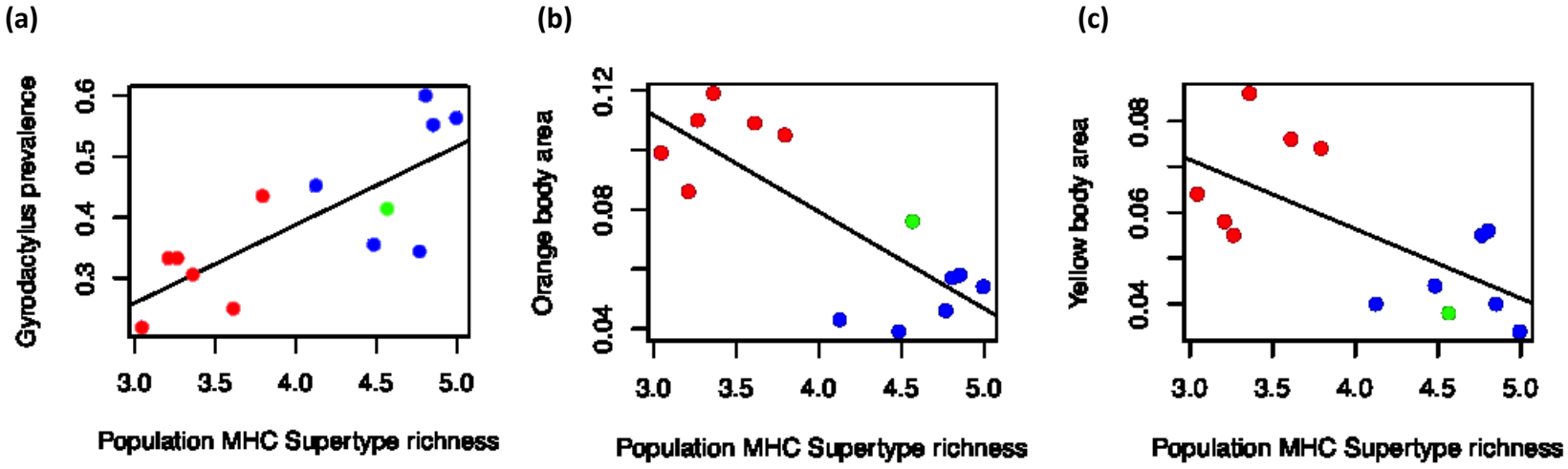

Figure 4.8. Pearson's correlation coefficients demonstrated significant positive association between *Gyrodactylus* prevalence and (a) MHC-ST_r (P=0.001, R^2=0.59). Conversely a significant negatively associated was observed between MHC-ST_r and (b) orange area (P=<0.001, R^2=0.64), and (c) yellow body area (P=0.006, R^2=0.45). The variation in relationships among traits (e.g. a) varies spatially among drainages: Caroni populations (blue), North Slope populations (Red), Oropouche population (Green).

Predation	Drainage	Population	Mean A_i	Mean ST_i	Range A_i	Range ST_i
High	Caroni	Arima-1	3.966	3.133	2-9	1-6
Low	Caroni	Arima-2	3.2	3	1-6	1-6
Low	Caroni	Aripo-1	3.068	2.689	1-5	1-4
High	Caroni	Aripo-2	4.875	3.812	2-9	2-6
Low	Caroni	El Cedro-1	3.366	3.1	1-5	1-4
High	Caroni	El Cedro-1	3.843	3.187	1-7	1-5
High	Caroni	Guanapo-1	3.903	3.225	2-6	2-5
Low	Caroni	Guanapo-2	3.75	3.166	1-6	1-5
High	North Slope	Damier-1	3.311	2.577	1-7	1-5
Low	North Slope	Damier-2	2.642	2.214	1-7	1-5
Low	North Slope	Marianne-10	2.148	1.851	1-3	1-3
Low	North Slope	Marianne-16	3.032	2.741	2-6	2-5
Low	North Slope	Marianne-3	3.111	3.111	3-4	3-4
Low	North Slope	Marianne-4	2.937	2.937	2-4	2-4
Low	North Slope	Paria-7	3.625	3.187	2-6	2-4
Low	North Slope	Yarra-1	2.489	2.326	2-5	1-4
High	North Slope	Yarra-2	3.043	2.586	1-6	1-5
High	Oropouche	Quare-1	3.310	2.724	1-6	1-4
Low	Oropouche	Quare-2	3.117	2.588	1-6	1-5
High	Oropouche (Caroni type)	Turure-2	3.709	2.750	2-5	2-3
Low	Oropouche (Caroni type)	Turure-3	3.655	1-4	1-5	3

Table 4.1. Summary metrics of MHC allelic richness (MHC-A_r), and MHC supertype richness (MHC-ST_r).

Trait	Predation		Drainages	
Genetic diversity	*W*	*P*	*W*	*P*
Micro-A_r	88	0.010*	38	0.859
MHC- A_r	76	0.089	64	0.039*
MHC-ST_r	67	0.301	78	<0.001*
Supertype-1	51	0.961	35	0.576
Supertype-2	32.5	0.168	24	0.157
Supertype-3	53.5	0.938	45.5	0.662
Supertype-4	77.5	0.062	48.5	0.5
Supertype-5	52.5	1	59	0.112
Supertype-6	46	0.666	43.5	0.808
Supertype-7	57.5	0.666	39	0.916
Supertype-8	70	0.179	28	0.257
Supertype-9	73	0.137	54	0.250
Supertype-10	64	0.401	69	0.012
Supertype-11	34	0.204	41	1
Supertype-12	54.5	0.863	36	0.687
Colouration				
Black area	48	0.804	27	0.258
Fuzzy black area	40	0.413	24	0.161
Orange area	39.5	0.384	4	0.001*
Yellow area	34	0.210	14	0.018*
Blue area	51.5	1	23	0.133
Green area	57	0.750	60	0.093
Violet area	44	0.595	44	0.796
Silver area	77	0.075	53	0.297
Total n. spots	37	0.301	29	0.340
n. black spots	37	0.301	53	0.297
n. fuzzy spots	49	0.859	7	0.001*
n. orange spots	40	0.413	34	0.596
n. yellow spots	52	1	28.5	0.309
n. blue spots	34.5	0.218	33	0.545
n. green spots	58	0.697	73	0.002
n. violet spots	62	0.500	39	0.929
n. silver spots	39.5	0.384	55	0.222
Parasite infection				
Gyrodactylus prevalence	97.5	<0.001*	51.5	0.344

Table 4.2. Results of Wilcoxon rank-sum test tests indicate significant variation (P=0.05) of genetic, and colour traits, and parasite prevalence between levels of predation (denoted by *).

Chapter 5
Supertypes explain paradoxes and reveal cryptic processes of MHC evolutionary ecology: A new perspective

Abstract

Evolution of the Major Histocompatibility Complex (MHC) is driven by immunological adaptation to fast evolving parasites. However, it is still not fully understood why contradictory observations among studies (i.e. directional selection *and* balancing selection; natural selection *and* genetic drift; high allelic diversity *and* low allelic diversity) persist. I outline a new perspective on MHC evolution that explains these issues, by focusing on the largely overlooked significance of MHC supertypes (groups of similarly/identically functioning MHC alleles) in natural populations. I describe how population structuring of MHC allelic diversity is affected by neutral demographic processes, whereas supertype population structuring is not. The study of MHC supertypes in comparison with their constituent alleles reveals detailed cryptic processes of MHC evolution that cannot be inferred by the study of MHC alleles alone, as is traditional done. I provide the first evidence to suggest that strong stabilizing selection has operated on MHC alleles *within* loci specific supertypes over millions of years in both the guppy and its relative, the swamp guppy (*Poecilia picta*). I also suggest that balancing selection operates directly on loci (supertypes) to produce complex patterns of CNV both within and among populations. The spatial and temporal patterns that stabilizing selection generates in MHC allelic diversity can be erroneously interpreted as widespread divergent selection among populations when supertypes are not considered. I suggest that haplotypes of MHC supertype CNV are a central unit upon which balancing selection operates, and high levels of functional similarity among alleles within a supertype render individual allele frequencies susceptible to inter-supertype random genetic drift. Alleles that differ in fitness effects may rapidly change in frequency due to inter-supertype Red Queen processes. The culmination is a description of a new paradigm in the study of MHC evolution, which resolves multiple unexplained and commonly observed paradoxes, and explains the enigma of MHC trans-species polymorphism.

Introduction

Genes of the Major Histocompatibility Complex (MHC) have contributed much of what we know about genetic adaptation (Bernatchez and Landry 2003, Piertney and Oliver 2006). Over the past 30 years a paradigm has emerged, which states that evolution of these highly variable genes is driven by immunological adaptation to fast evolving parasites (reviewed in Spurgin and Richardson 2010), as explained by the Red Queen hypothesis (van Valen 1973). This hypothesis suggests that host and parasite co-evolve in an evolutionary arms race, where parasites continually evolve strategies to evade the host immune system, and the host evolves more efficient immunity against parasites. It is believed that strong extrinsic selection pressures from pathogen infections maintain diverse MHC polymorphism over large spatial and temporal scales, though balancing selection, in the form of negative frequency dependent selection (NFDS), overdominance (heterozygote advantage) and fluctuating selection (Spurgin and Richardson 2010). Variation in MHC polymorphism among populations is commonly interpreted to represent differential selection pressures from dynamic pathogen communities, which may fluctuate temporally, resulting in directional selection of MHC through Red Queen dynamics. Despite NFDS and overdominance being the most popular interpretations of processes governing MHC polymorphism, convincing empirical evidence is yet to emerge that supports their influence on MHC genetic diversity. Moreover, this interpretation presents somewhat of an unanswered paradox in the understanding of MHC evolution: How can balancing selection maintain MHC allele polymorphism over large spatial and temporal scales in concert with widespread local adaptation to different parasite communities?

Paradoxically, MHC allele frequencies can be greatly influenced by demographic (random) processes (e.g. genetic drift or migration, Kamath & Getz 2011; Sutton *et al.* 2011; Strand *et al.* 2012). This contradicts the central paradigm in that the MHC evolves under strong selection. Rather, this observation suggests that MHC population genetics is affected both by adaptive processes as well as demographic processes. Moreover, it has become apparent that species may have greatly reduced MHC allelic diversity (e.g. Radwan *et al.* 2010), and this can be caused by the effects of genetic drift (e.g. though a population bottleneck) outweighing the

strength of parasite mediated natural selection (Sutton *et al.* 2011). However, species with very few MHC alleles among populations (traditionally presumed to be less adapted to diverse pathogens) may appear to be just as fit as those that have many alleles (traditionally presumed to be critically adapted to pathogen communities) (Radwan *et al*. 2010). It is still not fully understood why these contradictory observations among studies (i.e. directional selection *and* balancing selection; natural selection *and* genetic drift; high allelic diversity *and* low allelic diversity) persist. Here I outline a new perspective on MHC evolutionary that explains the persistence of these issues, by focusing on the largely overlooked significance of MHC supertypes (groups of similarly/identically functioning MHC alleles) in natural populations.

It is the understanding of how the MHC interacts with antigens that reveals its role in countering pathogens (e.g. Wucherpfennig 2001). This may help elucidate how MHC genes and the proteins they encode adapt to counteract pathogens. However, these data are lacking in non-model species, and difficult to acquire. As such very little is known about the relative functional properties of MHC polymorphism in natural populations of most vertebrates. An alternative approach is to classify MHC alleles into supertypes based on the level of shared similarity in inferred functional characteristics, using bioinformatic approaches (Lund *et al.* 2004; Doytchinova *et al.* 2004; Doytchinova & Flower 2005, Chapter 4). In this approach, functional characteristics of MHC alleles are represented by the physicochemical properties of the amino acids that are translated from the nucleotide sequence. MHC variants are grouped either by clustering or principal components analysis, using the properties of amino acids at positions in the peptide binding region (PBR) that are under strong positive selection and thus best reflect the functional differences among alleles (See Chapter 4). Correlative analysis between the frequency of a particular MHC supertype and the degree of infection in a population then suggests its functional significance (See Chapter 4).

Although the common philosophy of MHC population level analyses aims to uncover patterns of local adaptation at the allelic level by simply counting alleles (implying that allelic diversity directly reflects functional diversity; so every allele should have a distinct function), with very limited analysis on the translated amino acid sequence (e.g. Bernatchez & Landry

2003; van Oosterhout *et al.* 2006b; Piertney & Oliver 2006; Oliver *et al.* 2009; Sutton *et al.* 2011; Eimes *et al.* 2011; Spurgin *et al.* 2011; Nadachowska-Brzyska *et al.* 2012; Winternitz *et al.* 2013), very few have adopted the premise of studying MHC evolution in the context of supertypes comprised of alleles which have very similar or identical functions. Nonetheless, it has recently become evident that MHC diversity represented by supertypes may reveal patterns of selection and relative fitness benefits in relation to parasite infections (e.g. Schwensow *et al.* 2007; Sepil *et al.* 2013a; b). The observation that demographic processes may less affect patterns of supertype diversity, compared to allelic diversity, suggests that they may better represent the units upon which selection operates at the MHC (Chapter 4). Understanding the interactions among processes governing MHC supertype evolution and those governing, more conventionally, individual alleles could provide an important new perspective on MHC evolution.

A conceptual framework put forward by van Oosterhout (2013) described how alleles of particular supertypes are likely to be confined to specific loci (at least in most cases), and therefore diverse MHC functionality (different supertypes) can be maintained at disparate loci even in instances when overall allelic diversity is degraded within loci (e.g. by inbreeding). In Chapter 4, I compared geographic patterns of MHC supertype and allelic diversity, neutral microsatellite diversity, and important fitness related measurements (male colouration, and parasite infection) in natural populations of the guppy (*Poecilia reticulata*). I described several key findings that fit with predictions stemming from van Oosterhout (2013): (1) In a single genotype, each supertype was represented (largely) by a maximum of two alleles, suggesting particular supertypes may be locus specific, as observed in other poeciliid fishes (Ellison *et al.* 2012), (2) MHC allelic richness was strongly correlated with microsatellite richness, but MHC supertype richness was not, suggesting that alleles are more affected than supertypes by demographic processes, and (3) the total number of supertypes per-individual varied within, and among populations, suggesting spatial (and likely temporal) differences in selection maintaining different patterns of MHC loci CNV and functional haplotypes (see Discussion).

Here I expand on these initial findings by comparing the geographic distribution of MHC alleles, MHC supertypes, and microsatellite diversity in guppy populations across a large geographic scale to investigate some important yet largely unresolved questions: What are the relative differences in processes that operate on MHC alleles and MHC supertypes, and importantly, can inferences of MHC evolution be unduly biased by focusing on just alleles? Resolving these issues will allow a clearer understanding of how apparent paradoxes in MHC diversity and evolution are observed in natural populations.

Methods

Sampling

Guppies were collected between 2008 and 2012 from 59 populations distributed among 39 rivers/lakes, across Trinidad, Tobago, Barbados, and Hawaii. Each fish was euthanized in 0.02 % Tricaine Methanesulfonate (Finquel MS-222; Argent Laboratories, Redmond, WA, USA) buffered to a neutral pH with NaHCO3, and then preserved in 100% ethanol. Sites were chosen to represent a wide geographic sample of populations across Trinidad, and like the site in Tobago, the presence of guppies here represents natural colonization from ancestral South American populations. It is unknown if guppy populations in Barbados represent a natural colonization from South America or a human mediated introduction, as is the case with Hawaiian populations that were established in the early 1920's. In addition to guppies, a small number of individuals of the closely related swamp guppy (*Poecilia picta*) were sampled from Trinidad. The last shared common ancestor between *P. reticulata* and *P. picta* was estimated at around ~21-22 mya (Meredith *et al.* 2011).

Molecular methods

The methods to generate the MHC sequence data, microsatellite data, and estimate genotypes are described in Chapter 3 and Chapter 4. However, this study sequenced samples (and replicate PCRs) among four independent sequences runs, compared to a smaller number of replicate PCRs among just two sequencing runs in previous chapters. Estimating MHC IIb

supertypes was also carried out in a similar fashion as in Chapter 4. However, use of the *diffNgroup* criterion within *adagenet* package (Jombart 2008; Jombart & Ahmed 2011) was not required. Because this study revealed many more alleles in a greater number of individuals (see Results) than in Chapter 4, identification of clusters (supertypes) during the Discriminant Analysis of Principle Components analysis (DAPC; Jombart *et al.* 2010) was made clearer. Multiple instances of DAPC analysis confirmed 15 clusters. I calculated the robustness of supertype designations by comparing the supertype grouping of the 157 alleles from Chapter 4 with the estimated groupings when combined in the current supertype analysis, which includes many more alleles (see Results). This was calculated as the percentage of alleles within the supertypes estimated in Chapter 4 that also group together during the current analysis.

Population and supertype genetic diversity

Because MHC loci in guppies may be duplicated, are high in diversity, and locus affiliation of alleles in unknown, population differentiation was calculated using D_{est} (Jost 2008) and 1000 bootstrap replicates in the *SPADE* R package (Ma *et al.* 2014; R Core Team 2014). Differentiation was estimated independently using MHC allele, MHC supertype, and microsatellite allele frequencies. Pairwise values of D_{est} were compared among microsatellites, MHC alleles, and MHC supertypes using a Mantel test in the *ape* package (Paradis *et al.* 2004) with 10,000 iterations, and Holm corrected *P* values for multiple comparisons. For each supertype, I calculated the (1) total number of MHC alleles (hereafter defined as nucleotide variants), (2) the number of PBR amino acid sequences, (3) the mean distance among PBR amino acid sequences (number of differences) within a supertype, (4) the mean frequency of a supertype in populations where it was present, (5) the mean number of alleles within each supertype per population, and finally (6) the level of PBR redundancy among the constitutional MHC alleles within a supertype (S_r) as,

$$S_r = \frac{the\ number\ of\ unique\ MHC\ alleles\ of\ supertype\ x}{the\ number\ of\ unique\ PBRs\ of\ supertype\ x},$$

Where *x* is supertype 1 to 15. Co-variation among these metrics were examined using principle components analysis (PCA) in the *ade4* package (Dray & Dufour 2007) and *FactoMineR* (François Husson 2008), and subsequent Pearson's correlation coefficients were calculated. Sequence similarity and dendrograms of MHC alleles and PBR sequences were inferred in *MEGA 5* (Tamura *et al.* 2011), and edited in *FIGTREE* (www.tree.bio.ed.ac.uk/software/figtree/).

Results

MHC genotypes

MHC genotypes were confidently estimated for 94% (1732) of the total 1839 samples sequenced. The failure to acquire accurate genotypes in 7% of the samples was likely due to poor DNA template, sample contamination, or random sequencing effects, and this genotyping failure rate is similar to that observed in Chapter 3 (6%) and Chapter 4 (10%). The number of alleles observed within an individual (A_i) ranged from 1-9 (mean A_i = 3.25 ±1.187), and mean A_i varied among populations (range of population mean A_i = 1 – 4.76, Table S5.1, Appendix 5). Among four sequencing runs, 233 replicate amplicons were sequenced across 103 individuals. Genotyping repeatability among these independent runs was 99.83%, which is an improvement over the 83.6% repeatability between just two sequencing runs previously reported using the same genotyping protocol in guppies (Chapter 3; Lighten *et al.* 2014a). This improvement was made possible by an increased number of high quality replicate samples among more independent sequencing runs.

In total 539 MHC IIb alleles were observed. Of these 164 have been previously identified, and 375 were novel (GenBank KT003989 - KT004363). Cluster analysis revealed that these alleles formed 15 supertypes based on functional characteristics, which is an increase from the 12 supertypes identified in Chapter 4 using 159 alleles (Figure S5.1 and S5.2, Appendix 3). On average (±SEM), 22% (±12) of the alleles within a supertype designated in Chapter 4 were

differentially grouped in the current analysis which included more alleles. In all but 16 (<1%) of individuals, each supertype was represented by a maximum of two alleles, and the observation of three alleles was confined to just two supertypes and a few populations; ST-9 = 1 individual from Arima-1, 2 from El Cedro-1, 4 from Aripo 2, 1 from Shark, and 4 from San Souci; ST-3 = 1 individual from Damier-1, 1 from Paria-3, and 2 from Paria-4. This unusual observation was concordant with other unique properties of these two particular supertypes (see below). The number of supertypes within an individual (ST_i) ranged from 1 to 7 (mean = 2.79 ±0.95, Table S5.1, Appendix 5). Among all individuals the relationship between ST_i and A_i was positively associated (P=<0.001, R^2=0.73). However, when individuals had the same A_i, they did not necessarily have the same ST_i (Figure 5.1). For example, in all individuals with A_i =4, 8.1% had ST_i = 2, 60.6% had ST_i =3, and 31.3% had ST_i = 4.

Population differentiation

Population differentiation estimates of D_{est} (Jost 2008) were calculated separately using MHC allele, MHC supertype, and microsatellite allele frequencies. Microsatellite genotypes were obtained from 50 populations of the total 59 genotyped at the MHC, and so only populations that comprised both marker types were used in D_{est} comparisons. Across 50 populations the mean D_{est} estimate based on microsatellites was 0.741 (± 0.007, range 0.001 - 1) (Table S5.2, Appendix 5), 0.88 (± 0.003, range 0.027 - 1) based on MHC alleles (Table S5.3, Appendix 5), and 0.388 (± 0.014, range 0.002 - 1) based on MHC supertypes (Table S5.4, Appendix 5). Populations were consistently highly differentiated by MHC alleles, and similarly so with microsatellites, yet less so by with MHC supertype diversity (Figure 5.2). A Mantel test with Holm P value correction revealed that D_{est} estimates of microsatellites and MHC alleles were significantly correlated (correlation=0.10, P=0.012), yet microsatellite differentiation was not significantly correlated with that of MHC supertypes (correlation=0.06, P=0.151). Conversely, population differentiation estimates based on MHC alleles were highly correlated with those of MHC supertypes (correlation=0.43, P=<0.001).

MHC Supertype population characteristics

The total number of alleles within a supertype ranged from 16 (ST-1) to 55 (ST9) (mean 35.93±11.79, Table 5.1). Redundancy in the PBR amino acid sequences (S_r) (i.e. the degree to which allelic nucleotide sequences translated into the same PBR amino acid sequence) also varied among supertypes (Table 5.1). Supertype-9 showed the highest degree of redundancy (despite comprising the most alleles), where the 55 alleles translated into just 17 unique PBR sequences (Figure 5.3, Table 5.1). ST-9 had an S_r of 3.23 (approximately one unique PBR observed for every three unique nucleotide alleles), compared to an average S_r of 1.38 (range 1.18-1.65) in the remaining 14 supertypes. Remarkably, compared to all other supertypes, ST-9 also displayed more than double the mean population frequency (0.330), compared to a mean population range of 0.017 – 0.097 in other supertypes (Figure 5.3, Table 5.1, Figure S5.3.a-o, Appendix 3). When considering all supertypes, each was expressed on average in 17.75% (±18.62) of individuals. However, ST-9 was observed in 79.77 % of individuals, which lies 3.33 standard deviations away from the mean, and so is significantly more common among individuals than other supertypes ($p<0.003$, Figure S5.4, Appendix 3, Table S5.8, Appendix 5).

Supertype-9 alleles were absent from just 5% (3) of the sampled sites (Marianne-10, Marianne-11, and Cumana), and these populations had particularly unusual supertype compositions compared to other surrounding sites (Figure 5.4). Other supertypes were absent from 14 (23.7%) to 41 (49.5%) of populations, which highlights that ST-9 is a particularly common, almost ubiquitous, supertype. The number of ST-9 alleles within populations ranged from 1-15 (mean 4.38). Despite variation in the number of ST-9 alleles within populations, the presence/absence, and frequency of particular ST-9 alleles, the cumulative frequency of ST-9 alleles was remarkably similar among populations (mean = 0.330 ±0.129, range= 0.019 – 0.588, Figure 5.4, Figure S5.3.i, Appendix 3, Table S5.5, Appendix 5). This was evident in populations across Trinidad, Tobago, two Hawaiian Islands, and Barbados. Similar degrees of redundancy, cumulative ST-9 frequency, and a high proportion of ST-9 alleles were also observed among individuals of *P. picta* (Figure 5.4, Figure S5.2, Figure S5.3.i, Appendix 3, Table S5.6, S5.1 and S5.7, Appendix 5). In addition, the nine unique PBR sequences from 10 alleles observed within

five *P. picta* individuals tended to be more closely related to those found in particular supertypes of guppies (Figure S5.2), rather than describing species specific lineages. Critically, there was no correlation between the number of unique ST-9 alleles and the total ST9 frequency within populations (P=0.303, R^2=0.01), or the number of unique ST-9 PBR amino acid sequences and the total ST9 frequency (P=0.162, R^2=0.03) (Figure 5.5).

Because ST-9 population level characteristics differed from those of other supertypes, I compared co-variation between the six supertype metrics (see Methods) in the presence, and absence of ST-9. In the presence of ST-9 PCA axis 1 explained 60.97%, and axis 2 24.39 % of the variation (Figure 5.6a). There was a positive association between S_r and the mean population frequency of a supertype, and the mean number of unique alleles per supertype within a population (additional correlation coefficient, P=<0.001, R^2=0.82), yet this relationship was mainly driven by variation in ST-9 (Figure, 5.6b; additional correlation coefficient, P=0.30, R^2=0.08). Similarly, the mean number of unique alleles per supertype within a population was positively correlated with mean population frequency of a supertype (additional correlation coefficient, P=<0.001, R^2=0.89), yet was much weaker when ST-9 was excluded (Figure 5.6b; additional correlation coefficient, P=0.25, R^2=0.35). I observed extreme values in all of these metrics in ST-9 (Table 5.1), and collectively these metrics characterized ST-9 as distinct from the remainder (Figure S5.4, Appendix 3).

While ST-9 displayed the highest S_r (3.23), and the lowest level of amino acid differentiation among PBR amino acid sequences (3.794), ST-6 displayed the highest within ST differentiation among alleles (7.758) and lowest PBR redundancy (1.22), while still comprising a relatively high number of unique alleles (44) (Table 5.1). Although ST-6 was observed in a range of populations across different geographic regions, it was notably more common in southern Trinidad, and comparatively rare in the North Slope (Figure 5.4, Figure S5.3f, Appendix 3). ST-3 was even more localized in distribution, with high frequencies (>0.20) only in North Slope populations. In the North Slope, ST-3 was represented by just 16 alleles, with an overall S_r of 1.455, which is less than half of that observed in ST-9 (3.235) (Table 5.1). Moreover, in each population, one or two unique alleles tended to dominate the cumulative frequency of this

supertype (Table S5.7, Appendix 5). When supertypes were analysed without ST-9, relationships among metrics of the remaining supertypes were made clearer. Here, PCA axis 1 explained 53.64% of the variation, and axis 2 explained 24.34% (Figure 5.6b). A weaker signal similar to ST-9 was observed in ST-12 and ST-4, which both showed relatively high levels of PBR redundancy along with a high number of alleles. Conversely, ST-15, ST-13, and ST-10 all exhibited high numbers of alleles, yet these also represented a relatively high number of unique PBR sequences (Figure 5.6b, Table 5.1).

Discussion

Interpretations of processes governing the evolution of MHC genes have often resulted in disparate or even contradictory inferences regarding signals of neutral processes (Sutton, 2011), parasite mediated selection (Fraser & Neff 2010; van Oosterhout *et al.* 2006b, Penn *et al.* 2002; Summers *et al.* 2009), and sexual selection (Winternitz *et al.* 2013). The common approach has been to study MHC allelic diversity at the nucleotide level, while generally ignoring functional significance at the level of the amino acids within the PBR that are subject to parasite mediated selection. Here I discuss how consideration of MHC supertype diversity (which is derived from the inferred functionality of PBR amino acid sequences) can help elucidate complex processes of MHC evolution, and how the study of allelic diversity alone can bias such inferences, leading to contradictory observations. Accurate interpretations of the effects of parasite mediated selection on the MHC can only be made when simultaneously considering allelic, and supertype diversity.

Comparison of MHC allele and supertype diversity improves evolutionary inferences

Population differentiation based on MHC allele frequencies is significantly correlated with differentiation at neutral loci. However, I found no significant correlation between population differentiation based on MHC supertypes and microsatellites, which shows that MHC supertype diversity is less affected by genetic drift in this system. Despite this, there was a very strong

relationship between population differentiation based on MHC alleles and supertypes. Approximately 45% of the variation in the MHC allele frequency distributions could be explained by variation in MHC supertypes. Therefore, MHC allele frequencies (which have typically been the focus of MHC studies in natural populations) appear to be affected by both neutral process and changes in supertype frequency. So exactly what are the characteristics that describe the association among alleles and supertypes?

An MHC supertype is defined as a group of alleles that share similar functional properties, inferred from variation in amino acids within the PBR that are under strong positive selection. The fact that the number of supertypes identified in this chapter increased by just 24% with a 357% rise in the number of alleles, compared to Chapter 4, supports the robustness of the DAPC approach in characterizing well-defined functional clusters of alleles. Despite the addition of many more alleles in the current analysis, there was high concordance between the supertype groupings observed in Chapter 4 and these improved supertype estimates (mean concordance= 76% ±21, range 42-100). Moreover, the mean number of PBR amino acid differences among alleles increased by just 1% from those used in Chapter 4 (mean number of differences = 9.996) compared to alleles described here (mean number of differences = 10.179).

Guppy genotypes (in 99% of cases) displayed a maximum of two MHC alleles for any observed supertype. This supports previous studies, which infer that supertypes are (largely) loci specific (Ellison *et al.* 2012; van Oosterhout 2013, Chapter 4). In addition, guppies show extensive CNV, both within and among populations (Chapter 3; Lighten *et al.* 2014a), and loci can appear either fixed or nearly fixed for particular supertypes (e.g. Marianne-3, Marianne-4, Cumana). The inference that supertypes, and their constituent alleles, may be locus specific, and that alleles within each supertype may be affected by demographic processes, suggests that selection operates directly on the presence/absence of supertypes at loci (Chapter 4; see below). Because alleles are confined to the functional space of a supertype, they are affected by both intra-supertype selective, and demographic processes (Figure 5.7). Alleles present within a population are influenced by the amount of intra-supertype genetic drift and this will

be dependent on the relative fitness that each allele confers, where alleles with similar/identical fitness will drift more. The relative fitness of alleles within a supertype is defined by how well each is adapted to combat parasite infection (Figure 5.7). The alleles that occupy the functional space of a supertype will change in response to parasite evolution, which is geared towards evading the host immune system, and changes in allele frequencies will be driven by intra-supertype Red Queen Dynamics. As alleles within a supertype become less efficient in defense against a parasite species, they will reduce in frequency or be lost, whereas alleles better adapted to combat infection within a supertype will increase in frequency in a population. This results in the optimization of supertype functionality (Figure 5.7).

The evolution of supertypes should be largely independent from each other (excluding possible linkage and micro-recombination events) as they perform different functions, and so each will have a reduced number of alleles (compared to the entire gene pool), which can facilitate rapid changes in allele frequency and allelic turn-over by drift or Red Queen Dynamics. Also, because supertypes may likely be confined to particular loci, and each is adapted to a particular parasite(s), then it is likely that variation in parasitic community exerts balancing selection directly on loci. Specifically, a locus is maintained in a population when a supertype (and its constituent alleles) is advantageous in defense against the population specific parasite fauna. This hypothesis can explain the extensive patterns of CNV observed among guppy populations. However, CNV (and therefore supertype diversity) could likely also be affected by extreme demographic processes (e.g. a severe population bottleneck), which could result in either an increase or decrease of mean ST_i. This likely explains the extremely reduced allelic and supertype richness observed in the Cumana population, where this population may have been seeded by a small number of individuals from the nearby Tompire river, which shares the single haplotype observed in the Cumana population. However, other more common demographic processes (e.g. drift) are likely less influential on CNV and ST_i, which appear under selection.

The number of alleles within a supertype (or at a locus, which might harbour multiple supertypes) is also likely to be affected by the length of time which selection has operated to maintain its presence among populations (see below), as well as the amount of drift. Similarly,

populations where a supertype has remained present over long evolutionary time are also expected to have accumulated multiple alleles of that particular supertype (some of which will encode identical PBR amino acid sequences).

Stabilizing selection on MHC supertypes

Stabilizing selection is generally not implicated in MHC evolution as this process would result in highly homogenized allele frequencies among populations, and observations generally support high divergence at the MHC among populations. However, this interpretation of widespread divergent selection is based purely on allele frequencies, while generally ignoring the PBR amino acid functionality that each allele represents. It is now established that allele frequencies can be significantly affected by demographic processes (e.g. Sutton *et al.* 2011), so even the strength of apparent divergent selection based on alleles may be called in to question. I propose a new argument that stabilizing selection of MHC supertypes is a strong evolutionary force maintaining crucial functionality over millions of years. Similar processes have been observed in histone gene supertypes (H1 multigene family; Eirín-López *et al.* 2004), and in allele frequencies of the Toll-like receptor gene family (Mukherjee *et al.* 2014). Invoking stabilizing selection on supertypes much better explains the observation of trans-species polymorphism (TSP) than does the common inference of balancing selection acting strictly on alleles. Balancing selection acting on a single gene pool cannot simultaneously explain the observation of rapid allelic turnover (or high allelic diversity) and TSP (van Oosterhout 2009b). However, when intra-supertype Red Queen Dynamics are invoked, rapid allelic evolution may take place within the confines of a supertypes functional space, which is itself preserved by stabilizing selection acting against mutant alleles with poorer peptide binding properties relative to defense against the targeted parasite(s) (Figure 5.7). This explains the presence of TSP in terms of sharing of allelic lineages between species, and the sharing of supertypes across species and populations, despite significant divergence in the constituted alleles.

For simplicity I focus on a remarkable example of stabilizing selection observed within ST-9. This supertype comprised 55 MHC alleles, yet these corresponded to just 17 PBR amino acid sequence variants. This relatively reduced PBR amino acid variation was maintained over large geographic distances among populations that have long been isolated, despite the fact that allelic variation at the nucleotide level was quite diverse. Even more remarkable was the fact that despite different numbers of alleles and PBR amino acid sequence variants in populations, and long term isolation, the cumulative frequency of ST-9 alleles, and the frequency of individuals that contained the supertype was both high and similar among populations. The frequency of ST-9 is not significantly affected by the number of alleles or PBR amino acid sequence variants present in the population. These observations suggest that strong stabilizing selection is operating in concert on a diverse assemblage of alleles belonging to ST-9, despite variation in nucleotide and PBR amino acid sequences. This is because alleles are inferred to have similar functionality, and moreover, DAPC analysis suggests that this functionality is highly conserved and distinct from that of other supertypes. The selective force maintaining the functionally important ST-9 must be very strong indeed, as the characteristics of a relatively high number of alleles, high PBR similarity/redundancy, and high/similar population frequencies were also observed in *P. picta*. This maintenance of such trans-species functionality since the last shared common ancestor between *P. reticulata* and *P. picta* ~21-22 mya suggests a very important role for ST-9 (as well as the other shared supertypes) in poeciliid immune processes. In Chapter 4, I described associations among numerous other MHC supertypes with *Gyrodactylus* prevalence, and variation in fitness related colours. The results corroborated the homogenizing effect of *Gyrodactylus* on guppy MHC supertype diversity (Fraser & Neff 2010b), which are further explained by the model of stabilizing selection described here.

As no correlation between ST-9 and *Gyrodactylus* prevalence, and male colour was previously identified, inferences of its functional relevance remain elusive. It may be that this supertype functions to combat a common and ubiquitous parasite. This hypothesis is supported in part by the fact that guppies from the Cumana population (which lack ST-9) appear to have considerably higher rates of mortality and lower fecundity than guppies from Marianne-3 (which all express ST-9, and appear to have very good health) when reared in aquaria (data not

shown). Indeed, the fact that ST-9 is the only monophyletic supertype (based on its constituent alleles, and PBR amino acid sequences), and is under such strong stabilizing selection, implies that these alleles are very fastidious in function, where as other supertypes (which can be polyphyletic or paraphyletic) may be more promiscuous in function (or target rapidly evolving/generalist pathogens), and so recombination, and less stabilizing selection, is characteristic of their evolution. This signal of long term stabilizing selection was only detectable when examining the relationship among MHC supertypes and their constituent alleles. A conventional analysis that focused purely on the geographic distribution of nucleotide level allelic diversity would have led to an erroneous supposition that local adaptation, e.g. though balancing NFDS must be operating to drive strong patterns of MHC allelic differentiation.

When examining supertypes in the absence of ST-9, other interesting patterns emerge. For example, there is no correlation between the average number of alleles within supertypes and the average frequency of those supertypes in each population. This is consistent with stabilizing selection also acting on these supertypes. Another important observation is that as the number of different alleles within a supertype increases, so does the similarity among the PBR amino acid sequences that they encode. High similarity among alleles within a supertype (Figure S4.4, Appendix 2) supports stabilizing selection operating on the PBR amino acids of alleles, whereas convergent evolution would increase evolutionary distance among alleles within a supertype. The preservation of functionality among alleles within a supertype also explains how new (rare/private) alleles can be maintained over long periods of time, as they not as easily lost by genetic drift. If alleles were not confined to selection within the functional boundary of a supertype, the number of alleles within supertypes would decrease as a result of directional selection. This would prevent the wide spread observation of many rare and private alleles that are very similar in composition to those of higher frequency.

Finally, weaker signals of stabilizing selection were observed in ST-12 and ST-4, which both showed relatively high S_r values (1.520 and 1.652 respectively) along with a high number of alleles (38 and 38 respectively). However, stabilizing selection at each of these supertypes appears less evident than for ST-9, and was concentrated in the North Slope for ST-4, and outside of the North Slope for ST-12. This highlights how accurate interpretation of processes governing MHC polymorphism relies upon comparisons among populations across suitable spatial scales.

There is growing recognition in the value of studying MHC gene evolution at the supertype level. Previous studies have inferred functional roles of supertypes, by correlating supertype frequency with that of parasitic infections (Schwensow *et al.* 2007b; Fraser & Neff 2010; Sepil *et al.* 2013a), which overcomes the problems of resolving MHC allele specific effects in highly diverse study systems. Interestingly, it seems that variation in supertypes observed among populations of a species are not just driven by their own parasitic infections, but also by infection dynamics seen among parasite fauna in other host species at the community-level (Pilosof *et al.* 2014). This places importance on evolution on shared MHC functionality among species, either through trans-species polymorphism or convergence (Sette *et al.* 2012), and less so on attempting to resolve patterns of MHC evolution strictly through patterns of allelic diversity. Indeed, a recent study showed that supertypes can resolve patterns of selection operating on the MHC at the population level in Hochstetter's frog (*Leiopelma hochstetteri)*, which shows high diversity at the allelic level (Lillie *et al.* 2015). By assessing the pattern of population differentiation at the MHC, my study gains critical insight into the interrelated evolution of MHC alleles and supertypes. This provides the basis for a novel model of MHC evolution, which describes a complex of processes operating on alleles and supertypes, and importantly resolves the observation of numerous evolutionary paradoxes commonly observed in patterns of MHC diversity. Overall I highlight that consideration of supertypes is critical in understanding processes of MHC evolution.

Conclusion

This chapter examines how the consideration of supertypes can help explain the evolutionary significance of patterns of MHC diversity in natural populations. By comparing geographic patterns of MHC alleles, MHC supertypes, and neutral loci, previously undetected processes governing polymorphism at MHC loci can be examined. A significant correlation between MHC allele and microsatellite population structuring exists, however there is no significant correlation between MHC supertype and microsatellite structuring. Moreover, a significant correlation between MHC allele and supertype population differentiation suggests that alleles, and not supertypes, are affected by demographic processes as well as changes in supertype diversity. The maximum of two alleles per supertype (in >99% of genotypes), suggests that supertypes are locus specific. In connection with these points I closely examined one particular supertype (ST-9), and proposed that supertype functionality is maintained by strong stabilizing selection quickly eliminating alleles that fall outside of the functional boundary (and in between the functional boundaries of other supertypes). The frequency of alleles within a supertype that confer a similar/identical fitness are affected by random genetic drift, albeit less so than completely neutral loci. Frequencies of alleles that vary in relative fitness are likely affected by intra-supertype Red Queen Dynamics. Because evolutionary processes operating on alleles are confined within supertypes, and stabilizing selection operates on maintaining the supertype functionality, allelic lineages within supertypes can persist over large spatial and temporal scales, explaining TSP. This also explains the common observation of many unique rare, and private alleles at the nucleotide level, which are functionally similar or redundant at the PBR amino acid level. Balancing selection, driven by variable parasite communities likely operates to maintain over all supertype diversity among populations. Therefore balancing selection may act directly on the loci and so is complicit in driving the widespread CNV observed both within and among guppy populations. Overall this hypothesis of ‘stabilized supertypes and balanced loci’ represents a potential paradigm shift in the study of MHC evolutionary ecology.

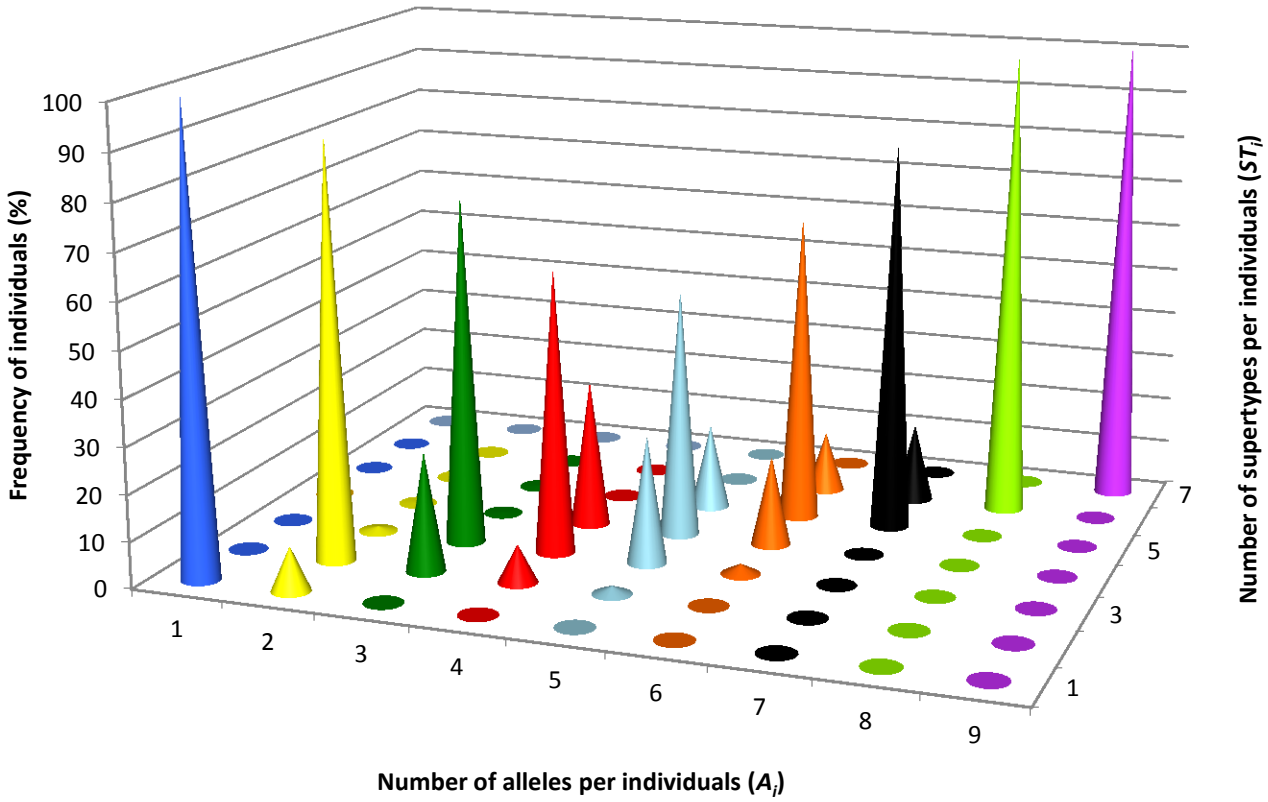

Figure 5.1. The relationship between the number of alleles within an individual (A_i) and the number of supertypes within an individual (ST_i) observed among all samples. In general, as A_i increases, so does ST_i; however, there is variability in the trend, with intermediate levels of A_i (A_i = 4-6) corresponding to more variation in ST_i. Individuals with a large A_i will never have a low ST_i, suggesting that variation in A_i among individuals is largely due to variation in the size of the functional repertoire, which can be explained as variation in locus specific supertypes.

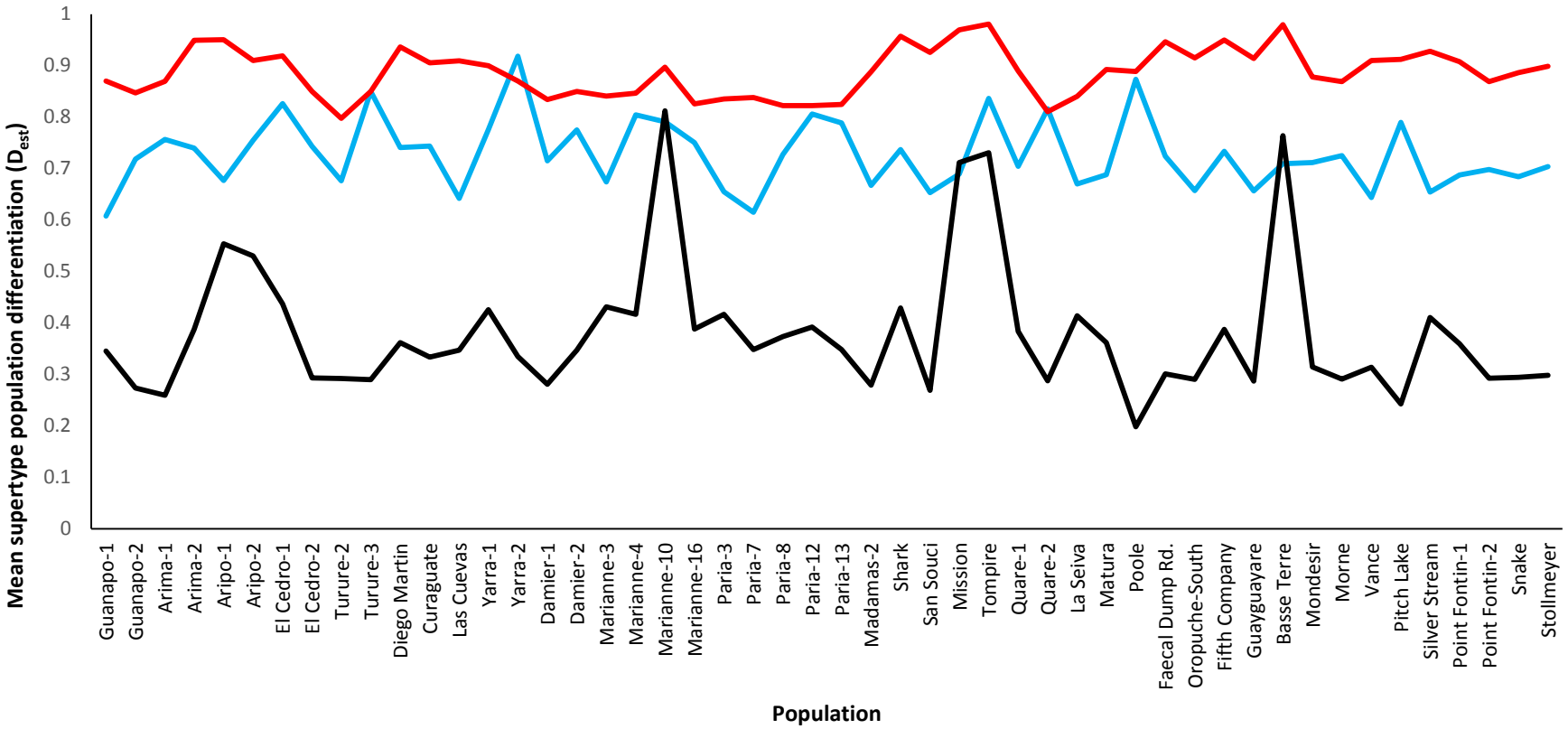

Figure 5.2. Comparisons of mean population differentiation estimates (D_{est}) based on microsatellite (Blue), MHC allele (Red), and MHC supertype (Black) frequencies. Generally guppy populations are highly differentiated based on MHC allele frequencies, as well as in microsatellite allele frequencies and these are significantly correlated (see Results). While the majority of populations are only moderately differentiated based on supertype frequencies, representing stabilizing selection, a few populations show higher differentiation similar to that observed in microsatellites. This indicated that although supertype and microsatellite frequencies are not correlated across the data set (See Results), that in some cases either supertype diversity within a population can be affected by demographic processes or local adaptation results in particular populations becoming more differentiated in their MHC functional repertoire. Examination of MHC alleles and microsatellites alone would lead to the erroneous conclusion that strong divergent selection is operating in concert with demographic processes driving high population differentiation in MHC alleles.

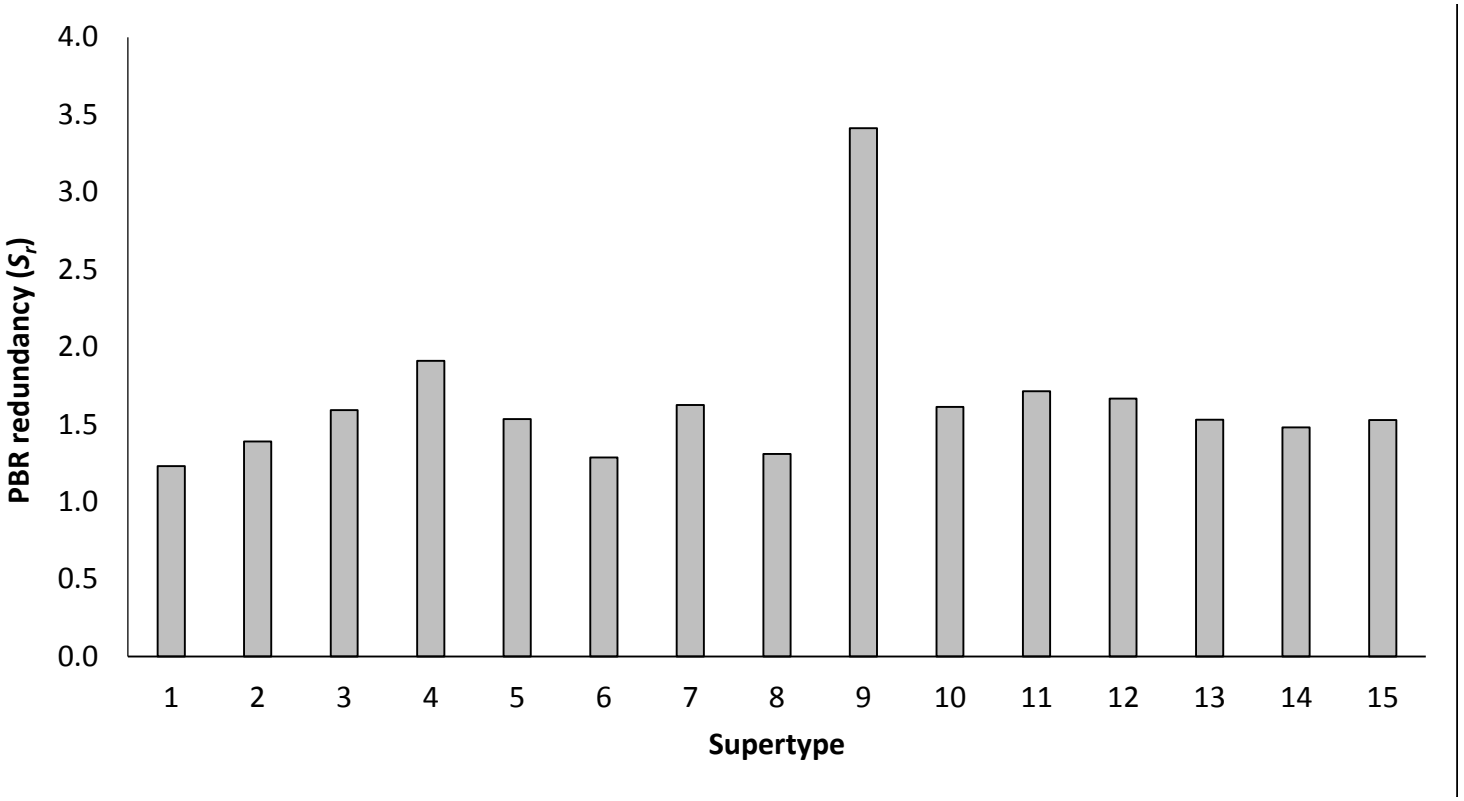

Figure 5.3. Redundancy of the protein binding region (PBR) translated from the unique MHC allelic nucleotide sequences in each supertype (S_r). Redundancy increases as the fraction of unique PBR sequences decreases among alleles within a supertype. In general, the majority of supertypes display a similar degree of PBR redundancy, while ST-9 displays almost double the amount of PBR redundancy compared to all other supertypes. In concert, ST-9 displays multiple other unique traits (see Results), for example this high redundancy is coupled with the highest number of MHC alleles of any supertype. In conjunction with the near ubiquitous nature of ST-9, this suggests that its functionality has been preserved over large temporal and spatial scales, expanding in the number of alleles through mutations that do not deviate from the functionality that is under strong stabilizing selection.

(a)

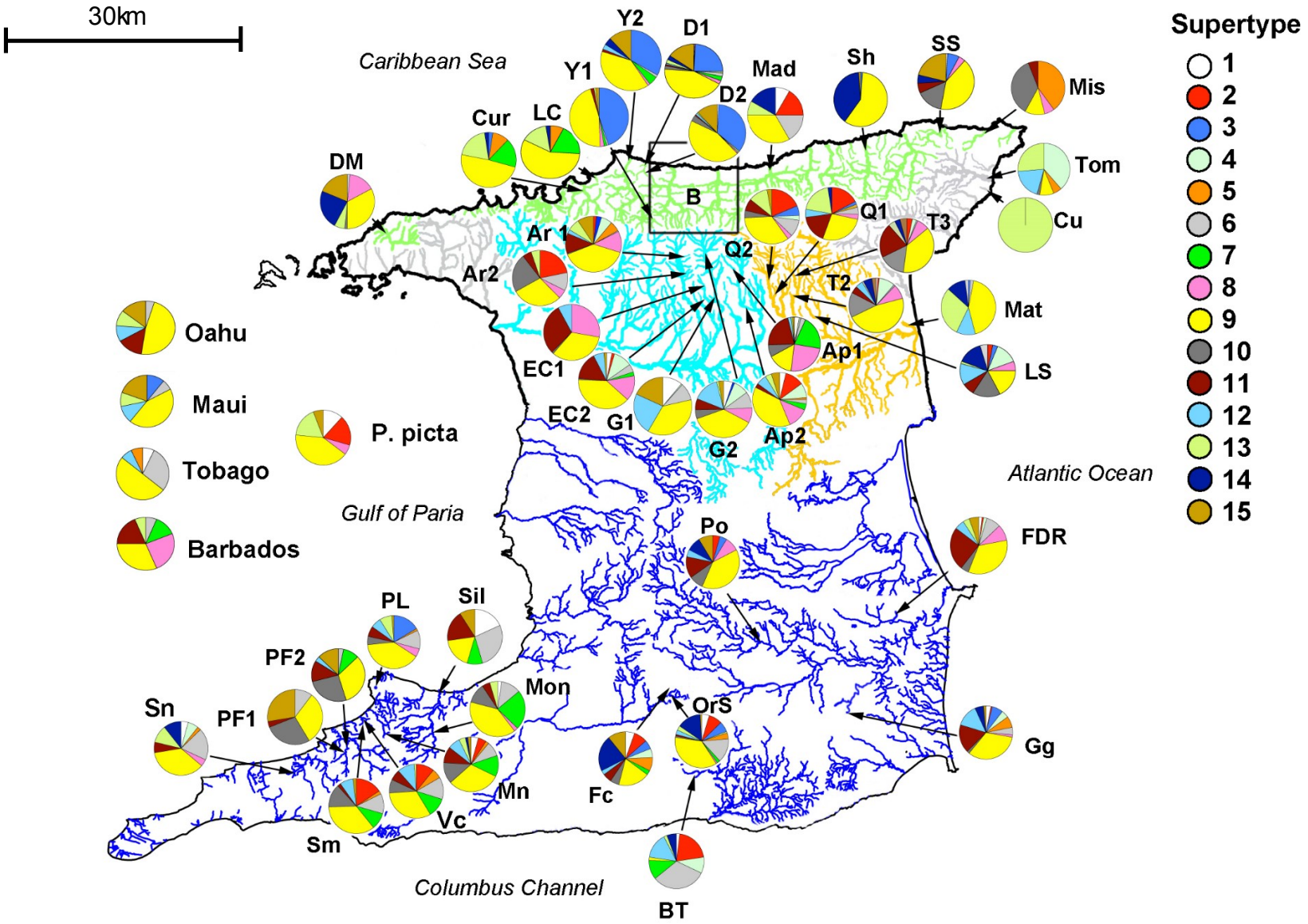
30km
Caribbean Sea
Gulf of Paria
Columbus Channel
Atlantic Ocean
Supertype
1
2
3
4
5
6
7
8
9
10
11
12
13
14
15
Oahu
Maui
Tobago
Barbados
P. picta
Y2
D1
Y1
Mad
D2
Sh
SS
Mis
Cur
LC
DM
Tom
B
Q1
T3
Cu
Ar 1
Q2
Ar2
T2
Mat
Ap1
EC1
LS
EC2
G1
G2
Ap2
Po
FDR
PL
Sil
PF2
Mon
Sn
PF1
OrS
Gg
Mn
Fc
Vc
Sm
BT

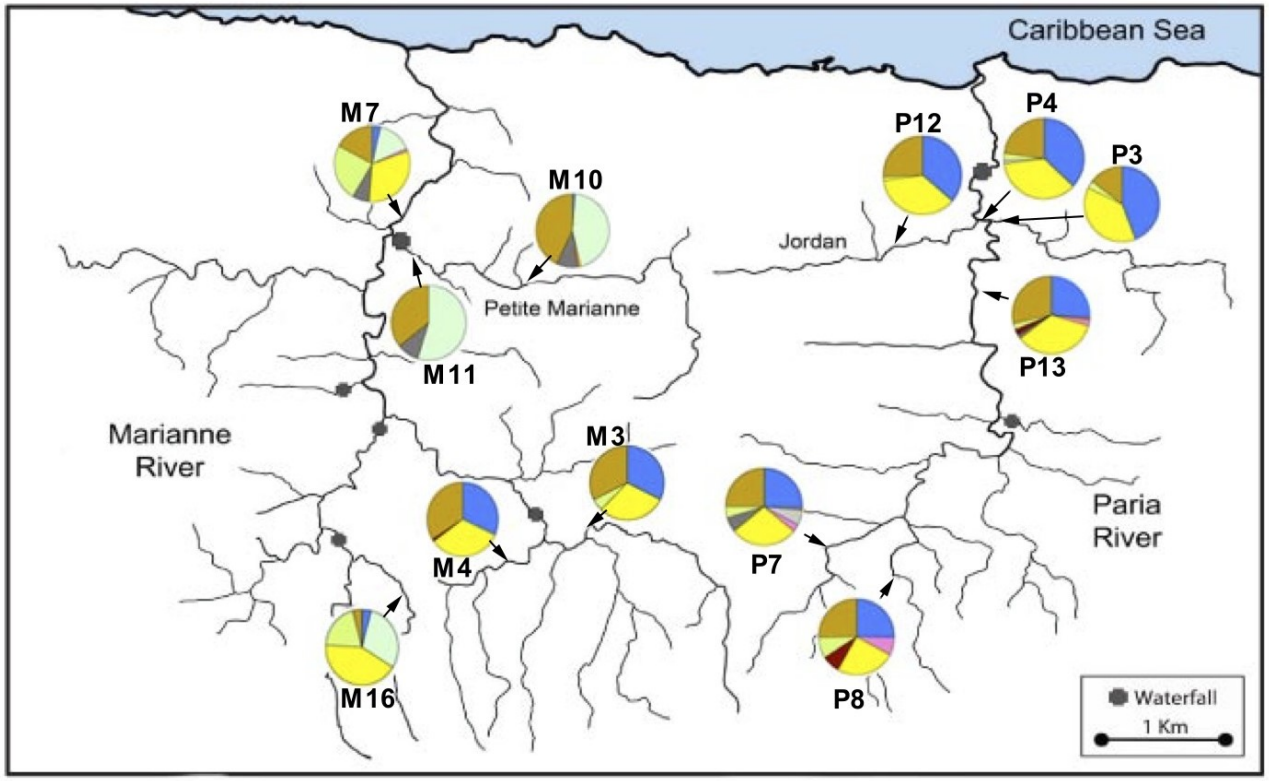

Figure 5.4. The geographic distribution of MHC supertypes in guppy populations across Trinidad and other oceanic islands. Rivers in the mountainous Northern Range comprise three major regions: The North Slope (green), Caroni Drainage (light blue), and Oropouche drainage (Orange). Separate drainages in the Northern range are shown in grey. Rivers in the relatively flat regions towards the south are shown in dark blue. Abbreviated populations comprise; Diego Martin (DM), Curaguate (Cur), Las Cuevas (LC), Yarra 1 (Y1), Yarra (Y2), Damier 1 (D1), Damier (D2), Marianne 3, 4, 7, 10, 11, 16 (M3, M4, M7, M10, M11, M16), Paria 3, 4, 7, 8 ,12, 13 (P3, P4, P7, P8, P12, P13) Madamas (Mad), Shark (Sh), San Souci (SS), Mission (Mis), Tompire (Tom), Cumana (Cu), Matura (Mat), Las Seiva (LS), Turure 2 (T2), Turure 3 (T3), Quare 1 (Q1), Quare 2 (Q2), Aripo 1 (Ap1), Aripo 2 (Ap2), Guanapo 1 (G1), Guanapo 2 (G2), El Cedro 1 (EC1), El Cedro 2 (EC2), Arima 1 (Ar 1), Arima 2 (Ar2), Silver Stream (Sil), Pitch Lake (PL), Point Fortin (PF1), Point Fortin 2 (PF2), SN (Snake), Stollmeyer (Sm), Vance (Vc), Morne (Mn), Mondesir (Mon), Fifth Company (FC), Oropouche-South (OS), Basse Terre (BS), Poole (Po), Faecal Dump Rd. (FDR), Guayguayre (Gg). Guppies were also collected from Oahu and Maui in the Hawaiian archipelago, Windward Rd. in Tobago, and Grahame Hall swamp In Barbados. (Cont'd)

Poecilia picta (P. picta) were collected from St. Joseph, East coast Trinidad.(A, B) Complex variation in supertype frequency distribution occurs across populations, and for clarity those in the Marianne and Paria are shown separately. However, ST9 is obviously maintained in similar frequencies across the majority of populations, despite wide variation in the frequencies of particular alleles that are present. Populations that are in close proximity tend to be similar in supertype composition, which is likely a consequence of similar selection pressures and gene flow. For example, Cumana is fixed for just one ST-allele that is found only in the neighboring Tompire River (and Pitch Lake in the South West). Populations in the Yarra, Damier, Marianne, and Paria also appear to be largely similar. Damier populations represent a human mediated introduction from the Yarra, but the similarity among (B) the eastern upland populations of the Marianne and those in the Paria likely represent recent colonization of the Paria from the Marianne, and microsatellite data support this (Baillie 2012). Populations M10 and M11 lack ST9, but are unique in displaying a large expansion of ST4 alleles, which are rare elsewhere.

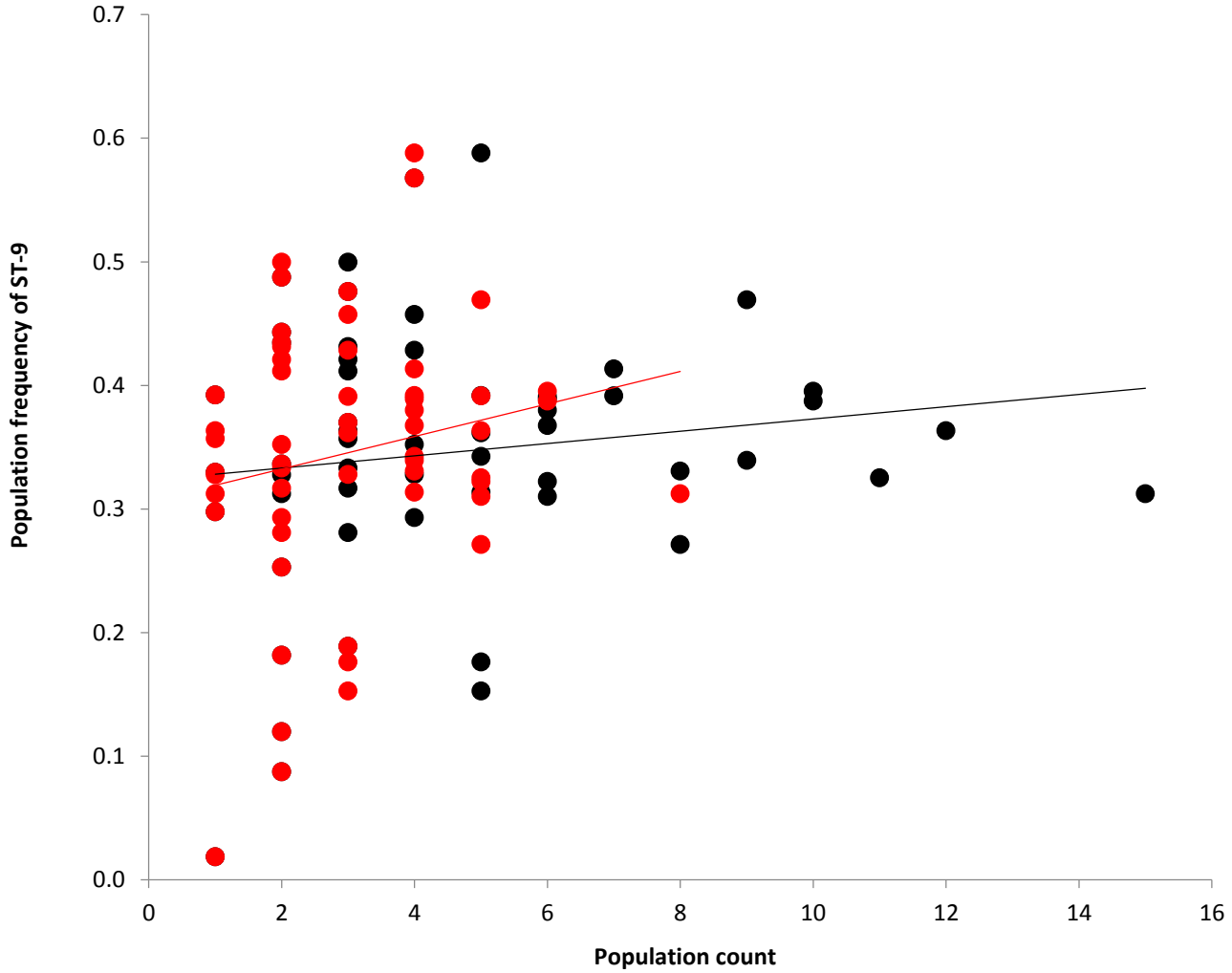

Figure 5.5. The lack of relationship between the number of unique alleles (black) and cumulative population frequency of supertype-9 (P=0.303, R^2=0.01), as well as between the number of unique PBR sequences (red) within a population, and the combined frequency of ST-9 alleles (P=0.162, R^2=0.03) present in a population again supports strong stabilizing selection

(a)

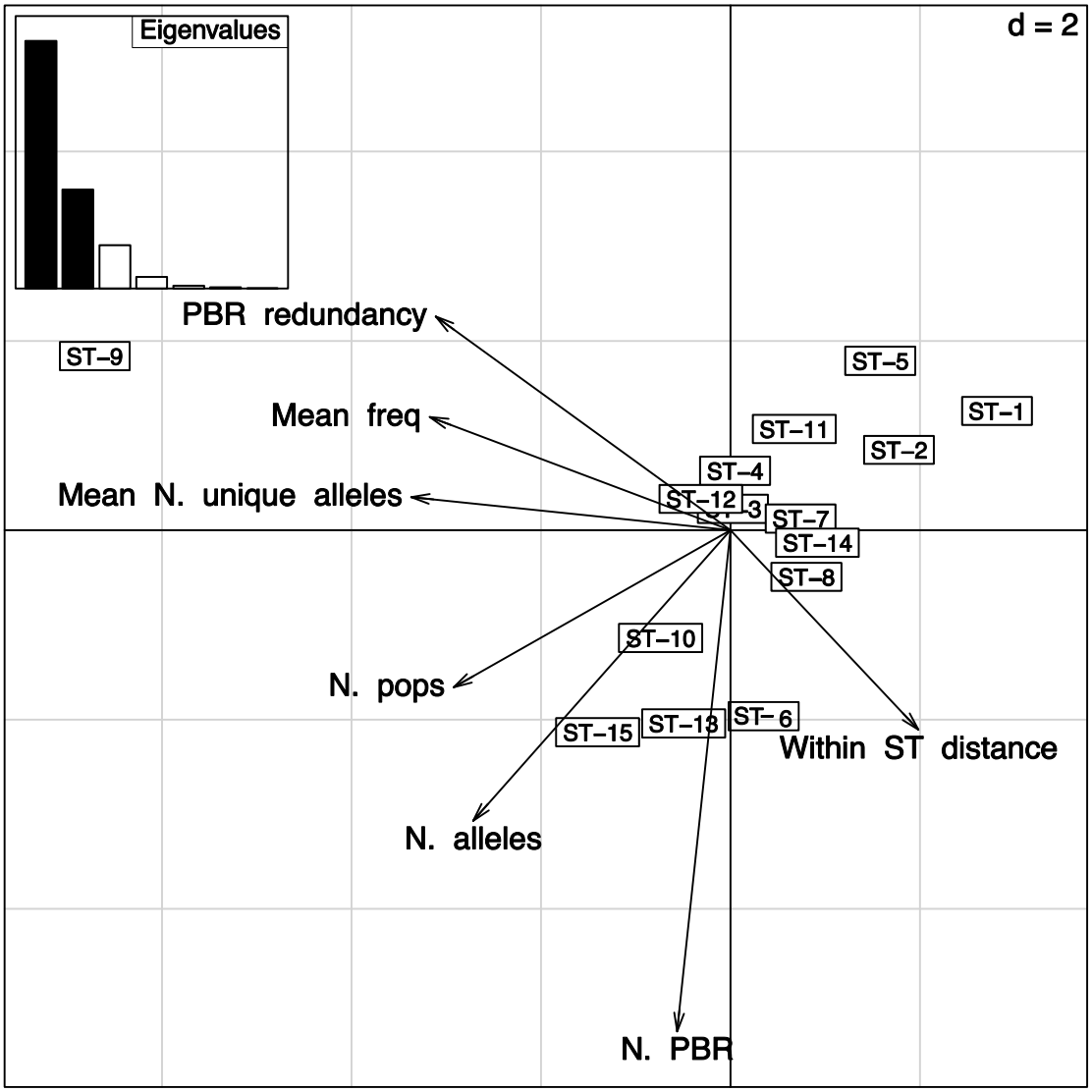
Eigenvalues
d = 2
PBR redundancy
Mean freq
Mean N. unique alleles
N. pops
N. alleles
N. PBR
Within ST distance
ST–9
ST–5
ST–1
ST–11
ST–2
ST–4
ST–12
ST–7
ST–14
ST–8
ST–10
ST–15
ST–13
ST– 6

(b)

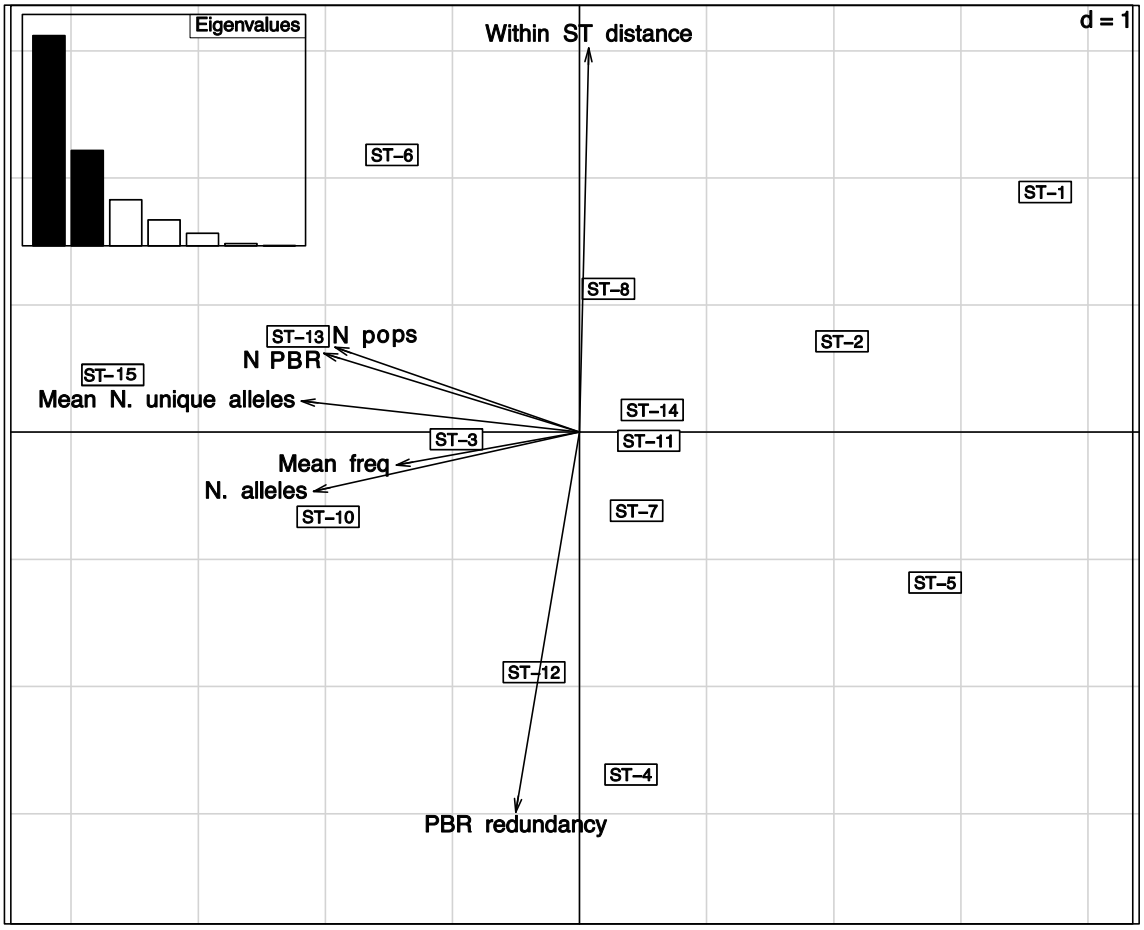

Figure 5.6. Principle components analysis displaying the variation among supertypes in (1) protein binding region (PBR) redundancy, (2) Mean population frequency (Mean freq), (3) mean number of unique alleles within a supertype within a population (Mean N. unique alleles), (4) the number of populations a supertype is observed (N. pops), (5) the total number of unique MHC alleles (nucleotide sequences) in a supertype across all populations(N. alleles), (6) the number of unique PBR sequences in a supertype (N. PBR), and (7) the mean distance among MHC PBR amino acid sequences (i.e. number of differences) within a supertype (Within ST distance). The distance of the position of each supertype from the center is proportional to its contribution to structuring the data set, and their position relative to the arrow heads of each metric depict either a positive or negative association. For example, (a) ST-9 shows the highest PBR redundancy, Mean freq, and Mean N. unique alleles, while ST-1 contains the least number of total alleles among the fewest number of populations. Conversely, ST-6 comprises a high mean number of unique alleles within a supertype, which are the most differentiated in nucleotide sequences compared to other supertypes. Because ST-9 is observed in the majority of populations and displays strong unique traits, the signal in its variation displays an overpowering contribution to the data set. (b) When ST-9 is removed, more fine scale patterns of variation immerge in the remaining supertypes. This reveals that ST-15, and ST-13 show a similar combination of traits that signify, although to a lesser degree, stabilizing selection similar to ST-9.

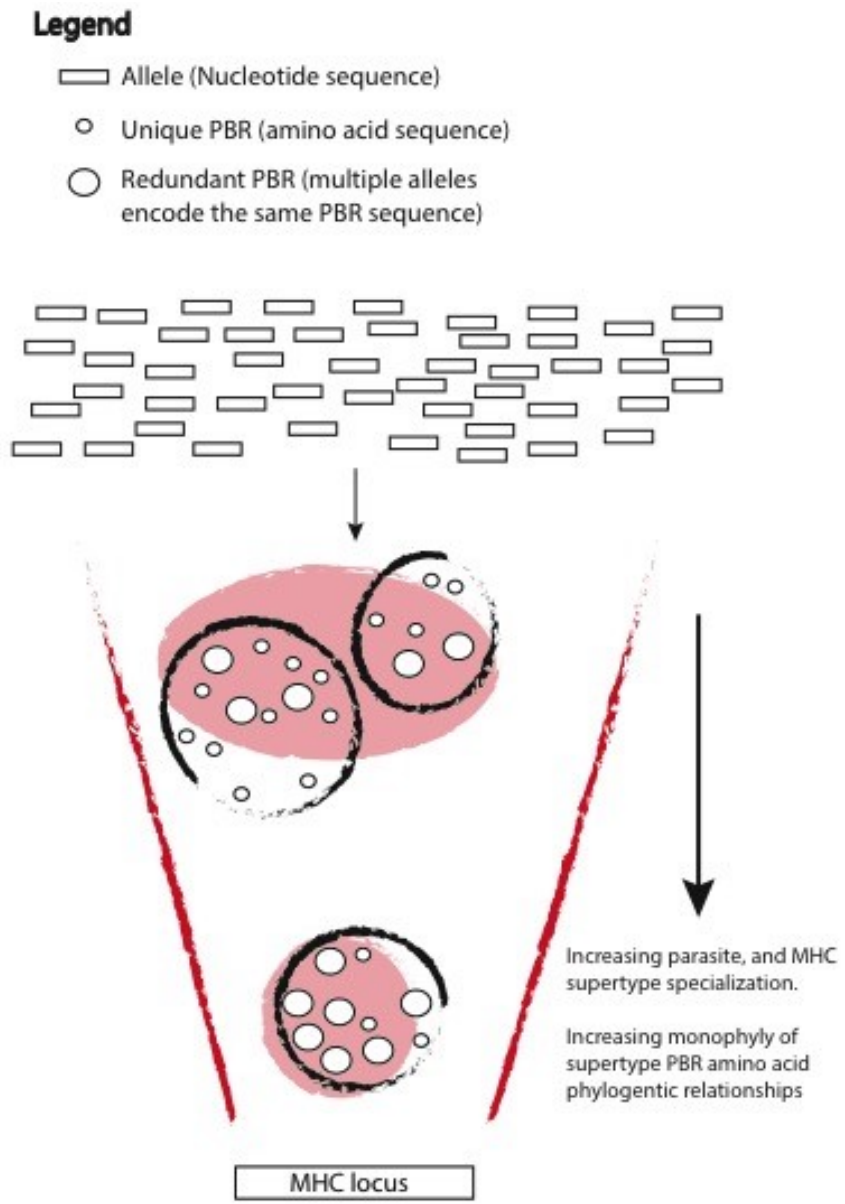

Schema of the evolutionary relationship between MHC alleles and supertypes:

A single MHC locus can express many MHC alleles. The functional role of these alleles is dependent on the PBR amino acids which they encode. PBR amino acid sequences fit inside a functional boundary of a locus (red lines), which has to recognize the phenotype of one or more parasites (shaded red ellipses). Within locus functionality is defined by specific functions of MHC supertypes, which are characterized by identical or similar PBR sequences.

The n-dimensional functional space of the supertype (black ellipses) is governed by stabilizing selection, acting to optimize its coverage of the parasite n-dimensional phenotypic space (for simplicity only two dimensions are shown here).

Evolution of parasites is geared towards reducing overlap between their phenotypic and the functional recognitional space that supertypes cover.

As parasites adapt, this leads to counter adaptation at the MHC by intra-supertype Red Queen Dynamics. PBR sequences are less functionally efficient when they fail to match the parasite's phenotype and so will be selected against, in favour of PBR sequences that better correspond to the phenotype of the parasite. The evolutionary dynamics of alleles within a supertype are largely independent from those in other supertypes (excluding possible linkage and micro-recombination events), resulting in a reduced effective population size of alleles, which can facilitate rapid changes in allele frequencies.

PBR sequences with similar functionality are under similar selective pressures, so their relative frequencies may be governed mainly by genetic drift. This is especially true when disparate alleles encode identical PBR amino acid sequences.

Parasites that encompass a large functional niche (generalists), and/or are rapidly evolving may be targeted by multiple 'generalist' supertypes. Parasites that are restricted in their functional niche and/or have evolved in concert with hosts for longer periods of time may be targeted by highly specialized supertypes. This results in an evolutionary equilibrium between parasite and host, which maintains supertype variation over long periods of time.

Figure 5.7

125

Supertype	N. alleles	N. PBR	Mean PBR amino acid distance (n. differences)	N. pops	Mean population frequency	Mean frequency of individuals that have supertype (%)	Mean number of unique alleles per population	S_r (measure of PBR redundancy among alleles)
ST1	16	13	7.857	21	0.017	5.99	0.458	1.231
ST2	25	17	6.891	21	0.032	10.42	0.661	1.471
ST3	32	22	6.794	30	0.079	23.05	1.136	1.455
ST4	38	23	4.607	24	0.047	12.39	1.136	1.652
ST5	21	17	4.971	17	0.018	4.92	0.508	1.235
ST6	44	36	7.758	37	0.055	16.54	1.237	1.222
ST7	35	24	6.232	18	0.030	8.93	0.881	1.458
ST8	32	27	6.335	32	0.041	13.81	1.000	1.185
ST9	55	17	3.794	56	0.330	78.41	4.390	3.235
ST10	48	33	5.391	34	0.053	15.86	1.441	1.455
ST11	21	15	7.267	37	0.058	18.95	1.085	1.400
ST12	38	25	3.886	29	0.038	12.25	1.085	1.520
ST13	49	33	7.065	41	0.068	17.60	1.322	1.485
ST14	35	25	6.558	20	0.034	10.32	0.831	1.400
ST15	50	40	6.296	45	0.097	29.82	1.780	1.250

Table 5.1. Comparisons of metrics that define each supertype across populations of guppies

Chapter 6

General Discussion and Conclusions

This thesis describes the use of Next Generation Sequencing (NGS) to elucidate patterns of Major Histocompatibility Complex (MHC) evolution in natural populations of the guppy (*Poecilia reticulata*). I have proposed a redefinition of the molecular and bioinformatic approaches used to gather NGS MHC sequence data, and the theoretical considerations required for accurate interpretation of MHC diversity. In addition, I provide novel evidence to suggest complex interactions between MHC polymorphism, parasite infection, and phenotypic traits believed to be associated with survival and mate choice. Comparisons among geographic distributions of MHC supertypes and their constituent alleles provides support of a novel model governing MHC evolution. This identifies a combination of parasite driven stabilizing selection acting on supertype functionality, and Red Queen Dynamics and random genetic drift acting on functionally similar MHC alleles *within* supertypes. I also propose that patterns of population differentiation may be misinterpreted to represent high levels of local adaptation at the allelic level if supertypes are ignored. Moreover, I suggest that patterns of MHC copy number variation (CNV) (or haplotype variation) may be maintained by balancing selection acting on individual loci (or groups of loci), driven by variable parasite communities. The culmination is a body of evidence to suggest not only that guppies provide a unique system to investigate the interplay between parasite mediated natural selection and sexually mediated natural selection, but also that the guppy is an ideal model species that can greatly improve our understanding of MHC evolution in natural populations.

Redefining NGS approaches to study MHC

In Chapter 2 and Chapter 3, I presented the basis for a re-definition of NGS MHC genotyping approaches by critically evaluating the relative merits of popular bioinformatic approaches, which use allele validation thresholds (AVT; e.g. Radwan *et al* 2012) or sequence clustering (e.g. Pavey *et al.* 2013). In conjunction, I introduced a novel molecular and bioinformatic procedure, which uses ultra-deep Illumina sequencing and relative amplicon sequencing depth modeling. This is advantageous over those that use AVTs and clustering of 454 or Ion Torrent sequencing data as it strictly adheres to genotyping assumptions and avoids compound-PCRs (unlike previous methods).

In these chapters, I clarified two major points of concern that had been previously overlooked: (1) Approaches that use AVTs are inappropriate to deal with NGS artifacts, and (2) The presence of contaminant DNA is a significant problem in NGS multigene family genotyping. Contamination of amplicons can result from direct DNA/PCR sample contamination, or MID barcode swapping during pooling of samples prior to sequencing. After many PCR cycles, even a minute amount of contamination may be amplified to form a significant amount of "noise" so that it will become increasingly difficult to distinguish it from the "true" amplicons (i.e. the alleles present in that individual genotype). Given that NGS techniques can sequence the PCR products with extremely high coverage, such artifacts can appear in the data read-out at convincingly high sequencing-depth alongside the true alleles (Chapter 2; Chapter 3, Lighten *et al.* 2014a; b). However, the process of dealing with contaminants and artifacts should not start at the stage of bioinformatic data processing. Here I add to my previous advice regarding bioinformatics, and outline important yet largely unspoken requirements for accurate genotyping of MHC loci, during the stages of sample collections and laboratory protocols.

Sample collection and laboratory protocols: If attention is given during experimental design to measures aimed at avoiding cross sample contamination, the ease of downstream analysis of sequence data can be significantly improved. Contamination may be particularly problematic when samples have been collected in the field, or yield small amounts of DNA. A recent example illustrates this. Herdegen *et al.* (2014) used fishnets to collect a shoal of guppies, and DNA of fish mucus could easily end up contaminating other samples. Furthermore, guppies have to be euthanized in an overdose of anesthetic (typically MS222) before being transferred to sample tubes with ethanol. Given that the same solution tends to be used to kill many individuals (often simultaneously), this can lead to further contamination. This thesis also used samples collected by batch-preserving individuals in the same vial, and I found that previously described AVT bioinformatic protocols could not reliably remove the sequence contamination that this process resulted in. However, contamination was significantly reduced when just a few scales per sample were preserved individually (samples from experimental pedigrees not used in this thesis), as opposed to preserving many whole individuals in the same vial.

This has severe implications on the validity of the AVT approach, which is founded on the ill-conceived idea that confirmation of the authenticity of an individual's alleles can be based on observing that allele in other samples even when present at very low sequencing depths. Given that sampling during fieldwork is hardly a sterile activity, low-level contamination is a practical inevitability (as is low-level barcode swapping during pooling of PCR products prior to sequencing), making AVTs a methodologically unsound approach. More so than ever, it is important that researchers make every effort to minimize cross-sample contamination, and when this is practically impossible (e.g. during fieldwork), the appropriate informatics should be applied to curtail the problems.

Recently, Herdegen *et al.* (2014) used NGS to genotype MHC loci in guppy populations of Northern Venezuela. They concluded that the AVT method (see Zagalska-Neubauer *et al.* 2010, Radwan *et al.* 2012) out-performs the procedure described in Chapter 3. This protocol uses the relative 'degree of change' (*DOC*) in sequencing depth to distinguish true alleles from artifacts (see Chapter 2; Chapter 3; Lighten *et al.* 2014a; b for full details). I demonstrated both empirically and theoretically that the *DOC* criterion is more suitable for NGS MHC genotyping than the various AVT approaches (Chapter 2; Chapter 3; Lighten *et al.* 2014a; b). However, why did the AVT approach in Herdegen *et al.* (2014) appear to outperform the *DOC* method? Herdegen *et al.* (2014) used two sequencing approaches to estimate MHC genotypes. First they amplified MHC loci using degenerate primers and 35 PCR cycles. Once amplified, these samples underwent an undisclosed number of additional emulsion-PCR cycles that form an integral part of the Ion Torrent sequencing protocol (which commonly uses between 30 to 70 cycles). To validate genotypes they also amplified independent replicate amplicons using 33 PCR cycles, which were then pooled and underwent an additional 12 PCR cycles during the Illumina MiSeq Nextera sequencing protocol. However, both of these approaches are ill-advised when sequencing multi-template PCR amplicons of unknown CNV with a multitude of potential errors (e.g. chimeras, base-mismatches etc.) and potential cross-sample contamination. I previously outlined this issue in brief (Chapter 2; Lighten *et al.* 2014b) but here expand of the importance of correct laboratory protocols, which are essential for multigene family genotyping.

Artifacts and contaminants can be relatively easily identified by the *DOC* method if just one independent PCR per sample is performed because they remain at a significantly lower sequence depth than true alleles (Chapter 2; Chapter 3; Lighten *et al.* 2014a; b). This is because (1) the high-copy number template DNA (i.e. the alleles) will outcompete the low-copy number contaminants during the first series of PCRs, and (2) the base mismatch error rates, as well as chimeras, are still sufficiently rare to be identified as artifacts. Post-PCR, however, all artifacts are at a significantly elevated frequency, and when introducing these artifacts into a new set of PCRs with a fresh batch of reagents, their frequencies can increase to such extents that it

becomes virtually impossible to distinguish them from the true alleles (Chapter 2; Lighten *et al.* 2014b).

Up until now, researchers have not acknowledged that the double-PCR in Ion Torrent and Illumina Nextera (as well as 454 sequencing) can be problematic when sequencing multigene families with unknown CNV (and possibly also in the analysis of samples collected in non-sterile conditions). The Illumina TruSeq protocol is in my opinion superior for these particular purposes because it involves just a single independent PCR for each sample (see Chapter 2; Chapter 3; Lighten *et al.* 2014a; b). Indeed, the *DOC* criterion was developed and validated using Illumina TruSeq, which guarantees that artifacts are kept at low frequencies so that they remain distinguishable from alleles. Moreover, because 'double-PCR' protocols can produce high frequency artefacts, these become the origin of further artificial sequences. This can produce further distortion to the depth profile of artificial variants (Chapter 2; Lighten *et al.* 2014b), in particular when artifacts produced during the first set of PCRs occur at much greater depths from those generated in the second PCR. After two rounds of PCRs, the amplified products may consist of (1) high-copy number artifacts, which are indistinguishable from high copy number true alleles, and (2) low-copy number complex artifacts generated from high-copy number artifacts. This makes it difficult to distinguish alleles from artifacts both using the *DOC* criterion and clustering protocols (Lamaze *et al.* 2014, Pavey *et al.* 2013, Sommer *et al.* 2013). An additional point worth emphasizing is the requirement for sequence error correction. In Chapter 3 (Lighten *et al.* 2014a), I identified repeatable base-mismatch errors and then added the total depth observed for these artificial variants back to the parental allele from which they originate. Error correction becomes even more critical when using Ion Torrent or 454 sequencing because they are particularly susceptible to higher incidences of repeatable base-mismatch and homopolymer indel errors. Critically, particular MHC alleles can be reduced in sequencing depth by over 50% by a repeatable indel error (unpublished data). The common practice to discard sequence variants that vary in the number of expected nucleotides (e.g. Herdegen *et al.* 2014) can severely impede accurate quantification of allelic sequences in an

amplicon.

Finally, clarification is required regarding an important misunderstanding that seems to have arisen about the *DOC* criterion, in Herdegen *et al.* (2014). This approach does not rely on the assumption of equal amplification of all allelic copies. I proposed two independent (and complementary) workflows for separating alleles from artifacts. One workflow uses the *DOC* criterion and its only assumption is that alleles are amplified at significantly greater depths than artifacts. This assumption is entirely reasonable given that it is universal to all NGS MHC genotyping procedures, and conveniently, this approach allows for the identification of CNV, potential PCR bias, and poor quality data. Confusion might have arisen because I also proposed a more advanced method that aims to both estimate CNV as well as an individual's multi-locus genotype. The CNV method could significantly advance the field given that currently MHC studies only score the presence of an individual's alleles. The additional assumption made by this method is that the relative sequencing depth of an allele is approximately proportional to its copy number in the genome (i.e. heterozygous and hemizygous alleles are present in one copy, alleles that are present in homozygous state in two copies, and so on). Admittedly, variable amplification of alleles can create unequal depth profiles that can bias the calling of an individual's multi-locus genotype (I.e. pattern of allelic and locus CNV). However, PCR bias should not impede actual allele identification when using the *DOC* criterion, given thorough primer design, as alleles should always be observed at significantly greater depth than artifacts. Further development and validation of the CNV method (e.g. using pedigree records and Mendelian segregation of alleles) is required to make this a standard multi-locus genotyping method in the future. Nevertheless, this could herald a step-change in MHC research because it would enable many population genetic analyses that are currently impossible (e.g. locus phasing, estimating true allele frequencies, genotypic testing of overdominance, etc.).

In summary, I provide new and important advice; when using NGS methods to study multigene families with CNV and/or samples collected in non-sterile environments, I recommend researchers should use the Illumina TruSeq protocol (or an equivalent protocol that avoids compound PCRs). Furthermore, I strongly advise researchers to apply the appropriate bioinformatics protocols (i.e. the *DOC* or novel clustering methods) to distinguish alleles from potential artifacts and avoid AVTs.

MHC supertypes play a role in disease susceptibility and phenotypic variability

The role of MHC in disease resistance and susceptibility (both infectious and autoimmune) is widely recognized in humans (Traherne 2008; Trowsdale 2011). Increasingly, similar relationships between particular MHC polymorphism and parasite infections have been observed in natural populations of non-model organisms (reviewed in Piertney & Oliver, 2006; Spurgin & Richardson, 2010). The use of supertypes in the study of MHC and disease resistance has several advantages over simply using assessing allelic diversity. Firstly, the presence and absence of particular MHC alleles can vary greatly among diverse populations, where many may be observed in just one population (private alleles). So the use of supertypes avoids including many missing data points (alleles) among populations, which would make correlative analysis very difficult. Secondly, supertypes allow characterization of variation in MHC functionality among populations, which is largely ignored in most MHC population genetic studies that focus purely on alleles.

In Chapter 4, I described two MHC supertypes (ST-2 & ST-11) that were correlated with decreased prevalence of *Gyrodactylus* infections among guppy populations. The inferred role in resistance of ST-11 appears to corroborate previous findings, where a group of alleles (supertype ‘a’) were also associated with resistance to *Gyrodactylus* infections (Fraser *et al.* 2010). These alleles were very closely related to supertype-11. However, the pattern associated

with ST-2 is novel. Male guppy colouration (implicated in mate choice and predator avoidance) was correlated with frequencies of these supertypes, as well as *Gyrodactylus* prevalence, and these correlations were governed by variability across river drainages. Colours that are important in mate choice (orange, yellow, and black) are of particular interest because they may be honest signals of fitness, derived from individual immunocompetence (Houde 1997; Saks *et al.* 2003; Aguilera & Amat 2007). Indeed, among infected populations, higher frequencies of ST-2, and ST-11 were associated with lower *Gyrodactylus* prevalence, and greater amounts of orange, yellow, and black coloration on males. The relative increase in health, which these colours may represent, may be a direct consequence of particular MHC supertypes providing better immunological defense against *Gyrodactylus,* thus reducing their prevalence in the populations.

The fact that microsatellite allelic richness (Micro-A_r) was not associated with variation among populations in either colouration or *Gyrodactylus* prevalence supports the hypothesis that these traits may experience strong selection pressures and are largely unaffected by demographic processes. Moreover, the associations between MHC supertype richness (MHC-ST_r), colouration and *Gyrodactylus* prevalence indicates that these important fitness related traits are associated with processes of natural selection operating on functional MHC diversity. Across all populations, greater MHC-ST_r was associated with less orange and yellow colouration on males. Critically, MHC-ST_r was not associated with Micro-A_r. This suggests that MHC-ST_r is under strong selection and little affected by demographic process, while MHC-A_r is affected by both demographic processes and changes in MHC-ST_r. Therefore the association between MHC-A_r and colouration is likely a consequence of links between MHC-ST_r (i.e. the measure of MHC functional diversity of MHC in a population) and fitness related traits, maintained by natural selection (see next section for more detail on the interplay between MHC alleles and supertypes).

The role of MHC diversity (or richness) in population viability is poorly understood (Radwan *et al.* 2010). Such data are important both in an evolutionary and species conservation perspective as it allows the investigation of relationships between MHC richness and pathogen community dynamics. The current paradigm suggests that greater genomic (and MHC) diversity within populations provides the evolutionary potential for populations to adapt to changing environmental conditions. However, if environmental dynamics remain in equilibrium for long periods of time, this can potentially reduce genetic (MHC) variation in populations through critical adaptation. Thus while such populations may not be able to deal with sudden dramatic shifts in their environments (e.g. introduction of an alien pathogen), individual fitness variability may be less than in populations in which environmental conditions are more complex and/or are subject to flux. Indeed, a recent study showed that MHC diversity reduced during critical adaptation to new environments of individual rainbow trout (*Oncorhynchus mykiss*) that were introduced to wild sites from aquaculture enclosures (Monzón-Argüello *et al.* 2013). However, the common premise is to examine MHC-A_r in relation to population adaptation, which may be problematic due to its susceptibility to demographic processes. Here I suggest that MHC-ST_r is a more biologically relevant and robust metric to assess the role of MHC diversity in population adaptation and viability. Notably, lower MHC-ST_r was strongly associated with lower *Gyrodactylus* prevalence, and greater expression of colours believed to signal health, across drainages, and so may represent critical adaptation. Importantly, MHC-ST_r did not significantly vary between populations suspected of being different sizes (low-land populations in high predation sites are generally thought to be larger than up-land low predation sites), and so is a robust measure of functional diversity, which is maintained by strong selection pressures. This is especially important as *Gyrodactylus* prevalence was observed to be significantly different between high- and low-predation sites, yet MHC-ST_r varied independently of population size and is likely implicit in changes in *Gyrodactylus* prevalence across drainages, driven by process of natural selection.

The fact that *Gyrodactylus* prevalence covaried with MHC-ST_r suggests that the diversity of supertypes in a population may be related to pathogen community diversity. That is, when a pathogen community is diverse, a population requires a larger repertoire of different functional supertypes in order to counteract diverse infection potentials. However, this reduces the adaptive strength of that population in combating a single particular pathogen relative to a population that is critically adapted to dealing with just one parasite species. So population viability in the face of many parasite species may require a 'Jack of all trades' approach, compared to a highly specialized approach (and so lower supertype diversity) in populations with fewer pathogens (Pilosof *et al.* 2014).

Supertypes are crucial in the understanding of MHC evolution

By comparing patterns of diversity of MHC alleles, MHC supertypes, and neutral microsatellites, I was able to uncover processes governing MHC evolution, which remain cryptic when assessing MHC allele polymorphism alone. The often observed pattern of high allelic differentiation among populations is traditionally interpreted as representing local adaptation of host species to fast evolving and divergent parasite fauna (reviewed in Piertney & Oliver, 2006; Spurgin & Richardson, 2010). However, this inference is commonly confounded by significant observed effects of demographic processes on patterns of MHC diversity, and the common approach is to quantify this effect by comparing MHC diversity to that of neutrally evolving microsatellite diversity (e.g. Sutton *et al.* 2011; Lamaze *et al.* 2014). By assessing allele nucleotide sequences and the translated PBR amino acid sequences within and among supertypes, high similarity in inferred MHC functionality was observed. Peptide binding region amino acid sequences were either similar or identical among alleles that appear unique at the nucleotide level. To my knowledge this is the first time that identical PBR amino acid sequences have been observed among divergent nucleotide alleles and populations. Such appraisals of functional comparisons among MHC alleles are important as they allow the scale of adaptive divergence at the MHC to

be assessed among populations. By conducting such appraisals, I have revealed that natural selection operates both directly on supertype functionality, and thus individual loci (supertypes appear to be loci specific), and on individual alleles *within* supertypes (which can also be significantly affected by demographic processes). Specifically, stabilizing selection operates upon the functional space of a supertype to maintain critical functionality at particular loci. Because alleles within a supertype have the same/similar function, they are subject to genetic drift, although new alleles will not be lost as easily as fully neutral loci, as they convey the same/similar fitness benefits as other high frequency alleles from which they originate. Alleles that confer relative variation of fitness within a supertype will be subject to intra-supertype Red Queen Dynamics. This explains the observation of many rare and private MHC alleles. The culmination of strong stabilizing selection acting on supertype functionality, and the rapid changes of allele frequencies within supertypes can simultaneously explain how long isolated populations can be highly divergent in MHC allele composition, yet the sharing of particular alleles over large spatial and temporal scales may also be maintained.

Stabilizing selection acting upon MHC alleles within supertypes is strong enough to maintain functionality beyond speciation events. Indeed, by comparing PBR amino acid sequences between individuals of guppies (*P. reticulata*) and the swamp guppy (*P. picta*), trans-species polymorphism was observed in the functionally important attributes of MHC alleles. Evidence supporting a role of stabilizing selection in maintaining MHC functionality over millions of years is important because it resolves the inconsistencies in the traditional hypothesis that balancing selection on MHC alleles is responsible for long term preservation of alleles. An allelic genealogy under balancing selection is similar to those of a neutral gene genealogy, but under a different time scale (Takahata 1990). Thus balancing selection cannot account for the topology, namely very long terminal branches, often observed in MHC allele genealogies. Long terminal branches can however be explained by long term stabilizing selection, and Chapter 5 outlined unique supertype characteristics which support its operation on the MHC.

However, balancing selection is still likely implicit in driving MHC allelic diversity within supertypes, as well as overall supertype diversity. Because supertypes may be MHC locus specific, parasite mediated balancing selection should operate directly on the frequency of particular loci among populations. This is because the unit of selection is the core functionality at these loci (which is restricted by stabilizing selection). The fact that MHC allelic population differentiation is strongly correlated with supertype population differentiation and neutral differentiation, whereas supertypes differentiation is not correlated with neutral differentiation, further supports the notion that individual loci are a unit of selection. This can explain why female mate choice is often associated with choosing MHC heterozygous or dissimilar males (Milinski 2006). In these cases it may be that specific allelic combination are not the unit of choice, but rather the increased likelihood of including diverse/particular supertypes. This goes further to explain why populations that are depauperate at the MHC allelic level can maintain high levels of fitness (or at least do not display unusually heavy parasite burdens; Radwan *et al.* 2010). Balancing selection maintains critically functioning loci independently, while not preventing loss of allelic diversity within groups of functionally similar supertype alleles. Indeed, a recent study of bottlenecked populations of Berthelot's pipit (*Anthus berthelotii*) revealed just 22 MHC IIb alleles among 310 individuals (Gonzalez-Quevedo *et al.* 2015). However, almost all of these alleles represented a unique supertype (22 alleles - 20 supertypes). Therefore, despite large losses of allelic diversity though demographic bottlenecks, selection for individual loci can maintain critical MHC functionality within populations. Spatially and temporally fluctuating balancing selection at MHC loci may also explain the high variance in MHC CNV observed in guppies, and other species. This model of 'stabilized supertypes - balanced loci' could be used to experimentally deduce the biological relevance of MHC CNV in wild populations, and to unveil a likely important and understudied unit upon which selection operates at the MHC.

The guppy is a unique model system to study MHC evolution

We are now in the genomic era, which holds unparalleled power to detect signatures of genome-wide adaptation. However, researchers in evolutionary ecology still look towards MHC genes as a well-established system to assess local adaptation in species. Over 50 years of empirical and theoretical analyses on these genes reflects their biological importance in fitness, and as such, a firm basis for understanding their evolution has materialized. While biomedical and immunology researchers focus on the MHC to better understand its critical function and evolution in general, it seems for the most part that ecologists' latch on to the MHC purely though an interest in their focal species. This has revealed a complex of varying evolutionary processes operating on the MHC among a wide range of taxa, yet often, observations in one species may be contradicted or absent in the next. These could arise though differences in life history, ecology, behavior, and sample/population accessibility. However, if we are to significantly progress our understanding of MHC evolutionary ecology, researchers would do well to focus on a model species that holds the most optimal or desirable traits, which would augment the myriad of complex evolutionary processes in a single MHC system.

Guppies appear to be such a system for several reasons: (1) In Trinidad alone there are hundreds, if not thousands, of isolated yet easily accessible replicate populations, (2) among different combinations of populations, ecological conditions are either similar or dissimilar, and so populations have been shown to demonstrate either parallel or non-parallel evolution (Houde 1997; Magurran 2005), (3) individuals are abundant and easily sampled, (4) guppies are among the fastest evolving vertebrates and local adaption can occur very quickly, (5) there is a wealth of knowledge surrounding guppy physiology, ecology, life history, behavior, and natural selection, (6) combinations of bottlenecked, and un-bottlenecked populations, (7) guppies have been introduced globally and have colonized many different habitat types containing diverse pathogen fauna, (8) wild individuals can easily be transported back to the lab and with simple husbandry experimental populations can be established, (9) poeciliid species are also known to

hybridize allowing the experimental study of trans-species polymorphism and introgression at the MHC, and finally (10) guppies have extraordinary MHC diversity.

The empirical data described in this thesis also demonstrate that guppies are an ideal species to study the interaction between parasite mediated and sexually mediated natural selection on the MHC. Moreover, they appear an elegant system in which future research could establish the long term role of MHC CNV in fitness among populations and species. While guppies should be recognized as a valuable resource in MHC studies, increasing caution should be exerted in conserving population sizes, especially in those that are well studied in Trinidad. Numerous population have experienced recent human mediated declines, and Trinidadian authorities are aiming to protect this valuable species so that its use as an exception biological model system can continue (Ryan Mohammed pers. comm).

Conclusion

Here I present a thesis that delineates novel approaches to both MHC sequence data collection and genotype estimation, and in the analysis of MHC diversity among natural populations of the guppy. Firstly, I have shown that significant improvements can be made to NGS MHC genotyping approaches, which allows high quality and repeatable genotype estimates, while discarding poor quality data that can severely bias downstream analysis. The overall lessons learned are that increased diligence is required to fully eradicate artificial sequences from NGS MHC data and that this can be accomplished by using sequence depth modelling approaches, which strictly adhere to genotyping assumptions.

Secondly, population level MHC supertype diversity, and particular MHC supertypes are related to changes in *Gyrodactylus* prevalence infecting guppy populations. By classifying alleles based on shared functional characteristics such inferences can be made, and this is especially

important in species where MHC allelic diversity significantly varies among populations. In using *Gyrodactylus* as a proxy for parasitism, I propose that individual parasite species exert parallel evolutionary effects (stabilizing selection) on MHC supertypes, which maintains critical functionality across large spatial and temporal scales. In addition, it is varying parasite communities (number of different species or parasitic phenotypes) that exert balancing selection on the MHC to maintain higher levels of loci specific supertype functionality. However, further experimental work is required to confirm this.

Finally, I have uncovered cryptic evolutionary processes operating on the MHC by comparing MHC alleles, MHC supertypes (loci specific functionality), and neutral microsatellite population diversity. The presence of stabilizing selection acting to maintain MHC supertype functionality, balancing selection maintaining supertype diversity, and intra-supertype evolutionary dynamics fueling allelic turn over, forms the basis for a novel model of MHC evolution in 'stabilized supertypes - balanced loci'. Critically this model explains numerous observations commonly present in MHC studies: (1) neutral processes and selective processes both apparently operating on MHC alleles, (2) high variance in allele frequencies within and among populations, (3) many rare and private alleles, (4) the maintenance of alleles over large spatial and temporal scales, and so the enigma of trans-species polymorphism.

References

Aguilera E, Amat JA (2007) Carotenoids, immune response and the expression of sexual ornaments in male greenfinches (Carduelis chloris). *Die Naturwissenschaften*, **94**, 895–902.

Altschul SF, Gish W, Miller W *et al*. (1990) Basic local alignment search tool. *Journal of Molecular Biology*, **215**, 403–410.

Antao T, Lopes A, Lopes R *et al.* (2008) LOSITAN: A workbench to detect molecular adaptation based on a Fst-outlier method. *BMC Bioinformatics*, **9**, 323.

Archard GA, Cuthill IC, Partridge JC *et al.* (2008) Female guppies (Poecilia reticulata) show no preference for conspecific chemosensory cues in the field or an artificial flow chamber. *Behaviour*, **145**, 1329–1346.

Arden B, Klein J (1982) Biochemical comparison of major histocompatibility complex molecules from different subspecies of Mus musculus: evidence for trans-specific evolution of alleles. *PNAS,* **79**, 2342–6.

Asthana S, Noble WS, Kryukov G *et al.* (2007) Widely distributed noncoding purifying selection in the human genome. *PNAS,* **104**, 12410–12415.

Babik W (2010) Methods for MHC genotyping in non-model vertebrates. *Molecular ecology resources*, **10**, 237–251.

Babik W, Taberlet P, Ejsmond MJ *et al.* (2009) New generation sequencers as a tool for genotyping of highly polymorphic multilocus MHC system. *Molecular ecology resources*, **9**, 713–9.

Baillie L (2012) Genetic population structure of the Trinidadian guppy (Poecilia reticulata) across Trrinidad and Tobago. Dalhousie University.

Balenger SL, Zuk M (2014) Testing the Hamilton-Zuk hypothesis: past, present, and future. *Integrative and comparative biology*, **54**, 601–13.

Barson NJ, Cable J, van Oosterhout C (2009) Population genetic analysis of microsatellite variation of guppies (Poecilia reticulata) in Trinidad and Tobago: Evidence for a dynamic source-sink metapopulation structure, founder events and population bottlenecks. *Journal of Evolutionary Biology*, **22**, 485–497.

Beaumont MA, Nichols RA (1996) Evaluating Loci for Use in the Genetic Analysis of Population Structure. *Proceedings of the Royal Society B: Biological Sciences*, **263**, 1619–1626.

Beck S, Trowsdale J (2000) The human major histocompatibility complex: Lessons from the DNA sequence. *Annual Review of Genomics and Human Genetics*, **1**, 117–137.

Beer AE, Quebbeman JF, Ayers JW *et al.* (1981) Major histocompatibility complex antigens, maternal and paternal immune responses, and chronic habitual abortions in humans. *American journal of obstetrics and gynecology*, **141**, 987–999.

Bernatchez L, Landry C (2003) MHC studies in nonmodel vertebrates : what have we learned about natural selection in 15 years ? *Journal of evolutionary biology*, **16**, 363–377.

De Boer RJ, Borghans JAM, van Boven M *et al.* (2004) Heterozygote advantage fails to explain the high degree of polymorphism of the MHC. *Immunogenetics*, **55**, 725–31.

Bolker BM, Brooks ME, Clark CJ *et al.* (2009) Generalized linear mixed models: a practical guide for ecology and evolution. *Trends in Ecology & Evolution*, **24**, 127–135.

Bondinas GP, Moustakas AK, Papadopoulos GK (2007) The spectrum of HLA-DQ and HLA-DR alleles, 2006: a listing correlating sequence and structure with function. *Immunogenetics*, **59**, 539–553.

Brown JH, Jardetzky TS, Gorga JC *et al.* (1993) Three-dimensional structure of the human class II histocompatibility antigen HLA-DR1. *Nature*, **364**, 33–39.

Burri R, Promerová M, Goebel J *et al.* (2014) PCR-based isolation of multigene families: Lessons from the avian MHC class IIB. *Molecular ecology resources*. **14**, 778-788

Bush AO, Lafferty KD, Lotz JM *et al.* (1997) Parasitology meets ecology on its own terms: Margolis et al. revisited. *The Journal of parasitology*, **83**, 575–583.

Cable J, van Oosterhout C (2007) The impact of parasites on the life history evolution of guppies (Poecilia reticulata): the effects of host size on parasite virulence. *International journal for parasitology*, **37**, 1449–1458.

Campbell PJ, Stephens PJ, Pleasance ED *et al.* (2008) Identification of somatically acquired rearrangements in cancer using genome-wide massively parallel paired-end sequencing. *Nature genetics*, **40**, 722–729.

Cao H, Wu J, Wang Y *et al.* (2013) An integrated tool to study MHC region: accurate SNV detection and HLA genes typing in human MHC region using targeted high-throughput sequencing. *PloS one*, **8**, e69388.

Carlsen T, Aas AB, Lindner D *et al.* (2012) Don't make a mista(g)ke: Is tag switching an overlooked source of error in amplicon pyrosequencing studies? *Fungal Ecology*, **5**, 747–749.

Carrington M (1999) Recombination within the human MHC. *Immunological Reviews*, **167**, 245–256.

Catchen J, Hohenlohe PA, Bassham S *et al.* (2013) Stacks: an analysis tool set for population genomics. *Molecular ecology*, **22**, 3124–40.

Del Cerro S, Merino S, Martínez-de la Puente J *et al.* (2010) Carotenoid-based plumage colouration is associated with blood parasite richness and stress protein levels in blue tits (Cyanistes caeruleus). *Oecologia*, **162**, 825–835.

Chen JM, Cooper DN, Chuzhanova N *et al.* (2007) Gene conversion: mechanisms, evolution and human disease. *Nature reviews. Genetics*, **8**, 762–775.

Cheng Y, Stuart A, Morris K *et al.* (2012) Antigen-presenting genes and genomic copy number variations in the Tasmanian devil MHC. *BMC genomics*, **13**, 87.

Chew BP, Park JS (2004) Carotenoid Action on the Immune Response. *Journal of Nutrrition*, **134**, 257–261.

Chiang DY, Getz G, Jaffe DB *et al.* (2009) High-resolution mapping of copy-number alterations with massively parallel sequencing. *Nature methods*, **6**, 99–103.

Crispo E, Bentzen P, Reznick DN *et al.* (2006) The relative influence of natural selection and geography on gene flow in guppies. *Molecular ecology*, **15**, 49–62.

Croisetière S, Bernatchez L, Belhumeur P (2010) Temperature and length-dependent modulation of the MH class IIβ gene expression in brook charr (Salvelinus fontinalis) by a cis-acting minisatellite. *Molecular Immunology*, **47**, 1817–1829.

Cullen M, Perfetto SP, Klitz W *et al.* (2002) High-resolution patterns of meiotic recombination across the human major histocompatibility complex. *American journal of human genetics*, **71**, 759–76.

Cummings SM, McMullan M, Joyce DA *et al.* (2009) Solutions for PCR, cloning and sequencing errors in population genetic analysis. *Conservation Genetics*, **11**, 1095–1097.

Danchin E, Vitiello V, Vienne A *et al.* (2004) The major histocompatibility complex origin. *Immunological Reviews*, **198**, 216–232.

Dawkins R, Leelayuwat C, Gaudieri S *et al.* (1999) Genomics of the major histocompatibility complex: haplotypes, duplication, retroviruses and disease. *Immunological reviews*, **167**, 275–304.

Doledec S, Chessel D (1994) Co-inertia analysis: an alternative method for studying species-environment relationships. *Freshwater Biology*, **31**, 277–294.

Doytchinova IA, Flower DR (2005) In silico identification of supertypes for class II MHCs. *Journal of immunology*, **174**, 7085–95.

Doytchinova IA, Guan P, Flower DR (2004) Identifiying Human MHC Supertypes Using Bioinformatic Methods. *The Journal of Immunology*, **172**, 4314–4323.

Dray S, Dufour AB (2007) The ade4 Package: Implementing the Duality Diagram for Ecologists. *Journal of Statistical Software*, **22**, 1 – 20.

Dzuris JL, Sidney J, Appella E *et al.* (2000) Conserved MHC class I peptide binding motif between humans and rhesus macaques. *Journal of immunology*, **164**, 283–291.

Edgar RC, Haas BJ, Clemente JC *et al.* (2011) UCHIME improves sensitivity and speed of chimera detection. *Bioinformatics*, **27**, 2194–200.

Edwards SV, Hedrick PW (1998a) Evolution and ecology of MHC molecules: from genomics to sexual selection. *Trends in Ecology & Evolution*, **13**, 305–311.

Eimes JA, Bollmer JL, Whittingham LA *et al.* (2011) Rapid loss of MHC class II variation in a bottlenecked population is explained by drift and loss of copy number variation. *Journal of evolutionary biology*, **24**, 1847–1856.

Eirín-López JM, González-Tizón AM *et al.* (2004) Birth-and-death evolution with strong purifying selection in the histone H1 multigene family and the origin of orphon H1 genes. *Molecular biology and evolution*, **21**, 1992–2003.

Eizaguirre C, Lenz TL, Kalbe M *et al.* (2012) Rapid and adaptive evolution of MHC genes under parasite selection in experimental vertebrate populations. *Nature communications*, **3**, 621.

Eizaguirre C, Lenz TL, Sommerfeld RD *et al.* (2011) Parasite diversity, patterns of MHC II variation and olfactory based mate choice in diverging three-spined stickleback ecotypes. *Evolutionary Ecology*, **25**, 605–622.

Eizaguirre C, Yeates SE, Lenz TL *et al.* (2009) MHC-based mate choice combines good genes and maintenance of MHC polymorphism. *Molecular Ecology*, **18**, 3316–3329.

Ejsmond MJ, Radwan J, Wilson AB (2014) Sexual selection and the evolutionary dynamics of the major histocompatibility complex. *Proceedings of the Royal Society B: Biological Sciences* **281**.

Ellison A, Allainguillaume J, Girdwood S *et al.* (2012) Maintaining functional major histocompatibility complex diversity under inbreeding: the case of a selfing vertebrate. *Proceedings of the Royal Society B: Biological Sciences*, **279**, 5004–5013.

Elphinstone MS, Hinten GN, Anderson MJ, Nock CJ (2003) An inexpensive and high-throughput procedure to extract and purify total genomic DNA for population studies. *Molecular Ecology Notes*, **3**, 317–320.

Endler J (1980) Natural selection on colour patterns in Poecillia reticulata. *Evolution*, **34**, 76–91.

Endler JA (1991) Variation in the appearance of guppy color patterns to guppies and their predators under different visual conditions. *Vision research*, **31**, 587–608.

Evans JP, Pilastro A, Schlupp I (Eds.) (2011) *Ecology and Evolution of Poeciliid Fishes*. University of Chicago Press.

Ezawa K, Ikeo K, Gojobori T *et al.* (2010) Evolutionary pattern of gene homogenization between primate-specific paralogs after human and macaque speciation using the 4-2-4 method. *Molecular Biology and Evolution*, **27**, 2152–2171.

Figueroa F, Günther E, Klein J (1988) MHC polymorphism pre-dating speciation. *Nature*, **335**, 265–267.

Figueroa F, Mayer WE, Sültmann H *et al.* (2000) Mhc class II B gene evolution in East African cichlid fishes. *Immunogenetics*, **51**, 556–575.

Fitzpatrick SW, Torres-Dowdall J, Reznick DN *et al.* (2014) Parallelism isn't perfect: could disease and flooding drive a life-history anomaly in Trinidadian guppies? *The American naturalist*, **183**, 290–300.

François Husson JJ (2008) FactoMineR: An R Package for Multivariate Analysis. *Journal of Statistical Software*, **25**, 1-18

Fraser BA, Neff BD (2010a) Parasite mediated homogenizing selection at the MHC in guppies. *Genetica*, **138**, 273–278.

Fraser B a, Neff BD (2010b) Parasite mediated homogenizing selection at the MHC in guppies. *Genetica*, **138**, 273–8.

Fraser BA, Ramnarine IW, Neff BD (2010) Temporal variation at the MHC class IIb in wild populations of the guppy (Poecilia reticulata). *Evolution: International Journal of Organic Evolution*, **64**, 2086–2096.

Gagnaire PA, Pavey SA, Normandeau E *et al.* (2013) The genetic architecture of reproductive isolation during speciation-with-gene-flow in lake whitefish species pairs assessed by RAD sequencing. *Evolution; international journal of organic evolution*, **67**, 2483–2497.

Galan M, Guivier E, Caraux G *et al.* (2010) A 454 multiplex sequencing method for rapid and reliable genotyping of highly polymorphic genes in large-scale studies. *BMC genomics*, **11**, 296.

Gasparini J, Bize P, Piault R *et al.* (2009) Strength and cost of an induced immune response are associated with a heritable melanin-based colour trait in female tawny owls. *The Journal of animal ecology*, **78**, 608–616.

Gasparini C, Congiu L, Pilastro A (2015) MHC-similarity and sexual selection: different doesn't always mean attractive. *Molecular ecology*. **In press**

Gilles A, Meglécz E, Pech N *et al.* (2011) Accuracy and quality assessment of 454 GS-FLX Titanium pyrosequencing. *BMC genomics*, **12**, 245.

Godin JGJ (2003) Predator preference for brightly colored males in the guppy: a viability cost for a sexually selected trait. *Behavioral Ecology*, **14**, 194–200.

Gomez-Alvarez V, Teal TK, Schmidt TM (2009) Systematic artifacts in metagenomes from complex microbial communities. *The ISME journal*, **3**, 1314–1317.

Gonzalez-Quevedo C, Phillips KP, Spurgin LG *et al.* (2015) 454 screening of individual MHC variation in an endemic island passerine. *Immunogenetics*, **67**, 149–162.

Gordon SP, López-Sepulcre A, Reznick DN (2012) Predation-associated differences in sex linkage of wild guppy coloration. *Evolution; international journal of organic evolution*, **66**, 912–918.

Gotanda KM, Delaire LC, Raeymaekers JAM *et al.* (2013) Adding parasites to the guppy-predation story: insights from field surveys. *Oecologia*, **172**, 155–166.

Gotanda KM, Hendry AP (2014) Using adaptive traits to consider potential consequences of temporal variation in selection: male guppy colour through time and space. *Biological Journal of the Linnean Society*, **112**, 108–122.

Gregersen JW, Kranc KR, Ke X *et al.* (2006) Functional epistasis on a common MHC haplotype associated with multiple sclerosis. *Nature*, **443**, 574–577.

Grether GF, Hudon J, Millie DF (1999) Carotenoid limitation of sexual coloration along an environmental gradient in guppies. *Proceedings of the Royal Society B: Biological Sciences*, **266**, 1317–1322.

Del Guercio MF, Sidney J, Hermanson G *et al.* (1995) Binding of a peptide antigen to multiple HLA alleles allows definition of an A2-like supertype. *Journal of immunology (Baltimore, Md. : 1950)*, **154**, 685–693.

Hamilton WD, Zuk M (1982) Heritable true fitness and bright birds: a role for parasites? *Science (New York, N.Y.)*, **218**, 384–387.

Harismendy O, Ng PC, Strausberg RL *et al.* (2009) Evaluation of next generation sequencing platforms for population targeted sequencing studies. *Genome biology*, **10**, R32.

Harris PD (1986) Species of Gyrodactylus von Nordmann, 1832 (Monogenea Gyrodactylidae) from poeciliid fishes, with a description of G. turnbulli sp. nov. from the guppy, Poecilia reticulata Peters. *Journal of Natural History*, **20**, 183–191.

Haskins CP, Haskins EF, McLaughlin JJA *et al.* (1961) Polymorphism and population structure in Lebistes reticulatus, an ecological study. In: *Vertebrate Speciation* (ed Blair WF), pp. 320–395. Austin: University of Texas Press.

Hayes JL, Tzika A, Thygesen H *et al.* (2013) Diagnosis of copy number variation by Illumina next generation sequencing is comparable in performance to oligonucleotide array comparative genomic hybridisation. *Genomics*, **102**, 174–181.

Hedrick PW (2002) Pathogen resistance and genetic variation at MHC loci. *Evolution; international journal of organic evolution*, **56**, 1902–1908.

Herdegen M, Babik W, Radwan J (2014) Selective pressures on MHC class II genes in the guppy (Poecilia reticulata) as inferred by hierarchical analysis of population structure. *Journal of evolutionary biology*, **27**, 2347–2359.

Högstrand K, Böhme J (1999) Gene conversion can create new MHC alleles. *Immunological reviews*, **167**, 305–317.

Hosomichi K, Miller MM, Goto RM *et al.* (2008) Contribution of mutation, recombination, and gene conversion to chicken MHC-B haplotype diversity. *Journal of immunology,* **181**, 3393–3399.

Houde AE (1997a) *Sex, Color, and Mate Choice in Guppies*. Princeton University Press.

Houde AE (1997b) *Sex, Color, and Mate Choice in Guppies*. Princeton University Press.

Houde AE, Torio AJ (1992) Effect of parasitic infection on male color pattern and female choice in guppies. *Behavioral Ecology*, **3**, 346–351.

Huchard E, Albrecht C, Schliehe-Diecks S *et al.* (2012) Large-scale MHC class II genotyping of a wild lemur population by next generation sequencing. *Immunogenetics*, **64**, 895–913.

Huchard E, Raymond M, Benavides J *et al.* (2010) A female signal reflects MHC genotype in a social primate. *BMC evolutionary biology*, **10**, 96.

Hughes AL, Nei M (1988) Pattern of nucleotide substitution at major histocompatibility complex class I loci reveals overdominant selection. *Nature*, **335**, 167–170.

Jacquin L, Lenouvel P, Haussy C *et al.* (2011) Melanin-based coloration is related to parasite intensity and cellular immune response in an urban free living bird: the feral pigeon Columba livia. *Journal of Avian Biology*, **42**, 11–15.

Jeffery KJM, Bangham CRM (2000) Do infectious diseases drive MHC diversity? *Microbes and Infection*, **2**, 1335–1341.

Johnson MB, Lafferty KD, van Oosterhout C *et al.* (2011) Parasite transmission in social interacting hosts: monogenean epidemics in guppies. *PloS one*, **6**, e22634.

Jombart T (2008) adegenet: a R package for the multivariate analysis of genetic markers. *Bioinformatics (Oxford, England)*, **24**, 1403–1405.

Jombart T, Ahmed I (2011) adegenet 1.3-1: new tools for the analysis of genome-wide SNP data. *Bioinformatics (Oxford, England)*, **27**, 3070–3071.

Jombart T, Devillard S, Balloux F (2010) Discriminant analysis of principal components: a new method for the analysis of genetically structured populations. *BMC genetics*, **11**, 94.

Jordan WC, Bruford MW (1998) New perspectives on mate choice and the MHC. *Heredity*, **81**, 239–245.

Jost L (2008) GST and its relatives do not measure differentiation. *Molecular Ecology*, **17**, 4015–4026.

Kamath PL, Getz WM (2011) Adaptive molecular evolution of the Major Histocompatibility Complex genes, DRA and DQA, in the genus Equus. *BMC evolutionary biology*, **11**, 128.

Katju V, Bergthorsson U (2013) Copy-number changes in evolution: rates, fitness effects and adaptive significance. *Frontiers in genetics*, **4**, 273.

Kemp D, Reznick DN, Grether GF (2008) Ornamental evolution in Trinidadian guppies (Poecilia reticulata): insights from sensory processing-based analyses of entire colour patterns. *Biological Journal of the Linnean Society, **95**, 734–747*.

Klein J (1987) Origin of major histocompatibility complex polymorphism: the trans-species hypothesis. *Human immunology*, **19**, 155–162.

Klein J, Sato A, Nagl S *et al.* (1998) Moleculare Trans-species polymorphism. *Annual Review of Ecology and Systematics*, **29**, 1–21.

Klein J, Sato A, Nikolaidis N (2007) MHC, TSP, and the origin of species: from immunogenetics to evolutionary genetics. *Annual review of genetics*, **41**, 281–304.

Klein, J, Ono H, Klein D *et al*.(1993) The Accordian Model of MHC evolution (J Gergely, M Benczúr, A Erdei, et al., Eds,). *Progress in Immunology*, **8**, 137-143.

Kloch A, Babik W, Bajer A *et al.* (2010) Effects of an MHC-DRB genotype and allele number on the load of gut parasites in the bank vole Myodes glareolus. *Molecular ecology*, **19,** 255–265.

Koboldt DC, Steinberg KM, Larson DE *et al.* (2013) The next-generation sequencing revolution and its impact on genomics. *Cell*, **155**, 27–38.

Kolluru GR, Grether GF, South SH *et al.* (2006) The effects of carotenoid and food availability on resistance to a naturally occurring parasite (Gyrodactylus turnbulli) in guppies (Poecilia reticulata). *Biological Journal of the Linnean Society*, **89**, 301–309.

Kondrashov FA (2012) Gene duplication as a mechanism of genomic adaptation to a changing environment. *Proceedings of the Royal Society B: Biological Sciences*, **279**, 5048–57.

Kulski JK, Shiina T, Anzai T *et al.* (2002) Comparative genomic analysis of the MHC: the evolution of class I duplication blocks, diversity and complexity from shark to man. *Immunological reviews*, **190**, 95–122.

Ladle RJ (1992) Parasites and sex: Catching the red queen. *Trends in ecology & evolution,* **7**, 405–408.

Lamaze FC, Pavey SA, Normandeau E *et al.* (2014) Neutral and selective processes shape MHC gene diversity and expression in stocked brook charr populations (Salvelinus fontinalis). *Molecular ecology*, **23**, 1730–1748.

Lamichhaney S, Berglund J, Almén MS *et al.* (2015) Evolution of Darwin's finches and their beaks revealed by genome sequencing. *Nature*, **518**, 371-375.

Lawrie DS, Messer PW, Hershberg R *et al.* (2013) Strong Purifying Selection at Synonymous Sites in D. melanogaster. *PLoS Genetics*, **9**.

Leffler EM, Gao Z, Pfeifer S *et al.* (2013) Multiple instances of ancient balancing selection shared between humans and chimpanzees. *Science*, **339**, 1578–1582.

Lenz TL, Becker S (2008) Simple approach to reduce PCR artefact formation leads to reliable genotyping of MHC and other highly polymorphic loci — Implications for evolutionary analysis. *Gene*, **427**, 117–123.

Li M, Stoneking M (2012) A new approach for detecting low-level mutations in next-generation sequence data. *Genome Biology*, **13**, R34.

Lighten J, van Oosterhout C, Paterson IG *et al.* (2014a) Ultra-deep Illumina sequencing accurately identifies MHC class IIb alleles and provides evidence for copy number variation in the guppy (Poecilia reticulata). *Molecular ecology resources*, **14**, 753-767.

Lighten J, van Oosterhout C, Bentzen P (2014b) Critical review of NGS analyses for de novo genotyping multigene families. *Molecular ecology*, **23**, 3957–3972.

Lillie M, Grueber CE, Sutton JT *et al.* (2015) Selection on MHC class II supertypes in the New Zealand endemic Hochstetter's frog. *BMC evolutionary biology*, **15**, 63.

Lindholm AK, Breden F, Alexander HJ *et al.* (2005) Invasion success and genetic diversity of introduced populations of guppies Poecilia reticulata in Australia. *Molecular Ecology*, **14**, 3671–3682.

Lippert C, Listgarten J, Davidson RI *et al.* (2013) An exhaustive epistatic SNP association analysis on expanded Wellcome Trust data. *Scientific reports*, **3**, 1099.

Llaurens V, McMullan M, Van Oosterhout C (2012a) Cryptic MHC polymorphism revealed but not explained by selection on the class IIB peptide binding region. *Molecular Biology and Evolution*, **29**, 1631–1644.

Llaurens V, McMullan M, van Oosterhout C (2012b) Cryptic MHC polymorphism revealed but not explained by selection on the class IIb peptide-binding region. *Molecular biology and evolution*, **29**, 1631–44.

Locke DP, Sharp AJ, McCarroll SA *et al.* (2006) Linkage disequilibrium and heritability of copy-number polymorphisms within duplicated regions of the human genome. *American journal of human genetics*, **79**, 275–290.

Lund O, Nielsen M, Kesmir C *et al.* (2004) Definition of supertypes for HLA molecules using clustering of specificity matrices. *Immunogenetics*, **55**, 797–810.

Ma K., Hsieh T., Chao A (2014) spadeR: species prediction and diversity estimation in R. R package version 1.0. *spadeR: species prediction and diversity estimation in R*.

Maan ME, Van Der Spoel M, Jimenez PQ *et al.* (2006) Fitness correlates of male coloration in a Lake Victoria cichlid fish. *Behavioral Ecology*, **17**, 691–699.

Magoc T, Salzberg SL (2011) FLASH: Fast Length Adjustment of Short Reads to Improve Genome Assemblies. *Bioinformatics*, **27**, 2957–2963.

Magurran AE (2005) *Evolutionary Ecology: The Trinidadian Guppy*. Oxford University Press.

Martin CH, Johnsen S (2007) A field test of the Hamilton–Zuk hypothesis in the Trinidadian guppy (Poecilia reticulata). *Behavioral Ecology and Sociobiology*, **61**, 1897–1909.

Martin JA, Wang Z (2011) Next-generation transcriptome assembly. *Nature reviews. Genetics*, **12**, 671–682.

Martinsohn JT, Sousa AB, Guethlein LA *et al.* (2000) The gene conversion hypothesis of MHC evolution: A review. *Immunogenetics*, **50**, 168-200.

Mays HL, Hill GE (2004) Choosing mates: good genes versus genes that are a good fit. *Trends in ecology & evolution*, **19**, 554–559.

McMullan M (2010) Host-parasite co-evolution and genetic variation at the Major Histocompatibility Complex in the Trinidadian guppy (Poecilia reticulata). University of Hull.

Meffe GK (1989) *Ecology and Evolution of Livebearing Fishes*. Prentice Hall.

Mehra NK, Kaur G (2003) MHC-based vaccination approaches: progress and perspectives. *Expert reviews in molecular medicine*, **5**, 1–17.

Meredith RW, Pires MN, Reznick DN *et al.* (2011) Molecular phylogenetic relationships and the coevolution of placentotrophy and superfetation in Poecilia (Poeciliidae: Cyprinodontiformes). *Molecular Phylogenetics and Evolution*, **59**, 148–157.

Milinski M (2006) The Major Histocompatibility Complex, Sexual Selection, and Mate Choice. *Annual Review of Ecology, Evolution, and Systematics*, **37**, 159–186.

Millar NP, Hendry AP (2012) Population divergence of private and non-private signals in wild guppies. *Environmental Biology of Fishes*, **94**, 513–525.

Monzón-Argüello C, Garcia de Leaniz C, Gajardo G *et al.* (2013) Less can be more: loss of MHC functional diversity can reflect adaptation to novel conditions during fish invasions. *Ecology and evolution*, **3**, 3359–3368.

Mougeot F, Martínez-Padilla J, Bortolotti GR *et al.* (2010) Physiological stress links parasites to carotenoid-based colour signals. *Journal of evolutionary biology*, **23**, 643–650.

Mukherjee S, Ganguli D, Majumder PP (2014) Global footprints of purifying selection on Toll-like receptor genes primarily associated with response to bacterial infections in humans. *Genome biology and evolution*, **6**, 551–558.

Nadachowska-Brzyska K, Zieliński P, Radwan J *et al.* (2012) Interspecific hybridization increases MHC class II diversity in two sister species of newts. *Molecular ecology*, **21**, 887–906.

Nei M, Gu X, Sitnikova T (1997) Evolution by the birth-and-death process in multigene families of the vertebrate immune system. *PNAS*, **94**, 7799–7806.

Nielsen R, Paul JS, Albrechtsen A *et al.* (2011) Genotype and SNP calling from next-generation sequencing data. *Nature reviews. Genetics*, **12**, 443–51.

Nowak MA, Tarczy-Hornoch K, Austyn JM (1992) The optimal number of major histocompatibility complex molecules in an individual. *PNAS*, **89**, 10896–10899.

O'Callaghan CA, Tormo J, Willcox BE *et al.* (1998) Structural features impose tight peptide binding specificity in the nonclassical MHC molecule HLA-E. *Molecular cell*, **1**, 531–541.

Ober C, Steck T, Van Der Ven K *et al.* (1993) MHC class II compatibility in aborted fetuses and term infants of couples with recurrent spontaneous abortion. *Journal of Reproductive Immunology*, **25**, 195–207.

Ohta T (1991) Role of diversifying selection and gene conversion in evolution of major histocompatibility complex loci. *Proceedings of the National Academy of Sciences of the United States of America*, **88**, 6716–6720.

Oliver MK, Telfer S, Piertney SB (2009) Major histocompatibility complex (MHC) heterozygote superiority to natural multi-parasite infections in the water vole (Arvicola terrestris). *Proceedings of the Royal Society B: Biological Sciences*, **276**, 1119–1128.

Oomen RA, Gillett RM, Kyle CJ (2013) Comparison of 454 pyrosequencing methods for characterizing the major histocompatibility complex of nonmodel species and the advantages of ultra deep coverage. *Molecular ecology resources*, **13**, 103–116.

van Oosterhout C (2009a) Transposons in the MHC: the Yin and Yang of the vertebrate immune system. *Heredity*, **103**, 190–191.

van Oosterhout C (2009b) A new theory of MHC evolution : beyond selection on the immune genes. *Proceedings of the Royal Society*, **276**, 657–665.

van Oosterhout C (2013) Maintenance of major histocompatibility supertype variation in selfing vertebrate is no evidence for overdominant selection. *Proceedings of the Royal Society B: Biological Sciences*, **280**, 20122501.

van Oosterhout C, Hutchinson WF, Wills DPM *et al.* (2004) MICRO-CHECKER: Software for identifying and correcting genotyping errors in microsatellite data. *Molecular Ecology Notes*, **4**, 535–538.

van Oosterhout C, Joyce DA, Cummings SM (2006a) Evolution of MHC class IIB in the genome of wild and ornamental guppies, Poecilia reticulata. *Heredity*, **97**, 111–118.

van Oosterhout C, Joyce DA, Cummings SM *et al.* (2006b) Balancing selection, random genetic drift, and genetic variation at the major histocompatibility complex in two wild populations of guppies (Poecilia reticulata). *Evolution: International Journal of Organic Evolution*, **60**, 2562–2574.

Padidam M, Sawyer S, Fauquet CM (1999) Possible emergence of new geminiviruses by frequent recombination. *Virology*, **265**, 218–25.

Papadopulos ASTP, Kaye M, Devaux C *et al.* (2014) Evaluation of genetic isolation within an island flora reveals unusually widespread local adaptation and supports sympatric speciation. *Philosophical transactions of the Royal Society of London. Series B, Biological sciences*, **369**

Paradis E, Claude J, Strimmer K (2004) APE: Analyses of Phylogenetics and Evolution in R language. *Bioinformatics*, **20**, 289–290.

Paterson IG, Crispo E, Kinninson MT *et al*.(2005) Characterization of tetranucleotide microsatellite markers in guppy (Poecilia reticulata). *Molecular Ecology Notes*, **5**, 269–271.

Pavey SA, Sevellec M, Adam W *et al.* (2013) Nonparallelism in MHCIIβ diversity accompanies nonparallelism in pathogen infection of lake whitefish (Coregonus clupeaformis) species pairs as revealed by next-generation sequencing. *Molecular ecology*, **22**, 3833–3849.

Piertney SB, Oliver MK (2006) The evolutionary ecology of the major histocompatibility complex. *Heredity*, **96**, 7–21.

Pilosof S, Fortuna MA, Cosson JF *et al.* (2014) Host-parasite network structure is associated with community-level immunogenetic diversity. *Nature communications*, **5**, 5172.

Posada D, Crandall KA (2001) Evaluation of methods for detecting recombination from DNA sequences: computer simulations. *PNAS*, **98**, 13757–13762.

Pröll J, Danzer M, Stabentheiner S *et al.* (2011) Sequence capture and next generation resequencing of the MHC region highlights potential transplantation determinants in HLA identical haematopoietic stem cell transplantation. *DNA research : an international journal for rapid publication of reports on genes and genomes*, **18**, 201–210.

R Development Core Team R (2011) R: A Language and Environment for Statistical Computing (RDC Team, Ed,). *R Foundation for Statistical Computing*, **1**, 409.

Radwan J, Biedrzycka A, Babik W (2010) Does reduced MHC diversity decrease viability of vertebrate populations? *Biological Conservation*, **143**, 537–544.

Radwan J, Zagalska-Neubauer M, Cichoń M *et al.* (2012) MHC diversity, malaria and lifetime reproductive success in collared flycatchers. *Molecular ecology*, **21**, 2469–79.

Raymond M, Rousset F (1995) GENEPOP (version 1.2): population genetics software for exact tests and ecumenicism. *Journal of Heredity*, **86**, 248–249.

Reznick D, Shaw F, Rodd F *et al.* (1997) Evaluation of the Rate of Evolution in Natural Populations of Guppies (Poecilia reticulata). *Science*, **275**, 1934–1937.

Rodd FH, Reznick DN (1991) Life history evolution III. The impact of prawn predation on guppy life histories. *Oikos*, **62**, 13–19.

Rousset F (2008) genepop'007: a complete re-implementation of the genepop software for Windows and Linux. *Molecular ecology resources*, **8**, 103–6.

Saks L, Ots I, Hõrak P (2003) Carotenoid-based plumage coloration of male greenfinches reflects health and immunocompetence. *Oecologia*, **134**, 301–307.

Samarakoon U, Gonzales JM, Patel JJ *et al.* (2011) The landscape of inherited and de novo copy number variants in a Plasmodium falciparum genetic cross. *BMC genomics*, **12**, 457.

Sandberg M, Eriksson L, Jonsson J *et al.* (1998) New chemical descriptors relevant for the design of biologically active peptides. A multivariate characterization of 87 amino acids. *Journal of medicinal chemistry*, **41**, 2481–2491.

Sato A, Figueroa F, O'hUigin C *et al.* (1996) Identification of major histocompatibility complex genes in the guppy, Poecilia reticulata. *Immunogenetics*, **43**, 38–49.

Von Schantz T, Wittzell H, Göransson G *et al.* (1996) MHC genotype and male ornamentation: genetic evidence for the Hamilton-Zuk model. *Proceedings of the Royal Society B: Biological Sciences*, **263**, 265–271.

Schmieder R, Edwards R (2011) Quality control and preprocessing of metagenomic datasets. *Bioinformatics*, **27**, 863–864.

Schneider C, Rasband W, Eliceiri K (2012) NIH Image to ImageJ: 25 years of image analysis. *Nature Methods*, **9**, 671–675.

Schwensow N, Fietz J, Dausmann KH *et al.* (2007) Neutral versus adaptive genetic variation in parasite resistance: importance of major histocompatibility complex supertypes in a free-ranging primate. *Heredity*, **99**, 265–277.

Sepil I, Lachish S, Hinks AE, Sheldon BC (2013a) Mhc supertypes confer both qualitative and quantitative resistance to avian malaria infections in a wild bird population. *Proceedings of the Royal Society B: Biological Sciences*, **280**.

Sepil I, Lachish S, Sheldon BC (2013b) Mhc-linked survival and lifetime reproductive success in a wild population of great tits. *Molecular ecology*, **22**, 384–396.

Sepil I, Moghadam HK, Huchard E *et al.* (2012) Characterization and 454 pyrosequencing of major histocompatibility complex class I genes in the great tit reveal complexity in a passerine system. *BMC evolutionary biology*, **12**, 68.

Sette A, Newman M, Livingston B *et al.* (2002) Optimizing vaccine design for cellular processing, MHC binding and TCR recognition. *Tissue antigens*, **59**, 443–451.

Sette A, Sidney J (1998) HLA supertypes and supermotifs: A functional perspective on HLA polymorphism. *Current Opinion in Immunology*, **10**, 478–482.

Sette A, Sidney J, Southwood S *et al.* (2012) A shared MHC supertype motif emerges by convergent evolution in macaques and mice, but is totally absent in human MHC molecules. *Immunogenetics*, **64**, 421–434.

Shafer ABA, Wolf JBW (2013) Widespread evidence for incipient ecological speciation: a meta-analysis of isolation-by-ecology. *Ecology letters*, **16**, 940–950.

Shaw PW, Carvalho GR, Seghers BH *et al.* (1992) Genetic Consequences Of an Artificial Introduction Of Guppies (Poecilia-Reticulata) In N-Trinidad. *Proceedings Of the Royal Society Of London Series B-Biological Sciences*, **248**, 111–116.

Shen X, Yang G, Liao M (2006) Development of 51 genomic microsatellite DNA markers of guppy (Poecilia reticulata) and their application in closely related species. *Molecular Ecology Notes*, **7**, 302–306.

Shiina T, Ota M, Shimizu S *et al.* (2006) Rapid evolution of major histocompatibility complex class I genes in primates generates new disease alleles in humans via hitchhiking diversity. *Genetics*, **173**, 1555–1570.

Siddle H V, Marzec J, Cheng Y, Jones M, Belov K (2010) MHC gene copy number variation in Tasmanian devils: implications for the spread of a contagious cancer. *Proceedings of the Royal Society B: Biological Sciences*, **277**, 2001–2006.

Sidney J, Grey HM, Kubo RT, Sette A (1996) Practical, biochemical and evolutionary implications of the discovery of HLA class I supermotifs. *Immunology Today*, **17**, 261–266.

Simpson E (1988) Function of the MHC. *Immunology. Supplement*, **1**, 27–30.

Sin YW, Annavi G, Newman C *et al.* (2015) MHC class II assortative mate choice in European badgers (Meles meles). *Molecular ecology*. **In press.**

Sommer S, Courtiol A, Mazzoni CJ (2013) MHC genotyping of non-model organisms using next-generation sequencing: a new methodology to deal with artefacts and allelic dropout. *BMC Genomics*, **14**, 542.

Spurgin LG, van Oosterhout C, Illera JC *et al.* (2011) Gene conversion rapidly generates major histocompatibility complex diversity in recently founded bird populations. *Molecular ecology*, **20**, 5213–5225.

Spurgin LG, Richardson DS (2010a) How pathogens drive genetic diversity: MHC, mechanisms and misunderstandings. *Proceedings of the Royal Society B: Biological Sciences*, **277**, 979–988.

Spurgin LG, Richardson DS (2010b) How pathogens drive genetic diversity : MHC, mechanisms and misunderstandings. *Proceedings of the Royal Society B: Biological Sciences*, **277**, 979–988.

Stahl W, Sies H (2003) Antioxidant activity of carotenoids. *Molecular Aspects of Medicine*, **24**, 345–351.

Stern LJ, Brown JH, Jardetzky TS *et al.* (1994) Crystal structure of the human class II MHC protein HLA-DR1 complexed with an influenza virus peptide. *Nature*, **368**, 215–221.

Stiebens VA, Merino SE, Chain FJJ *et al.* (2013) Evolution of MHC class I genes in the endangered loggerhead sea turtle (Caretta caretta) revealed by 454 amplicon sequencing. *BMC evolutionary biology*, **13**, 95.

Strand TM, Segelbacher G, Quintela M *et al.* (2012) Can balancing selection on MHC loci counteract genetic drift in small fragmented populations of black grouse? *Ecology and evolution*, **2**, 341–353.

Stuglik MT, Radwan J, Babik W (2011) jMHC: software assistant for multilocus genotyping of gene families using next-generation amplicon sequencing. *Molecular ecology resources*, **11**, 739–742.

Suk HY, Neff BD (2009) Microsatellite genetic differentiation among populations of the Trinidadian guppy. *Heredity*, **102**, 425–434.

Sutton JT, Nakagawa S, Robertson BC *et al.* (2011) Disentangling the roles of natural selection and genetic drift in shaping variation at MHC immunity genes. *Molecular Ecology*, **20**, 4408–4420.

Takahata N (1990) A simple genealogical structure of strongly balanced allelic lines and trans-species evolution of polymorphism. *PNAS*, **87**, 2419–2423.

Takahata N, Nei M (1990) Allelic genealogy under overdominant and frequency-dependent selection and polymorphism of major histocompatibility complex loci. *Genetics*, **124**, 967–978.

Takuno S, Nishio T, Satta Y *et al.* (2008) Preservation of a pseudogene by gene conversion and diversifying selection. *Genetics*, **180**, 517–531.

Tamura K, Peterson D, Peterson N *et al.* (2011) MEGA5: Molecular Evolutionary Genetics Analysis using Maximum Likelihood, Evolutionary Distance, and Maximum Parsimony Methods. *Molecular Biology*, **28**, 1530–1534.

The MHC sequencing consortium (1999) Complete sequence and gene map of a human major histocompatibility complex. The MHC sequencing consortium. *Nature*, **401**, 921–923.

Thompson JF, Milos PM (2011) The properties and applications of single-molecule DNA sequencing. *Genome biology*, **12**, 217.

Traherne JA (2008) Human MHC architecture and evolution: Implications for disease association studies. *International Journal of Immunogenetics*, **35**, 179–192.

Tripathi N, Hoffmann M, Willing EM *et al.* (2009) Genetic linkage map of the guppy, Poecilia reticulata, and quantitative trait loci analysis of male size and colour variation. *Proceedings of the Royal Society B: Biological Sciences*, **276**, 2195–2208.

Trowsdale J (1993) Genomic structure and function in the MHC. *Trends in Genetics*, **9**, 117–122.

Trowsdale J (2011) The MHC, disease and selection. *Immunology letters*, **137**, 1–8.

Trowsdale J, Knight JC (2013) Major histocompatibility complex genomics and human disease. *Annual review of genomics and human genetics*, **14**, 301–323.

Van Valen L (1973) A new evolutionary law. *Evolutionary Theory*, **1**, 1–30.

Vandiedonck C, Knight JC (2009) The human Major Histocompatibility Complex as a paradigm in genomics research. *Briefings in functional genomics & proteomics*, **8**, 379–394.

Völker M, Backström N, Skinner BM *et al.* (2010) Copy number variation, chromosome rearrangement, and their association with recombination during avian evolution. *Genome research*, **20**, 503–511.

Wang IJ, Glor RE, Losos JB (2013) Quantifying the roles of ecology and geography in spatial genetic divergence. *Ecology letters*, **16**, 175–182.

Warren RL, Choe G, Freeman DJ *et al.* (2012) Derivation of HLA types from shotgun sequence datasets. *Genome medicine*, **4**, 95.

Watanabe T, Yoshida M, Nakajima M *et al*. (2003) Isolation and characterization of 43 microsatellite DNA markers for guppy (Poecilia reticulata). *Molecular Ecology Notes*, **3**, 487–490.

Watson CT, Steinberg KM, Huddleston J *et al.* (2013) Complete haplotype sequence of the human immunoglobulin heavy-chain variable, diversity, and joining genes and characterization of allelic and copy-number variation. *American Journal of Human Genetics*, **92**, 530–546.

Wedekind C, Penn D (2000) MHC genes, body odours, and odour preferences. *Nephrology, dialysis, transplantation : official publication of the European Dialysis and Transplant Association - European Renal Association*, **15**, 1269–1271.

Weese DJ, Gordon SP, Hendry AP *et al.* (2010) Spatiotemporal variation in linear natural selection on body color in wild guppies (poecilia reticulata). *Evolution*, **64**, 1802–1815.

Wegner KM (2009) Massive parallel MHC genotyping: titanium that shines. *Molecular ecology*, **18**, 1818–20.

Willing EM, Bentzen P, van Oosterhout C *et al.* (2010) Genome-wide single nucleotide polymorphisms reveal population history and adaptive divergence in wild guppies. *Molecular ecology*, **19**, 968–984.

Wilson DJ, McVean G (2006) Estimating diversifying selection and functional constraint in the presence of recombination. *Genetics*, **172**, 1411–1425.

Winternitz JC, Minchey SG, Garamszegi LZ *et al.* (2013) Sexual selection explains more functional variation in the mammalian major histocompatibility complex than parasitism. *Proceedings of the Royal Society B: Biological Sciences*, **280**, 20131605.

Woelfing B, Traulsen A, Milinski M, Boehm T (2009) Does intra-individual major histocompatibility complex diversity keep a golden mean? *Philosophical transactions of the Royal Society of London. Series B, Biological sciences*, **364**, 117–128.

Wucherpfennig KW (2001) Insights into autoimmunity gained from structural analysis of MHC-peptide complexes. *Current Opinion in Immunology*, **13**, 650–656.

Xavier R, Faria PJ, Paladini G *et al.* (2015) Evidence for cryptic speciation in directly transmitted gyrodactylid parasites of Trinidadian guppies. *PloS one*, **10**, e0117096.

Xie T, Rowen L, Aguado B *et al.* (2003) Analysis of the gene-dense major histocompatibility complex class III region and its comparison to mouse. *Genome research*, **13**, 2621–2636.

Xie C, Tammi MT (2009) CNV-seq, a new method to detect copy number variation using high-throughput sequencing. *BMC bioinformatics*, **10**, 80.

Yang Z (2010) A likelihood ratio test of speciation with gene flow using genomic sequence data. *Genome Biology and Evolution*, **2**, 200–211.

Yoon S, Xuan Z, Makarov V *et al.* (2009) Sensitive and accurate detection of copy number variants using read depth of coverage. *Genome research*, **19**, 1586–1592.

Zagalska-Neubauer M, Babik W, Stuglik M *et al.* (2010) 454 sequencing reveals extreme complexity of the class II Major Histocompatibility Complex in the collared flycatcher. *BMC evolutionary biology*, **10**, 395.

Zhao M, Wang Y, Shen H *et al.* (2013) Evolution by selection, recombination, and gene duplication in MHC class I genes of two Rhacophoridae species. *BMC evolutionary biology*, **13**, 113.

Appendix 1

Supporting information for Chapter 3: *Ultra-deep Illumina sequencing accurately identifies MHC class IIb alleles and provides evidence for copy number variation in the guppy (Poecilia reticulata)*

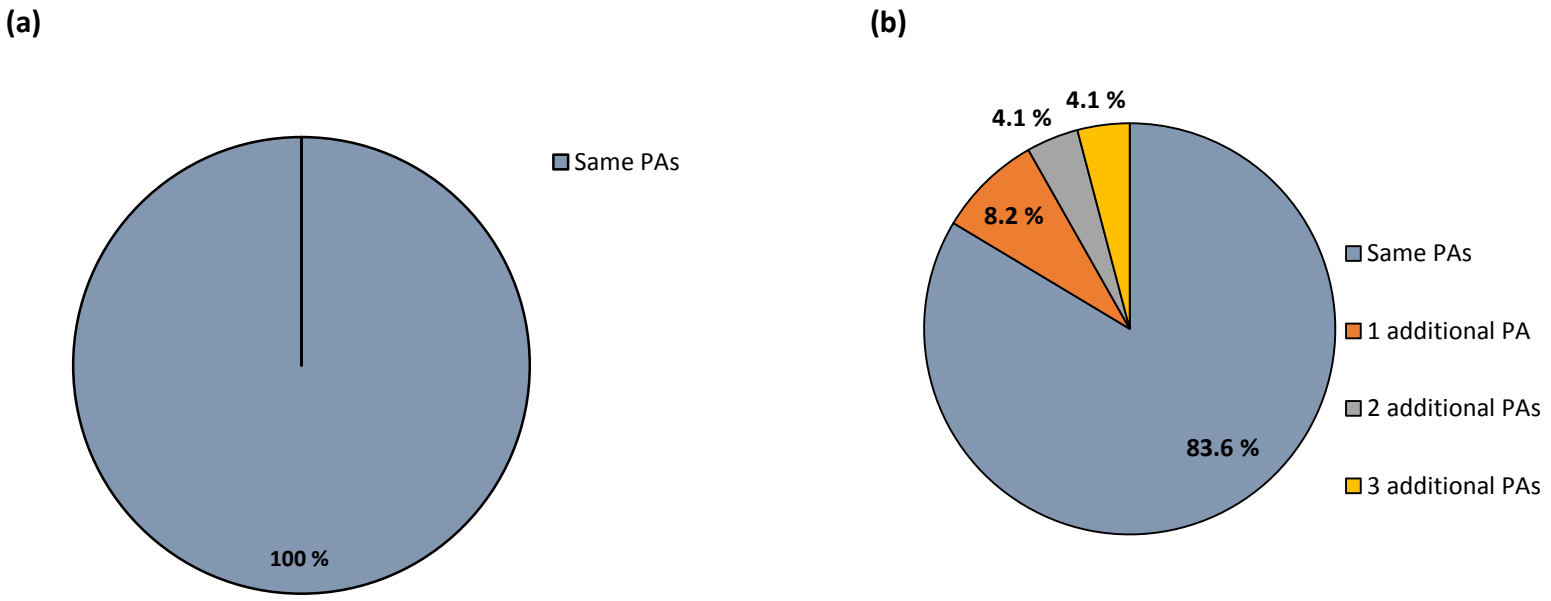

Figure S3.1: Genotype repeatability between re-sequenced samples

(a) Within the same sequencing run identical A_i estimates were observed in each replicated sample with 100% genotype replication. (b) However, when genotypes were compared between full independent replicates genotyping repeatability fell to 83.7%. This was due to some genotypes acquiring new alleles that were discarded in the original run due to low depth.

Figure S3.2

(a)

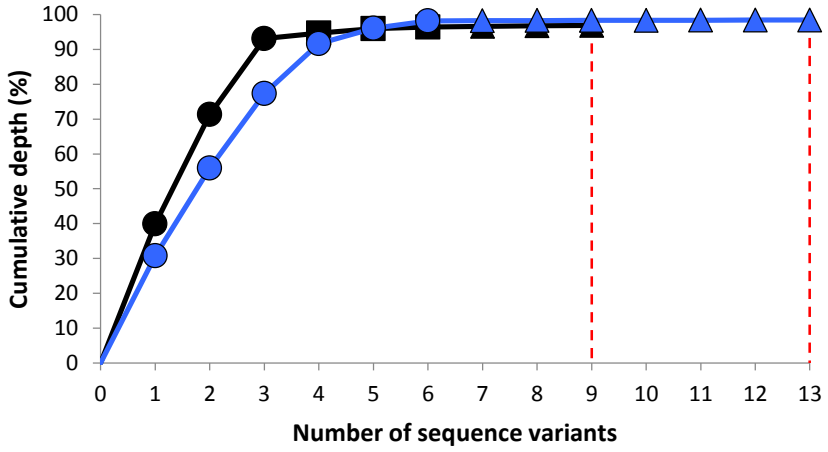

(b)

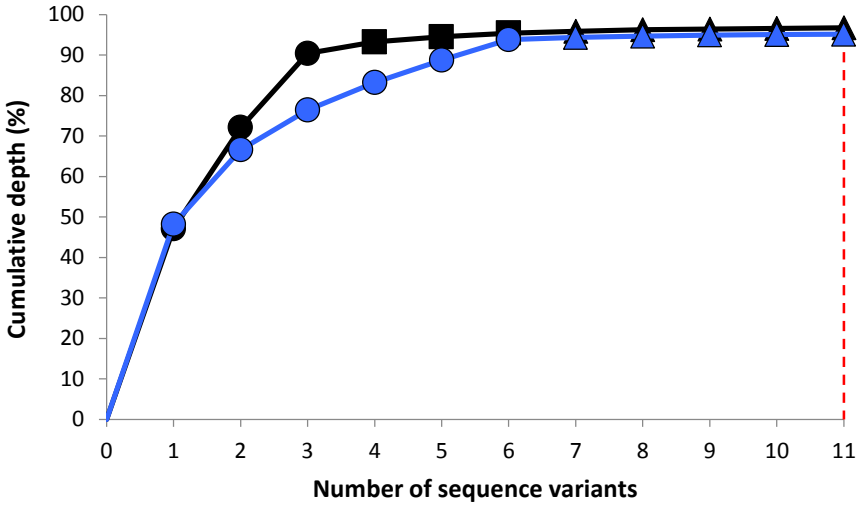

(c)

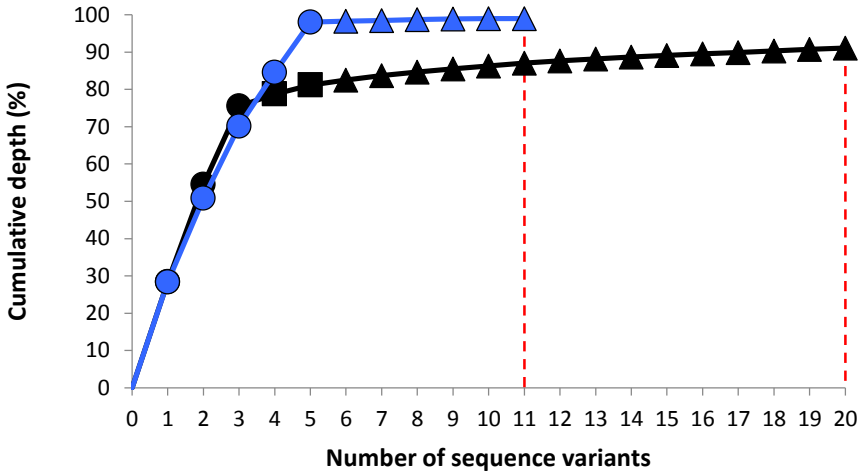
Cumulative depth (%)
100
90
80
70
60
50
40
30
20
10
0
0 1 2 3 4 5 6 7 8 9 10 11 12 13 14 15 16 17 18 19 20
Number of sequence variants

(d)

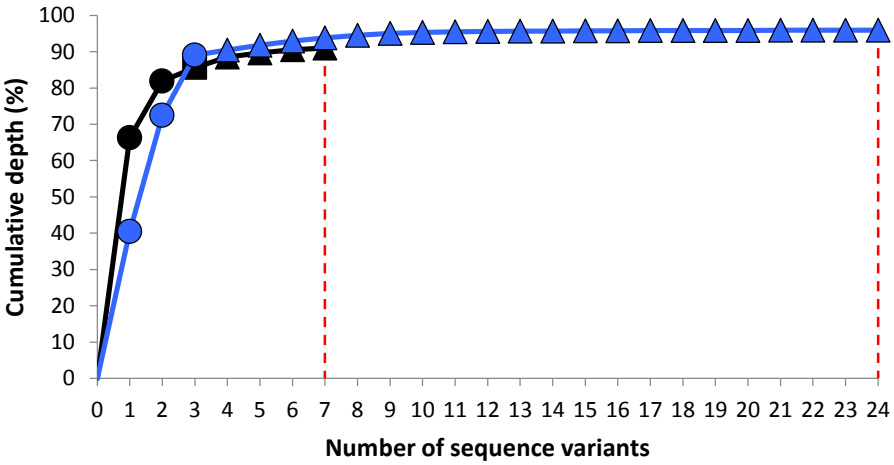
Cumulative depth (%)
100
90
80
70
60
50
40
30
20
10
0
0 1 2 3 4 5 6 7 8 9 10 11 12 13 14 15 16 17 18 19 20 21 22 23 24
Number of sequence variants

(e)

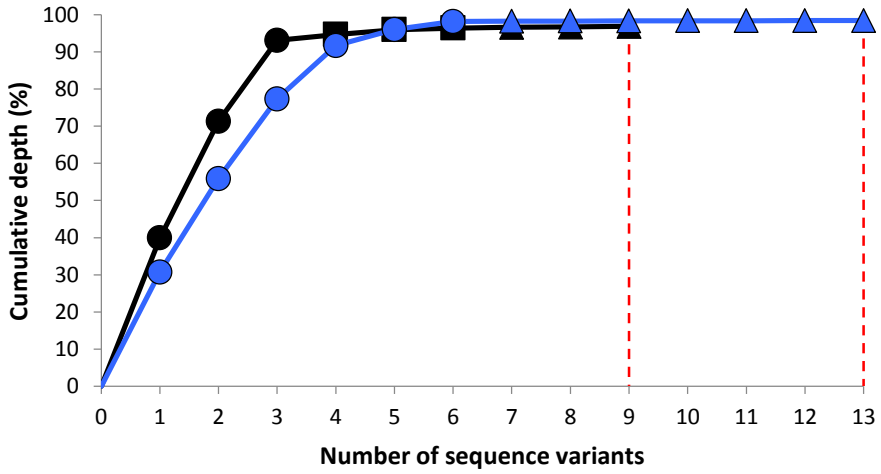
Cumulative depth (%)
100
90
80
70
60
50
40
30
20
10
0
0 1 2 3 4 5 6 7 8 9 10 11 12 13
Number of sequence variants

(f)

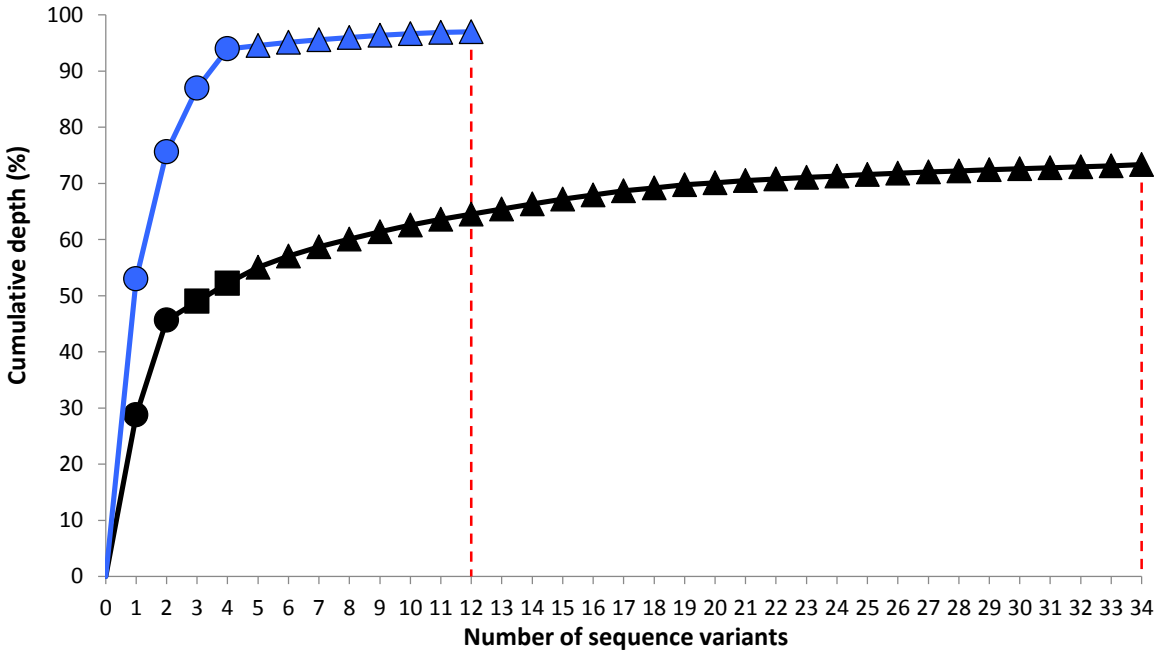
Cumulative depth (%)
100
90
80
70
60
50
40
30
20
10
0
0 1 2 3 4 5 6 7 8 9 10 11 12 13 14 15 16 17 18 19 20 21 22 23 24 25 26 27 28 29 30 31 32 33 34
Number of sequence variants

(g)

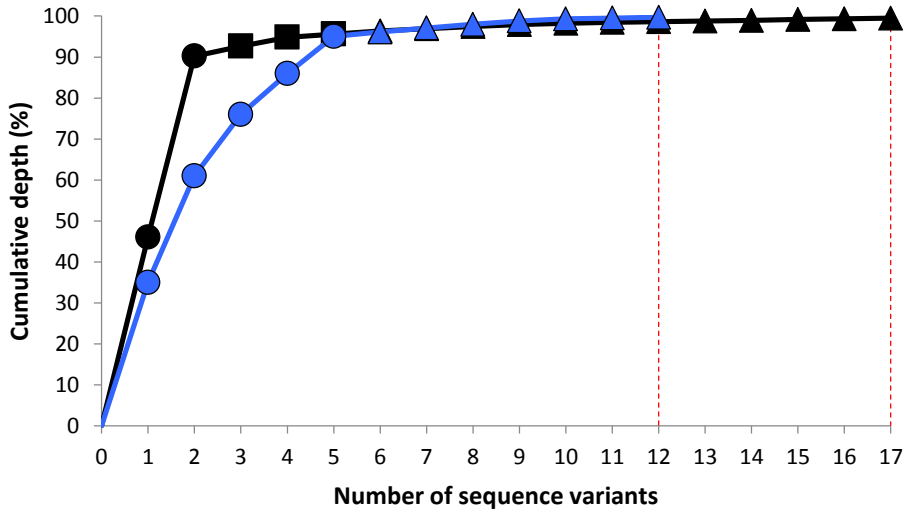

(h)

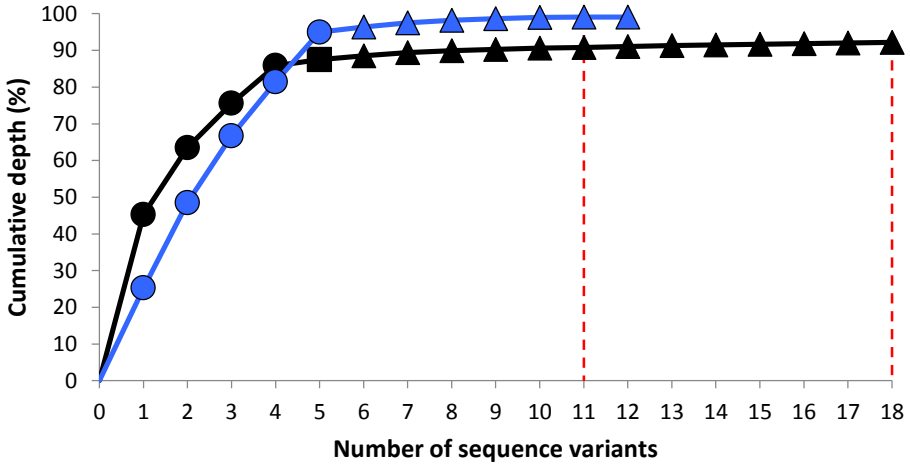

Figure S3.2: Comparison of A_i in independent replicates

For each replicated sample that produced different A_i estimates in independent sequencing runs (G100763Q1, G100786Q1, G100970G2, G100773Q1, G100788Q1, G100979G2, G101163M10 and G10077; a-h, respectively) the cumulative sequence depth is shown across variants (PAs: circles, artifacts: triangles) in the original sample (black), and the replicate (blue). Squares show PAs that were discarded in the original sample due to inadequate depth. The application of a low AVT (3x in this case)

would have retained these PAs in the original sample. However, the red-hashed lines indicate the artificially inflated A_i estimates that would result for each sample if low copy number contaminants are accepted under this criterion. Estimates of A_i are not replicated when a 3x depth threshold is implemented.

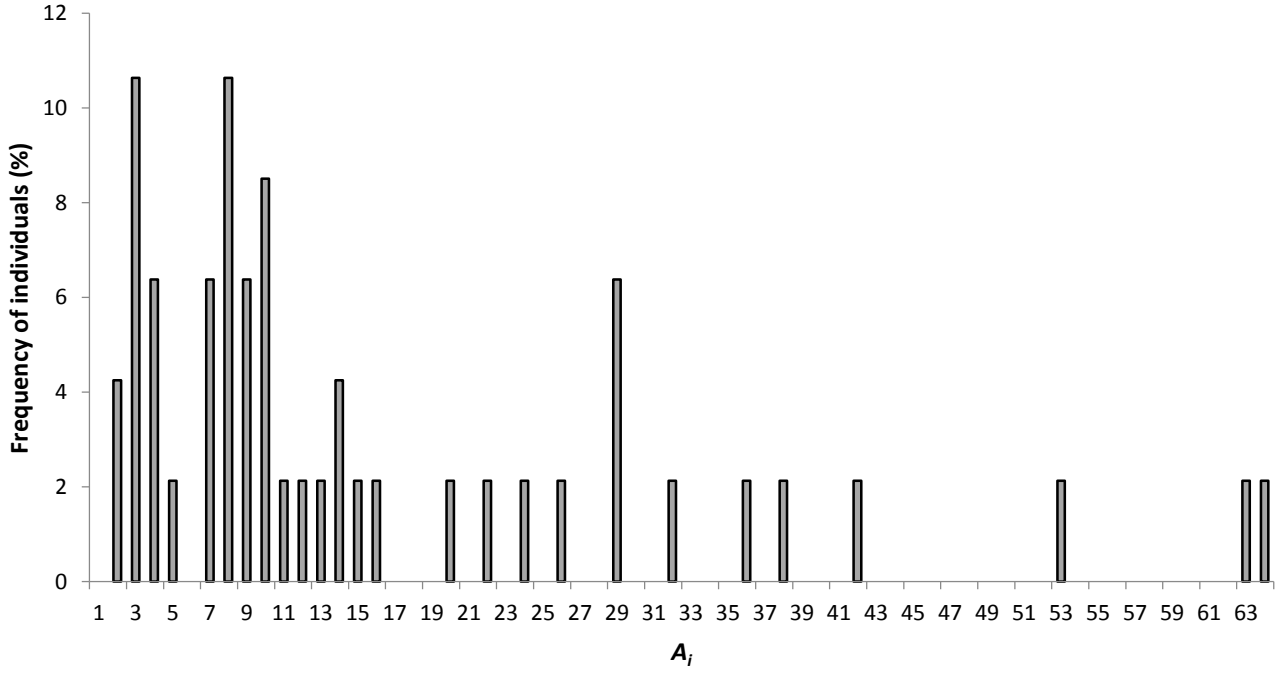

Figure S3.3: A_i distribution across individuals using a low AVT
When a low AVT (3x) is implemented across all samples that provided confirmed independent estimates of A_i using our method, A_i estimates range from 2 to 64 and the frequency distribution does not conform to expectation of the MHC optimality hypothesis or random segregation of alleles. This distribution reflects the error prone A_i estimates produced by using a low AVT.

(a)

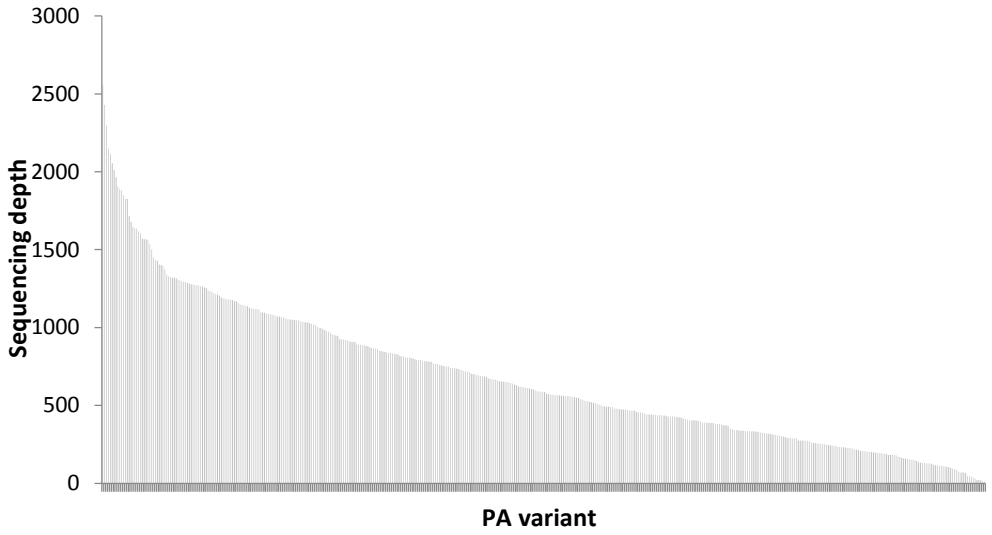

(b)

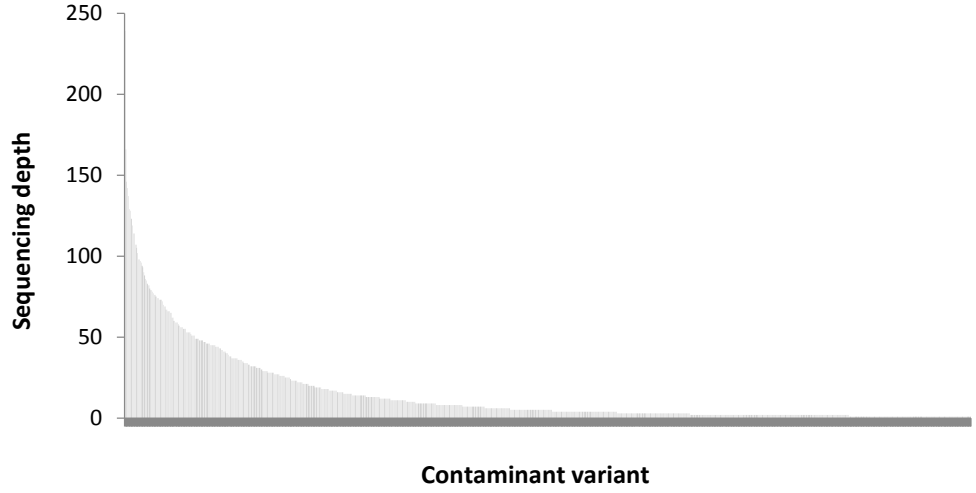

Figure S3.4: Raw sequencing depth distribution of variants among amplicons
(a) The raw depth distribution of variants accepted as PAs in genotypes ranged from 12 – 2,558x in the first sequencing run. (b) Artificial sequences representing low copy number contaminants obtained a sequencing depth distribution between 1-239x, and so overlapped that of real PAs. This highlights problems associated with using raw read depth distributions to estimate genotypes. Our protocol overcomes this issue by using relative comparisons of variant depths on a per-amplicon basis.

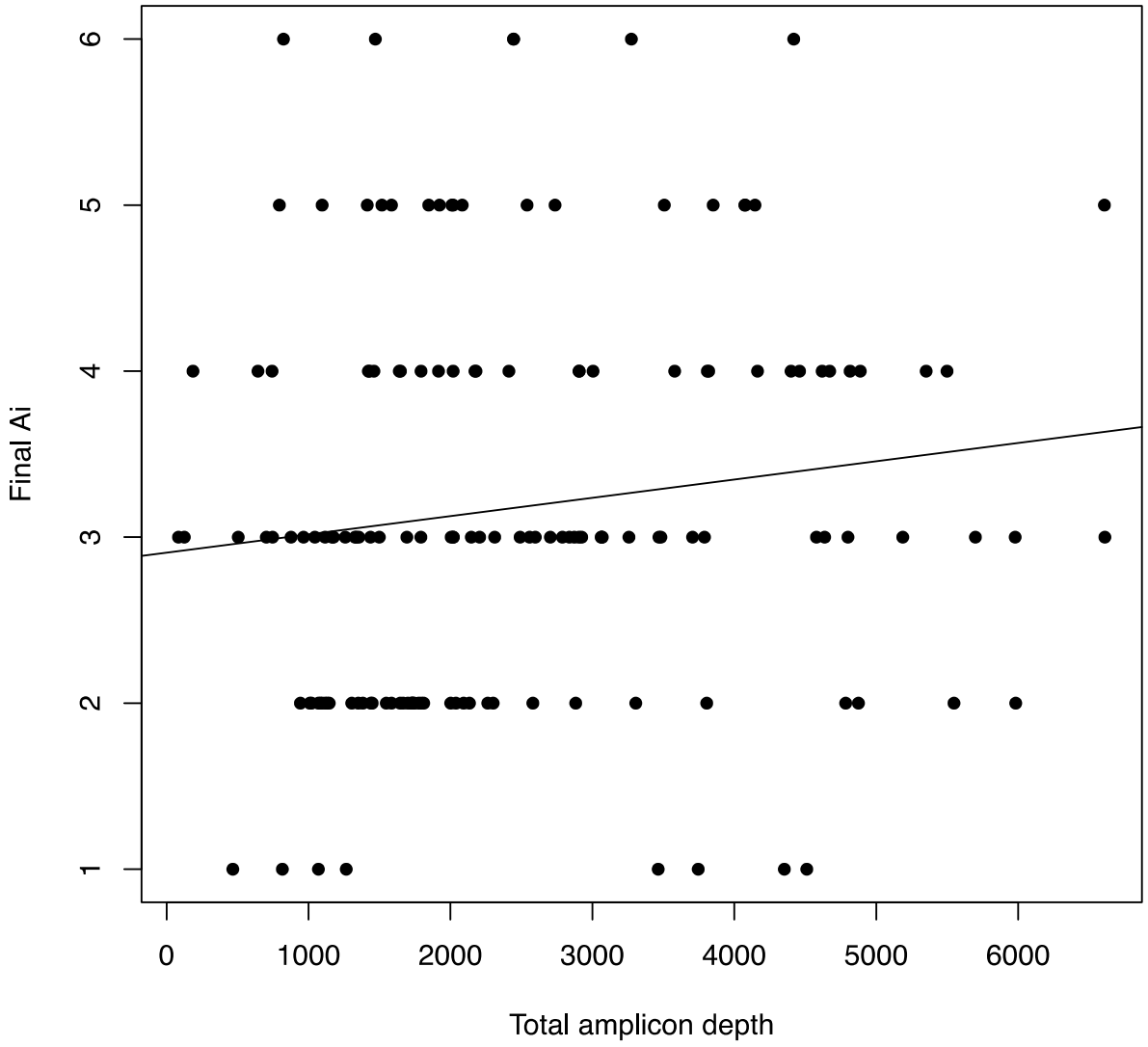

Figure S3.5: Linear relationship between total amplicon sequencing depth and A_i
The lack of correlation between total amplicon depth and the number of alleles characterized within an amplicon (A_i) (linear regression: p = 0.109, $r^2 = 0.01$) means that estimates of A_i are not significantly affected by sequencing depth.

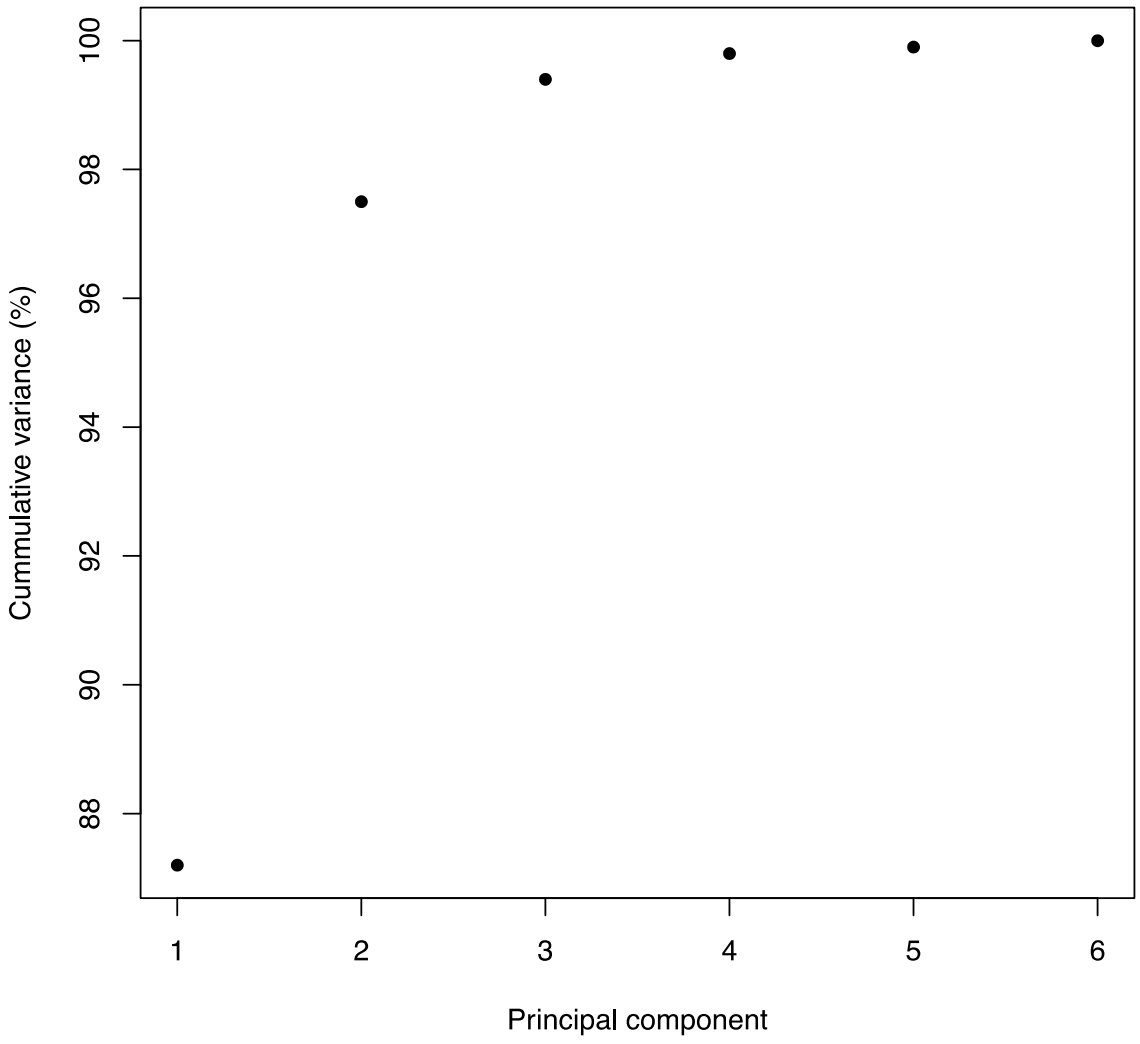

Figure S3.6: Confirmation of maximum A_i across samples using PCA
A PCA of mean sequencing depths of the top 10 most sequenced variants across all samples shows that 100% of the variance between variants within amplicons is attributed to PAs (PC 1 - 6). Although depth-percentages of up to 2.11% were observed for suspected contaminant variants, they accounted for 0% of the mean variance across samples. This corroborated that a maximum A_i of 6 explained the observed genotypes.

Figure S3.7

(a)

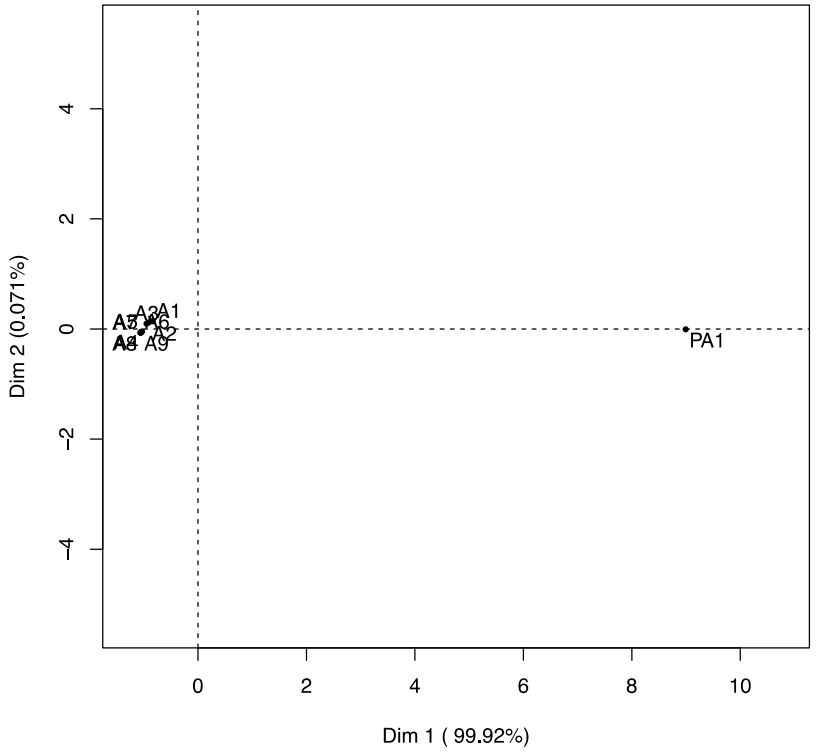

(b)

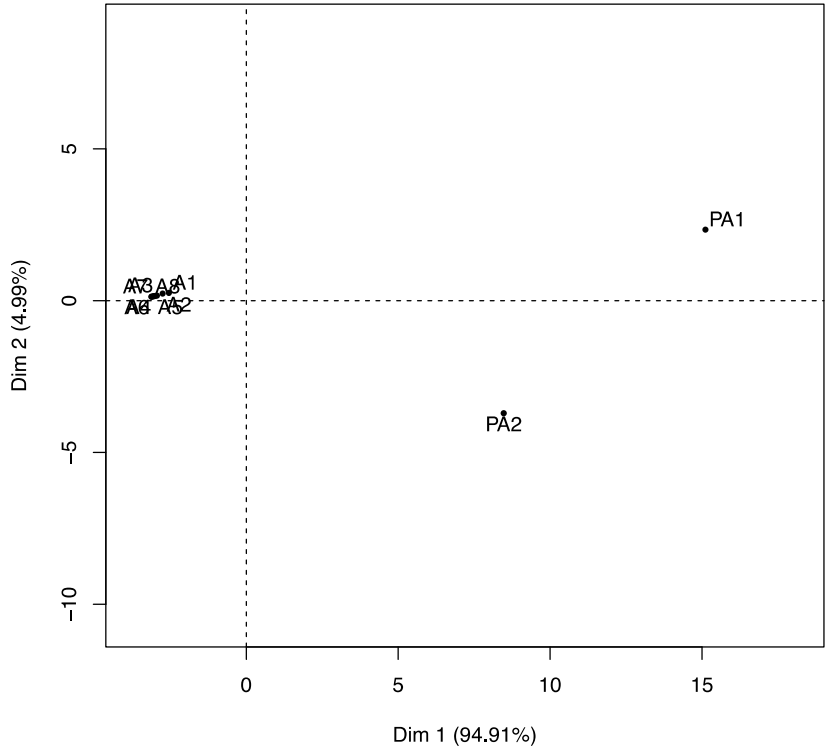

(c)

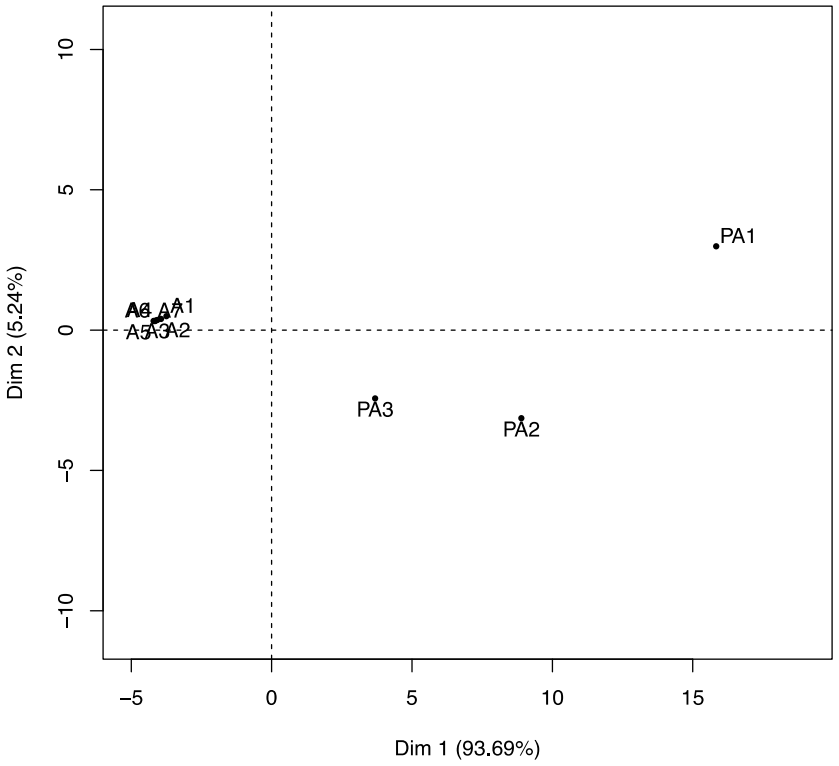
Dim 2 (5.24%)
Dim 1 (93.69%)
PA1
PA3
PA2
A1
A2
A3
10
5
0
−5
−10
−5
0
5
10
15

(d)

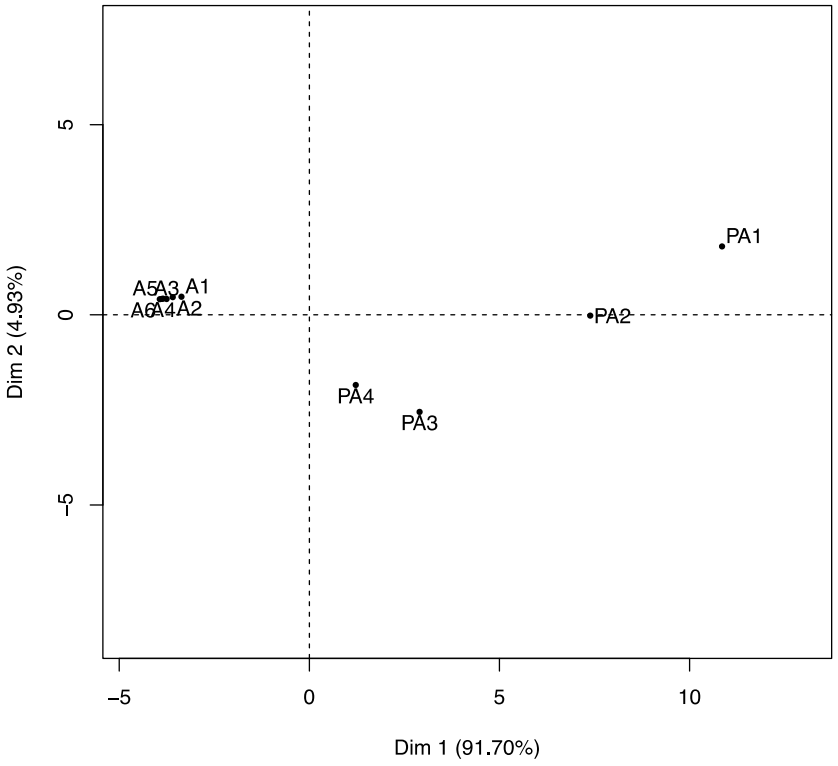
Dim 2 (4.93%)
Dim 1 (91.70%)
PA1
PA2
PA4
PA3
A1
A2
A3
5
0
−5
−5
0
5
10

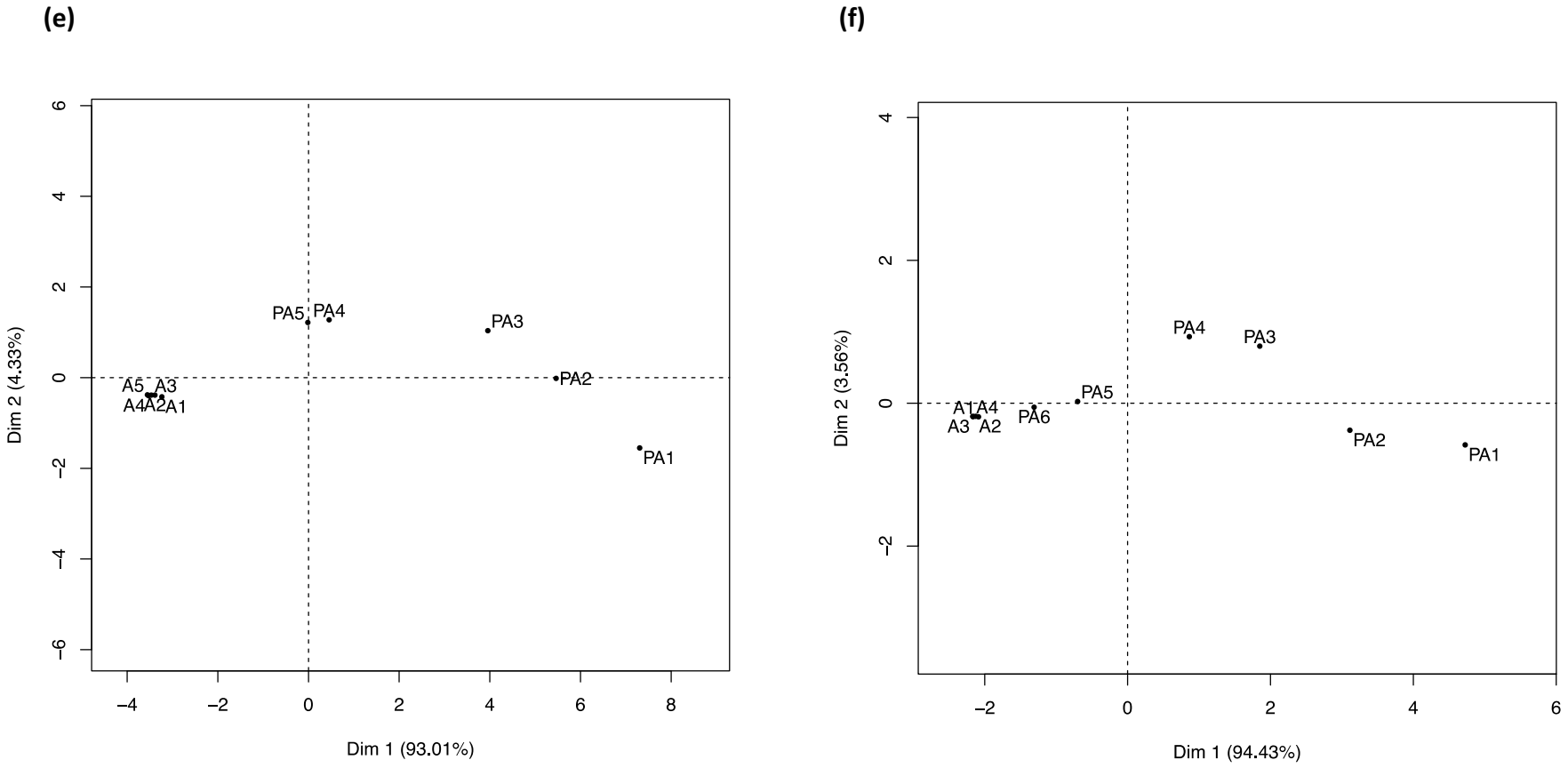

Figure S3.7: Confirmation of A_i estimates among samples
A PCA of mean sequencing depth of the top 10 most sequenced variants across samples within each A_i grouping (A_i =1 – A_i =6; a-f, respectively) correctly separates alleles (PA) and artifacts (A) based on mean sequencing depth. This corroborates A_i estimates illustrated in Figure 3.5 at the point of highest *DOC*.

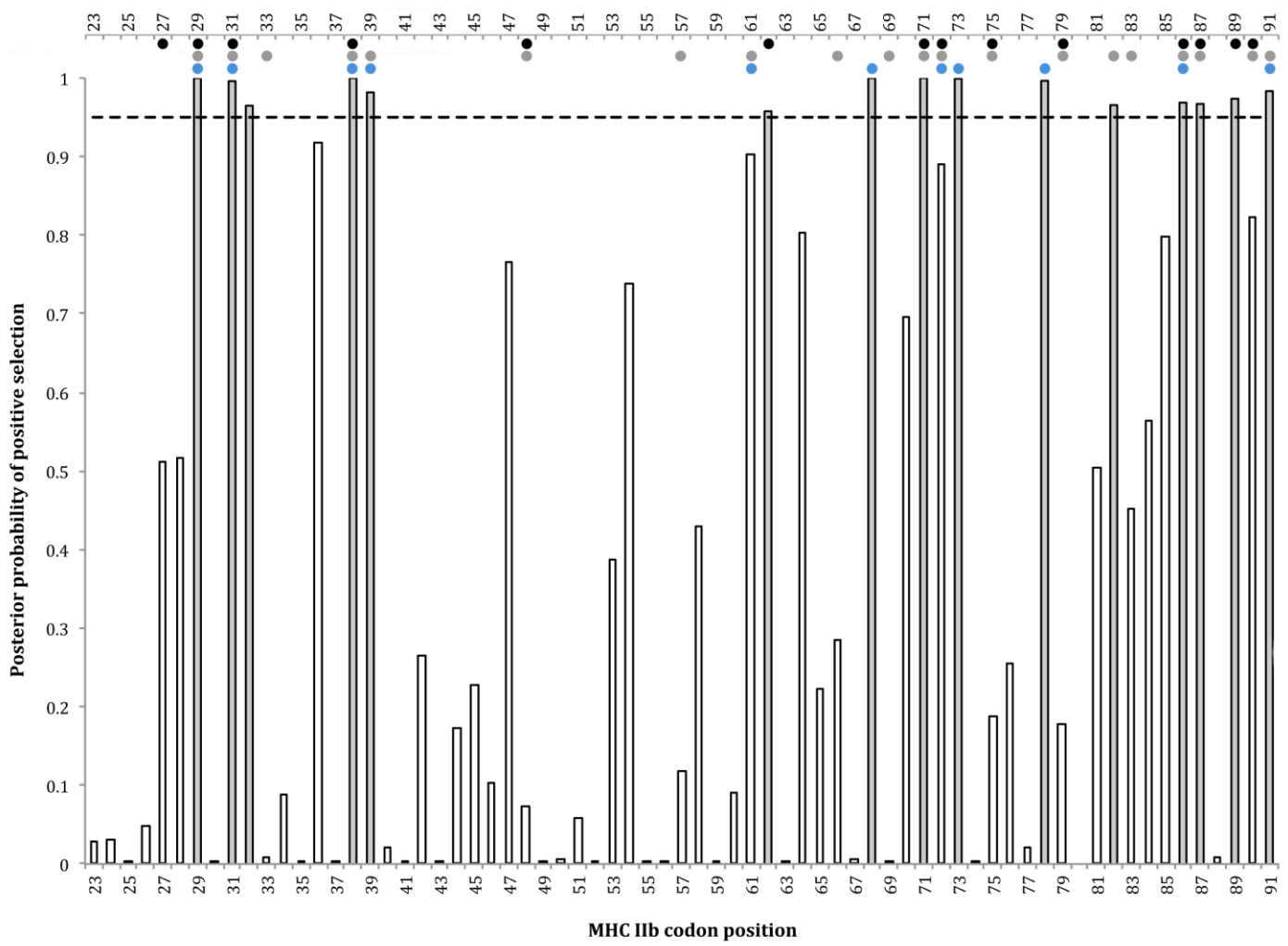

Figure S3.8: Analysis of selection on MHC class IIb sequences of guppies

The plot shows an estimate of the posterior probability of positive selection based on the d_N/d_S ratio at each codon (sliding window of 1 codon). Circles highlight PBR designation inferred in previous studies (black, Brown *et al.* 1993; grey, Bondinas *et al.* 2007; blue, McMullan 2011) shifted up by one codon to account for an insertion near the amino terminus of the fish MHC class IIb molecule (Figueroa *et al.* 2000). Grey columns highlight codons of the guppy MHC with a significant posterior probability (>0.95) of positive selection (codons 29, 31, 32, 38, 39, 62, 68, 71, 73, 78, 82, 86, 87, 89 and 91), where the dashed line indicates the 0.95 acceptance criteria for positive selection.

Appendix 2

Supporting information for Chapter 4: *The role of MHC and parasites in the secondary sexual colouration of guppies (Poecilia reticulata)*

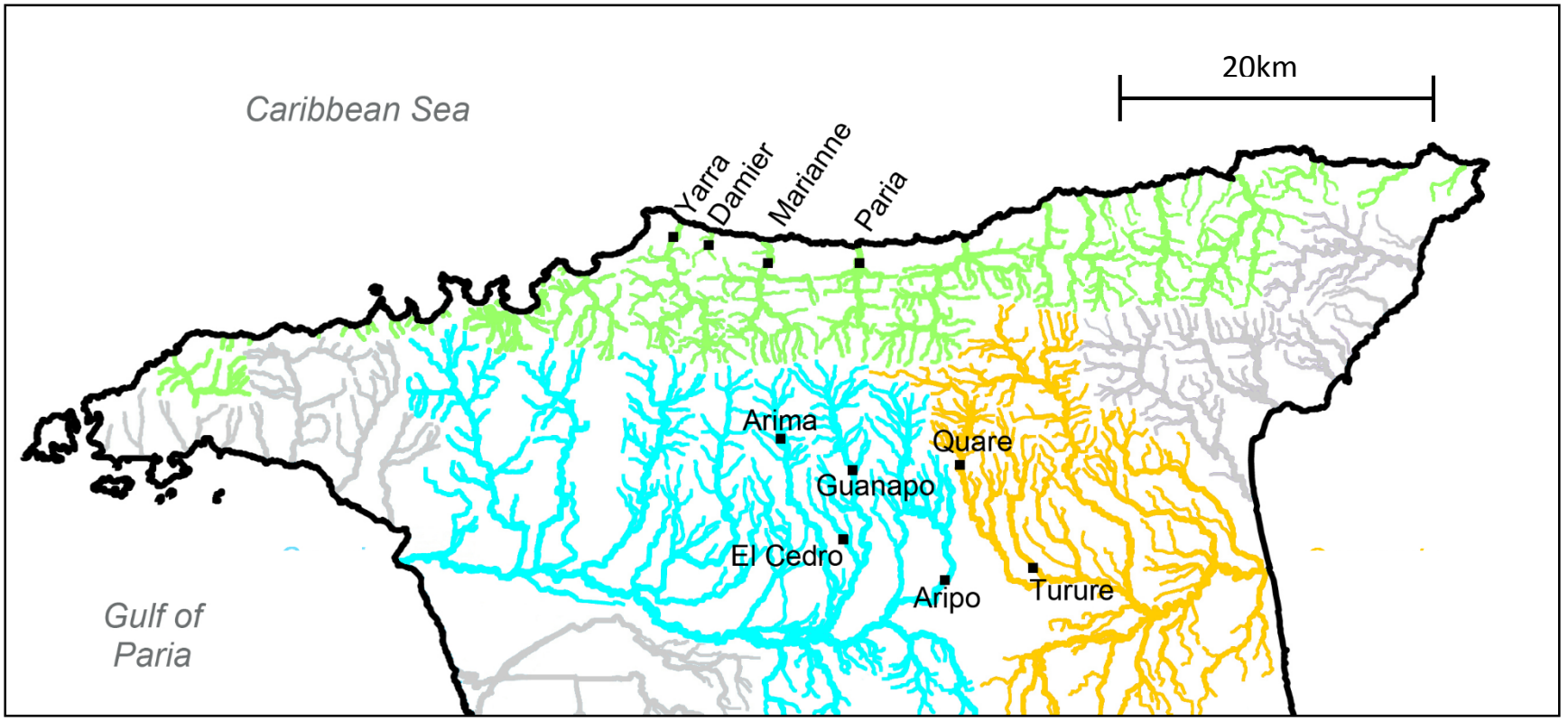

Figure S4.1. The three main drainage systems in northern Trinidad where the bulk of guppy research has been conducted (blue, Caroni; green, North slope; orange Oropouche) and the rivers where samples were collected. Additional river populations on the eastern and western coast (grey) maintain high genetic relatedness to populations in their associated drainage system and together form "Caroni type", "Oropouche type", and "North Slope type" genetic clades of neutral diversity (Willing *et al*. 2010).

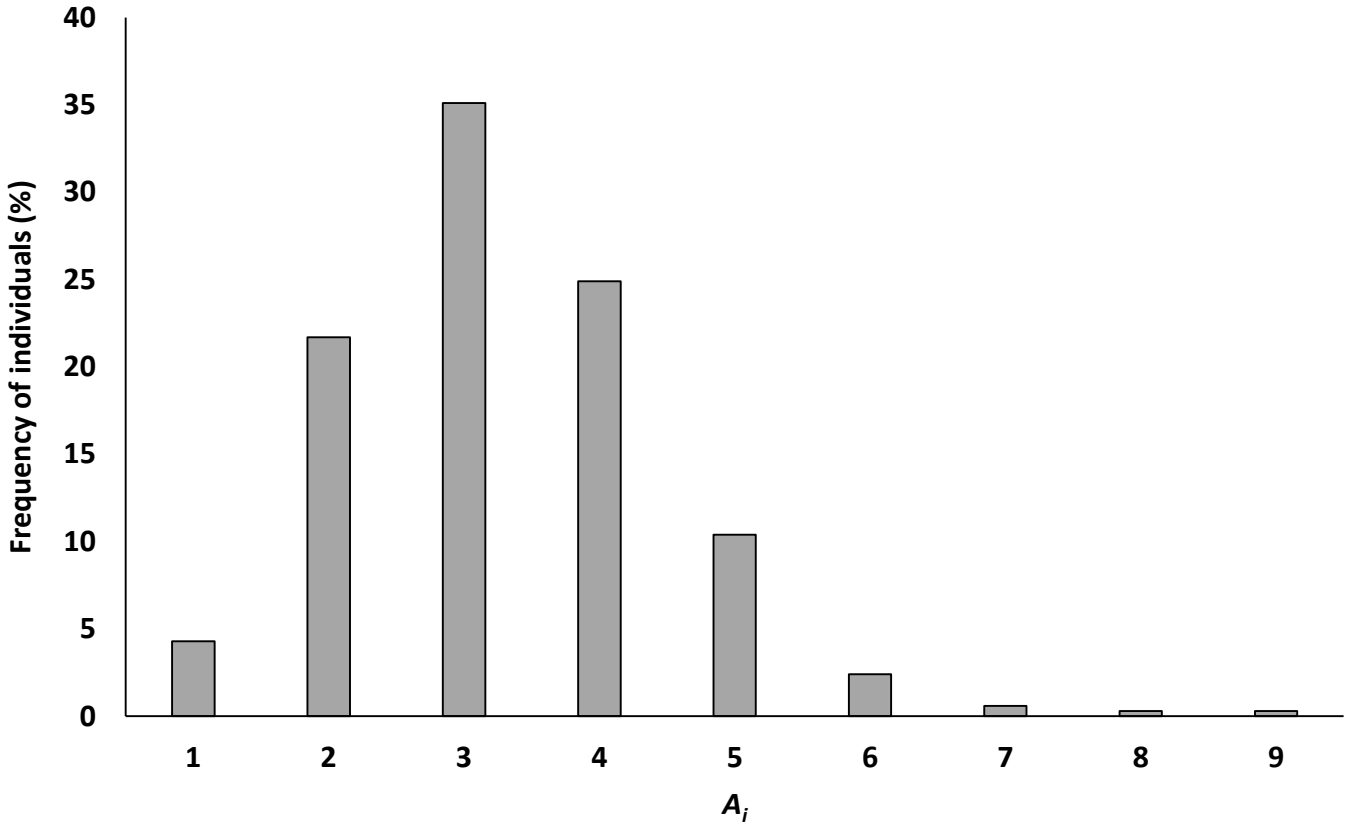

Figure S4.2. Frequency distribution of the percentage of individuals which had different total numbers of MHC alleles (A_i)

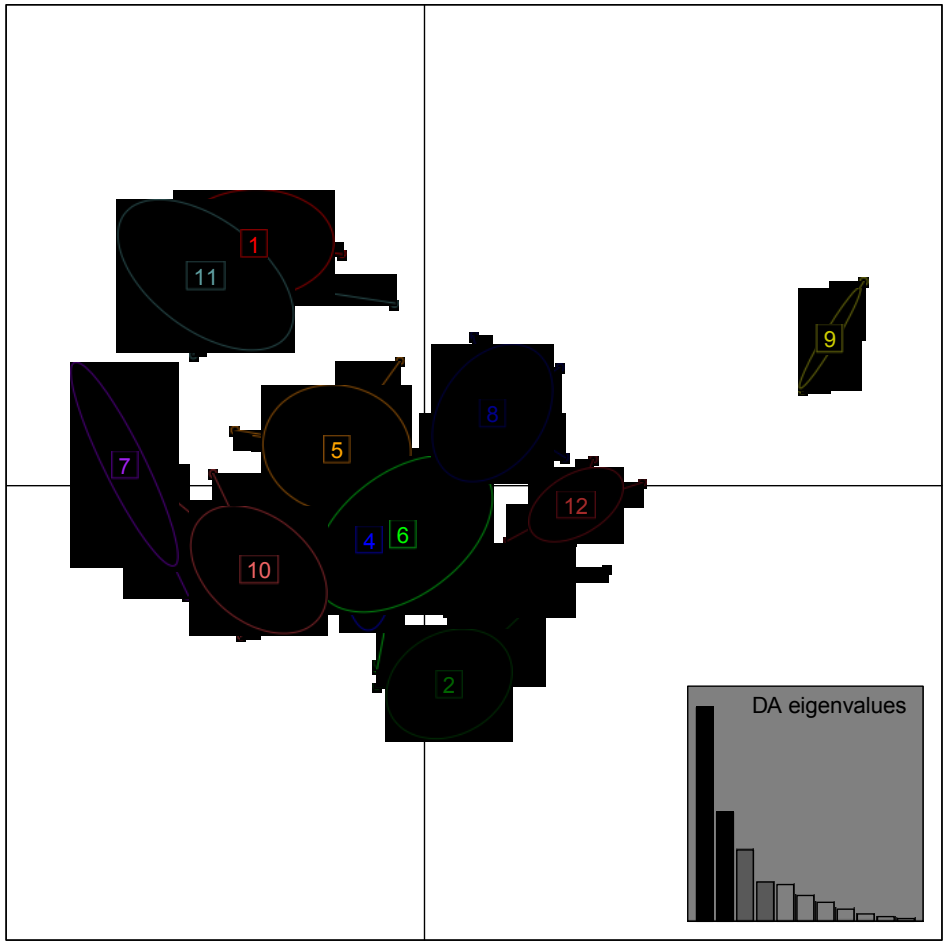

Figure S4.3. Clustering of MHC polymorphism by Discriminant Analysis of Principle Components was based on the physicochemical properties of the amino acids, which constitute the protein-binding region (PBR). Each point represents the positioning of each MHC allele within the first two discriminant functions (axis). Circles represent the positioning of each MHC supertype, which are largely represented by well-defined and minimally overlapping clusters.

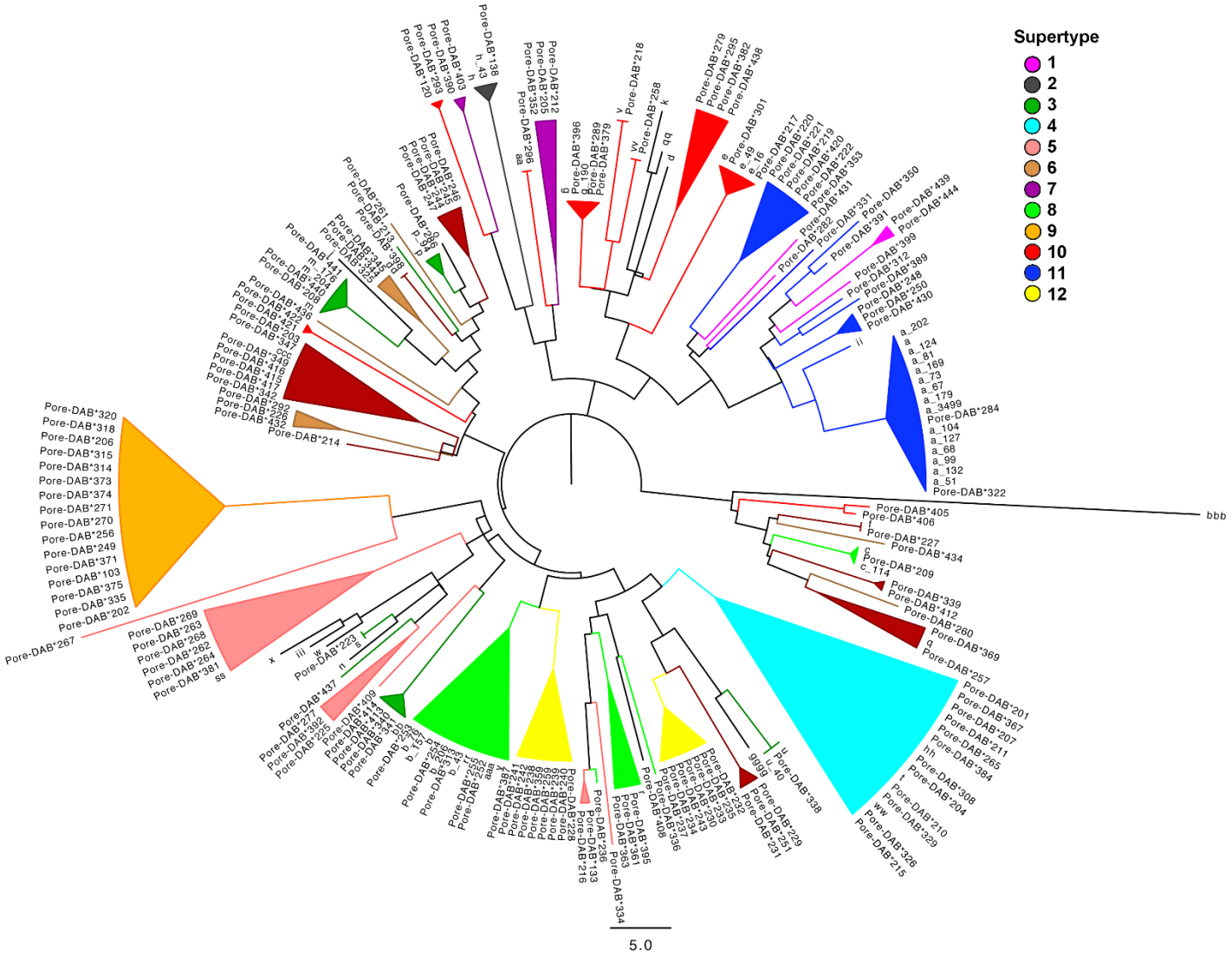

Figure S4.4 Bayesian inference of phylogenetic relationships among MHC alleles. Alleles are highlighted based on inferred membership to the 12 supertypes inferred though by Discriminant Analysis of Principle Components (DAPC). Alleles from Fraser *et al.* 2010 that formed 'supertype-a' and were correlated with reduced *Gyrodactylus* infections are closely related to alleles identified here (Pore*DAB) within supertype-11, which show a similar correlation. However, alleles pertaining to a supertype may form polyphyletic groups. This can be explained by the fact that micro-recombination and gene conversion events may redistribute genetic variation among duplicated MHC gene paralogues (Spurgin *et al.* 2011; van Oosterhout 2013). Therefore, defining supertypes based on DNA or peptide sequence similarity may not accurately reflect functional relationships among alleles.

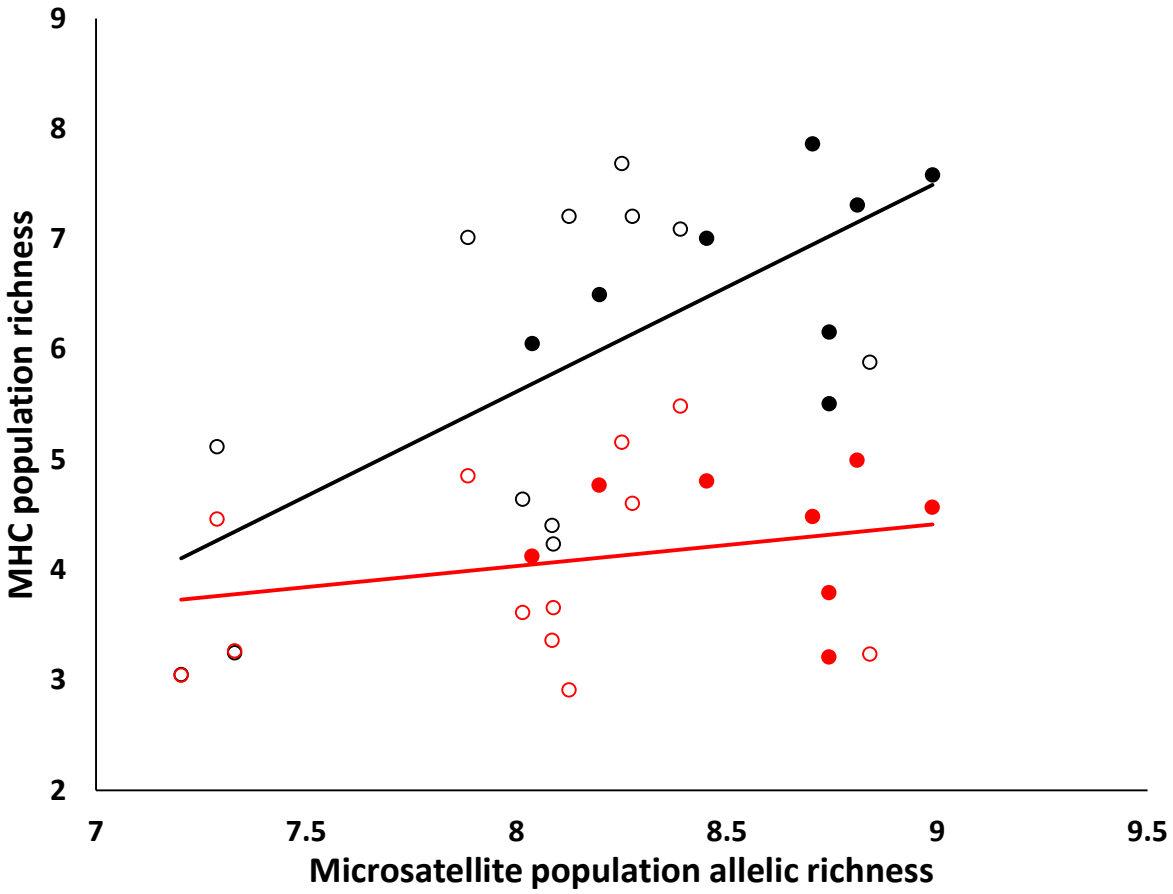

Figure S4.5. Linear models showing the relationship between MHC population allelic richness (MHC-$A_{r;}$ black circles), supertype richness (MHC-ST_r; red circles), and microsatellite population allelic richness (Micro-A_r). A strong and significant relationship is observed among all population estimates of MHC-A_r and Micro-A_r (solid line, P=0.001, R^2=0.41), and an insignificant relationship between MHC-ST_r and Micro-A_r (P= 0.289, R^2=0.01). Open circles denote low predation site, and closed circles denote high predation sites.

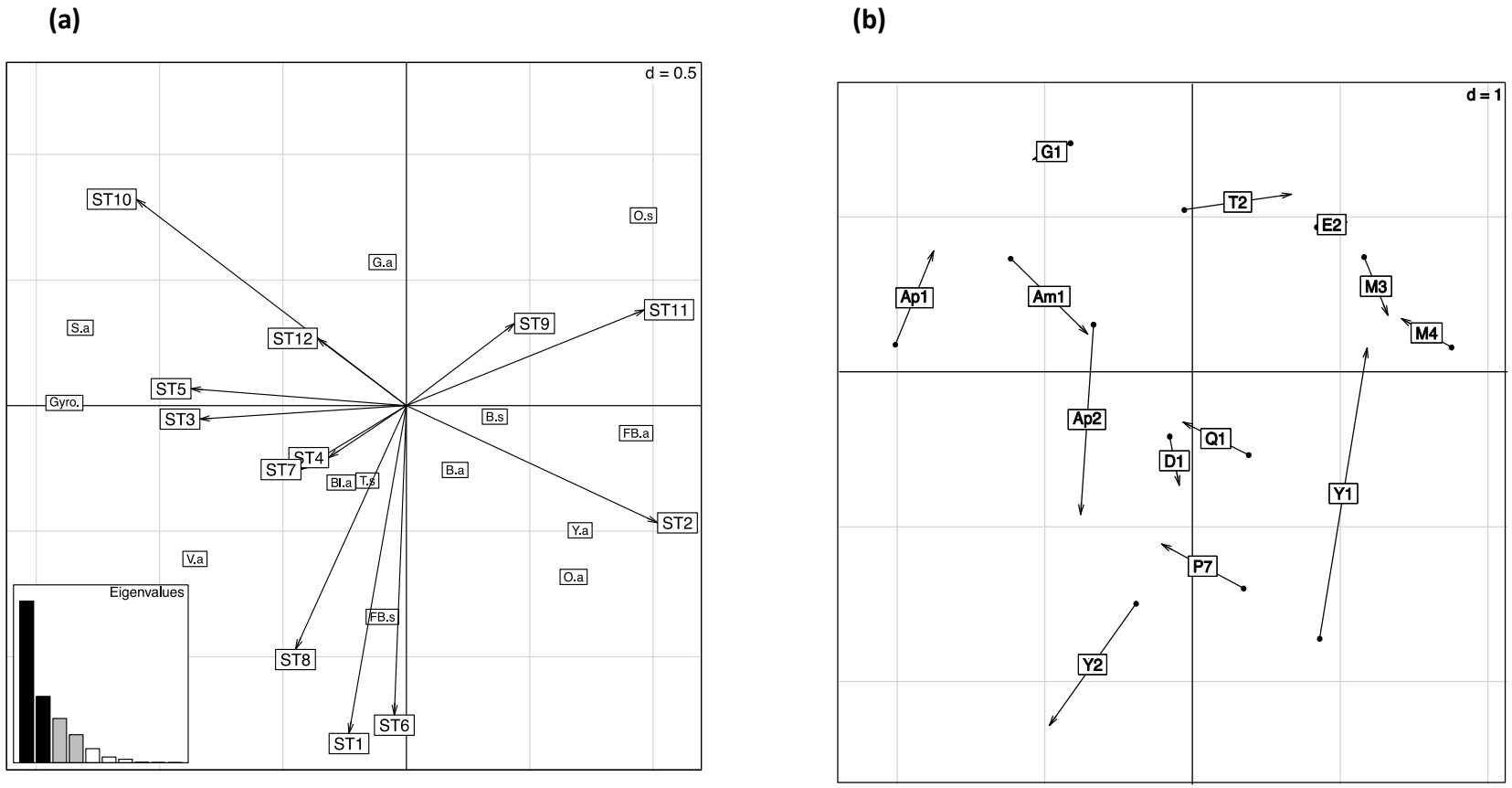

Figure S4.6. Coinertia analysis between datasets (1) MHC supertype frequencies, and (2) colour traits and *Gyrodactylus* prevalence (COIN[1]). (a) Vectors represent MHC supertype frequencies (ST-), whereas colour traits and *Gyrodactylus* prevalence are represented by a location on the first two factoral axis (Orange area (O.a), yellow area (Y.a), black area (B.a), fuzzy black area (FB.a), green area (G.a), blue area (Bl.a), silver area (S.a), violet area (V.a), number of orange spots (O.s), number of black spots (B.s), total number of spots (T.s), and *Gyrodactylus* prevalence (Gyro). Variables are positively associated when vectors and/or axis locations are in the same direction or close together. Variables are negatively associated when located in the opposite direction.

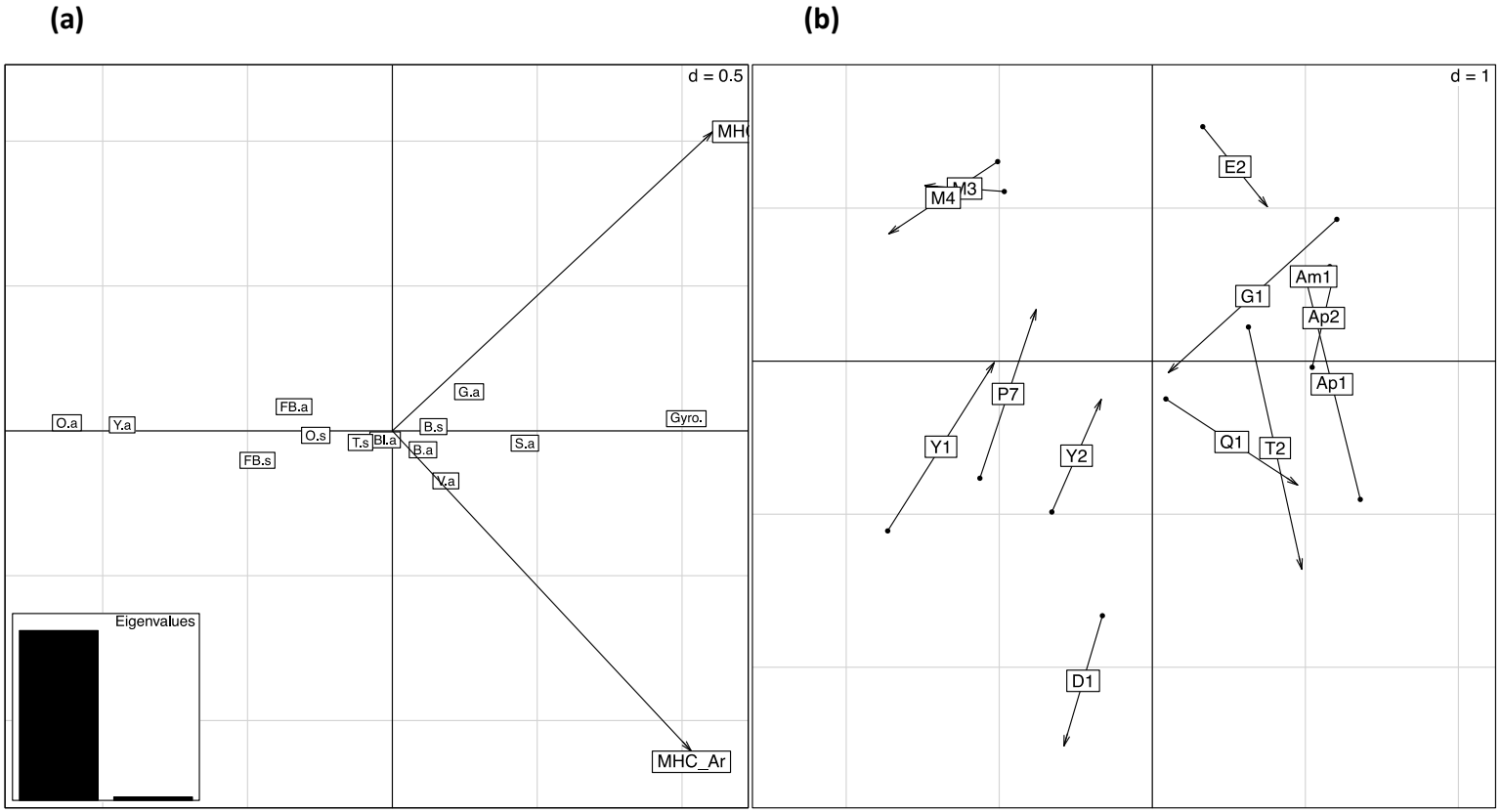

Figure S4.7. Coinertia analysis between datasets (1) Population MHC allelic richness (MHC-A_r) and Population MHC supertype richness (MHC-ST_r), and (2) colour traits and *Gyrodactylus* prevalence (COIN[2]). (a) Vectors represent MHC supertype frequencies (ST-), whereas colour traits and *Gyrodactylus* prevalence are represented by a location on the first two factorial axis (Orange area (O.a), yellow area (Y.a), black area (B.a), fuzzy black area (FB.a), green area (G.a), blue area (Bl.a), silver area (S.a), violet area (V.a), number of orange spots (O.s), number of black spots (B.s), total number of spots (T.s), and *Gyrodactylus* prevalence (Gyro). Variables are positively associated when vectors and/or axis locations are in the same direction or close together. Variables are negatively associated when located in the opposite direction. The distance of the variable from the center of the plot represents the strength of the variation in structuring the data. (b) Populations (Aripo-1 (AP1), Aripo-2 (AP2), Arima-1 (AM1), Guanapo-1 (G1), El Cedro-2 (EC2), Damier-1 (D1), Yarra-1 (Y1), Yarra-2 (Y2), Marianne-3 (M3), Marianne-4 (M4), Paria-7 (P7), and Quare-1 (Q1)) are positioned on the first two factorial axis of COIN[1] in accordance to the interaction between MHC supertype frequencies (tips of arrow) and colouration and *Gyrodactylus* prevalence (dot). The translational coefficient of the population position between datasets is given by the length and angle of the vector, where vector length is inversely correlated with the strength of the correlation between the two data sets

Locus	Primer sequence (5'-3')	Repeat sequence	Optimal T_A	Genbank #	Source Publication
Pre9	F: TTGCAAGTCAGTTGATGGTTG R: TGCCCTAGGGATGAGAAAAG	$(CAGA)_{13}$	60C	AY830941	Patterson *et al*. (2005)
Pre13	F: ACAGTACTGTCTGTCTGTCT R: TGTTTGAGACACTCATGGTGAAG	$(CTGT)_{18}$	65C	AY830942	Patterson *et al*. (2005)
Pre15	F: CTGAGGGACCAGGATGTTAAG R: CCATAAACACGCAAACCAAC	$(GATG)_{16}$	65C	AY830943	Patterson *et al*. (2005)
Pre26	F: GCTGACCCCAGAAAAGTGG R: TGGGACTTTCATGAGACTTGG	$(GATG)_{19}$	60C	AY830946	Patterson *et al*. (2005)
Pret-27	F: CACACGGGCTCTCATTTTT R: CTGTGTTTGTGTTCGGTCGTA	$(GT)_{53}$	60C	AB100321	Wantanabe *et al.* (2003)
Pret-28	F: ACATCGGCGTCCTCACCT R: GGGGGTTCAAACACATCCA	$(GT)_{32}$	60C	AB100322	Wantanabe *et al.* (2003)
Pret-38	F: AGGGAAAAGGAAAGAAAGAA R: CGAACAAGCCCAAATCTA	$(GT)_{19}$	50C	AB100328	Wantanabe *et al.* (2003)
Pret-46	F:AACCCTAATGACTCCCAACA R: CGACCCACCAGTAATCCAA	$(CA)_{27}$	60C	AB100334	Wantanabe *et al.* (2003)
Pret-80	F: GGAAGGGAGGGGAGGAT R:CACTTCAGCAGGGCAGACTA	$(GT)_{14}(GA)_{11}$	60C	AB100354	Wantanabe *et al.* (2003)
G145	F: TCTCCAAACCTCCCCTGTA R: GACGAGCCTCTGCTTCTTC	$(GT)_{11}$	60C	DQ855588	Shen *et al.* (2007)

Table S4.1: Details of microsatellite primers used

Predation	Drainage	Population	Mean A_i	Mean ST_i	Range A_i	Range ST_i
High	Caroni	Arima-1	3.966	3.133	2-9	1-6
Low	Caroni	Arima-2	3.2	3	1-6	1-6
Low	Caroni	Aripo-1	3.068	2.689	1-5	1-4
High	Caroni	Aripo-2	4.875	3.812	2-9	2-6
Low	Caroni	El Cedro-1	3.366	3.1	1-5	1-4
High	Caroni	El Cedro-1	3.843	3.187	1-7	1-5
High	Caroni	Guanapo-1	3.903	3.225	2-6	2-5
Low	Caroni	Guanapo-2	3.75	3.166	1-6	1-5
High	North Slope	Damier-1	3.311	2.577	1-7	1-5
Low	North Slope	Damier-2	2.642	2.214	1-7	1-5
Low	North Slope	Marianne-10	2.148	1.851	1-3	1-3
Low	North Slope	Marianne-16	3.032	2.741	2-6	2-5
Low	North Slope	Marianne-3	3.111	3.111	3-4	3-4
Low	North Slope	Marianne-4	2.937	2.937	2-4	2-4
Low	North Slope	Paria-7	3.625	3.187	2-6	2-4
Low	North Slope	Yarra-1	2.489	2.326	2-5	1-4
High	North Slope	Yarra-2	3.043	2.586	1-6	1-5
High	Oropouche	Quare-1	3.310	2.724	1-6	1-4
Low	Oropouche	Quare-2	3.117	2.588	1-6	1-5
High	Oropouche (Caroni type)	Turure-2	3.709	2.750	2-5	2-3
Low	Oropouche (Caroni type)	Turure-3	3.655	1-4	1-5	3

Table S2. Summary metrics of MHC allelic richness (MHC-A_r), and MHC supertype richness (MHC-ST_r).

Appendix 3

Supporting information for Chapter 5: *Supertypes explain paradoxes of MHC evolutionary ecology: A new perspective*

(a)

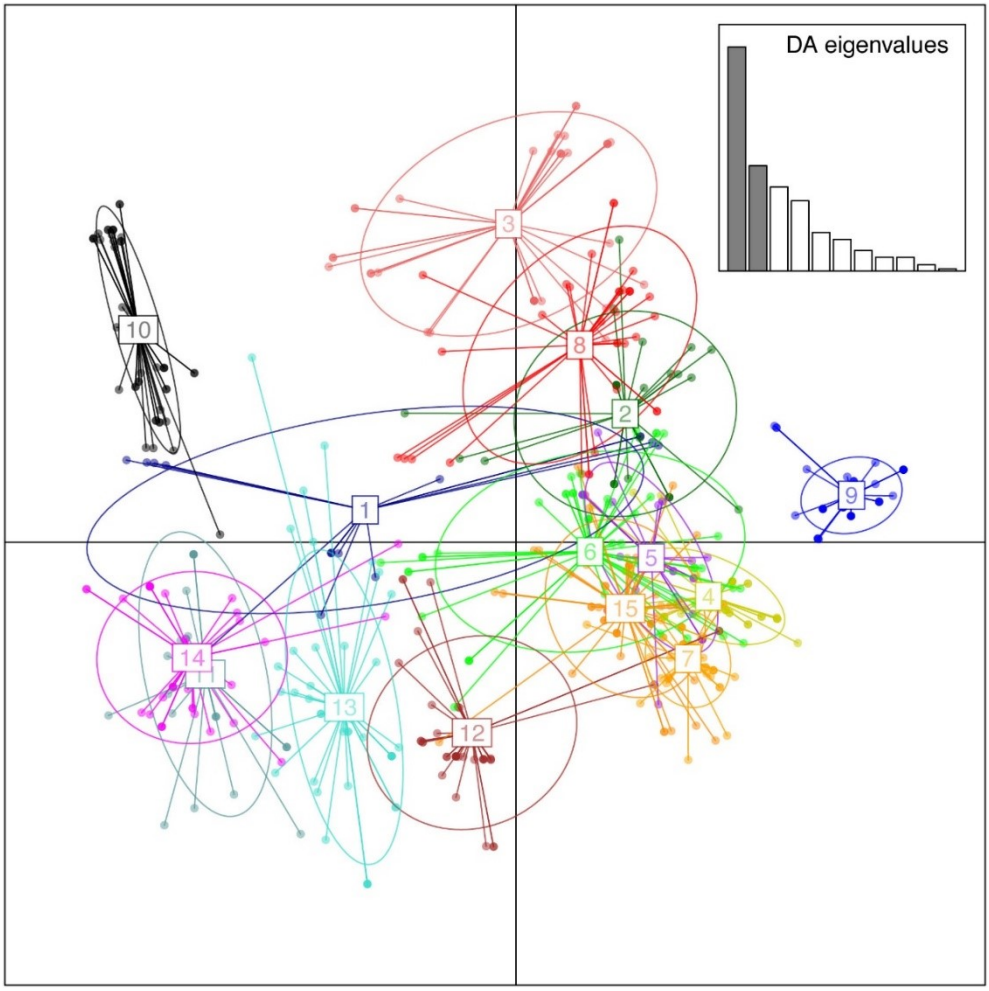

(b)

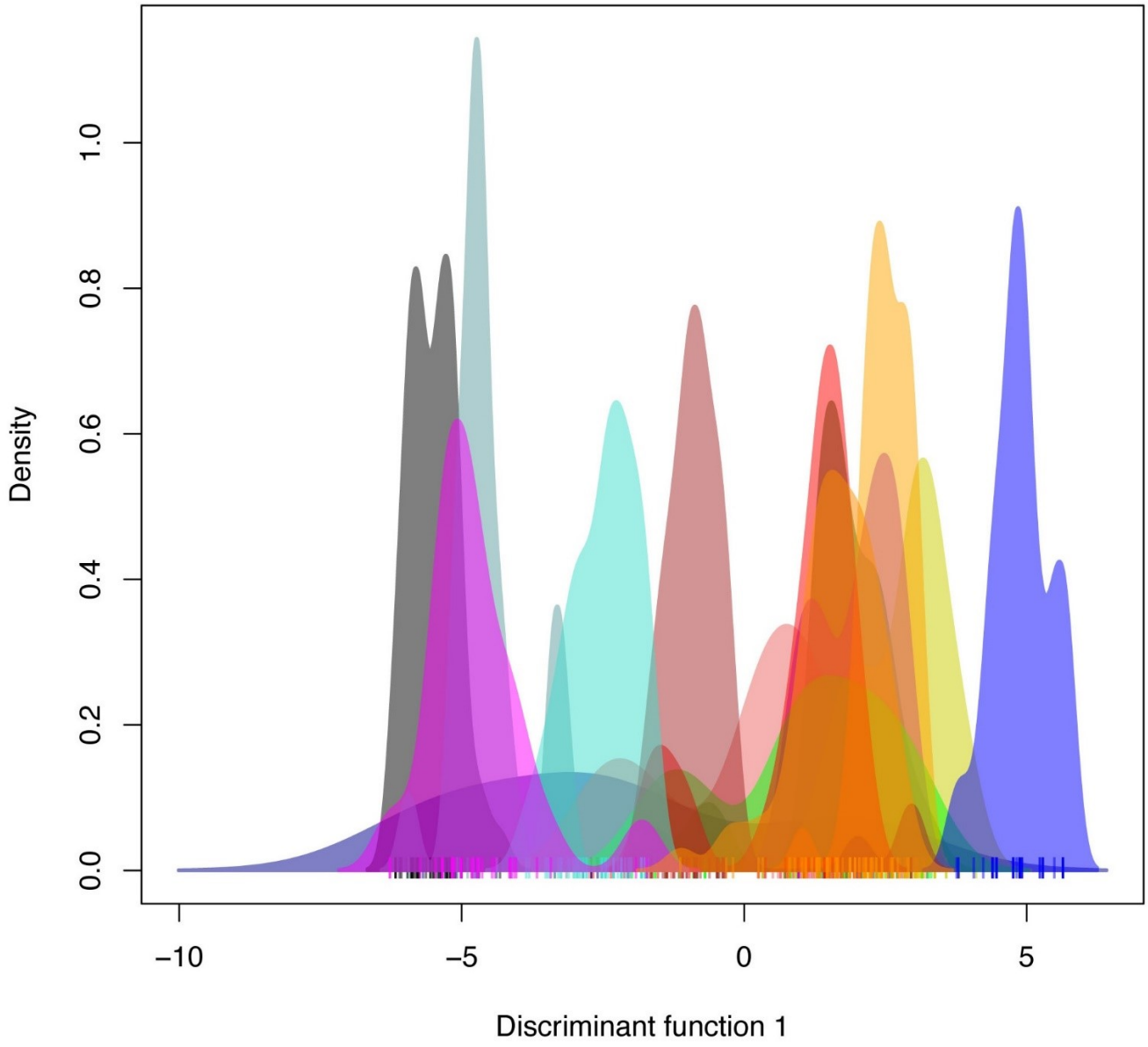

Figure S5.1. Clustering of MHC alleles by Discriminant Analysis of Principle Components (DAPC), based on the physicochemical properties of translated amino acids inferred to comprise the peptide binding region (PBR). DAPC inferred the presence of fifteen clusters, or supertypes, which are visualized on (a) two, and (b) one discriminant function.

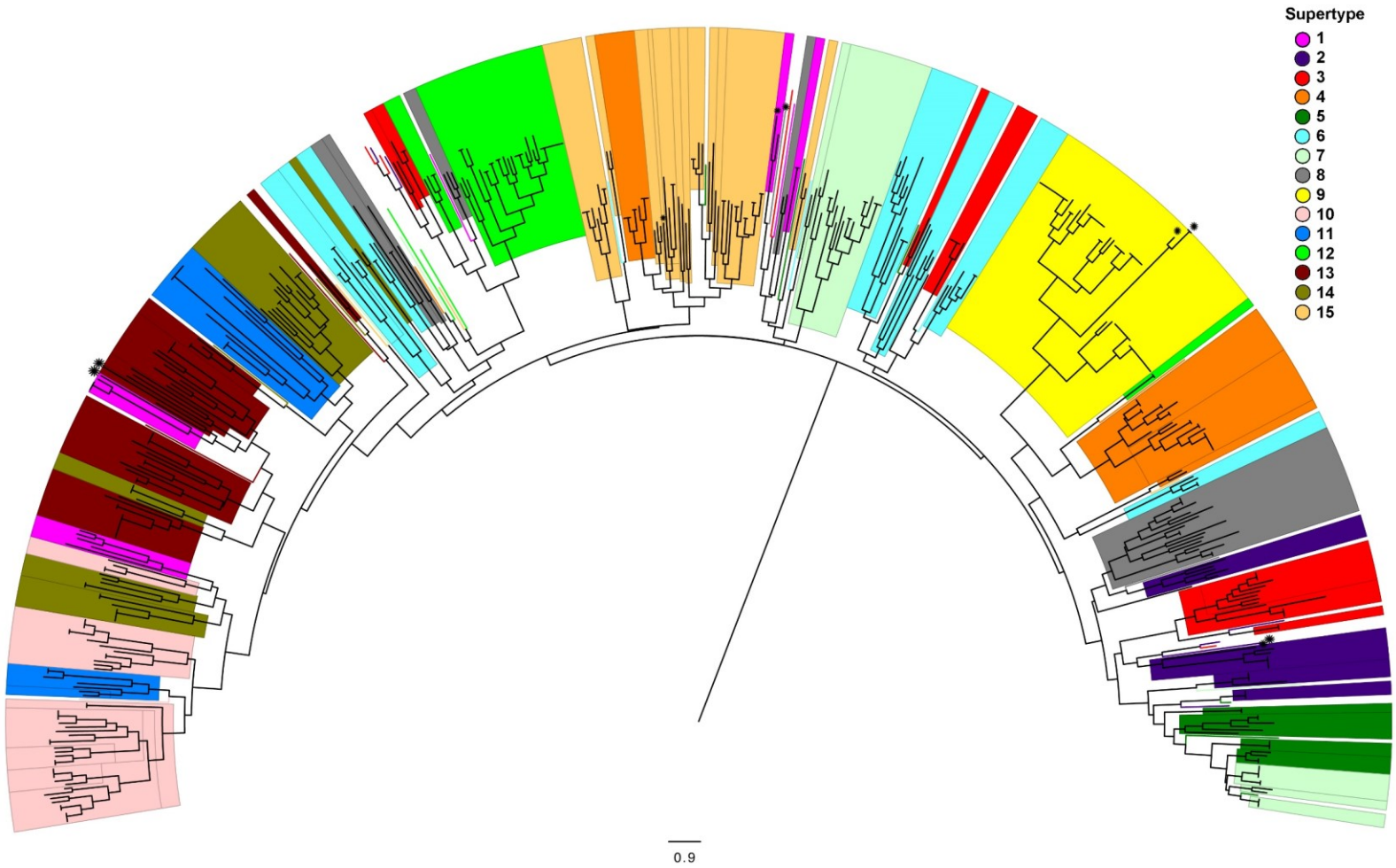

Figure S5.2. Neighbour-joining dendrogram of relationships among MHC alleles, based on the translated amino acids inferred to comprise the peptide binding region (PBR). For clarity, allele names have been removed. Alleles are highlighted based on inferred membership to the fifteen supertypes inferred though by Discriminant Analysis of Principle Components (DAPC). Perpendicular branch tips highlight identical PBR sequences derived from disparate MHC alleles (nucleotide sequences). The ten alleles observed in five Poecilia picta samples are denoted by a star symbol. Monophyly is on observed in supertype-9, and this is consistent with other unique characteristics of this supertype (See Results).

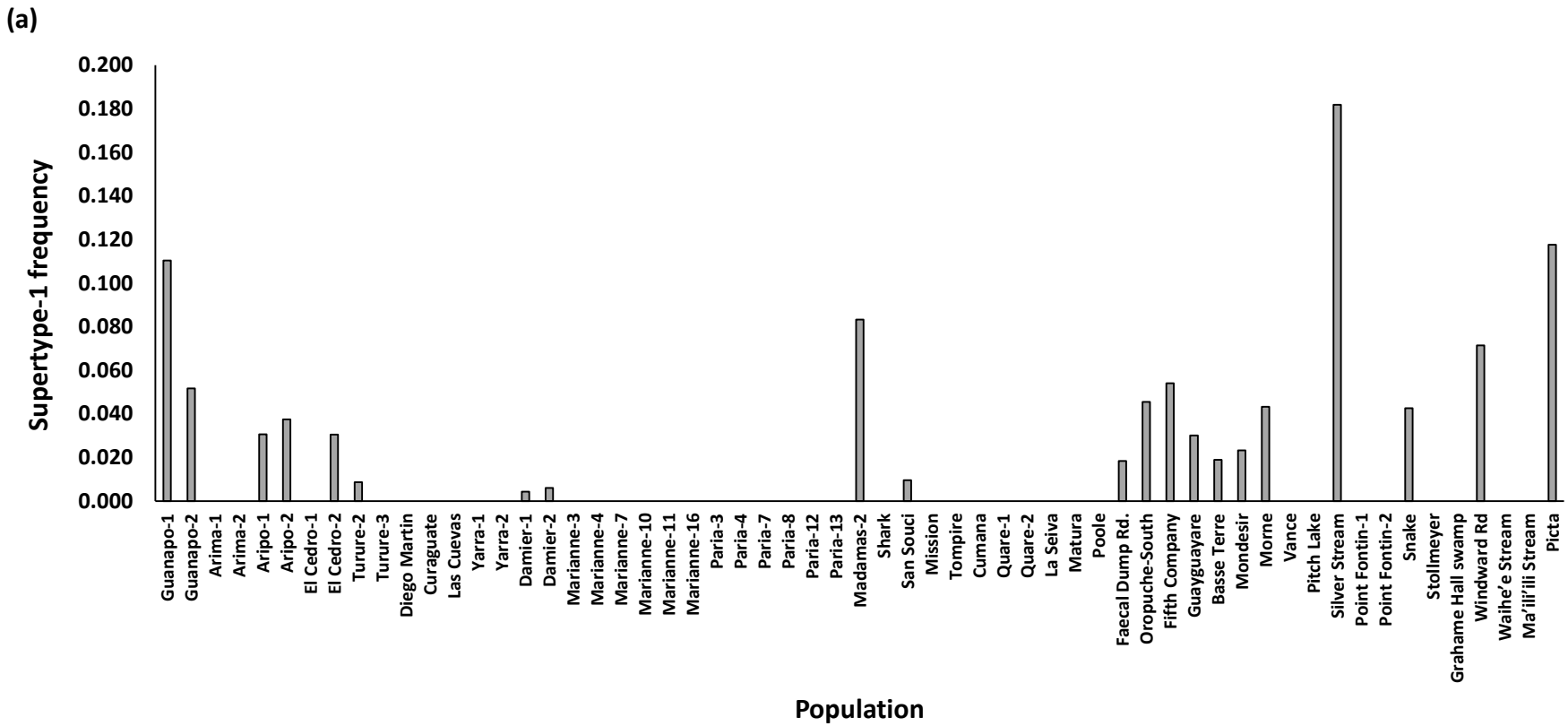

Figure S5.3. Population frequencies of (a) ST-1, (b) ST-2, (c) ST-3, (d) ST-4, (e) ST-5, (f) ST-6, (g) ST-7, (h) ST-8, (i) ST-9, (j) ST-10, (k) ST-11, (l) ST-12, (m) ST-13, (n) ST-14, (o) ST-15

(b)
Supertype-2 frequency
0.250
0.200
0.150
0.100
0.050
0.000
Guanapo-1
Guanapo-2
Arima-1
Arima-2
Aripo-1
Aripo-2
El Cedro-1
El Cedro-2
Turure-2
Turure-3
Diego Martin
Curaguate
Las Cuevas
Yarra-1
Yarra-2
Damier-1
Damier-2
Marianne-3
Marianne-4
Marianne-7
Marianne-10
Marianne-11
Marianne-16
Paria-3
Paria-4
Paria-7
Paria-8
Paria-12
Paria-13
Madamas-2
Shark
San Souci
Mission
Tompire
Cumana
Quare-1
Quare-2
La Seiva
Matura
Poole
Faecal Dump Rd.
Oropuche-South
Fifth Company
Guayguayare
Basse Terre
Mondesir
Morne
Vance
Pitch Lake
Silver Stream
Point Fontin-1
Point Fontin-2
Snake
Stollmeyer
Grahame Hall swamp
Windward Rd
Waihe'e Stream
Ma'ili'ili Stream
Picta
Population

(c)

Supertype-3 frequency
0.500
0.450
0.400
0.350
0.300
0.250
0.200
0.150
0.100
0.050
0.000
Guanapo-1
Guanapo-2
Arima-1
Arima-2
Aripo-1
Aripo-2
El Cedro-1
El Cedro-2
Turure-2
Turure-3
Diego Martin
Curaguate
Las Cuevas
Yarra-1
Yarra-2
Damier-1
Damier-2
Marianne-3
Marianne-4
Marianne-7
Marianne-10
Marianne-11
Marianne-16
Paria-3
Paria-4
Paria-7
Paria-8
Paria-12
Paria-13
Madamas-2
Shark
San Souci
Mission
Tompire
Cumana
Quare-1
Quare-2
La Seiva
Matura
Poole
Faecal Dump Rd.
Oropuche-South
Fifth Company
Guayguayare
Basse Terre
Mondesir
Morne
Vance
Pitch Lake
Silver Stream
Point Fontin-1
Point Fontin-2
Snake
Stollmeyer
Grahame Hall swamp
Windward Rd
Waihe'e Stream
Ma'ili'ili Stream
Picta
Population

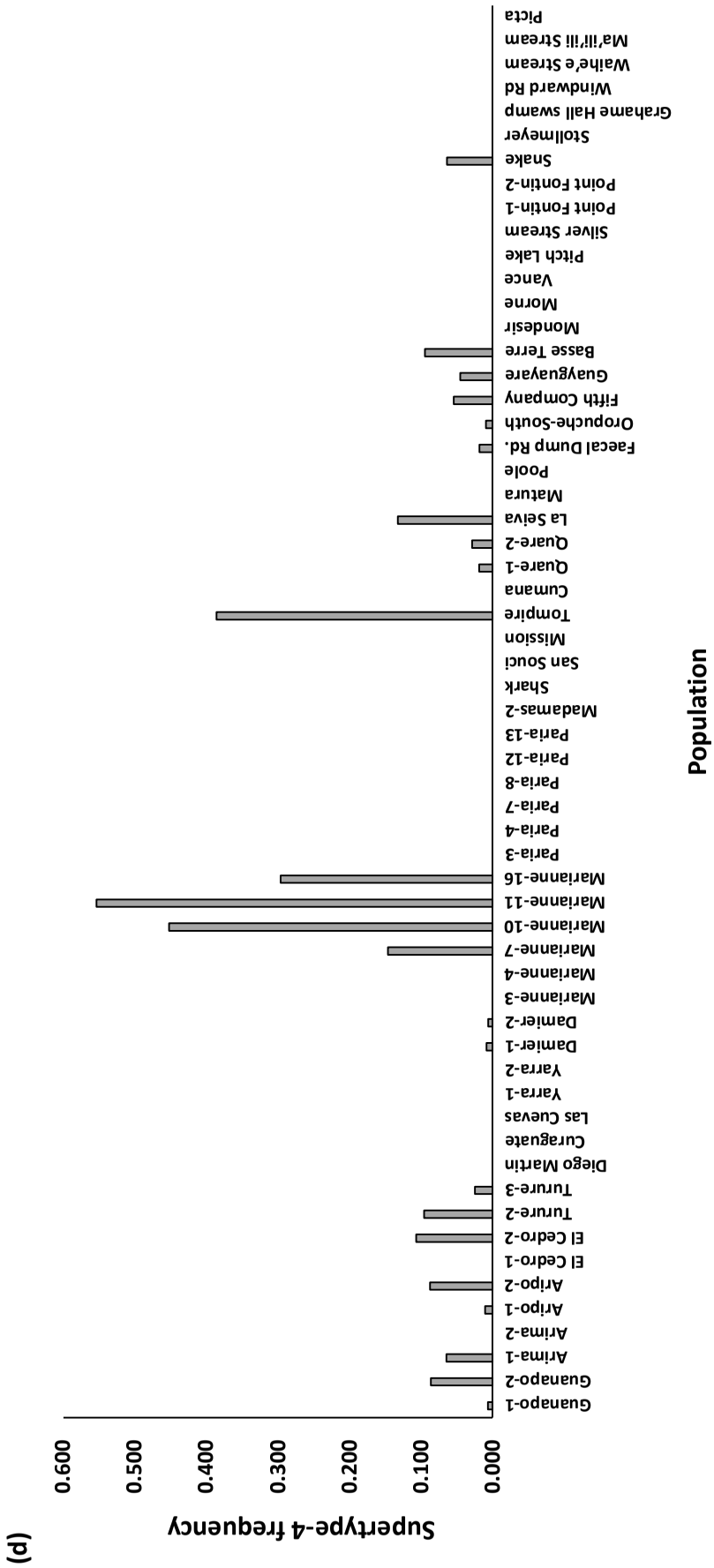
(p)
Supertype-4 frequency
0.600
0.500
0.400
0.300
0.200
0.100
0.000
Population
Guanapo-1
Guanapo-2
Arima-1
Arima-2
Aripo-1
Aripo-2
El Cedro-1
El Cedro-2
Turure-2
Turure-3
Diego Martin
Curaguate
Las Cuevas
Yarra-1
Yarra-2
Damier-1
Damier-2
Marianne-3
Marianne-4
Marianne-7
Marianne-10
Marianne-11
Marianne-16
Paria-3
Paria-4
Paria-7
Paria-8
Paria-12
Paria-13
Madamas-2
Shark
San Souci
Mission
Tompire
Cumana
Quare-1
Quare-2
La Seiva
Matura
Poole
Fecal Dump Rd.
Oropuche-South
Fifth Company
Guayguayare
Basse Terre
Mondesir
Morne
Vance
Pitch Lake
Silver Stream
Point Fontin-1
Point Fontin-2
Snake
Stollmeyer
Grahame Hall swamp
Windward Rd
Waihe'e Stream
Ma'ili'ili Stream
Picta

(e)

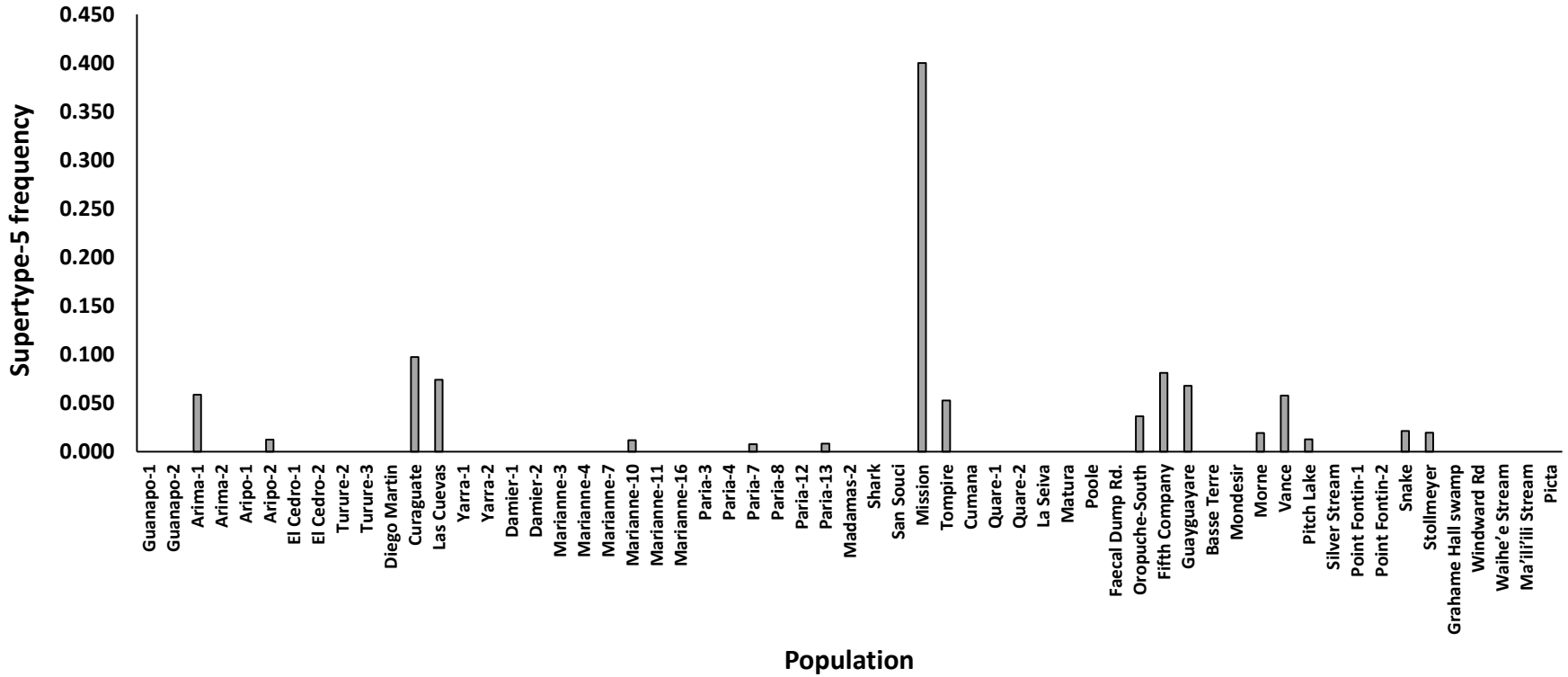
Supertype-5 frequency
0.450
0.400
0.350
0.300
0.250
0.200
0.150
0.100
0.050
0.000
Guanapo-1
Guanapo-2
Arima-1
Arima-2
Aripo-1
Aripo-2
El Cedro-1
El Cedro-2
Turure-2
Turure-3
Diego Martin
Curaguate
Las Cuevas
Yarra-1
Yarra-2
Damier-1
Damier-2
Marianne-3
Marianne-4
Marianne-7
Marianne-10
Marianne-11
Marianne-16
Paria-3
Paria-4
Paria-7
Paria-8
Paria-12
Paria-13
Madamas-2
Shark
San Souci
Mission
Tompire
Cumana
Quare-1
Quare-2
La Seiva
Matura
Poole
Faecal Dump Rd.
Oropuche-South
Fifth Company
Guayguayare
Basse Terre
Mondesir
Morne
Vance
Pitch Lake
Silver Stream
Point Fontin-1
Point Fontin-2
Snake
Stollmeyer
Grahame Hall swamp
Windward Rd
Waihe'e Stream
Ma'ili'ili Stream
Picta
Population

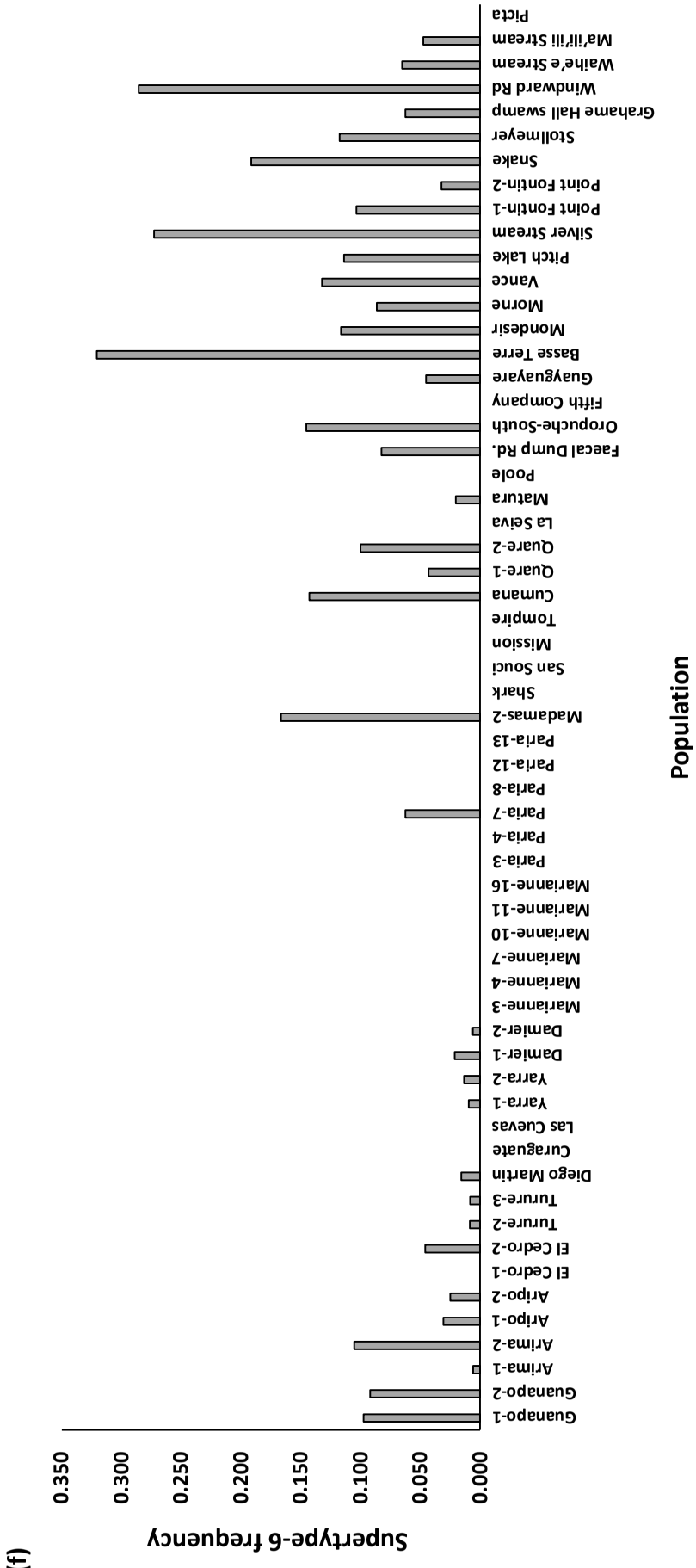
(f)
Supertype-6 frequency
0.350
0.300
0.250
0.200
0.150
0.100
0.050
0.000
Population
Guanapo-1
Guanapo-2
Arima-1
Arima-2
Aripo-1
Aripo-2
El Cedro-1
El Cedro-2
Turure-2
Turure-3
Diego Martin
Curaguate
Las Cuevas
Yarra-1
Yarra-2
Damier-1
Damier-2
Marianne-3
Marianne-4
Marianne-7
Marianne-10
Marianne-11
Marianne-16
Paria-3
Paria-4
Paria-7
Paria-8
Paria-12
Paria-13
Madamas-2
Shark
San Souci
Mission
Tompire
Cumana
Quare-1
Quare-2
La Seiva
Matura
Poole
Faecal Dump Rd.
Oropuche-South
Fifth Company
Guayguayare
Basse Terre
Mondesir
Morne
Vance
Pitch Lake
Silver Stream
Point Fontin-1
Point Fontin-2
Snake
Stollmeyer
Grahame Hall swamp
Windward Rd
Waihe'e Stream
Ma'ili'ili Stream
Picta

(g)

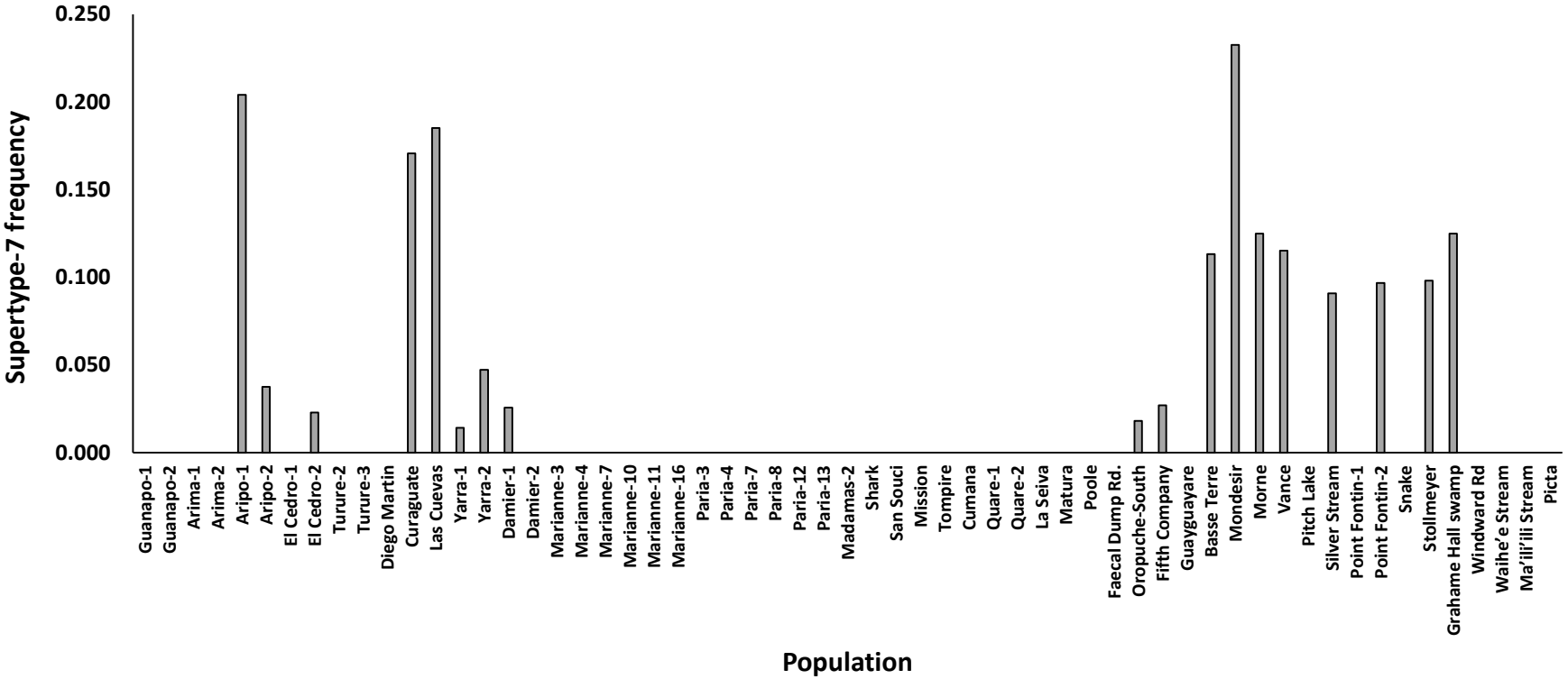
Supertype-7 frequency
0.250
0.200
0.150
0.100
0.050
0.000
Guanapo-1
Guanapo-2
Arima-1
Arima-2
Aripo-1
Aripo-2
El Cedro-1
El Cedro-2
Turure-2
Turure-3
Diego Martin
Curaguate
Las Cuevas
Yarra-1
Yarra-2
Damier-1
Damier-2
Marianne-3
Marianne-4
Marianne-7
Marianne-10
Marianne-11
Marianne-16
Paria-3
Paria-4
Paria-7
Paria-8
Paria-12
Paria-13
Madamas-2
Shark
San Souci
Mission
Tompire
Cumana
Quare-1
Quare-2
La Seiva
Matura
Poole
Faecal Dump Rd.
Oropuche-South
Fifth Company
Guayguayare
Basse Terre
Mondesir
Morne
Vance
Pitch Lake
Silver Stream
Point Fontin-1
Point Fontin-2
Snake
Stollmeyer
Grahame Hall swamp
Windward Rd
Waihe'e Stream
Ma'ili'ili Stream
Picta
Population

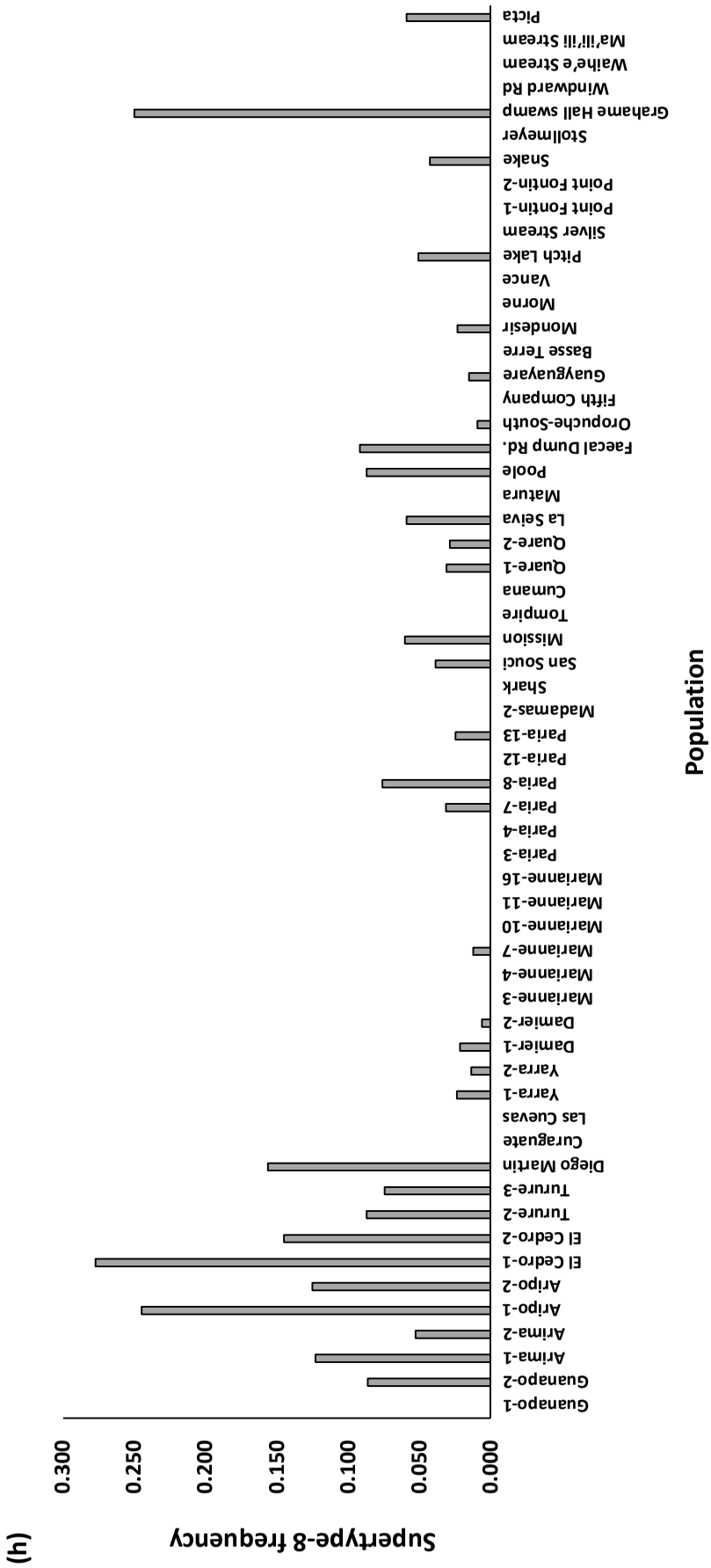
(u)
Supertype-8 frequency
0.300
0.250
0.200
0.150
0.100
0.050
0.000
Population
Guanapo-1
Guanapo-2
Arima-1
Arima-2
Aripo-1
Aripo-2
El Cedro-1
El Cedro-2
Turure-2
Turure-3
Diego Martin
Curaguate
Las Cuevas
Yarra-1
Yarra-2
Damier-1
Damier-2
Marianne-3
Marianne-4
Marianne-7
Marianne-10
Marianne-11
Marianne-16
Paria-3
Paria-4
Paria-7
Paria-8
Paria-12
Paria-13
Madamas-2
Shark
San Souci
Mission
Tompire
Cumana
Quare-1
Quare-2
La Seiva
Matura
Poole
Fecal Dump Rd.
Oropuche-South
Fifth Company
Guayguayare
Basse Terre
Mondesir
Morne
Vance
Pitch Lake
Silver Stream
Point Fontin-1
Point Fontin-2
Snake
Stollmeyer
Grahame Hall swamp
Windward Rd
Waihe'e Stream
Ma'ili'ili Stream
Picta

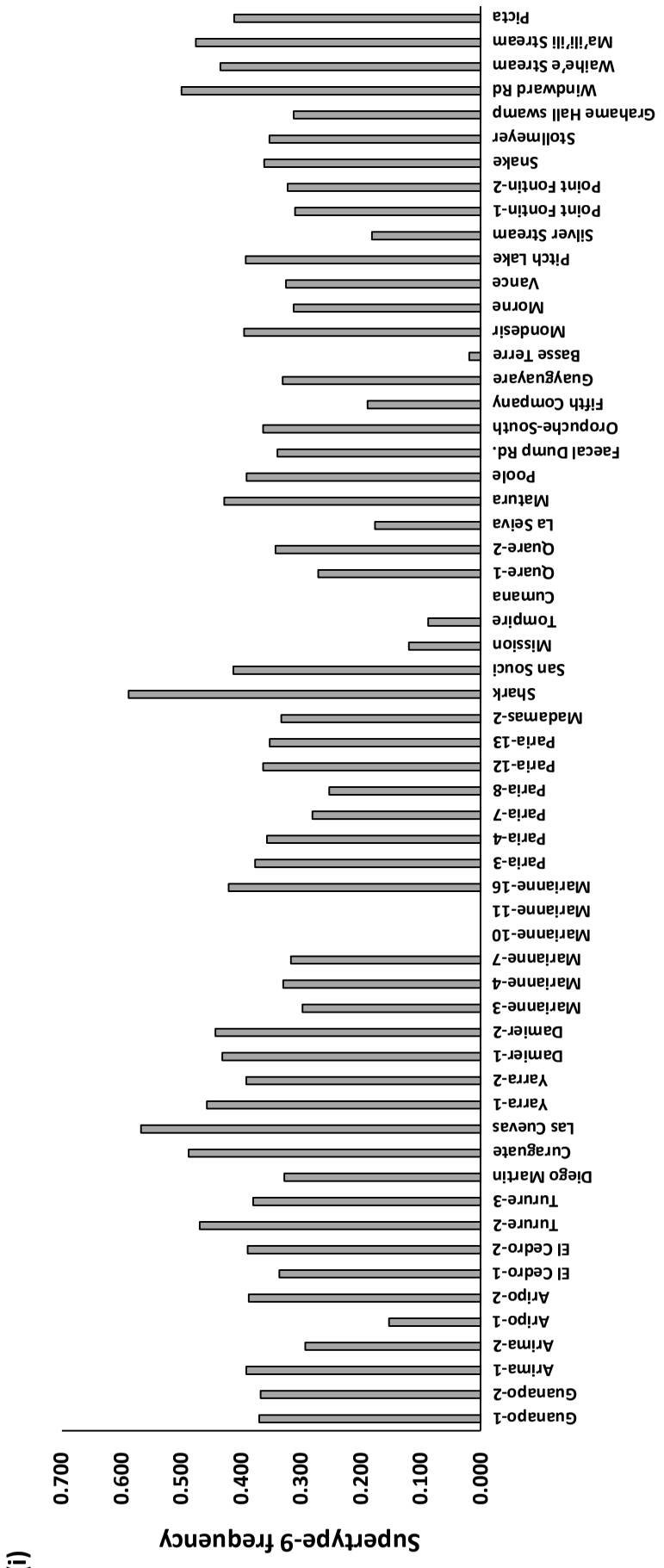
(i)
Supertype-9 frequency
0.700
0.600
0.500
0.400
0.300
0.200
0.100
0.000
Population
Guanapo-1
Guanapo-2
Arima-1
Arima-2
Aripo-1
Aripo-2
El Cedro-1
El Cedro-2
Turure-2
Turure-3
Diego Martin
Curaguate
Las Cuevas
Yarra-1
Yarra-2
Damier-1
Damier-2
Marianne-3
Marianne-4
Marianne-7
Marianne-10
Marianne-11
Marianne-16
Paria-3
Paria-4
Paria-7
Paria-8
Paria-12
Paria-13
Madamas-2
Shark
San Souci
Mission
Tompire
Cumana
Quare-1
Quare-2
La Seiva
Matura
Poole
Fecal Dump Rd.
Oropuche-South
Fifth Company
Guayguayare
Basse Terre
Mondesir
Morne
Vance
Pitch Lake
Silver Stream
Point Fontin-1
Point Fontin-2
Snake
Stollmeyer
Grahame Hall swamp
Windward Rd
Waihe'e Stream
Ma'ili'ili Stream
Picta

(j)

Supertype-10 frequency
0.400
0.350
0.300
0.250
0.200
0.150
0.100
0.050
0.000
Guanapo-1
Guanapo-2
Arima-1
Arima-2
Aripo-1
Aripo-2
El Cedro-1
El Cedro-2
Turure-2
Turure-3
Diego Martin
Curaguate
Las Cuevas
Yarra-1
Yarra-2
Damier-1
Damier-2
Marianne-3
Marianne-4
Marianne-7
Marianne-10
Marianne-11
Marianne-16
Paria-3
Paria-4
Paria-7
Paria-8
Paria-12
Paria-13
Madamas-2
Shark
San Souci
Mission
Tompire
Cumana
Quare-1
Quare-2
La Seiva
Matura
Poole
Faecal Dump Rd.
Oropuche-South
Fifth Company
Guayguayare
Basse Terre
Mondesir
Morne
Vance
Pitch Lake
Silver Stream
Point Fontin-1
Point Fontin-2
Snake
Stollmeyer
Grahame Hall swamp
Windward Rd
Waihe'e Stream
Ma'ili'ili Stream
Picta
Population

(k)

Supertype-11 frequency
0.350
0.300
0.250
0.200
0.150
0.100
0.050
0.000
Guanapo-1
Guanapo-2
Arima-1
Arima-2
Aripo-1
Aripo-2
El Cedro-1
El Cedro-2
Turure-2
Turure-3
Diego Martin
Curaguate
Las Cuevas
Yarra-1
Yarra-2
Damier-1
Damier-2
Marianne-3
Marianne-4
Marianne-7
Marianne-10
Marianne-11
Marianne-16
Paria-3
Paria-4
Paria-7
Paria-8
Paria-12
Paria-13
Madamas-2
Shark
San Souci
Mission
Tompire
Cumana
Quare-1
Quare-2
La Seiva
Matura
Poole
Faecal Dump Rd.
Oropuche-South
Fifth Company
Guayguayare
Basse Terre
Mondesir
Morne
Vance
Pitch Lake
Silver Stream
Point Fontin-1
Point Fontin-2
Snake
Stollmeyer
Grahame Hall swamp
Windward Rd
Waihe'e Stream
Ma'ili'ili Stream
Picta
Population

(l)

Supertype-12 frequency
0.250
0.200
0.150
0.100
0.050
0.000
Guanapo-1
Guanapo-2
Arima-1
Arima-2
Aripo-1
Aripo-2
El Cedro-1
El Cedro-2
Turure-2
Turure-3
Diego Martin
Curaguate
Las Cuevas
Yarra-1
Yarra-2
Damier-1
Damier-2
Marianne-3
Marianne-4
Marianne-7
Marianne-10
Marianne-11
Marianne-16
Paria-3
Paria-4
Paria-7
Paria-8
Paria-12
Paria-13
Madamas-2
Shark
San Souci
Mission
Tompire
Cumana
Quare-1
Quare-2
La Seiva
Matura
Poole
Faecal Dump Rd.
Oropuche-South
Fifth Company
Guayguayare
Basse Terre
Mondesir
Morne
Vance
Pitch Lake
Silver Stream
Point Fontin-1
Point Fontin-2
Snake
Stollmeyer
Grahame Hall swamp
Windward Rd
Waihe'e Stream
Ma'ili'ili Stream
Picta
Population

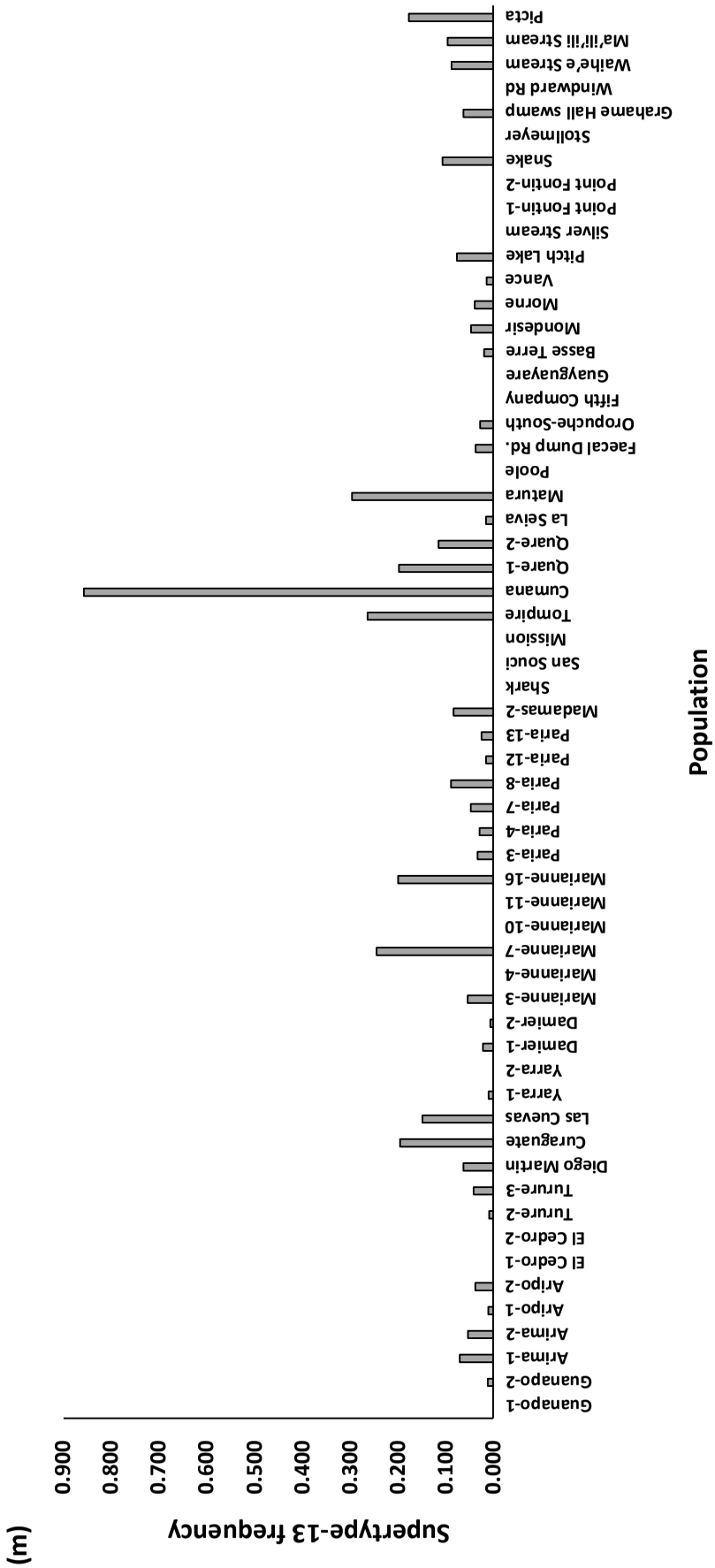
(m)
Supertype-13 frequency
0.900
0.800
0.700
0.600
0.500
0.400
0.300
0.200
0.100
0.000
Population
Guanapo-1
Guanapo-2
Arima-1
Arima-2
Aripo-1
Aripo-2
El Cedro-1
El Cedro-2
Turure-2
Turure-3
Diego Martin
Curaguate
Las Cuevas
Yarra-1
Yarra-2
Damier-1
Damier-2
Marianne-3
Marianne-4
Marianne-7
Marianne-10
Marianne-11
Marianne-16
Paria-3
Paria-4
Paria-7
Paria-8
Paria-12
Paria-13
Madamas-2
Shark
San Souci
Mission
Tompire
Cumana
Quare-1
Quare-2
La Seiva
Matura
Poole
Faecal Dump Rd.
Oropuche-South
Fifth Company
Guayguayare
Basse Terre
Mondesir
Morne
Vance
Pitch Lake
Silver Stream
Point Fontin-1
Point Fontin-2
Snake
Stollmeyer
Grahame Hall swamp
Windward Rd
Waihe'e Stream
Ma'iil'iil Stream
Picta

(n)

Supertype-14 frequency
0.450
0.400
0.350
0.300
0.250
0.200
0.150
0.100
0.050
0.000
Guanapo-1
Guanapo-2
Arima-1
Arima-2
Aripo-1
Aripo-2
El Cedro-1
El Cedro-2
Turure-2
Turure-3
Diego Martin
Curaguate
Las Cuevas
Yarra-1
Yarra-2
Damier-1
Damier-2
Marianne-3
Marianne-4
Marianne-7
Marianne-10
Marianne-11
Marianne-16
Paria-3
Paria-4
Paria-7
Paria-8
Paria-12
Paria-13
Madamas-2
Shark
San Souci
Mission
Tompire
Cumana
Quare-1
Quare-2
La Seiva
Matura
Poole
Faecal Dump Rd.
Oropuche-South
Fifth Company
Guayguayare
Basse Terre
Mondesir
Morne
Vance
Pitch Lake
Silver Stream
Point Fontin-1
Point Fontin-2
Snake
Stollmeyer
Grahame Hall swamp
Windward Rd
Waihe'e Stream
Ma'ili'ili Stream
Picta
Population

(o)

Supertype-15 frequency
0.450
0.400
0.350
0.300
0.250
0.200
0.150
0.100
0.050
0.000
Guanapo-1
Guanapo-2
Arima-1
Arima-2
Aripo-1
Aripo-2
El Cedro-1
El Cedro-2
Turure-2
Turure-3
Diego Martin
Curaguate
Las Cuevas
Yarra-1
Yarra-2
Damier-1
Damier-2
Marianne-3
Marianne-4
Marianne-7
Marianne-10
Marianne-11
Marianne-16
Paria-3
Paria-4
Paria-7
Paria-8
Paria-12
Paria-13
Madamas-2
Shark
San Souci
Mission
Tompire
Cumana
Quare-1
Quare-2
La Seiva
Matura
Poole
Faecal Dump Rd.
Oropuche-South
Fifth Company
Guayguayare
Basse Terre
Mondesir
Morne
Vance
Pitch Lake
Silver Stream
Point Fontin-1
Point Fontin-2
Snake
Stollmeyer
Grahame Hall swamp
Windward Rd
Waihe'e Stream
Ma'ili'ili Stream
Picta
Population

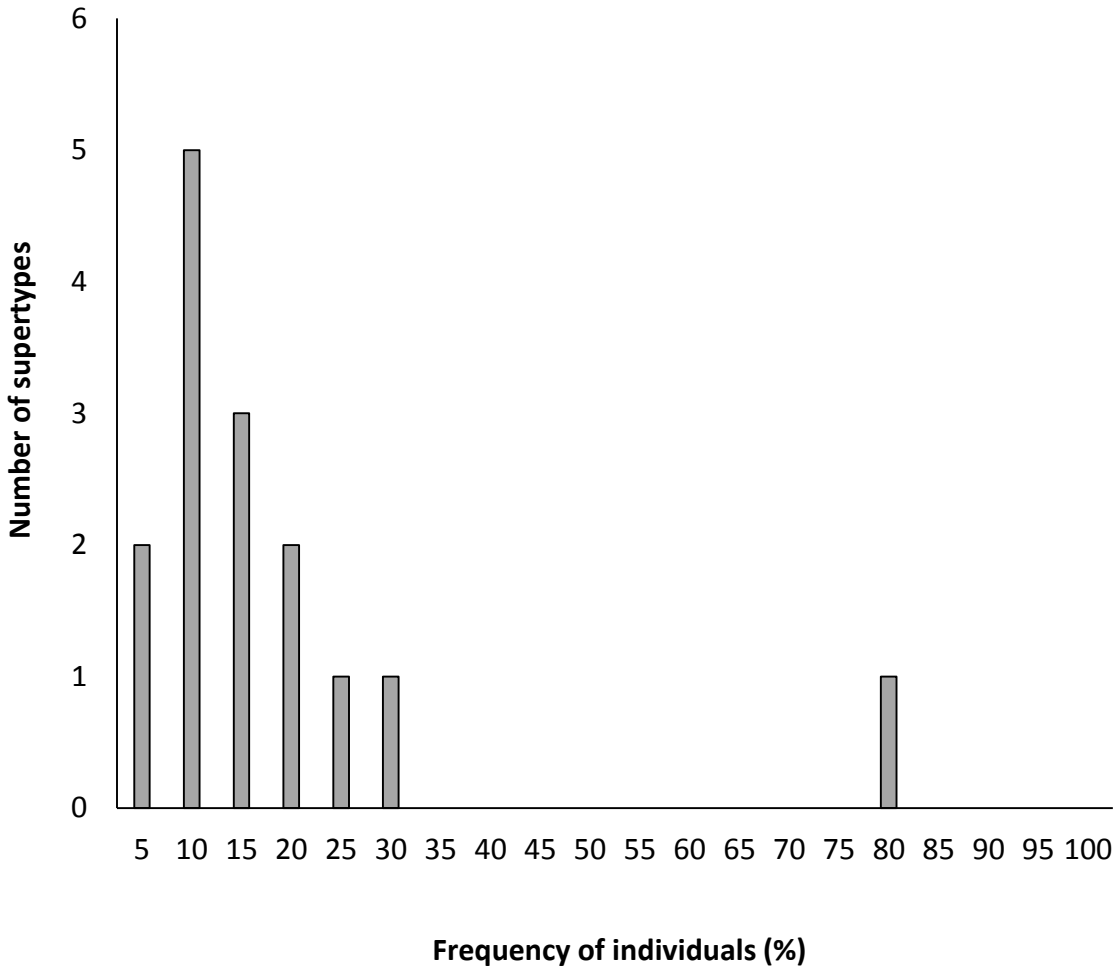

Figure S5.4. Frequency distribution of the occurrence of supertypes within individuals in populations. Supertype 9 is present in 79.77 % of individuals. The mean (and standard deviation) of the number of supertypes per individual equals 17.55 (18.62), and supertype 9 lies 3.33 standard deviations away from the mean, which is a significant outlier with $p<0.003$.

Appendix 4
Copyright agreements

JOHN WILEY AND SONS LICENSE

This Agreement between Jackie Lighten ("You") and John Wiley and Sons ("John Wiley and Sons") consists of your license details and the terms and conditions provided by John Wiley and Sons and Copyright Clearance Center.

License Number	3601291401895
License date	Apr 03, 2015
Licensed Content Publisher	John Wiley and Sons
Licensed Content Publication	Molecular Ecology Resources
Licensed Content Title	Ultra-deep Illumina sequencing accurately identifies MHC class IIb alleles and provides evidence for copy number variation in the guppy (*Poecilia reticulata*)
Licensed Content Author	Jackie Lighten, Cock van Oosterhout, Ian G. Paterson, Mark McMullan, Paul Bentzen
Licensed Content Date	Feb 5, 2014
Pages	15
Type of use	Dissertation/Thesis
Requestor type	Author of this Wiley article
Format	Print and electronic
Portion	Full article
Will you be translating?	No
Title of your thesis / dissertation	Elucidating patterns of Major Histocompatibility Complex polymorphism in the Trinidadian guppy (*Poecilia reticulata*) using Next Generation Sequencing
Expected completion date	July 2015
Expected size (number of pages)	250
Requestor Location	Jackie Lighten Dep. of Biology, Dalhousie University 1355 Oxford Street PO BOX 15000 Halifax, NS B3H 4R2 Canada

JOHN WILEY AND SONS LICENSE

This Agreement between Jackie Lighten ("You") and John Wiley and Sons ("John Wiley and Sons") consists of your license details and the terms and conditions provided by John Wiley and Sons and Copyright Clearance Center.

License Number	3601291401895
License date	Apr 03, 2015
Licensed Content Publisher	John Wiley and Sons
Licensed Content Publication	Molecular Ecology Resources
Licensed Content Title	Critical review of NGS analyses for *de novo* genotyping multigene families
Licensed Content Author	Jackie Lighten, Cock van Oosterhout, Paul Bentzen
Licensed Content Date	Jul 21, 2014
Pages	16
Type of use	Dissertation/Thesis
Requestor type	Author of this Wiley article
Format	Print and electronic
Portion	Full article
Will you be translating?	No
Title of your thesis / dissertation	Elucidating patterns of Major Histocompatibility Complex polymorphism in the Trinidadian guppy (*Poecilia reticulata*) using Next Generation Sequencing
Expected completion date	July 2015
Expected size (number of pages)	250
Requestor Location	Jackie Lighten Dep. of Biology, Dalhousie University 1355 Oxford Street PO BOX 15000 Halifax, NS B3H 4R2 Canada